ACCURATE DESCRIPTION OF THE CRITICAL REGION BY A MOLECULAR-BASED EQUATION OF STATE WITH A CROSSOVER TREATMENT

A dissertation presented to the
Departament de Química of the

Universitat Autònoma de Barcelona

in partial fulfillment of the requirements
for the degree of Doctor in Materials Science

by

Fèlix Lluís Llovell Ferret

under the supervision of Dr. Lourdes F. Vega

Molsim ICMAB

Bellaterra
(Barcelona)
October, 2006

Universitat
Autònoma
de Barcelona

ACCURATE DESCRIPTION OF THE CRITICAL REGION BY A MOLECULAR-BASED EQUATION OF STATE WITH A CROSSOVER TREATMENT

Thesis committee:

Prof. Cor Peters

Delft University of Technology, Holland

Dr. Josep Pàmies Corominas

Max-Planck Institute for Colloids and Interfaces, Germany

Dr. Amparo Galindo

Imperial College, UK

Dr. Isabel Marrucho

University of Aveiro, Portugal

Dr. Manuel Martínez Piñeiro

Universidade de Vigo, Spain

Dr. Jordi Fauraudo Gener (substitute)

Universitat Autònoma de Barcelona

Dr. Carlos Rey Castro (substitute)

Universitat de Lleida

La sotasignada

FA CONSTAR

que el present treball, que porta per títol

ACCURATE DESCRIPTION OF THE CRITICAL REGION BY A MOLECULAR-BASED EQUATION OF STATE WITH A CROSSOVER TREATMENT

i que presenta en Fèlix Lluís Llovell Ferret per a optar al grau de Doctor per la Universitat Autònoma de Barcelona, ha estat realitzat en aquesta universitat sota la seva direcció, i que tots els resultats presentats i l'anàlisi corresponent són fruit de la investigació realitzada per l'esmentat candidat.

I per a que se'n prengui coneixement i als efectes que correspongui, signa aquest certificat.

<div align="right">

Lourdes Vega Fernández
Investigadora Científica
Institut de Ciència de Materials de Barcelona
Consejo Superior de Investigaciones Científicas (CSIC)

</div>

Bellaterra (Barcelona), 30 d'octubre de 2006.

Declaration

The work reported in this thesis was carried out at the Molecular Simulation Group of the Institut de Ciència de Materials de Barcelona, Consejo Superior de Investigaciones Científicas (ICMAB-CSIC) (Campus de la Universitat Autònoma de Barcelona, 08193, Bellaterra, Spain) with financial support from the Ministerio de Educación y Ciencia (FPU grant). No part of this thesis has been submitted elsewhere for any other degree or qualification and it is all my own work unless referenced to the contrary in the text.

<div align="right">

Fèlix Llovell

October 2006

</div>

Als meus pares, avis i família, pel seu recolzament
incondicional, confiança i estimació

Contents

Agraïments
Agradecimientos
Acknowledgements

Quan s'arriba a la fi d'aquest llarg i intens periode un mira cap enrera i veu que quatre anys han passat, i que moltes persones han col·laborat en aquest camí traçat pel món de la ciència. En primer lloc, he d'agrair a la meva directora de tesi, la Dra. Lourdes Vega, el fet que ara mateix estigui presentant aquest treball. El seu entusiasme inicial em va fer decantar pel món de les equacions moleculars malgrat les "reserves" que tenia sobre les meves capacitats en el món de la física. Gràcies a ella, he après a estimar i valorar la meva pròpia feina i els seus savis consells han estat una bona guia per arribar a bon port. A més, el seu dinamisme s'ha traslladat a nivell personal, procurant activar sempre la convivència del grup de recerca.

I am also extremely grateful to Prof. Cor J. Peters for giving me the opportunity to do a stay for three months in his group in Delft. His experience helped me a lot, and the kindness of him and his wife Adri will never be forgotten. I also enjoyed a great time with the whole group in Delft: thanks to Sona, Ali, Bianca, Berend, Eliane, Laura, Susana and many others for doing my stay so greatful.

Continuando con este poupurri lingüístico, quiero agradecer al Prof. Hugo Segura la posibilidad de realizar una estancia de dos meses en su grupo en la Universidad de Concepción en Chile. Nunca olvidaré su paciencia, su carácter académico incansable para hacerme comprender hasta el más mínimo detalle y sus continuas ayudas para hacer mi estancia en Chile lo más confortable posible. Mis agradecimientos son extensivos a todas las personas que me rodearon durante mi estancia y que hicieron sentirme en mi casa a 12000km de distancia.

Vull fer una menció especial per tots els meus companys de grup i visitants amb qui he tingut el plaer de compartir un temps: al Carmelo, per dinamitzar sempre amb les seves bromes i bon humor al més pur estil veneçolà, a l'Aurelio, sempre receptiu a escoltar i ajudar en el que calgui, al Nuno, company de fatigues de la SAFT i el meu salvador en el món del Linux, al Carlos, sempre disposat a ajudar-me en tot, a l'Alexandra, el meu recolzament català dins del grup, a l'Andrés, que no només va contribuir al bon humor dintre del grup, sino que va ser la persona que més em va ajudar quan vaig estar a Xile, a la Rosa Marcos, amb qui vaig tenir la sort de viatjar a Portugal i Mèxic en dos congressos, a l'Ana Dias, amb les nostres llargues discussions al messenger sobre *el crossover* i a molts d'altres: el Daniel Duque, l'Ana Morales, el Krimo, etc. També vull agrair al meu predecessor, en Josep Pàmies, per la seva paciència extrema durant tots aquests anys a l'hora de discutir els detalls de la soft-SAFT. I com no, a totes les persones del ICMAB que m'han fet sentir totalment integrat dintre del centre.

No puc ni vull oblidar-me de tots els meus amics de Tarragona que sempre m'han donat suport: no puc mencionar-los a tots pero si vull destacar a 3 persones amb qui he compartit penes i alegries d'ençà l'inici de la carrera: Pol, Zoraida i Núria, moltes gràcies per acceptar-me com sóc. La llista de persones que han seguit (i patit) els meus bons i mals humors està repartida pel món, però agraeixo especialment al Vito (grazie), l'Amaia (eskerrik asko), la Mariana, la Nuria, la Maria Joao (obrigado) i l'Antje (danke) per tot el seu recolzament.

I finalment, vull donar les gràcies a la meva família, que m'estima amb bogeria i sé que sempre la tindré al meu costat. Gràcies a tots vosaltres per ajudar-me i valorar-me tant. Sense vosaltres no hauria arribat aquí.

Summary

The progress and the improvements made in the industrial field have pushed the researchers to look for refined tools to model these processes with a higher degree of accuracy. Thermophysical properties are needed and have to be known in a precise way, because an inaccurate prediction may affect the design of a unit property, with a result of a loss in yield and money.

Experimental work has always been the basis for having a database of properties of pure fluids and mixtures. However, nowadays the theoretical models have progressed as modern tools that can provide a huge amount of information of a fluid in a rapid, clean and cheap manner. In any case, there is still a long way to find a powerful tool able to calculate the thermodynamic behavior of any compound at any condition.

This work uses a robust equation of state called soft-SAFT. The original name comes from the Statistical Associating Fluid Theory (SAFT), which is an equation based on

statistical mechanics principles. It has a very strong molecular basis, proposing a "physical" model to describe the compound. Soft-SAFT is a variant of the original SAFT that uses a reference term based on a Lennard-Jones type interaction among the molecules.

Although the previous equation had already been successfully tested in many different works, it still failed in a very important region of the phase diagram: the critical region. In that region, the properties suffer strong fluctuations and change drastically due to the long-correlations established among the molecules. The original soft-SAFT version of the equation can not take into account these long-range fluctuations because it is based in a mean-field theory. However, this lack of the theory can be now overcome introducing a specific crossover treatment that considers these inherent fluctuations. The procedure is based in the renormalization group treatment of Wilson (1971) and it was developed by White (1992). It is written as a set of recursive relations where the correlations among the molecules are considered in several iterations.

The objective of this thesis work was to improve the molecular-based equation of state named soft-SAFT adding the specific crossover treatment before mentioned. The general aim was to develop a powerful predictive tool applicable under different conditions for thermodynamic calculations. Once the equation was improved, its application to experimental systems has covered a wide range of families of compounds like *n*-alkanes, *1*-alkanols and *n*-perfluoroalkanes, as well as mixtures among them and with carbon dioxide and chlorhydric acid. Several different properties including vapor-liquid equilibrium, critical lines and second order derivative properties have been calculated with this tool, proving its validity in most of the cases.

The extended equation, called crossover soft-SAFT, is first compared here to molecular simulations of the vapor-liquid equilibria of Lennard-Jones chains. Excellent agreement is obtained for different chain lengths. Then, the equation is employed to study three different families of hydrocarbons: the *n*-alkanes, the *1*-alkanols and the *n*-perfluoroalkanes. The molecular parameters are optimized using liquid density and vapor pressure data for the first eight members of each family. A correlation with molecular weight is then proposed, and the parameters are extrapolated to predict the phase behavior

of heavier members of the same family, with the same degree of accuracy as that one obtained for the lighter members of the series.

Another important test for the extended equation undertaken in this thesis work has been the evaluation of second order thermodynamic derivative properties. Heat capacities, isothermal and isentropic compressibility and the speed of sound have been calculated for these families obtaining very good agreement with experimental data in most of the cases. Results for these properties are very encouraging since calculations were performed in a pure predictive manner, with molecular parameters obtained to fitted vapor-liquid equilibrium data. The different singularities experimentally observed in the vicinity of the critical point have been reproduced and the universal critical exponents have also been found in agreement with the experimental measurements.

Finally the extension of the calculations to the critical region of binary and ternary mixtures is also presented and discussed here. Several groups of mixtures among n-alkanes, n-alkanes/1-alkanols, CO_2/n-alkanes, CO_2/1-alkanols and HCl/n-alkanes have been studied, paying special attention to the different critical transitions observed when increasing the chain length of the hydrocarbon. The crossover soft-SAFT equation is able to describe all these transitions from the parameters fitted from the pure compounds, although the adjustment of binary parameters is needed in some cases. Some preliminary results for the predictions of miscibility loops observed in ternary mixtures with supercritical CO_2 / n-alkane / 1-alkanol further support the strength of this tool for predictive purposes.

This work intends to be a step forward in the improvement of the molecular modeling tools for engineering applications. Although nature is always surprising and difficult to reproduce, the effort devoted to this task is encouraging enough to continue looking for new formulas that give us the possibility of getting closer to the real world.

Notation

Abbreviations

AAD(s)	Absolute Averaged Deviation(s)
AMQ(s)	Additive Molar Quantity(ies)
APACT	Associating Perturbed Anisotropic Chain Theory
ASOG	Analytical Solution of Groups
COR	Chain of Rotators
CL	Critical Line
EoS(s)	Equation(s) of State
LCEP	Lower Critical End Point
LJ	Lennard-Jones
LLV	Liquid-Liquid-Vapor
NRTL	Non-Random Two Liquid Model
PACT	Perturbed Anisotropic Chain Theory
PC	Perturbed Chain
PHCT	Perturbed Hard Chain Theory
PSCT	Perturbed Soft Chain Theory
PR	Peng-Robinson
PVT	Pressure-Volume-Temperature
RK	Redlich-Kwong
SAFT	Statistical Associating Fluid Theory
SPHCT	Simplified Perturbed Hard Chain Theory
SRK	Soave-Redlich-Kwong
SW	Square-Well

TPHCT	Truncated Perturbed Hard Chain Theory
TPT1	Thermodynamic Perturbation Theory (First order)
UCEP	Upper Critical End Point
UNIFAC	Universal Functional Activity Coefficient Model
UNIQUAC	Universal Quasi-Chemical Approach
vdW	van der Waals
VLE	Vapor-Liquid Equilibrium/a
VR	Variable Range

Latin symbols

A	Helmholtz free energy
a	Helmholtz free energy density
CN	carbon number
C_p	isobaric heat capacity
C_v	isochoric heat capacity
g	pair correlation function
k^{HB}	volume of association
k_B	Boltzmann constant
K	equilibrium constant for the formation of mono-disperse aggregates
L	cutoff length
M_w	molecular weight
m	chain length
N_A	Avogadro's number
P	pressure
R	ideal gas constant
T	temperature
w	range of the attractive potential in the crossover equation
X	fraction of nonbonded molecules
x	mole fraction
y	fraction of alkanol molecules present as single molecules
z	fraction of the alkane molecule in a ternary mixture
Z	compressibility factor

Greek symbols

α	interaction volume / thermal expansion coefficient
β	aggregation number for the alkanol molecules
Δ	association strength
ϵ	energy well-depth of the intermolecular potential / dispersive energy
ε^{HB}	association energy
η	size parameter of the generalized Lorentz-Berthelot combining rules
ϕ	average gradient of the wavelet function (crossover parameter)
κ	compressibility
μ	chemical potential / Joule-Thomson coefficient
ξ	energy parameter of the generalized Lorentz-Berthelot combining rules
ρ	density
σ	size parameter of the LJ intermolecular potential / diameter
ω	speed of sound
ν	index related to the average chain length for characterize a mixture

Superscripts

id	ideal
ref	reference
chain	chain
assoc	association
cross	crossover
av	average
agg	aggregate
HB	association

Subscripts

A	Avogadro
c	critical
r	reduced
w	weight

List of Tables

List of Figures

A. Introduction

1

Introduction

Nowadays, the industry has become the economic motor that makes the world to move. All the countries look at the industry to improve their economy, trying to refine their production. Moreover, the "globalization" is a current phenomena that has helped to transfer the knowledge through the countries but, at the same time, has increased their

competitive spirit to gain a place in the world market. It is clear that the optimization of resources is the key for the survival of any firm.

The needing for optimizing all the resources implies an accurate knowledge of the behavior of the prime materials employed. Some years ago, over sizing was the solution to any question when designing a new equipment. Now, although over sizing has to be taken into account for security reasons, the study of materials permits to refine the design, resulting in a save of money.

The behavior of a compound is always a world to discover. Thermodynamics is the key to enter in this world. It is absolutely necessary to know at which conditions a compound will be solid, liquid or gas, or will remain in a supercritical state; and also under which conditions these changes will occur. This need has resulted in the search for powerful tools able to give the answer to this question.

From the early times, experimental work has become the main solution. Researchers have been studying all kind of compounds in the laboratory. This work is difficult and sometimes risky because of the toxicity of some compounds. However, thanks to the amount of precise measurements done already, very important advancements have occurred.

At the same time, the possibility of modeling these measurements using a theoretical equation was considered. During the last century, hundreds of equations have been proposed, looking for the global one, able to reproduce the behavior of all the thermodynamic properties of all compounds. Sometimes, there have been some discussions between the experimental work and the modeling development. Experimental data always reports the reality, showing what happens at certain conditions, while modeling saves money and time and can be used to determine a set of experiments. This is, of course, assuming that both of them are done in a proper manner. As a conclusion, it can be said that both, the experimental work and the modeling part are equally necessary for a precise description of a fluid.

Great efforts have been done in the last decades in the modeling field. The development of theoretical equations based on statistical mechanics concepts opened a new window. It seemed that they would be able to describe the physics of the fluid and, as a consequence, they would become a powerful tool to study a fluid with a computer. In fact, their strong physical basis has acted in favor of these equations but it is also true that, due to some of the hypothesis employed when they are formulated, they are not describing the reality in a so perfect manner.

One of these limitations is centered in the critical region of the compounds. The particular behavior that fluids exhibit there makes them difficult to model. This is a real handicap, especially in the last years, because this region has become more important in many industrial processes. Near-critical and supercritical conditions are commonly found in several kind of extraction processes, for example.

Following this direction, the present work intends to go one step further in the searching of a global equation using a strong-molecular-based equation like soft-SAFT and coupling a specific treatment to improve their abilities in the critical region without prejudicing its predictions outside this region.

1.1. Scope and Objectives of the present work

As it has been mentioned, this work concerns the improvement of the molecular-based equation of state soft-SAFT (Blas and Vega, 1997), in order to look for a global equation able to predict all kind of thermodynamic properties in an accurate manner. Particularly, this thesis is focused in solving the problem of describing fluid properties near the critical region. The inherent fluctuations associated to this region make all the mean-field theories unable to capture the behavior of the compounds. It is necessary to couple a theory that considers these fluctuations to develop a physical realistic model for a fluid. The implementation of a crossover theory based on the renormalization group theory of Wilson

(1971, 1972) is done using a numerical approach proposed by White (1992) and applied into the soft-SAFT equation of state (Llovell et al., 2004). The extended equation has been tested for a wide range of temperatures and pressures of pure fluids, binary and ternary mixtures. Phase equilibria properties have been reproduced with accuracy, close to and far from the critical point. Single-phase calculations have also been performed and second derivative properties have been predicted as a further test. Some specific objectives are provided in the following list:

- Comparison with simulation results of Lennard-Jones chains of different molecular size.

- Calculation of phase equilibria properties for the *n*-alkanes, *1*-alkanols and *n*-perfluoroalkanes family.

- Obtention of reliable and transferable parameters to calculate heavier compounds.

- Performance of single-phase calculations and evaluation of critical exponents for pure fluids.

- Comparison with a classical equation of state with the same crossover approach.

- Analysis of critical behavior of binary mixtures of *n*-alkanes, *1*-alkanol/*n*-alkane, CO_2/*n*-alkane, CO_2/*1*-alkanol and HCl/*n*-alkane. Study of critical transitions from Type I to Type V and from Type II to Type III passing through Type IV.

- Description of the thermodynamic behavior of near-critical CO_2/*n*-alkane/*1*-alkanol ternary mixtures. Calculation of miscibility windows and two-phase holes.

- Calculation of heat capacities, compressibilities and speed of sound for pure fluids and binary mixtures. Study of the singularities observed in the vicinity of the critical point.

1.2. Organization of this thesis

Following this general introduction, the next chapter presents an overview about the main features of the critical region. The chapter illustrates why this region is important and, at the same time, why it is difficult to model.

Chapter 3 enters into the different tools for modeling presenting a historical review of the equations of state, from the first empirical relations established some centuries ago till the most modern theories based on statistical mechanics. The reader is invited to travel through the history and to see, briefly, the main achievements in this field with the pass of the years.

Chapter 4 is devoted to an explanation of the physical background of Wertheim's association fluid theory and the SAFT equation. The last section of this chapter describes the main versions of SAFT and the most recent improvements implemented in these versions. Chapter 5 is entirely dedicated to the soft-SAFT equation of state. The particularities of the equation are described in more detail, and a review of its capabilities is shown with a summary of the most relevant works published since its appearance in 1997. Then, the different known approaches to describe the critical region are presented and evaluated. Finally, the mathematical model for the chosen approach is shown in detail and its application is described, summarizing the main hypothesis done through the model. Results from the implementation of the theory are given in next chapter.

Chapter 6 is devoted to show the application of the equation to several kind of thermodynamic properties of pure compounds. In the first section, the equation is compared with molecular simulations to test their validity and robustness. In the second section, a systematic study for several families of compounds is done using the equation. Vapor-liquid equilibrium and derivative properties are evaluated close and far from the critical region, and the different singularities in the vicinity of the critical point are modeled for the *n*-alkanes, *1*-alkanols and *n*-perfluoroalkanes families. Other selected compounds like carbon dioxide or chlorhidric acid are also described. A comparison with a van der Waals type equation of state with the same implemented crossover treatment is also done.

Chapter 7 is entirely dedicated to the study of binary and ternary mixtures of compounds. Following the procedure employed when evaluating pure compounds, the study is repeated for different families of binary mixtures of industrial interest, with particular attention to the critical behavior. The different transitions from one type of critical behavior to another one are predicted with the equation for mixtures of *n*-alkanes, *n*-alkane/*1*-alkanol, CO_2/*n*-alkane, CO_2/*1*-alkanol and HCl/*n*-alkane. In the last section, some ternary systems are also calculated trying to reproduce several miscibility loops experimentally observed.

Finally, chapter 8 summarizes the concluding remarks of this thesis and outlines future work and recommendations to do in this research.

B. Methodology

A theory is the more impressive the greater is the simplicity of its premises, the more different are the kinds of things it relates and the more extended the range of its applicability.

(Albert Einsten) (1879-1955)
German-Swiss-U.S. scientist

2

Critical Region

This chapter is intended to give a general overview about the critical region. In fact, it is an introductory explanation about the interest of this region in the thermodynamic map of any compound. The first section is devoted to explain the basic concepts of the physics behind the critical area, with a brief description of the behavior of the main thermodynamic properties. The chapter continues showing the importance of these particularities in an industrial process, summarizing some of the most important ones where near-critical and supercritical conditions are encountered. Finally, last section classifies the different kinds of possible critical behavior when dealing with binary mixtures, following the classification of Scott and van Konynenburg (1970, 1980).

2.1. The "physics" in the critical region [1]

The transition between the vapor and liquid phases of a pure fluid is one of the most fundamental in nature. The reference point, from which all of the transition properties of such a fluid can be derived, is called the 'critical point'. This is the point, characterized by a fixed temperature, pressure and density, at which the distinction between the gas and the liquid phase simply disappears. It was the French baron Charles Cagniard de La Tour, in 1821, who first discovered this critical point, observing the disappearance of the gas/liquid interface of carbon dioxide in a sealed gun. He could not know at that time that this new 'state' of matter would lead later on to so many important discoveries for both fundamental science and technology, some of them thanks to exploiting the microgravity environment.
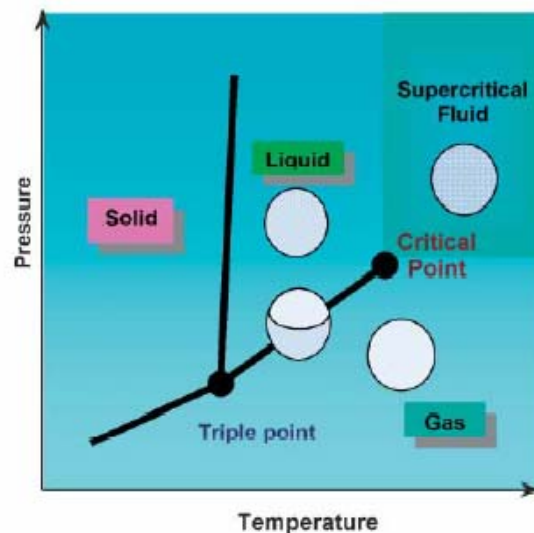
Figure 2.1 *Phase diagram of a pure substance in the temperature/pressure plane. The supercritical 'state' corresponds to a compressed gas that exhibits the density of a liquid (Image extracted from the book "A world without gravity", 2001).*

---

[1] *This section is inspired in section 2.3.5 of the book "A world without gravity" from the European Space Agency (2001)*

In a wide domain around the critical point, important parameters such as isothermal compressibility, the density of the gas and liquid phases, and the surface tension, obey universal power laws. These parameters can easily be varied by using small changes in temperature or pressure. The highly variable properties of near-critical fluids make them very appealing for studying many interesting phenomena that, because of the universality of the power laws, are valid for all fluids. Above the critical temperature and pressure, such fluids are called 'supercritical'. In this region, they exhibit a number of specific properties (high density, low viscosity, large diffusivity), which make them intermediate between liquids and gases. While their density approaches the liquid values, other properties like the diffusivity are closer to the gas characteristics. In addition, the isothermal compressibility becomes extremely large as one approaches the critical region, diverging at the critical point. Near the critical point of the solvent, its properties, like density and, with it, the ability for dissolving selectively non-volatile substances, change rapidly with only slight variations of temperature/pressure. For a better understanding of the phenomena, Figure 2.2 is presented and split in four parts. The figure shows the phase equilibrium of carbon dioxide. In the first image the separated phases (liquid and vapor) of carbon dioxide are easily observed. With an increase in temperature, the meniscus (the line between the two phases) begins to diminish (Fig. 2.2b). Increasing the temperature further causes the gas and liquid densities to become more similar. The meniscus is less easily observed but still evident (Fig. 2.2c). Once the critical temperature and pressure have been reached the two distinct phases of liquid and gas are no longer visible. The meniscus can not longer be seen. One homogenous phase called the "supercritical fluid" phase occurs which shows properties of both liquids and gases (Fig. 2.2d).

Fluids in their near-critical or supercritical state are affected by gravity. Consequently, gravity compresses the fluid under its own weight and the fluid stratifies. This prevents a very close approach to the critical point. Any measurements made on a cell of finite height will actually measure an averaged property of the fluid at differing densities, rather than the precise property approaching the critical point.
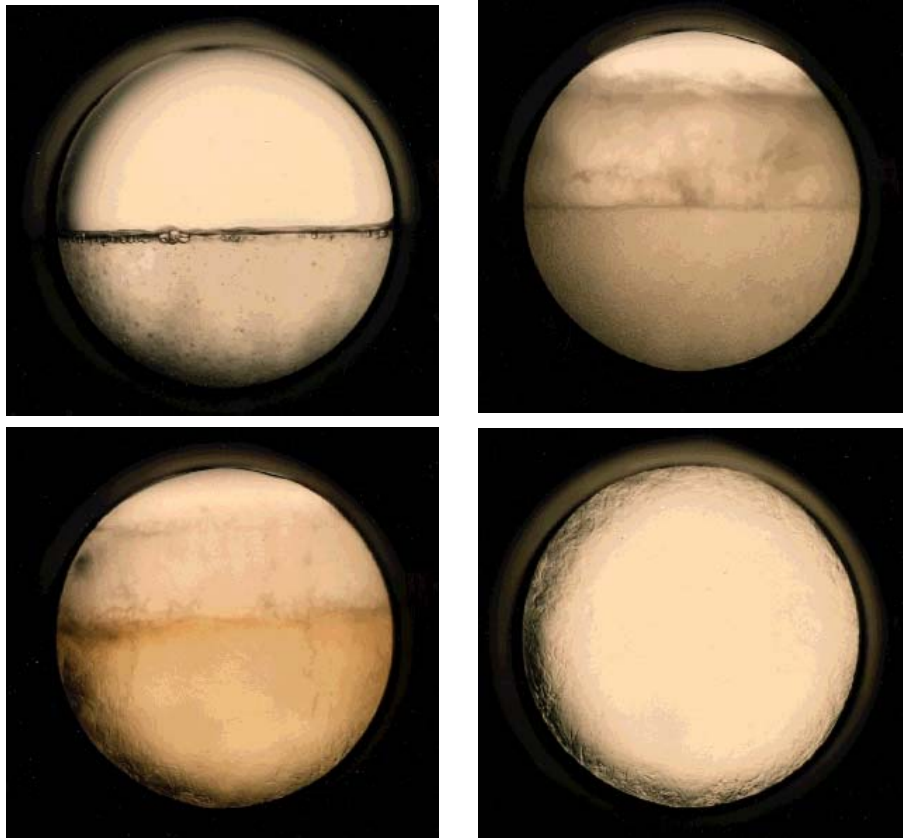
Figure 2.2. Images of the carbon dioxide transition from a vapor-liquid equilibrium till a supercritical state (Image extracted from the University of Leeds (England) webpage http://www.chem.leeds.ac.uk/People/CMR/criticalpics.html.)

An important aspect of the critical region is that most of the anomalies in the thermodynamic and transport properties can be set in the form of scaled, universal functions (power laws) with respect to the critical-point parameters. This has the very important consequence that any results obtained with one fluid can be immediately re-scaled to describe any member of a whole class of systems, called a 'universality class'. This class is defined by the space dimensionality d (=3 in normal space) and the

dimensionality n, of the fluctuating quantity, the 'order parameter'. This is the parameter (M) that describes the change in the symmetry of the system at the transition. In fluid systems, the order parameter M is usually the density but, in some cases, like in liquid-liquid equilibrium, it may be the concentration of each species.

Density is homogeneous above the critical point (the fluid is supercritical) and inhomogeneous below it, because the two phases (gas and liquid) coexist with different densities. All systems with the same 'd' and same 'n' show the same asymptotic, universal, scaled behavior. They all belong to the same 'universality class'. Fluids belong to the class defined by d=3, n=1 (density is a scalar). In addition to pure fluids (order parameter: density), another member of this same class are the partially miscible liquid mixtures (order parameter: concentration). This includes the polymer melts, polymer solutions, micro-emulsions, molten salts, and monotectic liquid metals. This universality and scaling is fundamental in nature. It stems from the universal behavior that the free energy must asymptotically obey at the critical point in order to fulfill the conditions of a second-order phase transition. (In such a transition, a specific property changes continuously, rather than discontinuously, on going through the transition). In this sense, universality and scaling are generic to all critical-point phenomena.

By permitting measurements extremely close to the critical point, space experiments have made possible the precise measurements of important, weak power law divergence, such as that of the specific heat at constant volume C_v. For example, from space experiments (Haupt and Straub, 1999), the temperature divergence of the specific heat has been determined with a very high precision, giving the universal critical α exponent. Its precise calculation was a key test of the "Renormalization Group Theory" (Wilson, 1971, 1972), which was developed to try to improve on the classical macroscopic description of the fluid behavior close to the critical point.

As the critical point is approached, the fluids become extremely compressible, much more than ideal gases. Excited by the thermal fluctuations and enhanced by the large compressibility of the fluid, the density fluctuates more and more strongly as the critical

point is approached. The vicinity of the critical point is thus characterized by the presence of very-large-scale density fluctuations (or more generally, order parameter fluctuations), which develop throughout the fluid. The density fluctuations give rise to unusually strong light scattering, called 'critical opalescence'. These order parameter fluctuations are correlated with the correlations having a spatial extent that can be characterized by a correlation length *L.*
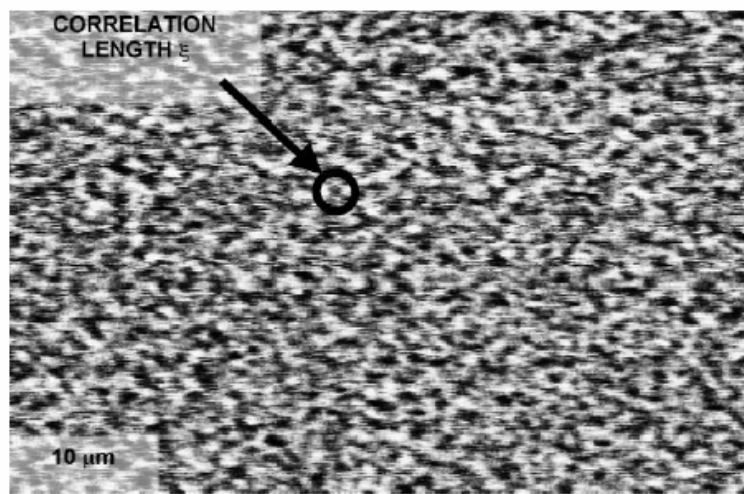
Figure 2.3 *Huge density fluctuations observed under Og in sulphur hexafluoride (SF$_6$) (Mir, 1996). Fluctuations in density diverge at the critical point and their typical size, the correlation length L, determines the length scale of all critical-point phenomena. (Image extracted from the book "A world without gravity", 2001).*

The specific nature of the critical region therefore involves the appearance of this new characteristic distance, which can become much larger than the inter-particle distance. The correlation length then becomes the natural length scale of critical-point phenomena. At that point where the correlation length becomes much larger than the range of the intermolecular forces, the specifics of the microscopic interactions cease to be relevant in the description of the critical behavior.

2.2. Summary of important industrial applications

The previous section has shown the basic features of the physics behind the critical region. It has been remarked that all the fluids approach the critical point following universal laws. However, it does not mean that they achieve the critical point at the same thermodynamic conditions. The critical point of each compound is reached at a different temperature and pressure for each compound and, sometimes, it implies a high energy cost.

Table 2.1 shows a list of the critical properties of some common fluids. Among them, carbon dioxide and water have been the most studied for supercritical applications, although both present strong differences. While supercritical water has a high critical temperature and pressure (T_c=647.3K, P_c=22.1MPa) that requires a considerable energetic effort, the CO_2 is considered the "ideal" supercritical fluid. Their critical conditions are easily achievable (T_c=304.1K, P_c=7.38MPa), and it is a non-toxic, cheap and easy-to-get gas. It is the most widely used compound in the supercritical processes.

Table 2.1. *Critical properties of various industrial solvents (Reid et al, 1987)*

Solvent	M_w (g/mol)	Temp. (K)	Press. (MPa)	Dens. (g/L)
Carbon dioxide	44.01	304.1	7.38	469
Water	18.02	647.3	22.12	348
Methane	16.04	190.4	4.60	162
Ethane	30.07	305.3	4.87	203
Propane	44.09	369.8	4.25	217
Ethylene	28.05	282.4	5.04	215
Propylene	42.08	364.9	4.60	232
Methanol	32.04	512.6	8.09	272
Ethanol	46.07	513.9	6.14	276
Acetone	58.08	508.1	4.70	278

Due to its characteristics, supercritical fluids become the ideal solvents because its enormous diffusivity lets them to go into the porous media. Taking advantage of these properties, new industrial technologies use a wide variety of fluid separation processes where critical conditions are encountered. There are different fields where the supercritical conditions are employed (for a complete review, see Bright and McNally, 1992; Perrut, 2000; Cooper, 2002):

- ❖ Natural products extraction processes are one of the most important industrial applications for the supercritical technology: the extraction of caffeine from green coffee beans with supercritical carbon dioxide (CO_2), the decaffeination of tea and the extraction of spices, aromas, hops, oils and fats from natural products are some good examples.

- ❖ Oxidation in a supercritical water reactor is done for transforming complex and dangerous organic compound wastes into their simple constituent components. These reactors operate at temperatures around 700K and pressures about 500 bar in a process that is harmless to the environment. The yields of these oxidation processes are extremely high.

- ❖ Fractionation in oil processes: The Residum Oil Supercritical Extraction (ROSE process), the separation and isomer purification, etc.

- ❖ Impregnation processes like wood treatment, textile dyeing, etc.

- ❖ Materials: precipitation and crystallization of medicines, pigments, catalyzers, etc.

- ❖ Microelectronics (dry lithography): photoresist stripping, supercritical spinning, metal deposition, silylation,etc.

- ❖ Production of finely divided materials based on the use of compressed CO_2 as cosolvent in CO_2-expanded organic solutions (DELOS process) (Ventosa et al., 2001).

Consequently, their current use without such knowledge inevitably raises fundamental questions concerning fluid dynamics, heat transfer, interfacial phenomena and chemical processes. It is evident that an accurate modeling for pure fluids and multicomponent mixtures involving critical conditions is needed. However, this task is difficult due to the particular nature of the critical region and the various phenomena observed, not only for pure fluids, but also when describing the binary mixtures. A systematic study of the fundamental behavior is necessary for the understanding of the possible phenomena. The classification of Scott and van Konynenburg (1970, 1980) offers a way to classify the binary mixtures describing possible types of critical phase behavior. As a main part of this thesis work is involved with the evolution from one type of critical behavior to another one, the last section of this chapter proceeds to briefly describe each one of the different possible behaviors according to this classification.

2.3. The classification of Scott and Van Konynenburg

The graphical representation of two thermodynamic properties in a plane of two or more phases and their mutual coexistence is called a phase diagram. The ability to determine phase diagrams for fluid mixtures is important, from both a theoretical as well as a practical point of view. For binary fluid mixtures, the classification of van Konynenburg and Scott (1970, 1980), based on the shape and location of the mixture critical curves, identifies six possible classes of fluids (see Figure 2.4):

❖ Type I phase behavior is characterized by having a continuous vapor-liquid critical curve without any liquid-liquid miscibility. This behavior occurs with two substances that are chemically similar and/or have critical properties that are comparable (e.g. ethane + 2-methylpropane).

❖ Type II phase behavior has, in addition to the continuous vapor-liquid critical curve that connects both pure critical points, a three-phase line liquid-liquid-vapor, ending at an upper critical endpoint (UCEP). From this point, a second critical curve of liquid-liquid nature goes to infinite pressures where the fluid mixture approaches closest packing. An example of a type II system is carbon dioxide + *n*-octane.

❖ Type III phase behavior has two different critical curves: one starts at the critical point of the heavier compound and goes to infinite pressures, and the other curve starts at the critical point of the component with the lower critical temperature and meets a three-phase line liquid-liquid-vapor (LLV) at an UCEP. This behavior is found in many mixtures with carbon dioxide and heavy hydrocarbons, like, for instance, CO_2 + *n*-hexadecane.

❖ Type IV phase behavior is a transition state between type II and type III behavior. In type IV, three different critical curves exist: One of them is a liquid-liquid critical curve that starts at the UCEP of a three-phase line liquid-liquid-vapor and goes to infinite pressures. The second one starts at the critical point of the component with the lower critical temperature and ends in another UCEP of a second three-phase line liquid-liquid-vapor. Finally, the third critical line starts at the critical point of the component with the higher temperature and ends at a Lower Critical End Point (LCEP) of the second three-phase line liquid-liquid-vapor. This last critical line changes its nature near the LCEP, passing from a vapor-liquid equilibrium to a liquid-liquid equilibrium. This is the particular behavior observed for the mixture CO_2 + *n*-tridecane.

❖ Type V phase behavior is characterized by two distinct critical curves: one going from the heavier compound till a LCEP and a second one going

from an UCEP till the lighter pure compound. Between the LCEP and the UCEP, a three-phase LLV line is found. The critical line diagram is identical to type IV, excepting for the liquid-liquid critical line. This is the typical behavior observed in mixtures between two asymmetric compounds of the same family, like the system methane + *n*-hexane.

❖ Type VI phase behavior have a continuous vapor-liquid critical curve between the critical points of the pure compounds. Moreover, the main characteristic is a closed liquid-liquid critical curve that starts at a LCEP of a three-phase line liquid-liquid-vapor and ends at an UCEP on the same three-phase line. Type VI phase behavior is found in mixtures with strong intermolecular bonding, like, for instance, the system water + *2*-butoxyethanol.

All the types are connected among them and a slight modification in a mixture may involve passing from one type of critical behavior to another one. Some series of mixtures may pass through several phase behaviors as a function of the chain length of the hydrocarbon. For example, mixtures of *n*-alkanes with carbon dioxide begin with the simple type I phase behavior (CO_2 + ethane), go through Type II when the *n*-alkane increases the chain length (i.e. both compounds become more dissimilar and liquid-liquid immiscibility appears), like the mixture CO_2 + *n*-heptane, pass through Type IV (CO_2 + *n*-tridecane) to arrive to a Type III phase behavior (CO_2 + *n*-tetradecane). Some of these evolutions are studied with soft-SAFT and presented in chapter 7.
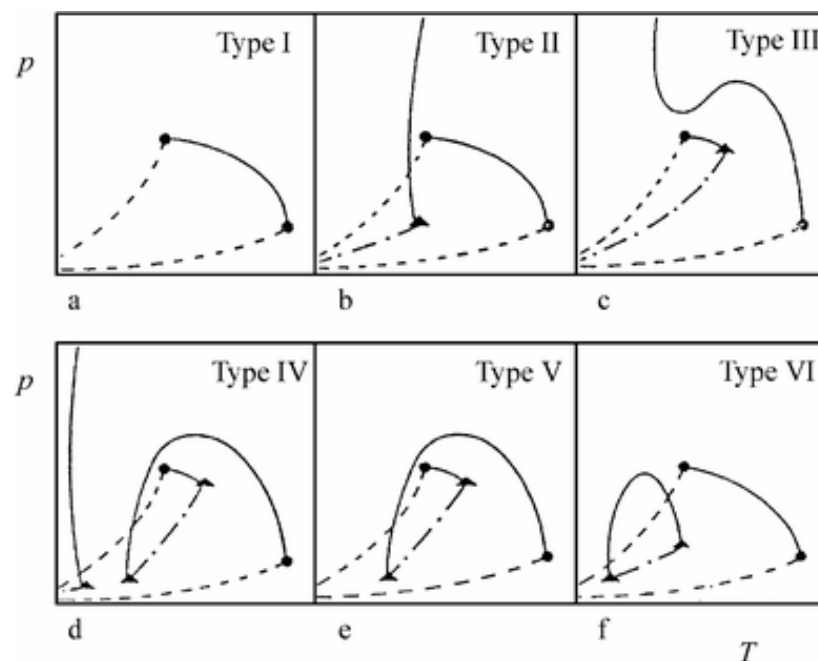
Figure 2.4 *Schematic Pressure-Temperature projections of types of binary fluid phase behavior according to the classification of Scott and van Konynenburg (1970, 1980).*

In the same manner, an accurate modeling will be required to avoid predicting a wrong behavior in a particular mixture. The inclusion of binary parameters in the equation of state will determine the type of critical behavior in a mixture. In fact, the various types of phase behavior can be located on a map depending on these parameters. This map is called the "global phase diagram" (Furman et al., 1977) and it is very useful to facilitate the discussion of binary fluid phase behavior from a theoretical point of view.

In the following chapters (3, 4 and 5), a description of the different tools for modeling the thermodynamic behavior of a substance and, in particular, its critical region is presented.

3
Equations

In this chapter, a review in the development of equations of state for the calculation of thermodynamic properties in pure fluids and mixtures is presented. From the first modeling before 1800, the reader is invited to a follow a brief summary of some different approaches through the history. The chapter explains some basic features about the main cubic equations of state, the empirical methods and the molecular equations, finishing in the Wertheim's theory of association, which provided the mathematical basis and structure to the Statistical Associating Fluid Theory (SAFT).

3.1. Chronology of classical equations of state[1]

An equation of state (EoS) is a constitutive equation describing the state of matter under a given set of physical conditions. It provides a mathematical relationship between two or more state functions associated with the matter, such as its temperature *(T)*, pressure *(P)*, volume *(V)*, or internal energy *(U)*. The term "state" is also used to designate the physical phase of the system, i.e., solid, liquid, or gas. In some cases, it is necessary to give the phase of a substance, in addition to values of such properties as *P, T, V*, and number of moles *(n)*, in order to completely and unequivocally designate its state. Equations of state are useful in describing the properties of fluids, mixtures of fluids, solids, and even the interior of stars.

Hundreds of equations have been developed through history and this research field keeps active because, at present, there is no single equation of state that accurately predicts the properties of ALL substances under ALL conditions.

Based on experimental measurements, Robert Boyle (1662) developed an equation in which there is a reciprocal relationship between the pressure and the volume of gases, when the temperature and the amount of gas are kept constant. The work of Jacques Charles in 1787 and of Joseph-Louis Gay-Lussac in 1808 demonstrated that the volume of a given amount of gas is directly proportional to the temperature, when its pressure remains constant.

Amedeo Avogadro proposed in 1811 that equal volumes of all gases, at the same pressure and temperature, contain the same number of molecules. In other words, an equal number of moles of all gases occupy the same volume at constant temperature and pressure.

---

[1] *This section is inspired in the work of Valderrama (2003) and the information that can be found in the video The World of Chemistry, produced by the University of Maryland and the Educational Film Center (1990).*

This proposal, combined with the relationships discovered by Boyle, Charles, and Gay-Lussac led to an equation of state for gases:

$$P = \frac{RT}{V_m} \tag{3.1}$$

where P is the pressure, V_m is the molar volume, T is the absolute temperature and R is the universal gas constant. The equation is written for one mol of molecules of a compound.

This equation is known as the equation of state for ideal gases or the ideal gas law. Although the behavior of real gases closely follows the ideal gas equation under circumstances of low pressure and reasonably high temperature, it becomes increasingly inaccurate at higher pressures and lower temperatures, and fails to predict condensation from a gas to a liquid. Therefore, a number of much more accurate equations of state have been developed for gases and liquids as well as others for predicting the volume of solids, including the transition of solids from one crystalline state to another. Although it is impossible to mention all the equations developed up-to-date, in this section it is intended to briefly review the most important advancements through the last century.

The most widely used equation of state for real gases is that of Johannes van der Waals (1873). The van der Waals equation (vdW) was one of the first to perform markedly better than the ideal gas law and the first one in successfully describing both the liquid and the vapor phase simultaneously. Instead of using the measured value of pressure in the equation of state for ideal gases, he substituted a term which takes into consideration the reduced pressure on the walls of a container due to the attractive forces. This magnitude of the pressure term increases with the density of molecules: when they are closer together, the molecules are more constrained by their mutual attraction. The van der Waals equation also corrects the volume term in the ideal gas equation by subtracting the space that is taken up by the molecules themselves. The equation looks like this:

$$P = \frac{RT}{(V_m - b)} - \frac{a}{V_m{}^2} \tag{3.2}$$

In this landmark equation, a is called the attraction parameter and b the repulsion parameter or the effective molecular volume. a and b were first calculated using PVT data but were later related to critical properties by applying the condition of continuity of the critical isotherm (inflexion point) at the critical point:

$$a = \frac{27}{64} \frac{(RT_c)^2}{P_c} \tag{3.3}$$

$$b = \frac{1}{8} \frac{RT_c}{P_c} \tag{3.4}$$

The study of real gases in relationship to the van der Waals equation yields valuable information about intermolecular forces and the volume of molecules. The concepts developed by van der Waals on the separation of repulsive forces caused by molecular size from cohesive forces caused by molecular attraction still remain as the basis of several theories concerning the prediction of fluid properties and of computer simulations based on statistical mechanics. Unfortunately, although the equation is definitely superior to the ideal gas law and does predict the formation of a liquid phase, the agreement with experimental data is limited for conditions where the liquid forms. In spite of this limitation, the vdW equation still remains as the basis for more refined cubic equations of state for engineering purposes

A very old and appreciated effort is the virial expansion suggested by Heike Kammerlingh-Onnes (1901). Following the idea of modifying the ideal gas equation of state adding new terms to account the interaction among the molecules, the virial expansion, also called the virial equation of state, is the most interesting and versatile of the equations of state for gases. The virial expansion is a power series in powers of the variable, V_m, and has the form,

$$P = \frac{RT}{V_m}\left(1 + \frac{B}{V_m} + \frac{C}{V_m^2} + \frac{D}{V_m^3}\dots\right) \qquad (3.5)$$

It adds correction terms to the ideal gas equation by multiplying the right side of the equation (RT) by the mathematical progression $(1 + B/V + C/V^2 + D/V^3 + E/V^4 +...)$ where the constants A, B, C, etc. are temperature dependent. The coefficient, B(T), is a function of temperature and is called the "second virial coefficient". C(T) is called the "third virial coefficient", and so on. The expansion is, in principle, an infinite series, and as such should be valid for all isotropic substances. In practice, however, terms above the third virial coefficient are rarely used in chemical thermodynamics. Although it is only applicable to the gas phase, the virial equation is important because it can be derived directly from statistical mechanics. If appropriate assumptions are made about the mathematical form of the intermolecular forces, theoretical expressions can be developed for each of the coefficients. In this case *B* corresponds to interactions between pairs of molecules, *C* to triplets, and so on. Accuracy can be increased by considering higher order terms.

In 1940, Benedict, Webb and Rubin developed an empirical equation with several parameters to correlate and predict the thermodynamic properties of light hydrocarbons and their mixtures. Later on, Starling (1973) modified the original equation and published a book with the parameters for a total of fifteen substances.

$$P = \rho RT + \left(B_0 RT - A_0 - \frac{C_0}{T^2} + \frac{D_0}{T^3} - \frac{E_0}{T^4}\right)\rho^2 + \left(bRT - a - \frac{d}{T}\right)\rho^3$$
$$+ \alpha\left(a + \frac{d}{T}\right)\rho^6 + \frac{c\rho^3}{T^2}\left(1 + \gamma\rho^2\right)\exp\left(-\gamma\rho^2\right) \qquad (3.6)$$

where ρ is the density of the compound and A_0, B_0, C_0, D_0, E_0, *a*, *b*, *c*, *d*, α and γ are coefficients.

In a similar way, other nonanalytic empirical equations were developed (Lee and Kesler, 1975). This type of equations offer improved thermodynamic property correlations

but does not offer any better results for the correlation of mixture phase behavior due to the large number of coefficients and the lack of theoretical guidelines. Another drawback of this type of equations is the large amount of volume roots that can be obtained from them.

With the pass of the years, several cubic equations were developed from modifications of the basis of the van der Waals equation looking for improvement in vapor-liquid equilibria calculations. The differences were established by modifying the way of calculating the parameters *a* and *b*.

The Redlich-Kwong equation of state (1949) was a considerable improvement over other equations of the time. It has the following form:

$$P = \frac{RT}{(V_m - b)} - \frac{a}{V_m(V_m + b)} \tag{3.7}$$

$$a = 0.42748 \frac{(RT_c)^2}{P_c} T_r^{-1/2} \tag{3.8}$$

$$b = 0.08664 \frac{RT_c}{P_c} \tag{3.9}$$

where T_r is the reduced temperature. By the time of this proposal, there were about 200 equations of state (Vukalovich and Novikov, 1948). Redlich and Kwong looked for correct representations at low and high density for gases, adding temperature dependence in the attractive parameter. Their equation, while superior to the van der Waals equation of state, performs poorly with respect to the liquid phase and thus cannot be used for accurately calculating vapor-liquid equilibria. However, it can be used in conjunction with separate liquid-phase correlations for this purpose. The Redlich-Kwong equation is adequate for calculation of gas phase properties when the ratio of the pressure to the critical pressure (reduced pressure) is less than about one-half of the ratio of the temperature to the critical temperature (reduced temperature).

During fifteen years, the Redlich-Kwong proposal became extremely popular and several RK-type equations were proposed. Wilson (1964) made one of the major contributions when he introduced Pitzer's acentric factor ω into the attractive term to consider the variations in behavior of different fluids at the same reduced temperature and pressure, depending on their shape.

In 1972, Soave, following Wilson's idea, replaced the $a\mathrm{T}^{1/2}$ term of the Redlich-Kwong equation with a function $\alpha(T,\omega)$ involving the temperature and the acentric factor:

$$a = 0.42748 \frac{(RT_c)^2}{P_c} \left(1 + m\left(1 - \sqrt{T_r}\,\right)\right)^2 \tag{3.10}$$

The *m* parameter is a specific function of the acentric factor ω:

$$m = 0.47979 + 1.576\omega + 0.1925\omega^2 + 0.025\omega^3 \tag{3.11}$$

The α function was devised to fit the vapor pressure data of hydrocarbons and the equation does fairly well for these materials. The Soave-Redlich-Kwong (SRK) equation has become one of the most common equations and it is still widely employed for phase equilibria calculations.

The Peng-Robinson equation was developed in 1976 in order to satisfy the following goals:

1. The parameters should be expressed in terms of the critical properties and the acentric factor.

2. The model should provide reasonable accuracy near the critical point, particularly for calculations of the compressibility factor and liquid density.

3. The mixing rules should not employ more than a single binary interaction parameter, which should be independent of temperature, pressure and composition.

4. The equation should be applicable to all calculations of all fluid properties in natural gas processes.

The Peng-Robinson equation looks like this:

$$P = \frac{RT}{(V_m - b)} - \frac{a}{\left(V_m + \left(1 - \sqrt{2}\right)b\right)\left(V_m + \left(1 + \sqrt{2}\right)b\right)} \tag{3.11}$$

$$a = 0.45724 \frac{(RT_c)^2}{P_c}\left(1 + m\left(1 - \sqrt{T_r}\right)\right)^2 \tag{3.12}$$

$$b = 0.07780 \frac{RT_c}{P_c} \tag{3.13}$$

$$m = 0.37464 + 1.54226\omega + 0.26992\omega^2 \tag{3.14}$$

The Peng-Robinson equation exhibits performance similar to the SRK equation, although it is generally superior in predicting the liquid densities of many materials, especially nonpolar ones.

If one rewrites equations 3.2-3.4 in a more general form, it is observed how the Redlich-Kwong (RK), Soave-Redlich-Kwong (SRK) and Peng-Robinson (PR) equations are obtained from the original van der Waals equation of state:

$$P = \frac{RT}{(V_m - b)} - \frac{a}{\left(V_m + c_1 b\right)\left(V_m + c_2 b\right)} \tag{3.15}$$

$$a = \Omega_a \frac{(RT_c)^2}{P_c}\alpha(T) \tag{3.16}$$

$$b = \Omega_b \frac{RT_c}{P_c} \tag{3.17}$$

Table 3.1 summarizes the parameters of these cubic equations of state.

Table 3.1. *Summary of the parameters value for the most common cubic type equations of state*

Model	Ω_a	Ω_b	c_1	c_2	$\alpha(T_r)$
vdW	27/64	1/8	0	0	1
RK	0.42748	0.08664	0	1	$[T_r]^{-1/2}$
SRK	0.42748	0.08664	0	1	$[1 + m\,(1-\sqrt{T_r}\,)]^2$
PR	0.45724	0.07780	$1-\sqrt{2}$	$1+\sqrt{2}$	$[1 + m\,(1-\sqrt{T_r}\,)]^2$

Several other equations of state could be mentioned in this section (there is a total of 400 cubic EoSs proposed to date in the literature) but SRK and PR have remained as the most used for engineering calculations. The newest contributions have tried to modify the expression of $\alpha(T_R)$ (Stryjek and Vera, 1986), the volume dependence of the attractive pressure term or to use a third-substance dependence parameter (Patel and Teja, 1982). Some other equations were developed to treat fluids at a very certain specific conditions (high pressure in liquid phases, Bose gases, etc.), but they are not the aim of this summary.

More information about the different equations of state can be found in the reviews of Valderrama (2003) and Prausnitz and Tavares (2004).

3.2. Molecular-based equations of state

The phenomenological basis of a traditional EoS of the van der Waals form is based on molecules that are quasi-spherical. This is not appropriate for fluids with chain-like molecules, especially polymers, not only because molecules are not spherically

symmetric in shape, but also because such molecules exercise rotations and vibrations that depend on density and should be taken into account.

The advancement in the field of statistical mechanics permitted to develop a series of new equations based on a deeper study of the molecular behavior of the fluid. These equations are able to take into account the different shapes of the molecules and they relate the microscopic functions that describe the molecular nature of the compound to the obtention of macroscopical properties through the calculation of the Helmholtz free energy. In some way, all the van der Waals equations are also molecular equations, taking into account the volume of the molecules and the attraction among them in the *a* and *b* parameters, although they are categorized into another class because their "molecular" considerations are oversimplified. It is also interesting to notice that even the virial equation of state can be derived from statistical mechanics.

The first published molecular-based equations of state started with a hard body equation plus some terms to account the effect of molecular attraction. Different hard-body terms have been proposed through the years. The most significant are the Wertheim-Thiele equation (Wertheim, 1963; Thiele, 1963), the Carnahan-Starling equation for hard spheres (1969, 1970), and the equation of Gibbons (1969), the one from Boublik (1970) and the one from Nezbeda and Leland (1979) for non-spherical rigid molecules. The most well-known equation for chains are the Perturbed Hard Chain Theory (Beret and Prausnitz, 1975) (and its versions) and the Flory-Huggins Theory for polymers (1953).

The Perturbed Hard Chain Theory (PHCT) is a phenomenological EoS for chain-like molecules proposed by Beret and Prausnitz (1975) based on Prigogine's theory for liquid polymers (Prigogine, 1957). The PHCT is similar to the van der Waals model but it allows for contributions from so-called external degrees of freedom (density-dependent rotational and vibrational motions) in addition to translations to the EoS.

The PHCT is a successful equation but mathematically complex. Some versions have simplified the original equation. The most important are the Truncated Perturbed Hard

Chain Theory (TPCHT) of Gmehling et al. (1979) and the Simplified Perturbed Hard Chain Theory (SPCHT) of Kim et al. (1986). In the TPCHT, the perturbation expansion in the attractive term is truncated after the second term. In the SPCHT, the attractive term is replaced by a theoretical but simple expression based on the local composition model of Lee et al. (1985).

The PHCT has also been modified in terms of the selected intermolecular potential. The substitution of the square-well potential by a soft-core Lennard-Jones potential energy function by Morris et al. (1987) has created the Perturbed Soft Chain Theory (PSCT), with accurate results for non-polar mixtures.

Vimalchand and Donohue (1986) developed the Perturbed Anisotropic Chain Theory (PACT) combining the PHCT with an additional perturbation expansion where multipolar interactions were explicitly considered.

Another EoS similar to PHCT is the chain-of rotators (COR) (Chien et al., 1983). In this equation of state, a chain of molecules is not composed of spherical segments but is seen as a dumbbell-shaped molecule. Chien et al. (1983) obtained an accurate correlation for pure fluid properties using this theory. Unfortunately, calculations for mixtures required large values of binary interaction parameters.

The Deiters equation (1981) is also similar to the PHCT and the COR. This equation of state contains corrections for non-spherical molecular shape, softness of the repulsive potential and three-body effects.

When paying more attention to the liquid phase, several attempts have been proposed extending the original Flory-Huggins lattice theory for polymer solutions (1953). Among them, the Sanchez-Lacombe equation of state (1976, 1978) has become quite popular because of its relative simplicity. The essential contribution of this equation is the inclusion of holes (empty sites) into the lattice.

Although this kind of equations involve more complexity, they become a promising route to the calculation of phase equilibria in different kind of systems because their molecular nature contributes to extrapolate the parameters within the same family. Moreover, the expressions are usually written as a sum of contributions where the different effects can be separated and quantified. This is the key for a continuous improvement, because there exists the possibility of adding a new term in order to consider a particular interaction (multipolar effects, associating sites, etc.)

In some cases, the existence of strong and highly directional attractive forces leads to the formation of long-lived molecular clusters. Electrolytes, hydrogen-bonded fluids, polymers, liquid crystals or plasmas fall into this category. The new intermolecular forces present in these compounds (Coulombic forces, strong polar forces, complexing forces, etc.) produce large deviations from ideality (for instance, the closed loop phase behavior [Jackson, 1991]) and should be specifically taken into account in any modeling for an accurate description. This group of compounds constitutes the so-called associating fluids. However it is important to remark that the distinction between an associating and a non-associating fluid is completely arbitrary, because there is a continuous transition between the two types. For instance, the hydrogen sulfide molecule has a bond strength of approximately 6 KJ/mol that could be considered in the border of both types, either a compound with a stronger van der Waals interaction, or a compound with a small association effect (around 10 kJ/mol and above).

Several approaches have been developed to model associating fluids, being categorized among chemical, quasi-chemical and physical theories. The oldest known method is the chemical theory proposed by Dolezalek (1908), which considered the different anisotropic physical interactions to be treated as a chemical reaction. The association phenomena would be a chemical reaction where two substances A and B are in equilibrium with a dimer AB. It can be assumed that the different species form an ideal mixture or take into account the non-ideality trying to evaluate the different activity coefficients through an empirical equation. Although this theory has been quite successful

in describing solution properties for some compounds (like alcohols), it presents serious limitations because of the arbitrary way in which the number of species and chemical reactions are determined. Moreover, the evaluation of the different equilibrium constants as adjustable parameters and the estimation of the activity coefficients makes the theory quite inefficient and with little predictive power.

Heidemann and Prausnitz (1976) combined a classical EoS for non-associating systems with a chemical theory, supposing consecutive "chainlike" association reactions forming dimers, trimers, etc., where all the equilibrium constants had the same value. Although this treatment is not straightforwardly extended to mixtures and the arbitrary separations of the physical and the chemical part can be thermodynamically inconsistent, it has become a basis for more refined approaches like the associating perturbed anisotropic chain theory (APACT) of Ikonomou and Donohue (1986), which comes from the Perturbed Anisotropic Chain Theory (PACT). Although the APACT equation gives good fits for hydrogen bonding systems, it is lenghtly and cumbersome. Another essay of Ikonomou and Donohue was the COMPACT equation (1987), a derivation from the SPHCT for hydrogen systems. Although it was simpler than the APACT, the equation was not able to model properly high complex phase behavior. The particular form of the combining rules for the associated species and the number and type of reactions considered continued posing a problem for an efficient and accurate application.

The quasi-chemical approach was originally formulated by Guggenheim (1944, 1948) and it supposed a nonrandom mixing at the molecular level to explain the nonidealities observed in fluids. The concept of several associating species disappears and the association effect is treated as a stronger van der Waals type interaction assigning large energy parameters to the associating interactions. Many important methods were developed from this theory, using several excess Gibbs energy models, especially for the estimation of liquid mixtures, like the Wilson's equation (Wilson, 1964), the nonrandom two-liquid model (NRTL) of Renon and Prausnitz (1968) or the group contribution methods.

Group contribution methods, also known as Group Additivity relationships, are useful for correlating a material property with the chemical composition and state of matter of a substance. Useful methods have arisen for correlating properties of gases and liquids with small molecules, crystals, and polymeric materials. The underlying idea of any Group Contribution method is as follows: whereas there are thousands of chemical compounds of interest to science and technology, the number of structural and functional groups which constitute all these compounds is much smaller. The basic assumption is made that the physical property of a material (gas, liquid or solid) is a sum of contributions from each of the material's component parts. The fundamental assumption is additivity of these contributions.

The development and use of Group Contribution methods proceeds in two stages:

1. The properties of known materials are correlated with their chemical structure, in order to identify the basic groups and their Additive Molar Quantities (AMQ's).

2. The properties of unknown materials are estimated through direct addition of AMQ's from constituent chemical groups, or through the use of additive quantities to estimate parameters in more accurate correlations.

The most important models in use are the universal quasi-chemical approach (UNIQUAC) of Abrams and Prausnitz (1975); the universal functional activity coefficient model (UNIFAC) of Fredenslund et al. (1977) and the analytical solution of groups (ASOG) of Kojima and Tochigi (1979).

Among the above mentioned models, UNIFAC has been the most commonly used model because of its simplicity: its parameters are independent of temperature and it does not require any experimental mixture data. The equation was modified by several authors to improve their capabilities. Oishi and Prausnitz (1978) extended the equation to polymer solutions. Some efforts were made to the calculation of solutions with electrolytes and charged particles, as well as for supercritical components. However, such extensions were

quite limited because the data is confined to aqueous systems and lattice models are not able to reproduce highly mobile gaseous solute.

Another related method was developed from Panayiotou and Sanchez (1991), separating the partition function into a physical part, treated using a lattice-fluid equation, and a chemical part, using the quasi-chemical approach. All this second group of methodologies presents again serious drawbacks concerning the evaluation of the equilibrium constant. Moreover, lattice theories assume that the fluid structure can be approximated by a solid-like structure and accurate results will only be obtained for very well structured fluids.

Later on, the physical theories for describing the behavior of associating fluids provided a framework in which the interaction effects could be separated and quantified using recipes for establishing the structure and thermodynamics, given its intermolecular potential function.

One of the first statistical mechanical theories was the one developed by Andersen (1973, 1974), who introduced the geometry of the interaction in an early stage of the theory. He considered an only short-ranged, highly directional attraction site embedded in a repulsive core. Andersen wrote a cluster expansion in terms of two densities: the overall density and a density weighted by the strength of the hydrogen bond. The idea was that the repulsive core would only allow dimers and no higher *s*-mers and, due to this fact, many diagrams in the cluster expansion were negligible. Although no calculations of thermodynamic properties were achieved with this method, Andersen's work inspired several theories for associating fluids that used similar expansions with respect to fugacity, for convergence reasons. Chandler and Pratt (1976), for instance, developed a theory to describe the intramolecular structure of molecules based on intermolecular and external forces modeling the atom-atom bond with a spherically symmetric attraction. Hoye and Olaussen (1980) presented a renormalized perturbation expansion that introduced the multidensity formalism. Finally, from that point and Andersen's work, Wertheim (1984a,b, 1986a,b) developed an elegant theory that improved the previous essays. This solid theory

has become the basis of the Statistical Associating Fluid Theory (SAFT). In the next chapter, the main features of Wertheim's theory of association and the derivation towards the SAFT equation of state are described.

4

SAFT

In the previous chapter, we have traveled through the history of the equations of state, from the first modeling 200 years ago, till the recent and modern equations based on the microscopic behavior of the fluid. This chapter presents the background of the Statistical Associating Fluid Theory (SAFT), which is the basis of the work implemented and presented in this thesis work. A brief summary of the Wertheim's theory of association and the assumptions underlying the theory is done in the first section. Later, a detailed description of the different contributions calculated in SAFT is given, remarking the approximations made from the original theory. Finally, a brief note about different SAFT versions is done.

4.1. Wertheim's theory of association

As it was stated in the previous chapter, Wertheim (1984a,b, 1986a,b), inspired from Andersen's work (1973, 1974), developed a solid theory for associating fluids. The molecules are treated as different species according to the number of bonded associated sites. He showed that graph cancellation due to steric effects is simpler and more effective using the fugacity expansion in terms of two densities: the equilibrium monomer density and the overall number density. He also considered that the repulsive core restrict the formation to a single bond at each attraction site. The key result of Wertheim's cluster expansion is written as a first-order perturbation theory (TPT1) that establishes a direct relation between the change in the residual Helmholtz energy due to association and the monomer density. This monomer is, in turn, related to a function characterizing the "association strength".

Wertheim presented an initial work for pure hard-core molecules with one attractive site (1984a,b), and he extended the theory to compounds with multiple bonding sites per molecule (1986a,b). Later, Chapman et al. (1986, 1987) extended Wertheim's theory to the treatment of binary mixtures of components A and B that interact with off-center point charge dipoles of equal magnitude and opposite sign, where only AB dimers could be formed.

Although Wertheim's theory considers that the potential has a short-range highly directional component that is the cause of the formation of associated species, it does not specify any particular intermolecular potential for the reference fluid. It is necessary to select one in order to implement the theory. In a first stage, the known hard-sphere model was used in order to study the influence of the molecular association on the phase coexistence properties of hard-sphere molecules with one or two bonding sites (Wertheim, 1987, Jackson et al., 1988). Wertheim (1987) and Chapman et al. (1988a) deduced that in the limit of infinite association (in an infinitesimal small volume), the system becomes a polymer. The hard-sphere model has accurate analytical expressions for its equation of state and pair distribution. Results obtained showed excellent agreement compared to Monte

Carlo simulations. Chapman et al (1988a) obtained an equation of state for hard-sphere chains by imposing the condition of total bonding (i.e. zero nonbonded segments condition is imposed) and establishing the correct stoichiometry of segments with bonding sites (i.e. a stoichiometric ratio of *m* segments with either one or two associating sites). This work can be considered as the birth of the Statistical Associating Fluid theory.

The obtention of an equation of state through the derivation of Werheim's TPT1 involves some approximations that have to be considered in order to see the limitations when applying the theory. The main approximations are:

❖ Only three-like structures are permitted in theory, neglecting more complex structures like the ring bonding.

❖ Only one single bond is allowed at each associating site. It implies that:

  o Two bonded associating sites (each one from a different molecule) prevent a third core of another molecule to bond to any of the occupied sites.

  o Two associating sites of the same molecule cannot bond at the same time to another site of a different molecule.

  o Double bonding between two molecules is not allowed.

Figure 4.1. shows in several graphics all the hypothesis mentioned in the list.
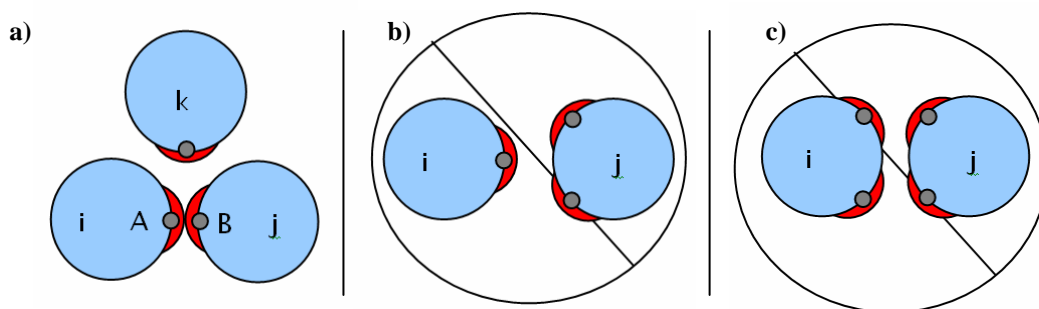
Figure 4.1. *Approximations in first-order Wertheim's theory; **a)** two bonded associating sites cannot bond to a third one; **b)** one site on molecule i cannot bond simultaneously to two sites on molecules j; **c)** double bonding is forbidden. Fig. from Chapman et al. (1990).*

❖ The activity in each site is not affected by the activity in other sites of the same molecule. It means that the possible repulsion interactions of two molecules trying to join at two sites of a third molecule are neglected.

❖ The first order approximation does not make any difference among the actual positions of the sites. As a consequence, the angles among the bonding sites are not specified and the properties are evaluated independently of the angle between the sites.

In spite of all these simplifications, the resulting SAFT equation has shown to be a powerful tool to calculate and predict phase equilibria of different kind of pure fluids and mixtures and, excepting in special cases (Chapman, 1988b; Blas and Vega, 2001), no more structural information will be needed to obtain accurate results.

4.2. The SAFT EoS and related approaches

As it was mentioned in the last section, the work of Chapman et al. (1988) constituted the first stone in the SAFT history. However, the pure formalism of the SAFT equation was presented in the papers of Chapman et al. (1989, 1990) and Huang and Radosz (1990, 1991). SAFT has been especially successful in some engineering applications for which other classical EoSs failed. In addition, the microscopic components of the equation make it a very challenging approach from the fundamental point of view, since extensions and modifications of the equation can be systematically performed and compared to simulation data for the same underlying model. The success of the equation in its different versions is proved by the amount of published works since its development. Figure 4.2 shows the number of published papers per year related to SAFT modeling. The growth of the equation in the last 10 years demonstrates its applicability in a wide range of different fields.
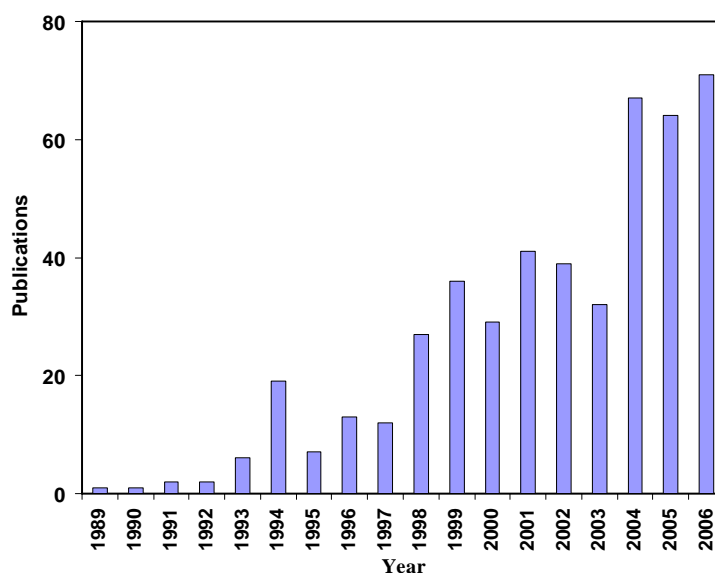
Figure 4.2 *Number of papers related to SAFT published per year in Journals ranked in the ISI Web of Knowledge from 1989 till today.*

The key of the success of SAFT-based equations is its solid statistical-mechanics basis, which lets a physical interpretation of the system. It provides a framework in which the effects of molecular shape and interactions on the thermodynamic properties can be separated and quantified. Besides, its parameters are few in number, with physical meaning and transferable, which makes SAFT a powerful tool for thermodynamic predictions.

SAFT equations are usually written in terms of the residual Helmholtz free energy, where each term in the equation represents different microscopic contributions to the total free energy of the fluid. The general equation is written as:

$$a^{res} = a - a^{id} = a^{ref} + a^{chain} + a^{assoc} \tag{4.1}$$

where a^{res} and a^{id} represent the residual and ideal Helmholtz free energy of the system. The superscripts *ref*, *chain* and *assoc* refer to the contributions from the interaction among segments, the formation of the chain from identical segments and the association bonds between two segments or chains, respectively.

The different contributions depend on several molecular parameters that will define a physical model for the molecule. In the original SAFT, the reference and the chain contribution have a total of three parameters to define the compound: *m*, which is the number of spherical segments forming a chain molecules; σ, which is the diameter of the segments and ε, which is their dispersive energy. The association contribution adds two more parameters that define the strength of the association bond between a site α on specie *i* and a site β on specie *j*: $k_{i_j}^{\alpha\beta}$ and $\varepsilon_{i_j}^{\alpha\beta}$ which are the volume and the energy of association respectively.

4.2.1. The reference term

A^{ref} considers the residual Helmholtz free energy of nonassociated spherical segments, and it is not specified within SAFT. It can refer to atoms, functional groups or even a full molecule (methane, argon). Most SAFT equations differ in the reference term, keeping formally identical the chain and the association term, both obtained from Wertheim's theory. The original SAFT of Chapman et al. (1988, 1990) and Huang and Radosz (1990, 1991) use a perturbation expansion using a hard-sphere fluid as a reference term and a dispersion term as a perturbation. The hard-sphere term is represented in both cases by the Carnahan-Starling expression while the dispersion term changes depending on the authors. Chapman et al. (1988, 1990) used an expression originally proposed by Cotterman et al. (1986), whereas Huang and Radosz (1990, 1991), used an expression based on molecular dynamics simulation data for the square-well fluid (Alder et al. 1972). Some other different intermolecular potentials have been proposed to try to improve the capabilities of SAFT. Among the most important proposals, we remark the following ones:

- The square-well potential (SW), employed by several authors (Banaszak et al., 1993; Tavares et al., 1997). Using the square-well potential, Gil-Villegas et al. (1997) developed a generalized potential function with an attractive part of variable range. The SAFT equation with an intermolecular potential of variable range is known as SAFT-VR. More recently, SAFT-VR has been slightly modified extending the potential range λ to higher values (Patel et al., 2005).

- The Lennard-Jones (LJ) potential, which accounts for both the repulsive and attractive interactions of the monomers in the same term. This potential has been used to develop different SAFT versions like the LJ-SAFT (Müller and Gubbins, 1995), a modified SAFT of Kraska and Gubbins (1996) and the soft-SAFT equation of state (Blas and Vega, 1997).

- The Yukawa potential (Davies et al., 1999), which has also been used with variable range in SAFT-VR.

- A hard-chain potential, which also considers the chain attraction (Sadowski, 1998). This model is known as the perturbed-chain SAFT (PC-SAFT) (Gross and Sadowski, 2000, 2001).

Since the Hemholtz free energy density is calculated by adding different contributions, each of them should be expressed in terms of composition for mixture studies. It is important to remark that the reference term is written and established for a pure compound (in contrast with the chain and association term, which are directly applicable to mixtures). Multicomponent mixtures, with different numbers of segments, different size and/or different dispersive energy, have to be averaged to "create" a pseudo-compound with the same thermodynamic properties as the mixture. Several mixing rules exist on this purpose (Economou and Tsonopoulos, 1997) and some studies about them have been done using SAFT-type equations (Galindo et al., 1998). Among all of them, the van der Waals' one fluid theory is the most popular due to its simplicity. Very good agreement has been obtained when comparing some results to simulation data for spheres of similar size (Rowlinson and Swinton, 1982) and different sizes and/or energies (Tang et al., 1995). The

corresponding expressions for the three molecular parameters involved in the reference term are:

$$m = \sum_{i=1}^{n} x_i \, m_i \tag{4.2}$$

$$\sigma_m^3 = \frac{\sum_{i=1}^{n}\sum_{j=1}^{n} m_i \, m_j \, x_i \, x_j \, \sigma_{ij}^3}{\sum_{i=1}^{n}\sum_{j=1}^{n} m_i \, m_j \, x_i \, x_j} \tag{4.3}$$

$$\varepsilon \, \sigma_m^3 = \frac{\sum_{i=1}^{n}\sum_{j=1}^{n} m_i \, m_j \, x_i \, x_j \, \varepsilon_{ij} \, \sigma_{ij}^3}{\sum_{i=1}^{n}\sum_{j=1}^{n} m_i \, m_j \, x_i \, x_j} \tag{4.4}$$

The above expressions involve the mole fraction x_i and the chain length m_i of each of the components of the mixture of chains. The crossed interaction parameters σ_{ij} and ε_{ij} are calculated using the generalized Lorentz-Berthelot combining rules:

$$\sigma_{ij} = \eta_{ij} \, \frac{\sigma_{ii} + \sigma_{ij}}{2} \tag{4.5}$$

$$\varepsilon_{ij} = \xi_{ij} \, \sqrt{\varepsilon_{ii} \, \varepsilon_{jj}} \tag{4.6}$$

where the factors η_{ij} and ξ_{ij} modify the arithmetic and geometric averages between components i and j, being the adjustable binary parameters of this equation. With the expressions (4.2)-(4.6), the reference term is expressed as a function of the chain molar fractions. More information about advantages and disadvantages of several combination rules can be found in a works of Diaz Peña et al. (1982), Halgren (1992) and Al-Matar and Rockstraw (2004).

4.2.2. The chain term

The chain contribution comes from an analytical expression obtained from Wertheim's work. It is derived from the energetic contribution given for the association of the segments in the limit of an infinite strong bonding on a small association site placed at the edge of a given molecule. The resulting equation for tangent spherical segments looks like this:

$$a^{chain} = \rho \ k_B T \sum_i x_i (1 - m_i) \ln y^{ref}$$

(4.7)

where ρ is the molecular density of the fluid, T is the temperature, m is the chain length, k_B the Boltzmann constant and y^{seg} is the pair correlation function of the selected reference fluid at density $\rho_m = m\rho$, evaluated at the segment contact σ. This function is given by:

$$y^{ref} = \exp\left(\Phi^{ref} / kT\right) g^{ref}$$

(4.8)

For most of the potentials, expression 4.8 can be reduced to simply: $y^{ref} = g^{ref}$, being g, the radial distribution function of the reference fluid.

One of the limitations of the first order theory is that the bond angles are not considered inside the molecule. It means that, while the theory is able to give a very good result for linear chains (Muller and Gubbins, 1993), it may fail in the limit where the bonding site angles are so small that cannot avoid a simultaneous bonding at the same site. Branched and linear isomers are conformal from the modeling point of view. It would be necessary to take into account higher order terms of the perturbation expansion (Wertheim, 1987, Muller and Gubbins, 1993) to consider this simultaneous bonding. Going to a second-order level, this situation can be overcome. However, *n*-order expressions imply a more complex calculation, involving *m*-body correlation functions (being *m=n+1*) of the reference fluid that would depend on the bond angles. Müller and Gubbins (1993)

suggested that, for hard-sphere chain fluids, there was not a significant improvement to justify the effort unless the chains have rigid bond angles less than 110º. Blas and Vega (2001) established a comparison using the first and second-order perturbation approach for modeling branched Lennard-Jones chains, modeling the branches as rigid bonds of 120º. They tested the new equation, called SAFT-B, and obtained lower pressures at high densities and higher pressures at low densities, compared to the results for linear chains, in qualitative agreement with the experimental data.

Wertheim's theory does not specify a particular reference fluid. Generally, most SAFT equations refer to a spherical segment with diameter σ equal to the distance at which the intermolecular potential vanishes. However, additional information into the reference fluid can improve the predictions for TPT. Chang and Sandler (1994) and Ghonasgi and Chapman (1994) developed a dimer reference TPT1 for hard chains, where the pair correlation function g^{Dseg} corresponds to the pair correlation function of dimers. Blas and Vega (2001) also studied the effect of a dime version for the Lennard-Jones potential. In the same direction, the PC-SAFT (Gross and Sadoswski, 2000, 2001) uses a hard-chain reference (instead of the monomer reference) and adds a Barker-Henderson type perturbation term (Barker and Henderson, 1967a,b) to consider the chain attraction. PC-SAFT has been successfully applied to polymer systems in the last five years.

Finally, it is interesting to remark that the theory does not consider the intramolecular attraction beyond the formation of bonds when taking into account only the first term of Wertheim's Perturbation Theory (TPT1). As a result, low densities are not properly calculated (Johnson et al., 1994) because at that level, intramolecular interactions become more significant compared to the intermolecular forces, and SAFT does not account for coil up of the chains, predicting higher energies than those observed from simulations. It is necessary a second-order term to overcome this limitation.

4.2.3. The association term

The basis of Wertheim's perturbation theory is the fact that it considers the possibility of association. A molecule can have one or more associating sites. The theory allows an infinite number of sites, although in practice, more than four seems quite unrealistic for a molecule. An association site is characterized by a noncentral potential placed near the perimeter of a molecule.

As already stated, the association term, within the first-order Wertheim's perturbation theory for associating fluids, assumes that the activity in one site is independent of a possible bonding in another site of the same molecule. This hypothesis lets estimate the fraction of molecules present in a cluster of size N as:

$$X(N-mer) = NX^2(1-X)^{N-1} \tag{4.9}$$

being X the mole fraction of molecules of one specie not bonded at one site. It is important to remark the difference between x (component composition) and X. The cluster average size would be:

$$\bar{N} = \frac{1}{X} \tag{4.10}$$

Equation 4.10 is the "most probable distribution" of Flory (1953) and it is in agreement with experimental results for polymer polydispersity.

The association contribution to the Helmholtz energy is expressed as the sum of contributions of all associating sites of component i:

$$a^{assoc} = \rho \; k_B T \sum_i x_i \sum_\alpha \left(\ln X_i^\alpha - \frac{X_i^\alpha}{2} \right) + \frac{M_i}{2} \tag{4.11}$$

being M_i the number of associating sites of component i, and X_i^α the mole fraction of molecules of component i non bonded at site α, which accounts for the contributions of all the associating sites in each species. From the solution of mass balances:

$$X_i^\alpha = \frac{1}{1 + N_A \rho \sum_j x_j \sum_\beta X_j^\beta \Delta^{\alpha_i \beta_j}} \tag{4.12}$$

The double summation refers to a sum over all possible association sites on all the species involved, considering the possibility of self-association and cross-association among the species. The term $\Delta^{\alpha_i \beta_j}$ is related to the strength of the association bond between site α in molecule i and site β in molecule j. It is formally given by:

$$\Delta^{\alpha_i \beta_i} = \int g^{ref}(12) f_{ij}(12) d(12) \tag{4.13}$$

where g^{seg} is again the reference fluid pair correlation function, f is the Mayer function of the association potential, given by: $f_{ij} = \exp\left[\dfrac{-\phi_{ij}(12)}{kT}\right] - 1$; ϕ_{ij} is the potential function that is used to define the association, and *d(12)* represents an unweighted average over all orientations and an integration over all separations of molecules 1 and 2. In order to simplify the integration, it is assumed (Chapman et al., 1988) that the segment pair correlation function is equivalent to that of the segment as part of a chain. This approximation has been proved to be valid if the bonding site is located diametrically opposed to the backbone of the chain (Müller et al. 1994). Several models have been proposed for the evaluation of ϕ_{ij}, like the realistic fractional point charge model (Walsh, 1993). However, a more simplified model based in a square-well potential has become the standard for most of the applications.

The geometry of the association sites is normally chosen to be spherical for both, simplicity and reality, compared to other models (Walsh, 1993). When the reference

fluid is made of hard-spheres, the association sites are situated with its centre lying on the surface of the reference spherical core. Expression 4.13 cannot be analytically obtained and, for that reason, another reasonable approximation is made. It is supposed that $r^2 g_{HS}(12)$ is equal to the value at contact $\sigma^2 g_{HS}(\sigma)$ (Jackson et al., 1988).

With all the assumptions considered, the simplified expression for a square-well bonding potential with a spherical geometry of the association sites is:

$$\Delta^{\alpha_i \beta_i} = 4 \pi \, g(\sigma)_{ref} \left(\exp\left[\frac{\varepsilon^{\alpha_i \beta_j}}{T} \right] - 1 \right) k^{\alpha_i \beta_j} \tag{4.14}$$

where $\varepsilon^{\alpha_i \beta_j}$ is the association energy and $k^{\alpha_i \beta_j}$ represents the association volume for each association site and compound. Equation 4.14 may be more simplified when a particular kind of bonding potential is selected.

4.2.4. SAFT Versions

As it has been said, different versions of SAFT have appeared through the last years that, although formally identical, they differ in the form of the reference term. Among them, the most commonly used are (apart of the original SAFT of Chapman et al. [1989,1990] and Huang and Radosz [1990,1991]) the SAFT-VR (Gil-Villegas et al., 1997), the soft-SAFT (Blas and Vega, 1997) and the PC-SAFT (Gross and Sadowski, 2001), although there are other successful versions: the copolymer SAFT (Banaszak, 1996), the SAFT-BACK of Pfhol and Brunner (1998), the SAFT1 of Adidharma and Radosz (1998), etc.

SAFT-VR (Gil-Villegas et al. 1997) has shown that it could be used to deal with homonuclear chains of hard spheres segments of equal diameter σ, which interact via different intermolecular potentials such as the square-well, the Sutherland, or the Yukawa

potentials (Davies et al. 1999). Generally, most of the works are performed with the variable square-well fluid, showing its applicability in a large number of works. The equation correlated accurately the pure *n*-alkane and *n*-perfluoroalkane phase equilibrium over a wide temperature range. The equation has also shown good predictions for binary (McCabe et al., 1998) and ternary mixtures (Colina et al., 2004). Galindo et al. (1998) extended SAFT-VR to aqueous electrolyte systems. Long-range Coulombic ion-ion interactions are calculated with the restricted primitive model using the mean-spherical approximation. With one transferable fitted parameter per ion, the vapor pressure and liquid density for a number of single-salt aqueous solutions and one mixed-salt system of strong electrolytes were correlated. Several relevant works have been published in this field (Patel et al., 2003; Behzadi et al. 2005).

The perturbed chain SAFT (PC-SAFT) (Gross and Sadowski, 2001) uses a hard-chain reference fluid by applying the Barker-Henderson perturbation theory truncated at the second-order term. The integral expressions for the first and second-order terms were refitted to appropriate Taylor series expansions in density using pure *n*-alkane data. PC-SAFT has also shown good accuracy when modeling pure fluids and binary mixtures (Gross and Sadowski, 2002; Tumakaka et al., 2005), with good applications for polymers (von Solms et al., 2005; Arce et al., 2006; Pedrosa et al., 2006) and polar compounds (Karakatsani et al., 2005; Karakatsani and Economou, 2006).

This thesis work has been devoted to the improvement of a particular version of SAFT, the soft-SAFT equation of state. More details about this equation are given in the next chapter.

5

soft-SAFT

This chapter is devoted to the soft-SAFT equation. The differences between soft-SAFT and the original SAFT are described in the first section. Afterwards, a description of the different extensions and applications made to the equation since its creation is exposed. Then, the chapter is concerned to the methodology for implementing a specific treatment for critical region calculations into the equation. Several approaches are mentioned and discussed. The mathematical model for the chosen approach is shown in detail. Finally, some details about phase equilibria, critical lines and derivative properties calculations are described.

5.1. The soft-SAFT equation of state

Soft-SAFT is a variant of the original SAFT which is based on a reference Lennard Jones (LJ) intermolecular potential. Following the ideas of Müller and Gubbins (1995) and Kraska and Gubbins (1996), soft-SAFT was presented by Blas and Vega (1997) and, in the last ten years, has been applied with success to several types of mixtures over a broad range of thermodynamic conditions, and it has proved to be very strong for phase equilibria conditions. The main differences between soft-SAFT and the original SAFT from Chapman et al. (1990) are:

- Soft-SAFT uses a Lennard-Jones intermolecular potential to describe the interactions among the molecules in the reference term. There exist two accurate LJ equations of state that are temperature and density dependent functions: the Benedict-Webb-Rubin EoS from Johnson et al. (1994), fitted to computer simulation data for the LJ fluid, and a perturbed virial expansion with a reference hard sphere term from Kolafa and Nezbeda (1998). Although the second one is theoretically more robust, the first one is slightly more accurate in the vapor phase and close to the critical region (Pàmies and Vega, 2002). This is logical considering that the hard sphere term proposes a model which is very realistic in the liquid phase but deviates from real in the gaseous systems (where the molecules move faster) and the critical region (where the long fluctuations among the molecules are very significant). The EoS from Johnson is employed for all the calculations shown in this work.

- Soft-SAFT uses a radial distribution function (g_{LJ}) of a LJ fluid of nonbonded spheres. A fitted expression for LJ chains, as a function of the reduced temperature and density, from Johnson et al. (1993) is employed.

- Soft-SAFT also uses a Lennard-Jones fluid in the association term. It means that association sites are allowed to be embedded in the referent core, tangent to the surface. This location is forcing the bonded molecules to have some degree of

overlapping, as it would be expected in real fluids. With this bonding potential and the spherical geometry for the associating sites, expression 4.14 is simplified to:

$$\Delta^{\alpha_i \beta_i} = 4\pi \left(\exp\left[\frac{\varepsilon^{HB}}{T} \right] - 1 \right) k^{HB_j} I^{ij} \tag{5.1}$$

where *I* is a dimensionless integral which is defined as:

$$I^{ij} = \frac{1}{24b^2\sigma^3} \int_{2b-\sigma}^{2b+\sigma} g_{ref}(r)(\sigma_a + 2b - r)^2 (2\sigma_a - 2b + r)\, r\, dr \tag{5.2}$$

This integral can be evaluated numerically using accurate values for g_{ref} obtained from molecular simulations, and the results can be converted into an analytical-fitted function of the temperature and density (Müller and Gubbins, 1995).

- Soft-SAFT places association sites tangent to the reference core using this geometry: *b=0.4σ* and *σ$_a$=0.2σ*. This geometry has been previously tested in other works (Johnson and Gubbins, 1992; Walsh and Gubbins, 1993, Müller and Gubbins, 1995) obtaining accurate results.

The different terms of the soft-SAFT equation for calculating the total Helmholtz energy, the pressure and the chemical potential can be found in the PhD work of Pàmies (2003).

5.2. Soft-SAFT extensions and improvements

A main advantage in the use of SAFT-type equations versus classical ones is that they are accurate for complex fluids with different molecular architectures and intermolecular forces in a straightforward manner. The soft-SAFT equation is a powerful tool that has been applied to calculate the phase behavior of several pure components and mixtures in a broad range of thermodynamic conditions.

In addition, as any other SAFT-type equation of state, soft-SAFT is written as a sum of contributions where the different effects are separated and quantified. This formulation offers the possibility of improving the equation by adding a specific treatment or just extending it to the calculation of other properties. It is convenient to establish the difference between the addition of a new term to take into account a new molecular effect (like multipolar terms, charges, etc.), which can be considered as an extension of the equation, and the implementation of a treatment for a specific region of the phase space (like the crossover treatment for the critical region or the density gradient theory for the interfacial space), which is an improvement.

One of these contributions concerns the accounting for multipolar interactions. The quadrupole was already introduced following the work of Twu and Gubbins (1978) and employed in the calculation of quadrupolar substances like CO_2 (Pedrosa et al., 2005; Dias et al., 2006), achieving excellent improvements in the performances of mixtures.

Another relevant extension concerns the calculation of derivative properties because they constitute a strong test for any equation of state. These properties are second-order properties of a primary thermodynamic function and, as a consequence, are more sensitive to errors. The evaluation of derivative properties of pure fluids (Llovell and Vega, 2006) and binary mixtures (Llovell et al., 2006) has shown the robustness of the soft-SAFT equation of state.

The evaluation of interfacial properties using soft-SAFT was also performed by adding an extra term to take into account the density inhomogeneities that are found in a liquid-vapor interface. The van der Waals gradient theory (1894) provided a general expression for the Helmholtz energy density of an inhomogeneous system. Cahn and Hilliard (1958) rediscovered this expression relating an equation of state to interfacial

properties of a classical fluid system. The density gradient theory was coupled to the soft-SAFT in the PhD Pàmies thesis work (2003) and presented in the works of Duque et al. (2004), Mejia et al. (2005) and Mejia and Vega (2006). The equation showed excellent agreement in the calculation of interfacial tensions and density profiles of Lennard-Jones chains when it was compared to molecular simulations. Then, it was applied to the *n*-alkanes and *1*-alkanols family, reproducing vapor-liquid interfacial tensions with a high degree of accuracy. Results for binary mixture of *n*-alkanes were also in good agreement with experimental information.

Finally, it was also necessary a specific treatment for the evaluation of critical properties of pure compounds and mixtures. This PhD work has been devoted to this improvement of the equation: the implementation of a crossover treatment to reproduce the physics of the critical region. Soft-SAFT is a mean-field theory that does not take into account the long-range fluctuations near the critical region. Following the approach proposed by White (1992), based in the renormalization-group theory (Wilson, 1971), an additional term to take into account these fluctuations has been added into soft-SAFT. As a result, the equation has provided quantitative agreement with experimental data for vapor-liquid equilibria calculations far from and close to the critical region for pure fluids (Llovell et al., 2004) and mixtures (Llovell and Vega, 2006).

Table 5.1 is presented in next page and gives a summary to the reader of some of the most relevant modeling works performed with the soft-SAFT equation of state till now. The table is organized in terms of families of compounds that have been studied.

The following sections are entirely dedicated to the critical region, describing the different approaches for considering the fluctuations and the implementation of the mathematical treatment for the model chosen into the soft-SAFT EoS.

Table 5.1. *Summary of some of the most relevant works published using soft-SAFT.*

Applied to	Study	Reference
LJ chains	VLE of homonuclear and heteronuclear LJ molecules	Blas and Vega (1997)
	VLE using a dimer reference fluid	Blas and Vega (2001$_a$)
	VLE of branched LJ chains	Blas and Vega (2001$_b$)
	Critical Region of LJ chains	Llovell et al. (2004)
	Interfacial properties of LJ chains	Duque et al. (2004)
	Phase and Interfacial properties of Type I and Type V LJ mixtures	Mejia et al. (2005)
	Three phase equilibrium and interfacial properties in Type II LJ mixtures	Mejia and Vega (2006)
n-alkanes	VLE for C1-C8 alkanes and prediction of heavier compounds (C16, C24, C48)	Blas and Vega (1997) Pàmies and Vega (2001)
	Critical region of the *n*-alkanes family	Llovell et al. (2004)
	Derivative properties of some light *n*-alkanes.	Llovell and Vega (2006)
	Binary and ternary phase diagrams of *n*-alkanes	Blas and Vega (1998$_a$) Pàmies and Vega (2001)
	VLE and critical behavior of *n*-alkane mixtures	Blas and Vega (1998$_b$) Llovell and Vega (2006$_c$)
	Tricritical phenomena	Vega and Blas (2000)
	Inversion curves of *n*-alkanes and CO_2	Colina et al. (2002)
	Solubility of hydrogen in heavy *n*-alkanes.	Florusse et al. (2003)
	Excess thermodynamic properties in alkane binary mixtures.	Blas (2000); dos Ramos and Blas (2005)
	VLE and critical transitions in CO_2/alkanes	Llovell and Vega (2006$_a$)
	Solubility of polyethylene in different solvents	Pedrosa et al. (2006)
	Derivative properties of alkane mixtures	Llovell et al. (2006)

	Solubility of hydrogen chloride and critical transitions in some n-alkanes	Llovell et al. (2006)
n-alkenes	VLE for C2-C5 alkenes	Blas and Vega (1998[a])
1-alkanols	VLE for C1-C8 *1*-alkanols	Blas and Vega (1998[a])
		Pàmies (2003)
	Derivative properties of some light *1*-alkanols.	Llovell and Vega (2006[b])
	Excess properties in self-associating systems	Blas (2002)
	VLE and critical transitions in CO_2/*1*-alkanols	Llovell and Vega (2006[a])
	VLE and critical lines of alkane/1-alkanol mixtures	Llovell and Vega (2006[c])
	Derivative properties of alkane/1-alkanol mixtures	Llovell et al. (2006)
Perfluoro-alkanes	VLE for C1-C9 perfluoroalkanes	Dias et al. (2004)
	Solubility of gases in perfluoroalkanes	Dias et al. (2004)
	VLE of various fluorinated compounds	Dias et al. (2005)
	LLE of alkanes and perfluoroalkanes,	de Melo et al. (2006)
	VLE of CO_2/perfluoroalkane mixtures	Dias et al. (2006)
	Derivative properties of perfluoro-propane	This work
Polymers, surfactants	VLE of homopolymers	Pàmies and Vega (2002)
	VLE and aggregate formation characteristics of surfactant-like molecules.	Herdes et al. (2004)
	VLE of Ethylene glycol oligomers and mixtures with CO_2, benzene and N_2.	Pedrosa et al. (2005)
	Solubility of polyethylene in different solvents	Pedrosa et al. (2006)
	VLE and LLE of polystyrene systems	Pedrosa et al. (2006)

5.3. The different approaches to the critical region

As it has been stated before, the particular behavior of the critical region implies that slight variations in one property can increase or decrease thee density and the solubility in a process very rapidly. From a microscopic point of view, the classical theory of critical points corresponds to a mean-field approximation, which neglects local inhomogeneities (fluctuations) in density. It is well-known that the nonclassical critical behavior of the thermodynamic properties is a consequence of the long-range fluctuations of an order parameter, the density for the case of pure fluids. The spatial extend of the density fluctuations diverges at the critical point and becomes larger than any molecular scale in the critical region. Only theories which account for these density fluctuations can provide the correct approach to the critical region.

The classical formulation of SAFT (and all the available equations of state) makes the theory unable to correctly describe the scaling of thermodynamic properties as the critical point is approached, unless an specific treatment is considered. Two are the alternatives used up to now to overcome this problem in SAFT-type equations: a rescaling of molecular parameters so that the experimental critical point of the pure compound is matched and a rigorous treatment based on renormalization-group (RG) arguments, in which the approach to the critical point is explicitly considered. There are several advantages and inconveniences in each one of them. The simple rescaling of molecular parameters has been used by several authors (Blas and Vega, 1998; McCabe and Jackson, 1999; Pàmies and Vega, 2001). Although it improves predictions of the critical behavior of several mixtures, a new set of different molecular parameters for each family of components is required for the near-critical region. Also, note that in this case, *the fluctuations inherent to the critical region are ignored*. The result is that there is no possibility to describe the near-critical region and the rest of the phase envelope with the same set of parameters and the same equation, a real drawback of the methodology. It is therefore clear that, for practical applications, an accurate theory valid both close to and far from the critical point with a unique set of parameters is required. In the second case, the asymptotic behavior near the critical point is coupled with a classical equation, which works well far from the critical region. This rigorous crossover treatment should give exact results far from and close to the critical region, provided that both terms are accurate

enough. Nevertheless, there are some additional adjustable parameters in this case and care must be exercised in the way they are fitted, and the possible transferability of them.

Renormalization-group methods have been very successful in describing the properties of systems near their critical point (Wilson, 1971; Wilson and Fischer, 1972). However, to obtain a realistic representation of the thermodynamic properties of fluids close to and far from the critical region, it is necessary to develop an equation that not only incorporates the fluctuation-induced scaled thermodynamic behavior of fluids asymptotically close to the critical point, but that also accounts for a crossover to classical behavior of the thermodynamic properties sufficiently far away from the critical point, where the effect of fluctuations becomes negligible (Wyczalkowska et al., 2004). There are different approaches in which the long-wavelength density fluctuations can be taken into account in the near critical region, searching for a global equation for real fluids. An excellent review on the subject was provided by Anisimov and Senger (2000). Following these authors the efforts on this direction can be summarized in three different approaches: a renormalized Landau expansion, followed by Senger and co-authors (Anisimov and Senger, 2000; Wyczalkowska et al., 2004); numerical approaches based on the hierarchical theory (Parola et al., 1989a,b; Meroni et al., 1990) and the phase-space cell approximation method of White and collaborators (White, 1992; Salvino and White, 1993; White and Zhang, 1993,1995).

Chen et al. (1990a,b) were among the first who used a renormalized Landau expansion. They formulated a procedure for transforming a series expansion of the classical Helmholtz free energy density into an equation that incorporates the fluctuation-induced singular scaling laws near the critical point, and reduces to the classical expansion far away from the critical point. Their procedure was based on an attempt to solve the nonlinear RG equations by matching the solution of the renormalization transformation to the classical equation at an appropriate matching point. More recently, Wyczalkowska et al.(2004) have used the same transformation to develop a crossover van der Waals equation of state, incorporating the near-critical scaling-law behavior of the thermodynamic properties.

Based on the renormalized Landau expansion, Kiselev (1998) and collaborators (Kiselev et al, 1991; Kiselev and Ely, 1999) have developed a phenomenological parametric crossover EOS. In this approach, one starts from a revised and extended parametric equation for the Helmholtz free energy and modifies each term so that all become analytic far away from the critical point. The approach is quite useful for

engineering purposes, and it has been successfully applied to several classical EoS's, including the original SAFT of Huang and Radosz (Kiselev et al., 2001, 2006) and SAFT-VR (McCabe and Kiselev, 2004a,b; Sun et al., 2005) equations. A main drawback of this methodology is that the crossover equation has several empirical system-dependent coefficients. It is difficult then to transfer these parameters for other compounds, even within the same chemical family.

Parola, Reatto and Meroni presented the Hierarchical Reference Theory (HRT), in which they reformulated the liquid-state theory to take into account density fluctuations in successively larger length scales, without grouping them into packets. The theory was successfully applied to Lennard-Jones fluids and mixtures (Parola et al., 1989a,b; Meroni et al., 1990). However, the intensive computing time required makes this methodology not suitable, yet, for engineering applications.

The procedure followed in this thesis work is the third one, which is based on Wilson's RG theory. Wilson developed a very successful RG method (Wilson, 1971, 1972) to incorporate density fluctuations in the critical region using the phase-space cell approximation. The theory was developed just for the critical region and it needed to be extended to the rest of the phase space (White, 1992; Salvino and White, 1993; White and Zhang, 1993,1995). White and co-workers extended the range of applicability of this method, developing a global RG theory. They proposed a set of recursive equations based on a phase-space cell approximation for the semiquantitative analysis of the behavior of systems near the critical point. That includes a renormalization of all the variables giving the correct non-analytical asymptotic behavior of real fluids inside the critical region, and reducing to the ideal gas law at low density. Based on White's work, Tang (1998) proposed a new theory, combining White's RG transformation, the density functional theory, and the superposition approximation. The new theory was implemented within the mean spherical approximation (MSA), providing a global theory for the LJ fluid, that has been applied successfully to pure fluids (Mi et al., 2004, 2005) and mixtures (Mi et al., 2006) . Lue and Prausnitz (1998a,b) extended the accuracy and range of White's equations through an improved Hamiltonian. They also stated the approximations made in the theory. The theory was applied to square-well fluids and results compared to simulation and experimental results, using the square-well model. The approach was then used by Jiang and Prausnitz (1999, 2000) to describe the pure *n*-alkanes family and some of their mixtures. Jiang and Prausnitz were the first who applied the theory to chain molecules, modeled as square-well

chains. An advantage of this method versus Kiselev's is that it is an easy-computing numerical method based on recursive equations, and the two additional parameters can be transferred within the same series. Moreover, in spite of its numerical character, versus the analytical nature of Kiselev's method, the resolution of the involved recursive equations is very fast in nowadays' available computers.

White's global RG theory consists of a set of recursion relations where the contribution of longer and longer wavelength density fluctuations up to the correlation length is successively taken into account in the free energy density. In this way, properties approach the asymptotic behavior in the critical region, and they exhibit a crossover between the classical and the universal scaling behavior in the near-critical region.

5.4. The phase-space cell approximation

This section is devoted to give a more detailed explanation about the phase-cell approximation to calculate long-range fluctuations in a similar way of Salvino and White (1992).

An intuitive phenomenological explanation for the cell space approximation may be described as it follows: it is supposed that our fluid is divided into many small cells each containing only a few number of molecules (Figure 5.1a). The total volume of the cell is considered to be the sum over all density distributions in each cell. If the cells are small enough, it can be assumed that the average potential of all molecules can be approximated using a mean-field theory, because there is not space for long-range correlations. Then, a mean-field model (the few molecules in the building block cell interact with all particles in the mean field way) is applied (Figure 5.1b) for each cell, having thousands of Helmholtz energy contributions in our fluid. The first iteration of the free energy only includes the lowest order short wavelength fluctuation correction term. Next, the neighbour cells are considered and each cell is treated as a whole molecule with a calculated energy (Figure 5.1c). The "intercell" potential is estimated again with the mean field theory but, in some way, the fluctuations among further molecules are taken into account. The procedure is repeated several times till the whole physical space of the compound is covered (Figure 5.1d). Following this approach, the estimated energy value obtained considers the longer wavelength contributions needed to introduce the long range correlations that are crucial in the critical region.
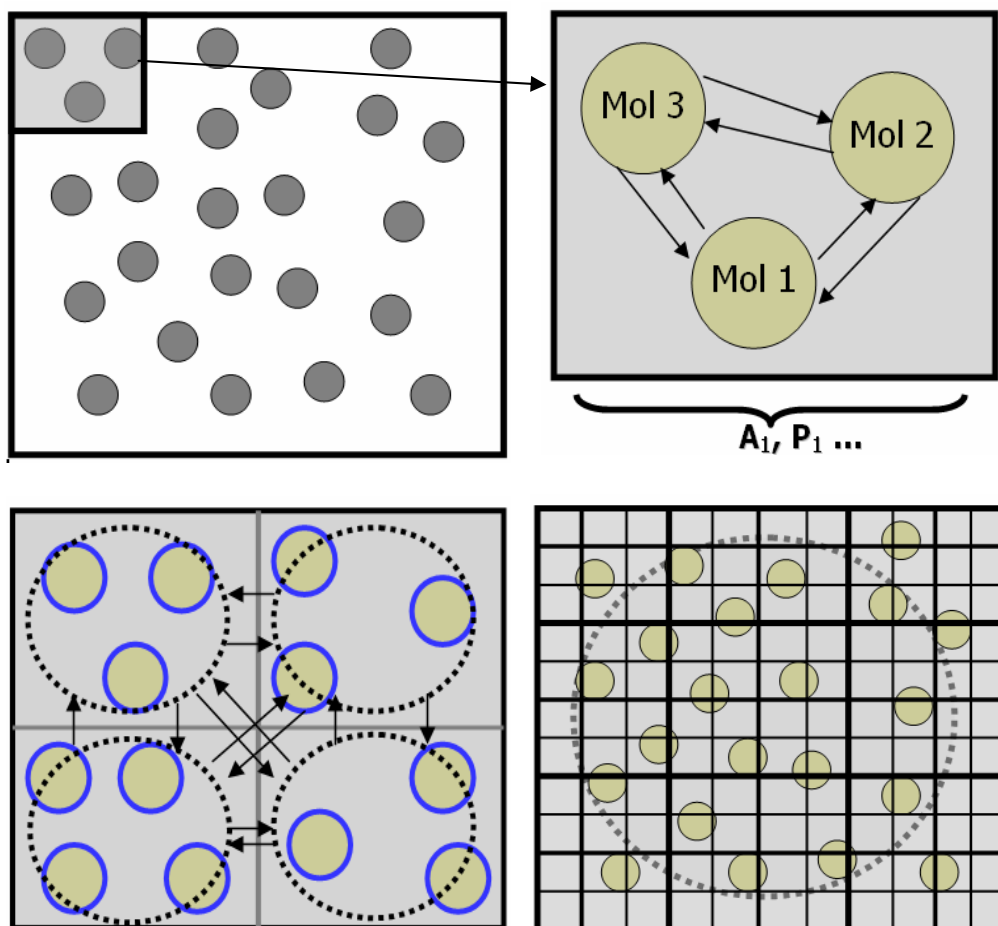
Figure 5.1 *A cartoon description of the phase space cell approximation.* ***a****) Model of a fluid with several molecules. A small cell of length L is selected.* ***b****) The properties of the small cell are calculated using a mean field theory.* ***c****) Each cell is considered as a single molecule that interacts with its neighbors using again a mean-field theory.* ***d****) The procedures is repeated till the whole amount of molecules is considered.*

5.5. Mathematical model

The implementation of White's global RG method is done in the same way as Lue and Prausnitz (1998a,b) and Jiang and Prausnitz (1999, 2000). In order to include the long-wavelength fluctuations into the free energy, the grand canonical partition function for simple fluids is transformed into a functional integral. The interaction potential is then divided into a reference contribution, due mainly to the repulsive interactions, and a perturbative contribution, due mainly to the attractive interactions ($u(r) = u_{ref}(r) + u'(r)$).

The RG theory is only applied to the attractive part, since it is considered that the other term contributes mainly with density fluctuations of very short wavelengths. The effect of the density fluctuations due to the attractive part of the potential is then divided into short-wavelength and long-wavelength contributions, with the assumption that contributions from fluctuations of wavelengths less than a certain cutoff length L can be accurately evaluated by a mean-field theory.

The effect of short-wavelength contributions is taken into account by the functional

$$A^s(\rho) = \int d^D r a^s(\rho) \tag{5.3}$$

where a^s is the Helmholtz free energy density of a homogeneous system with density ρ. This can be calculated using the soft-SAFT equation, or any other mean-field theory. The choice of the mean-field theory is of relevance for the overall behavior of the crossover equation, as will be discussed later. This is why different crossover equations have been developed and continue under development nowadays. It is important to note that because a^s should include only short-wavelength density fluctuations, it is necessary to subtract the long-wavelength fluctuations. As a first approximation this can be done by adding $-\alpha(m\rho)^2$.

$$a^s = a^{classical\,EOS} + \alpha(m\rho)^2 \tag{5.4}$$

where α is given by

$$\alpha = -\frac{1}{2}\int d^D r u'(r) \tag{5.5}$$

Using the saddle-point approximation (Negele and Orland, 1988), the zero order solution of the grand partition function gives

$$a_0 = a^s - \alpha(m\rho)^2. \tag{5.6}$$

Substitution of equation (5.4) into equation (5.6) gives that the zero order contribution to the Helmholtz free energy density is just the Helmholtz free energy density provided by the classical equation (soft-SAFT in our case) at molecular density ρ. Note that the saddle-point approximation used neglects the contribution of density fluctuations of all wavelengths that are not already accounted for by the reference fluid.

The contribution of the long-wavelength density fluctuations is taken into account through the phase-space cell approximation (Wilson, 1971, 1972; Salvino and White, 1992). In a recursive manner, the Helmholtz free energy per volume of a system at density ρ can be described as,

$$a_n(\rho) = a_{n-1}(\rho) + da_n(\rho) \tag{5.7}$$

where a is the Hemholtz free energy density and da_n the term where long wavelength fluctuations are accounted for in the following way:

$$da_n(\rho) = -K_n \cdot \ln \frac{\Omega_n^s(\rho)}{\Omega_n^l(\rho)} \qquad (5.8)$$

where Ω^s and Ω^l represent the density fluctuations for the short-range and the long-range attraction respectively, and K_n is a coefficient:

$$K_n = \frac{k_B T}{2^{3n} \cdot L^3} \qquad (5.9)$$

T is the temperature and L the cutoff length.

$$\Omega_n^\beta(\rho) = \int_0^{\min(\rho, \rho_{\max} - \rho)} \exp\left(\frac{-G_n^\beta(\rho, x)}{K_n} \right) \cdot dx \qquad (5.10)$$

$$G_n^\beta(\rho, x) = \frac{\bar{a}_n^\beta(\rho + x) + \bar{a}_n^\beta(\rho - x) - 2\bar{a}_n^\beta(\rho)}{2} \qquad (5.11)$$

The superindex β refers to both long (l) and short (s) range attraction, respectively, and G^β is a function that depends on the evaluation of the function $\bar{a}$, calculated as:

$$\overset{l}{\bar{a}}_n(\rho) = a_{n-1}(\rho) + \alpha \cdot (m \cdot \rho)^2 \qquad (5.12)$$

$$\overset{s}{\bar{a}}_n(\rho) = a_{n-1}(\rho) + \alpha \cdot (m \cdot \rho)^2 \cdot \frac{\phi \cdot w^2}{2^{2n+1} \cdot L^2} \qquad (5.13)$$

where m is the LJ segment parameter, ϕ an adjustable parameter, α is the interaction volume with units of energy-volume, and w refers to the range of the attractive potential. For the LJ fluid, α and w are given by:

$$\alpha = \frac{-1}{2} \int_\sigma^\infty u_{LJ} \, 4\pi r^2 \, dr = \frac{16\pi \varepsilon \sigma^3}{9} \qquad (5.14)$$

$$w^2 = \frac{-1}{3!\alpha} \int_{\sigma}^{\infty} r^2\, u_{LJ}\, 4\pi r^2\, dr = \frac{9\sigma^2}{7} \qquad (5.15)$$

ρ_{max} is the maximum possible molecular density and it depends on the selected model. The maximum value of the density accounted for in the reference equation employed (Johnson, 1993) depends on the temperature considered, but it is at least 1 in terms of monomer density and non-dimensional units, for the lowest temperature reported. The maximum density is set as:

$$\rho_{max} = \frac{1}{m \cdot N_A \cdot \sigma^3} \qquad (5.16)$$

The chemical potential and the pressure can be obtained by standard thermodynamic relationships. A detailed derivation of the recursive equations is shown in the appendix B of this thesis work.

The above procedure can be interpreted as the ratio of non-mean field contributions to mean-field contributions as the wavelength is increased. In practice, it has been observed, as some other authors did (Salvino and White, 1992; Tang, 1998; Lue and Prausnitz, 1998; Jiang and Prausnitz, 1999), that after five iterations (n=5), there is not further change in the Helmholtz free energy. However, as will be discussed later, more iterations are needed to obtain accurate values for the critical exponents.

The integral in equation 5.8 is evaluated numerically, by the trapezoid rule. The superior limit of the integral depends on how close we are from the maximum package density. This condition is given to assure that all calculations will be in the range of application of the selected intermolecular potential. The density step has been set to obtain good accuracy, without compromising the speed of the calculations. A density step $\rho/500$ gives accurate results for the critical region.

To extend White's theory to mixtures, the isomorphism assumption (Fisher, 1968) is used. Following the RG theory, it is assumed that the order parameter plays a crucial role in the Hamiltonian. Since the density is the order parameter in this case, according to the isomorphism assumption, the order parameter to describe vapor-liquid equilibria in mixtures is the total density of the system. Therefore, the one-component density must be replaced by the total density of the components. However, according to the isomorphism assumption, the chemical potentials must be chosen as independent variables when the integration in equation (5.10) is calculated, i.e. the integration should be performed at fixed chemical potential. This requirement makes computation extremely difficult. Therefore, following other authors (Cai and Prausnitz, 2004; Sun et al, 2005; Cai et al., 2006), Kiselev and Friend's approximation (1999) is used, replacing constant chemical potentials by constant mole fractions in performing the integral. It is important to remark that the choice of an order parameter or another will make the equation suitable for a particular kind of mixture equilibria. For instance, the approximations made here make the equation suitable for vapor-liquid equilibria; a different order parameter will be required in the case of liquid-liquid equilibria.

In addition to Kiselev and Friend's approximation (1999), the extension of the equation to mixtures also requires to introduce the mixing rules to determine the crossover parameters L and ϕ. Due to the fact that the cut off length L is the diameter of the three-dimensional space for characterizing density fluctuations, we have chosen the simplest possible expression for the mixture:

$$L^3 = \sum_{i=1}^{n} x_i L_i^3 \tag{5.17}$$

The crossover parameter ϕ is calculated in the same way as the chain length:

$$\phi = \sum_{i=1}^{n} x_i \, \phi_i \tag{5.18}$$

In addition to these crossover parameters, the soft-SAFT parameters for mixtures presented in equations 4.2-4.6 are used, instead of the pure component parameters m_i, σ_i, ε_i.

5.6. Phase equilibria, critical lines and derivative properties calculations

For phase-equilibria calculations, the commonly used fugacity method is employed (Fotouh and Shukla, 1996). Chemical, thermal and mechanical stability are satisfied by imposing the equality of chemical potentials of each component in the coexisting phases at fixed temperature and pressure. Because SAFT is formulated as an explicit function of temperature, density and phase compositions, the fugacity method is applied by equating chemical potentials and the pressure at a fixed temperature:

$$P^I(T, \rho^I, x^I) = P^{II}(T, \rho^{II}, x^{II}) \tag{5.19}$$

$$\mu_i^I(T, \rho^I, x^I) = \mu_i^{II}(T, \rho^{II}, x^{II}) \tag{5.20}$$

The calculation of critical properties of pure fluids and mixtures is done by numerically solving the necessary conditions (Sadus, 1992), which involves second and third derivatives of the Gibbs free energy with respect to the molar volume (pure systems) or the composition (in mixtures):

$$\left(\frac{\partial^2 G}{\partial x^2} \right)_{P,T} = \left(\frac{\partial^3 G}{\partial x^3} \right)_{P,T} = 0 \tag{5.21}$$

In addition to these equations, classical stability for critical points is required through the extra condition:

$$\left(\frac{\partial^4 G}{\partial x^4} \right)_{P,T} > 0 \tag{5.22}$$

Since the soft-SAFT EoS is given in terms of the Helmholtz energy, its natural thermodynamic variables are temperature, volume, and composition. Hence, it is more convenient to express the critical conditions in terms of derivatives of the Helmholtz free energy with respect to volume and composition, at constant temperature:

$$A_{2x}A_{2v} - A_{Vx}^2 = 0 \qquad\qquad (5.23)$$

$$A_{3x} - 3A_{V2x}\left(\frac{A_{Vx}}{A_{2V}}\right) + 3A_{2Vx}\left(\frac{A_{Vx}}{A_{2V}}\right)^2 - A_{3V}\left(\frac{A_{Vx}}{A_{2V}}\right)^3 = 0 \qquad\qquad (5.24)$$

where the notation $AnVmx = (\delta^{n+m}A/\delta V^n \delta x^m)$ is used for the derivatives of the Helmholtz free energy.

As a further test, derivative properties have been also calculated because, besides their technological importance, there is also a scientific interest in accurately obtaining these properties. As their name specifies, derivative properties are second derivatives of a thermodynamic potential function. They can be obtained by derivation respect to the temperature and density, and all of them are connected by straightforward mathematical relationships. It has been shown that second derivatives are more sensitive to errors than the first derivatives of the thermodynamic function from which they proceed, i.e, while first derivatives may provide accurate results (such as phase equilibria calculations), second derivatives of the same thermodynamic function lead to inaccurate results (heat capacities, speed of sound, etc.) for the same compound. In fact, as pointed out by Gregorowicz and co-authors (1996), the precise description of the features second derivative show is a challenge for any EoS model. For instance, cubic EoS, which have proved to be an accurate method for phase equilibria calculations, are unable to describe some of the singularities observed in the derivative properties, (Gregorowicz et al., 1996) such as the density extrema in isothermal variations of the isochoric heat capacity, isothermal compressibility and speed of sound. Some of these limitations may come from the way in which these classical equations were developed, ignoring some of the microscopic contributions to the macroscopic properties. This physical information may be of relevance when testing the equations for other applications than phase equilibria calculations. For this reason, the use of a crossover molecular equation of state overcomes some of these limitations. The new equation was tested to reproduce the singularities observed in the vicinity of the critical point.

Second-order derivative properties were obtained from the Helmholtz energy and the pressure, which are direct calculations from the soft-SAFT equation. Hence, the expressions for the main derivative properties calculated in this thesis work are:

$$C_v = -T\left(\frac{\partial^2 A}{\partial T^2}\right)_v \tag{5.25}$$

$$k_T^{-1} = \rho\left(\frac{\partial P}{\partial \rho}\right)_T \tag{5.26}$$

$$\mu = T\left(\frac{\partial P}{\partial T}\right)_v - \rho\left(\frac{\partial P}{\partial \rho}\right)_T \tag{5.27}$$

$$\alpha = k_T\left(\frac{\partial P}{\partial \rho}\right)_\rho \tag{5.28}$$

$$C_p = C_v + \frac{T\alpha^2}{k_T\rho} \tag{5.29}$$

$$\omega = \sqrt{\frac{C_p}{C_v}\left(\frac{\partial P}{\partial \rho}\right)_T} \tag{5.30}$$

being C_v the isochoric heat capacity, k_T the reduced bulk modulus, α the thermal expansion coefficient, μ the Joule-Thomson coefficient, C_p the isobaric heat capacity and ω the speed of sound. All these properties were developed for each soft-SAFT contribution, quantifying the different microscopic contributions to the total derivative properties. Regarding the ideal term, note that it contains the de Broglie wavelength, which includes temperature dependence. This directly affects the C_v and C_p calculations, and indirectly the speed of sound. For practical reasons we have used the ideal heat capacity correlations obtained from a database library (Perry and Green, 1999) to complete the calculations.

The two following chapters are devoted to the performance of the new equation for the whole ensemble of thermodynamic properties for pure fluids and mixtures.

C. Results

The essence of knowledge is, having it, to apply it; not having it, to confess your ignorance.

Confucius (BC 551-BC 479)
Chinese philosopher.

6

Pure fluids

In this chapter, the results of this thesis work concerning pure compounds are presented. The chapter is split in three main sections. First of all, the results of the soft-SAFT equation are tested against molecular simulations using the same underlying molecular model. The influence of the crossover parameters is also analyzed. Once the equation has been tested, it is applied to the calculation of several pure fluids of industrial interest. This second section presents results for three different families of hydrocarbons. The molecular model for each family is described, the molecular parameters are fitted to experimental data for the lighter compound and a correlation is calculated to predict the behavior of heavier compounds. The third section is devoted to the implementation of the critical region treatment to a van der Waals type equation of state in order to check the accuracy of the methodology when it is implemented into a cubic equation of state.

6.1. Comparison with molecular simulations[1]

      A main advantage of using a molecular-based equation is that it can be directly compared to simulation results for the same molecular model. In this case, there are two adjustable parameters, those related to the crossover approach, ϕ and L; while m, σ and ϵ are the same in both cases. Several studies have been devoted to the influence of both values (ϕ and L) in predicting the phase envelope when compared to simulation data, and the main results are presented here.

      Figure 6.1 shows the vapor-liquid coexistence curves for several LJ chains. Circles are computer simulation results, (Lofti et al., 1992; Escobedo and de Pablo, 1996; Vega et al., 2003) dashed lines are predictions with the original soft-SAFT equation (Pàmies and Vega, 2001) and solid lines are those obtained from the crossover soft-SAFT equation. As expected, the improvement is significant in the near critical region.
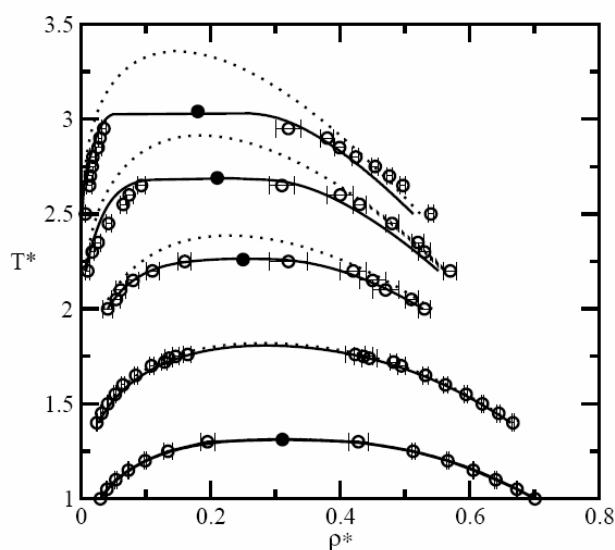
Figure 6.1: *Temperature-density diagram of LJ chains of length m=1, 2, 4, 8 and 16. Circles are simulation data from Lofti et al., 1992; Escobedo and de Pablo, 1996; and Vega et al., 2003. Dotted lines correspond to the original soft-SAFT, and solid lines the soft-SAFT + crossover.*

      The optimized crossover parameters for the LJ chains are given in table 6.1.

---

[1] *The results of this section have been published in the J. Chem. Phys. (Llovell et al., 2004)*

Table 6.1 *Crossover parameters for flexible LJ chains, optimized using simulation data for chain lengths m = 1, 2, 4, 8 and 16*

	ϕ	L/σ
m=1	10.0	1.26
m=2	10.5	1.35
m=4	10.6	1.48
m=8	13.0	1.80
m=16	15.0	2.33

Original soft-SAFT clearly overestimates the critical point for all length chains, except for m = 1. This is due to the fact that the LJ equation used for the reference term in the soft-SAFT equation is a fit to simulation data, including the critical point. The crossover soft-SAFT equation is able to predict the critical region with higher accuracy. Saturated liquid density values are in good agreement with simulation results. Note that vapor densities predictions are also improved compared to the original soft-SAFT equation, although some deviations from the simulation data are still observed. In fact, the crossover treatment takes into account the long-wavelength fluctuations in order to correct the behavior in the near critical region, where these fluctuations are important, but *it does not correct any other limitation the original equation may have*. This means that if soft-SAFT underestimates the vapor densities for long chains away from the critical point, the crossover soft-SAFT equation will also underestimate this density, as it happens for longer chains (m = 8, 16). As pointed out by other authors (Johnson et al., 1994), the original soft-SAFT equation does not consider the intramolecular interactions of chains. This is not a defect of the theory, but a consequence of the first-order perturbation approach used in describing the formation of the chains.

Additional structural information can be introduced into the equation to overcome this problem. The dimer version of the soft-SAFT equation (Blas and Vega, 2001; Pàmies and Vega, 2002) includes more structural information in the Helmholtz free energy, building the chains through LJ dimers, as the reference fluid, instead of monomers. This

improves predictions of LJ chains for vapor densities and in the near critical region (Blas and Vega, 2001). Figure 6.2 shows a comparison with simulation results of m = 8 for the monomer and dimer soft-SAFT versions, with and without the crossover treatment. Here the best fit is shown, with different values of ϕ and L, optimized for each equation. As expected, predictions of vapor densities near the critical region are improved with the dimer version, in both cases (with and without crossover); and the critical point is captured when the crossover treatment is included. However, liquid densities deviate from the simulation results more that those from the soft-SAFT monomer equation.

Figure 6.2: Temperature-density diagram of LJ chains of length m = 8. Circles are simulation data, dotted lines represent monomer and dimer versions of soft-SAFT, and solid and dashed lines represent monomer and dimer versions of the crossover soft-SAFT equation, respectively. For the monomer version, ϕ=13.0 and L=1.80σ, and for the dimer version, ϕ=13.8 and L = 1.56σ.
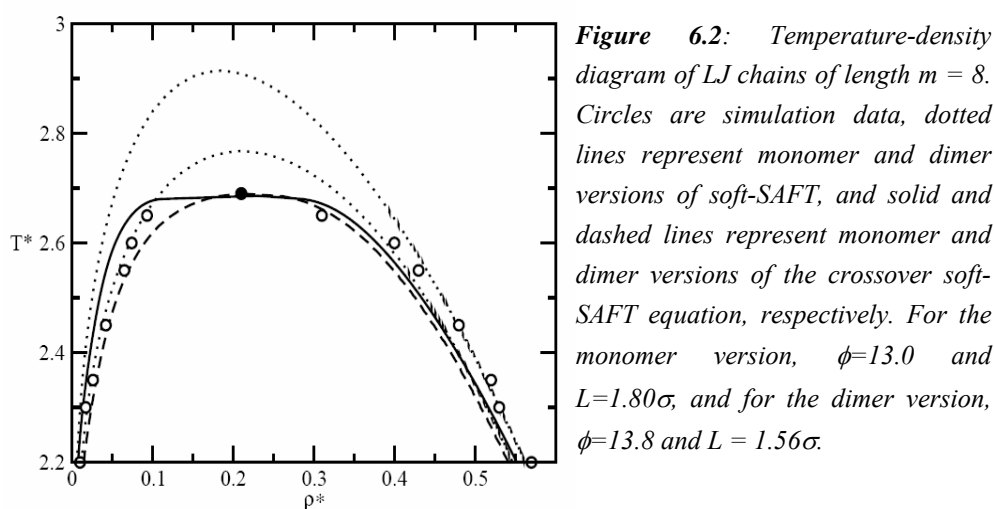
The influence of both adjustable parameters L and ϕ has also been investigated on the phase envelope. As it has been already mentioned, ϕ is used to adjust the critical temperature. Figure 6.3a shows different coexistence curves for several values of ϕ for LJ chains with m = 4, at a constant value of L (= 1.48σ). From bottom to top ϕ = 10, 10.67, 12, 13 and 14. The top curve corresponds to the original soft-SAFT equation, clearly overestimating the critical temperature. As the value of ϕ decreases, the crossover correction becomes more and more important, improving the final result until an optimized value of ϕ = 10.67 is found. Further decreases of its value underestimate the critical point, as observed at the bottom coexistence curve.

The influence of L for a given value of ϕ is shown in figure 6.3b, for the particular case of m = 4, when ϕ = 10.67. The particular values chosen have been L = 1.40, 1.45, 1.48, 1.60, 1.65 and 1.70σ. Again, as it happens when holding L constant while changing ϕ, an optimum value of L is found, 1.48σ, in this case. Shorter values of L are unable to capture the range of the correlations among molecules, even far from the critical point, while larger values of L lead to a mean-field like behavior.

Hence, for the particular case of LJ chains with four segments, the optimum crossover parameters are ϕ = 10.67 and L = 1.48σ. Excellent agreement with simulation results are found in this case, far from and near to the critical point. A compromise should be found regarding the optimization of both parameters for each molecule. Note that since these two parameters are somehow coupled, several combinations of them can provide accurate results.
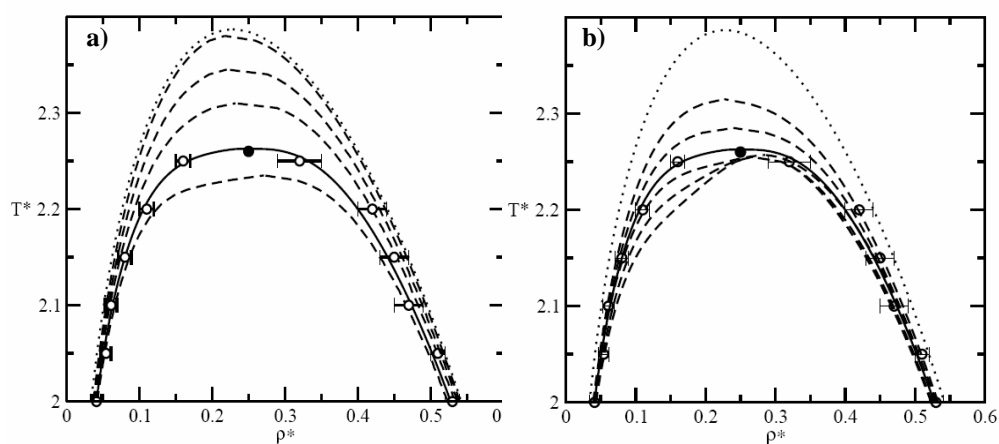
Figure 6.3 *Temperature-density diagram of LJ chains of length m=4.* ***a)*** *Influence of parameter ϕ when L = 1.48σ. Circles are experimental data, the solid line represents the optimized value ϕ=10.6, and the dotted line is the original soft-SAFT. Long-dashed lines are crossover soft-SAFT calculations with ϕ = 10, 12, 13 and 14.* ***b)*** *Influence of cut off length L in the temperature-density diagram of LJ chains of length m = 4, when ϕ = 10.6. L = 1.40, 1.45, 1.48, 1.60, 1.65 and 1.70. Symbols and lines as in 6.3a.*

6.2. Families of pure fluids

Once the accuracy of the equation has been tested with the aid of molecular simulations, it is applied to real fluids, where some additional parameters need to be adjusted. The aim of the generalization of the soft-SAFT equation in this context is to propose a reliable equation for real fluids, accurate enough near to and far from the critical point, and with transferable parameters, able to calculate different kind of properties in a wide range of thermodynamic conditions.

6.2.1. The n-alkanes family[2]

The *n*-alkanes family is selected, due to its relative simplicity, from the modeling point of view, and to its practical importance. Several works have been published concerning its study. A systematic analysis has been done using soft-SAFT (Blas and Vega, 1997; Pàmies and Vega, 2001) and SAFT-VR (McCabe and Jackson, 1999) without any specific crossover treatment. Other works already included a renormalization group treatment, like Jiang and Prausnitz (1999), who implemented White's approach into an equation of state for chain fluids (EOSCF, developed by Hu et al. [1996]). Following a different crossover theory (Kiselev, 1998), McCabe and Kiselev (2004a,b) also included the treatment into the SAFT-VR equation, extending the capabilities of the equation and applying them to the study of this family. Now, the extended soft-SAFT is applied to describe the main thermal behavior of the *n*-alkanes.

n-Alkanes are described as homonuclear chainlike molecules, modeled as *m* Lennard-Jones segments of equal diameter σ, and the same dispersive energy ε, bonded tangentially to form the chain. According to this model, the three molecular parameters plus the crossover parameters ϕ and *L*, are enough to describe all thermodynamic properties.

---

[2] *The results of this section have been published in the J. Chem. Phys. (Llovell et al., 2004) and in the J. Phys. Chem. B (Llovell and Vega, 2006b).*

Since it is known that the three molecular parameters m, $m\sigma^3$ and $m\varepsilon$ increase linearly with molecular weight (Pàmies and Vega, 2001) and $m\phi$ has shown a similar behaviour (Jiang and Prausnitz, 1999), a new set of transferable parameters is proposed as a function of the molecular weight of the compounds, including mL/σ. The correlation comes from optimized parameters for the eight first members of the alkanes series, obtained by fitting experimental saturated liquid densities and vapor pressures, in a similar manner as done by Pàmies and Vega (2001). The values of these parameters are presented in table 6.2.

Table 6.2. *Molecular parameters for the light members of the n-alkanes family (C1-C8).*

	m	σ (Å)	ε/k (K)	ϕ	L/σ
methane	1.000	3.741	151.1	5.50	1.04
ethane	1.392	3.770	207.5	6.20	1.10
propane	1.776	3.831	225.8	6.75	1.16
n-butane	2.134	3.866	240.3	7.25	1.22
n-pentane	2.497	3.887	250.2	7.57	1.27
n-hexane	2.832	3.920	259.8	7.84	1.33
n-heptane	3.169	3.937	266.0	8.15	1.38
n-octane	3.522	3.949	271.0	8.30	1.43

As stated, the molecular parameters can be easily correlated respect to the molecular weight. The new proposed correlation is given by:

$$m = 0.0255 M_w + 0.628 \tag{6.1a}$$

$$m\sigma^3 = 1.68 M_w + 25.4 \tag{6.1b}$$

$$m\varepsilon / k_B = 8.08 M_w + 38.9 \tag{6.1c}$$

$$m\phi = 0.244 M_w + 1.32 \tag{6.1d}$$

$$mL/\sigma = 3.99 \times 10^{-3} M_w + 0.981 \tag{6.1e}$$

Units of σ and ε/k_B are Å and K respectively. M_w is the *n*-alkane molecular weight expressed in g/mol. It is important to stress that this new set of parameters is able to

describe equally well the vapor-liquid equilibria diagram and critical region of these fluids, in contrast to previous correlations, accurate for only one of the two regions.

The experimental critical temperature, pressure and density and those predicted from the original soft-SAFT and the crossover soft-SAFT equation for the first eight members of the *n*-alkanes series are presented in table 6.3.

Table 6.3 *Critical constants for n-alkanes (C$_1$-C$_8$). Experimental data from NIST Webbook.*

	T$_c$ (K)			P$_c$ (MPa)		
n-alkane	Exp.	Crossover soft-SAFT	soft-SAFT	Exp.	Crossover soft-SAFT	soft-SAFT
methane	190.6	190.4	193.3	4.60	4.59	5.10
ethane	305.3	305.0	311.0	4.87	5.07	5.70
propane	369.8	370.2	378.6	4.25	4.43	5.14
n-butane	425.1	425.2	445.2	3.80	3.94	4.70
n-pentane	469.7	469.0	493.7	3.37	3.41	4.29
n-hexane	507.8	507.8	535.5	3.03	2.98	3.88
n-heptane	540.1	539.6	572.7	2.74	2.66	3.57
n-octane	568.9	567.2	603.9	2.49	2.31	3.26

	D$_c$ (mol/L)		
n-alkane	Exp.	Crossover soft-SAFT	Soft-SAFT
methane	10.14	10.79	9.93
ethane	6.87	7.25	6.86
propane	4.96	5.18	4.89
n-butane	3.92	4.06	3.69
n-pentane	3.22	3.37	2.95
n-hexane	2.71	2.87	2.45
n-heptane	2.32	2.47	2.07
n-octane	2.03	1.76	1.79

While soft-SAFT overestimates the critical temperature and pressure, as expected, crossover soft-SAFT is able to predict both critical properties with high accuracy. However, as already observed by other authors using a similar approach, the critical density is slightly overestimated. This is the price paid by fitting the crossover parameters to the critical temperature in the temperature-density diagram.

Figure 6.4a shows the coexistence curve for *n*-pentane, chosen as a member example of the *n*-alkanes series. The purpose of this figure is twofold: to study the influence of the crossover treatment in the phase envelope, with the molecular parameters obtained by fitting with the original soft-SAFT, and to optimize predictions from the equation by fitting new parameters with the crossover treatment included in the equation. Circles are experimental data (NIST), the dotted line represents original soft-SAFT calculations, the dashed line comes from the crossover soft-SAFT equation with the original parameters, and the solid line is from the crossover soft-SAFT equation with the new fitted parameters.
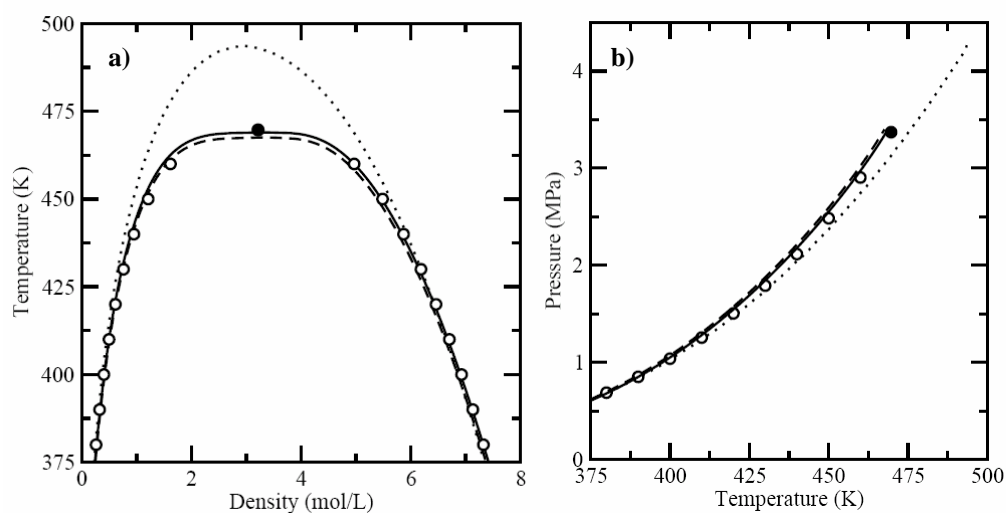
Figure 6.4 a*): Temperature-density diagram for n-pentane. **b)** Pressure-density diagram for n-pentane. See text for details.*

As it can be observed, original soft-SAFT overestimates the critical region, while with the crossover treatment this region is well-described, even with the "old" parameters. The parameters have been readjusted (except the chain length) and excellent agreement has been obtained with the experimental data, also far away from the critical point, where long wavelength fluctuations are unimportant. Figure 6.4b shows the vapor pressure plot of *n*-pentane. It is clearly shown how the original soft-SAFT equation overestimates the critical pressure and how results are improved with the new equation.

Figure 6.5a shows the coexistence curve for the eight first members of the *n*-alkanes series from experimental data and soft-SAFT predictions, with and without the crossover treatment. Agreement is excellent in all cases, correcting the behavior in the critical region due to the incorporation of density fluctuations into the equation. It can hardly be appreciated a slight deviation in the vapor density in *n*-heptane and *n*-octane, the heaviest members represented here. As already discussed in the previous section when compared to simulation data, this is due to the lack of intramolecular chain interactions in the soft-SAFT equation, which becomes more important as the chain length is increased. Figure 6.5b shows vapor pressures for the same members of the series. Again, excellent agreement is obtained in all cases.

Since SAFT is a molecular equation, its molecular parameters can be transferred within the same family, if there are physically sound. A test of the accuracy of the correlations proposed in equations (6.1a-e) is to compare predictions from soft-SAFT with experimental or simulation data for heavier members of the family. Note that these correlations have been obtained just from the eight first members of the series. Phase equilibria predictions for *n*-hexadecane (n-$C_{16}H_{34}$), *n*-tetracosane (n-$C_{24}H_{50}$), *n*-octatetracontane (n-$C_{48}H_{98}$) are shown in figure 6.6. Symbols represent simulation vapor-liquid equilibrium data taken from Nath et al. (1998), while the critical points are from Errington and Panagiotopoulos (1999).
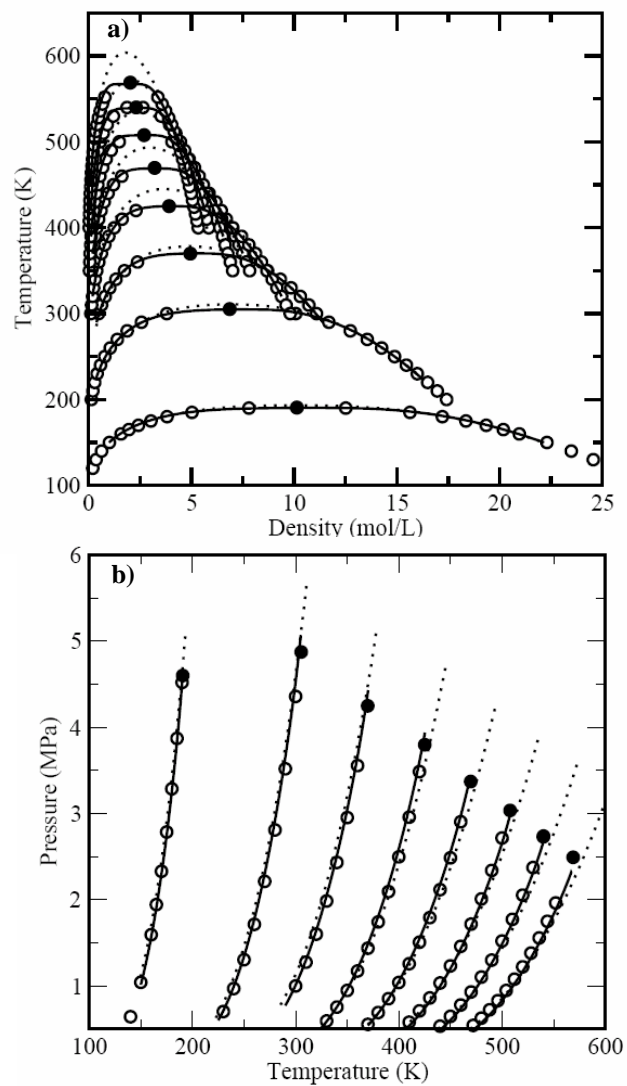
Figure 6.5 *The light members of the n-alkanes series, from methane to n-octane. **a**): Temperature-density diagram **b**) Pressure-density diagram. Symbols represent the experimental data taken from NIST Chemistry Webbook. Dashed lines correspond to soft-SAFT predictions, and the solid line to soft-SAFT + crossover predictions.*
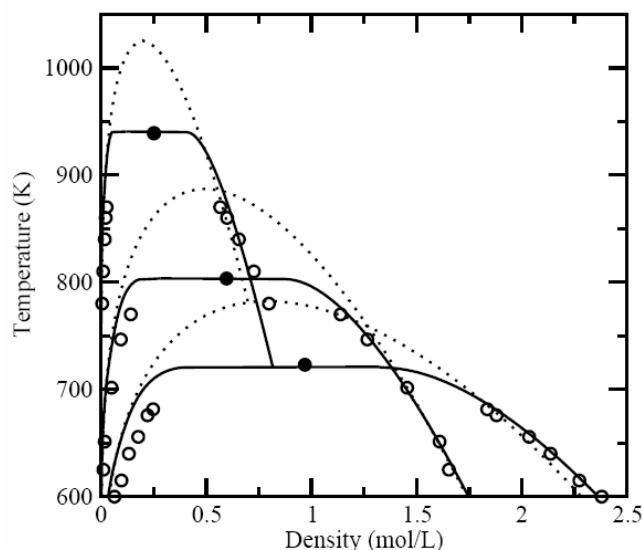
Figure 6.6: *Phase equilibria predictions for n-hexadecane ($C_{16}H_{34}$), n-tetracosane ($C_{24}H_{50}$) and n-octatetracontane ($C_{48}H_{98}$). Circles represent simulation data from Nath et al. (1998). Simulation critical points are from Errington and Panagiotopoulos (1999). Dashed lines correspond to predictions of the original soft-SAFT and solid lines to crossover soft-SAFT.*

Two comments are in order here: soft-SAFT gives excellent predictions for the VLE data, as already shown by Pàmies and Vega (2001)**,** and the new set of parameters is able to capture the whole phase envelope, including the critical region. It is remarkable to see how the crossover parameters adjusted to fit the critical temperature of the light members of the series predict the critical point of the heavier members of the series with the same degree of accuracy.

The accuracy of the equation near to, but above, the critical point has also been tested. It is clear that the modification of the shape of the phase envelope in the critical region will affect the prediction of thermodynamic properties at near-critical conditions. Figure 6.7a presents *n*-butane data for reduced temperatures $T_r = T/T_c$ = 1.05, 1.10 and 1.15. The symbols represent the experimental data taken from the NIST Chemistry Webbook, the dashed lines are predictions from the original soft-SAFT equation, while the solid lines represent the crossover soft-SAFT predictions.

As expected, the original equation is unable to capture the singular behavior of the fluid in the near-critical region; on the contrary, the crossover equation is able to give the

correct shape of the isotherms in this region. In fact, the agreement between the predicted isotherms with the crossover treatment and the experimental data is excellent in all cases, including the high density region. As expected the crossover equation reduces to the original equation as the one leaves the critical region. Three selected supercritical isobars of *n*-butane are presented in figure 6.7b, corresponding to reduced pressures $P_r = P/P_c = 1.05$, 1.10 and 1.15. As for the case of the supercritical isotherms, soft-SAFT with renormalization group corrections gives quantitative agreement with the experimental data, while the original equation overestimates the temperature and pressure in the near critical region, giving an incorrect shape to the curve. The curves shown in figures 6.7 represent pure predictions, since the molecular parameters used in both cases (with and without crossover) were fitted from vapor-liquid equilibrium data (from table 6.2 and the work of Pàmies and Vega [2001], respectively).
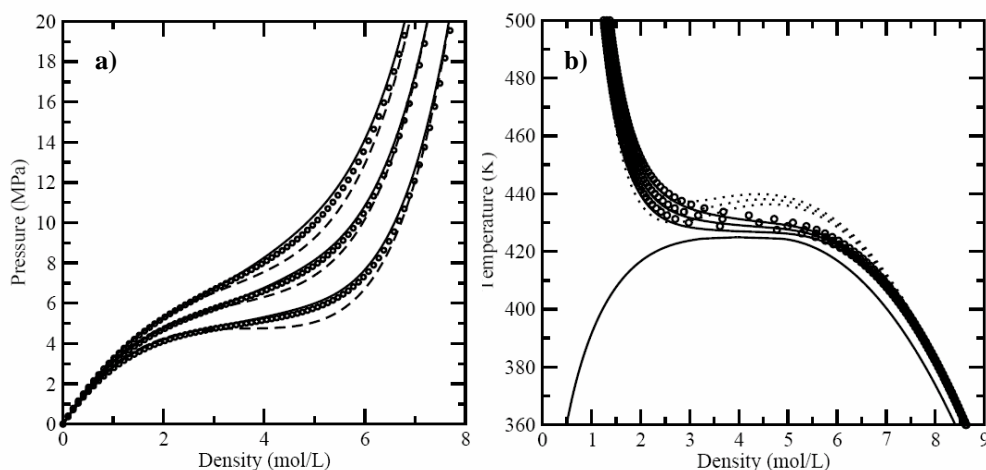
Figure 6.7: a) *Pressure-density diagrams for three temperatures above the critical point, T_r=1.05, 1.10 and 1.15 for n-butane.* ***b)*** *Temperature-density diagrams for three pressures above the critical point, P_r=1.05, 1.10 and 1.15 for n-butane. The predicted coexistence curve is also shown. Circles are experimental data from NIST Chemistry Webbook, dashed lines are original soft-SAFT predictions, and solid lines are crossover soft-SAFT predictions.*

A further test of the equation has been performed by calculating the critical exponents. The β and δ exponents have been obtained by the following equations (Salvino and White, 1992):

$$\ln\left(\frac{\rho_l - \rho_v}{\rho_c}\right) = \beta \cdot \ln\left|\frac{T - T_c}{T_c}\right| + const \; (\rho = \rho_c, T \to T_c^-) \tag{6.2a}$$

$$\ln\left|\frac{\mu - \mu_c}{\mu}\right| = \delta \cdot \ln\left|\frac{\rho - \rho_c}{\rho}\right| + const \; (T = T_c, \rho \to \rho_c) \tag{6.2b}$$

where $\rho_{l,v}$ are the coexistence densities values and μ is the chemical potential.

Since the procedure is the same in all cases, propane has been selected as an example for calculations; results for the rest of the *n*-alkanes studied are very similar and are omitted here. The critical exponent values obtained for propane $\beta = 0.331 \pm 0.009$ and $\delta = 4.82 \pm 0.04$. These values are in accordance to the universal critical values provided by modern critical phenomena theory (Wyczalkowska et al., 2004), within the error bars, implying that the equation and the molecular parameters used in the model reproduce the correct asymptotic behavior close to the critical point. Furthermore, by using the scaling law relation $\gamma = \beta(\delta - 1)$, a value of γ=1.264 is obtained, within the range of the experimental universal critical exponent values. The β exponent was calculated for temperatures between 0.2% and 1.5% below the critical point. The log-log plot of $\Delta\rho/\rho_c$ versus $\Delta T/T_c$ is shown in figure 6.8a, for the range of temperatures considered. The value of β was obtained from the slope of the linear regression to this data. A value of five iterations was enough to obtain accurate results for β. The δ exponent was calculated in a similar manner, by plotting $\Delta\mu/\mu_c$ versus $\Delta\rho/\rho_c$ in a log-log graph. As in previous works (Salvino and White, 1992), higher values of n were needed in order to obtain accurate results; a value of n = 7 iterations was enough to accurately obtain the chemical potential isotherm in our case. The value of δ was found by averaging the two slopes of the regression lines, representing the two sets of data, one from densities below the critical point and the second one from densities above the critical point. The log-log plot is shown

in figure 6.8b, for the range of densities considered. The points used for the regressions were in the range $0.1 < |\Delta\rho/\rho_c| < 0.3$ and $0.005 < |\Delta\mu/\mu_c| < 0.1$.
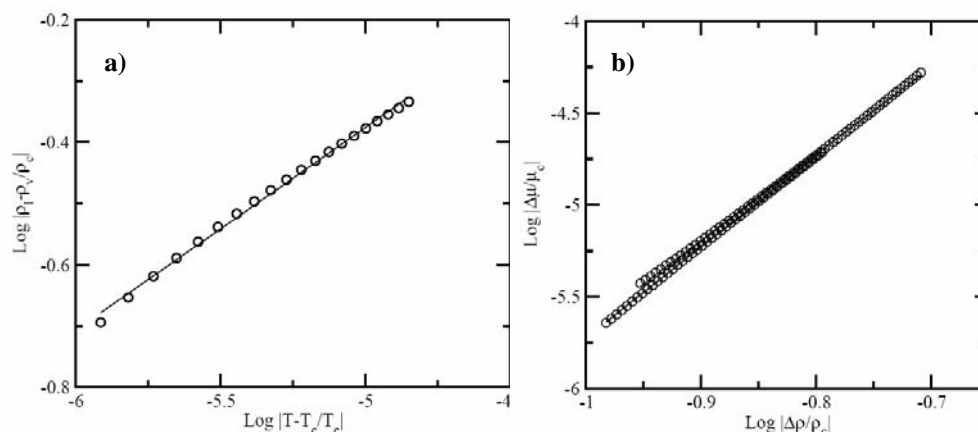
Figure 6.8: *Determination of the critical exponents for propane **a**) β critical exponent **b**) δ critical exponent. Circles are obtained from the crossover soft-SAFT EoS, and the solid line is the regression of these points. The value of δ is found by averaging the slope of the two fitted solid lines (see text for details).*

The thermodynamic behavior of a fluid also includes the prediction of other properties outside the phase diagram. As it has been said, derivative properties are crucial in order to understand the behavior of a compound. Till now, the number of published works related to the application of molecular-based EoS to derivative properties is very scarce. Colina et al. (2002) have shown the validity of soft-SAFT to predict the inversion curves of pure heavy *n*-alkanes, impossible to obtain with accuracy with classical EoSs (Segura, 2003); however, no systematic study on the behavior of the equation for other derivative properties was performed at that time.

In a very recent paper, Laffite at al. (2006) have published the application of different versions of SAFT (PC-SAFT [Gross and Sadowski, 2001] , SAFT-VR [Gil-Villegas et al, 1997], SAFT-VR LJC [Davies et al., 1998] and a modified SAFT-VR EoS, named SAFT-VR Mie [Lafitte et al., 2006]) to the calculation of derivative properties of n-

alkanes. They first checked the performance of the PC-SAFT, SAFT-VR and SAFT-VR LJC EoS's to obtain derivative properties with molecular parameters obtained by fitting vapor-liquid equilibrium data. They focused on the derivative properties of condensed liquid phases at selected temperatures and plotted them as a function of pressure; no calculations near the critical region were considered in this study. Results obtained with the different equations and the original parameters provided poor agreement as compared to experimental data. Hence, assuming the problem in accurately describing the derivative properties was the description of the repulsive interactions between the monomers forming the chain, they modified this term in the SAFT-VR equation, proposing the SAFT-VR Mie equation. This implies the addition of an extra parameter related to the shape of the repulsive part of the potential between monomers forming the chains. In addition, they used a fitting procedure in which two types of properties were included, vapor-liquid equilibrium data and the speed of sound in the condensed liquid phase. The new SAFT-VR Mie equation and the extended fitting procedure showed better agreement with experimental vapor-liquid equilibria and speed of sound data than the other SAFT equations (with the original parameters); notice that both type of properties were included in the fitting procedure. However, the new parameters provided poor agreement when compared to experimental isobaric heat capacities (nothing was mentioned above the isochoric heat capacities). The authors attributed these deviations to the need of further refinements of the Mie potential model, including higher order perturbation terms. Although they did not mention it, the fact is that this property was not included, directly or indirectly, into the fitting procedure. The deviations with respect to experimental data can also be due to this fact, showing, in this case, the lack of transferability of the parameters for predicting properties not included in the fitting set. This work is a clear step forward on testing the accuracy of SAFT-type equations for describing derivative properties. A point raised by Laffite et al. (2006) is the need of an accurate description of the reference potential for precisely describing derivative properties; the investigation of the performance of the soft-SAFT equation, which includes an accurate Lennard-Jones equation as the monomer reference term, is of great relevance in this context.

This work evaluates next the singular behavior of derivative properties in the vicinity of the critical point of the members of the *n*-alkane family. In this calculation, there is not any additional molecular parameter fitting. As derivative properties were not included in the fitting, results obtained are pure predictions of the equation. The compounds are selected depending on the available experimental data of systems near to and above the critical point of the compounds, for comparative purposes.

Results for propane are shown as an illustrative example in Figure 6.9. The data used for comparison were taken from the correlated data provided in the NIST Chemistry Webbook. Figure 6.9a depicts the vapor-liquid equilibria as obtained by two versions of soft-SAFT (with and without a crossover treatment) versus a correlation to the experimental data of propane (NIST Chemistry Webbook) from which the molecular parameters were obtained. As already shown in Figures 6.4 and 6.5., the addition of long-range density fluctuations in the vicinity of the critical point improves the critical region, while keeping the accuracy of the original equation far from the critical point. Figures 6.9b-6.9e show the residual isochoric heat capacity, residual isobaric heat capacity, isothermal compressibility, the Joule-Thomson coefficient and speed of sound of propane. The chosen reduced temperatures for comparison where $T^* = T / T_c$ = *1.1, 1.25* and *1.5*. T_c is the critical temperature of the fluid (three different values are used in this case, the experimental, that obtained from the original soft-SAFT and the equivalent one with crossover soft-SAFT). The overall agreement is very good in all cases. The largest deviations are obtained for the residual heat capacities very close to the critical point. Soft-SAFT with the original parameters is able to capture the extrema (maxima and minima) in very good agreement with the experimental data, except very close to the critical region.
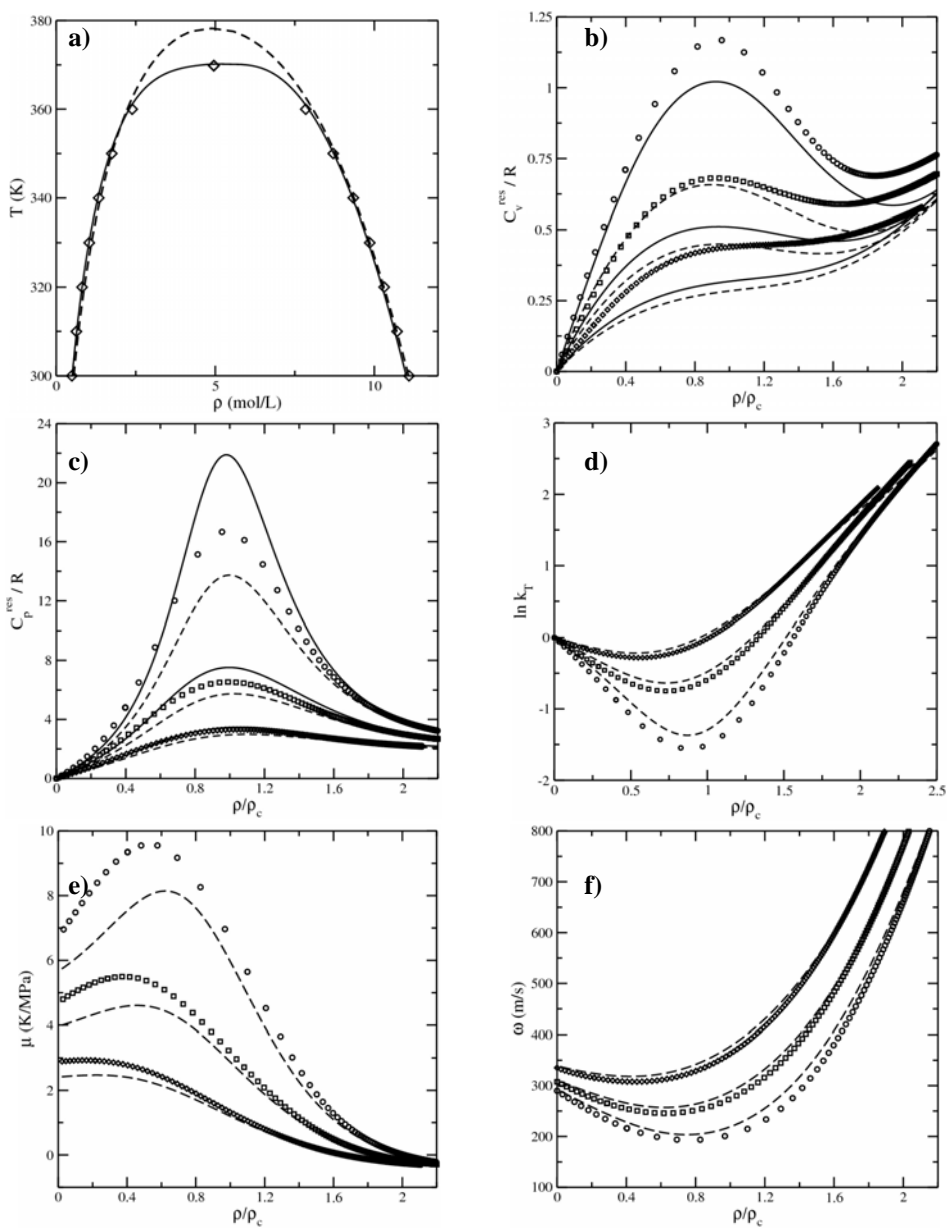
Figure 6.9: *The behavior of n-propane. **a)** temperature-density diagram. **b)** residual isochoric heat capacity. **c)** residual isobaric heat capacity. **d)** isothermal compressibility. **e)** the Joule-Thomson coefficient. **f)** speed of sound.*

Symbols represent correlation data obtained from NIST Chemistry Webbook, while the solid line stands for calculations performed with the crossover soft-SAFT equation and the dashed line with the original soft-SAFT equation. Derivative properties were calculated at three different reduced temperatures 1.1, 1.25 and 1.5 and all of them are represented versus reduced density.

The crossover treatment improves estimations for heat capacities (see Table 6.4, where the absolute average deviation of the soft-SAFT and crossover soft-SAFT calculations respect to the correlated data is shown for the compounds exposed in this section). However, no appreciable changes were observed for the rest of the derivative properties, and hence the results for these properties are presented with the original equation (it is unnecessary to use a technique that implies a greater computational effort to obtain the same result). It is striking to observe the excellent agreement predicted for the speed of sound; in fact, and due to way in which this property is obtained (see equation 5.30), the speed of sound is the derivative property most sensitive to deviations. The excellent agreement obtained here acts in favor of the reliability of the soft-SAFT equation for predicting this property.

Table 6.4: *Absolute average percentage deviation (AAD%) of isochoric and isobaric heat capacities for n-propane, n-heptane. Results were obtained at temperatures above the critical point, using the original soft-SAFT and crossover soft-SAFT equations.*

Compound	Property	T / T_c	AAD % Res. Value soft-SAFT	AAD % Res Value crossover-soft-SAFT
n-propane	C_v	1.10	32.7	10.9
		1.25	27.9	18.6
		1.50	25.9	19.0
	C_p	1.10	13.6	12.2
		1.25	10.9	9.7
		1.50	9.20	7.2
n-heptane	C_v	1.10	55.9	38.2
	C_p	1.10	24.0	13.5

It has been observed that although the equation is able to capture the behavior of these properties in all cases, the agreement with correlated experimental data deteriorates as the chain length increases. Results for *n*-heptane are shown as an example in Figure 6.10. As in the previous case, the molecular parameters of the equation were taken from table 6.2 (crossover soft-SAFT) and the work of Pàmies and Vega (2001) (original soft-SAFT). The total and residual isochoric heat capacities are shown in Figures 6.10a and 6.10b, while Figures 6.10c and 6.10d depict the isobaric residual heat capacity and the speed of sound, respectively. Comparisons with correlated data are presented just for a reduced temperature of *1.1* because this is the only available data. Note that, as shown in Figure 6.9, this is precisely the reduced temperature at which greater deviations were found for propane. The best results obtained from the original equation are those related to the speed of sound, while significant deviations are observed for the residual heat capacities close to the critical point (see Table 6.4). The crossover term clearly improves the isobaric heat capacity and the speed of sound descriptions, providing almost quantitative agreement, except very close to the critical density, in both cases. Although the isochoric heat capacities improve with respect to the soft-SAFT Eos without the crossover correction, results are still far from being accurate with either version of the equation.

Soft-SAFT has also been used in the same manner for the rest of the light members of the *n*-alkanes series, showing similar trends. A summary of the main results obtained with the original equation is provided in Table 6.5, where the absolute average percentage deviations (AAD%) in heat capacities and speed of sound for selected members of the series (methane, *n*-propane, *n*-hexane and *n*-heptane) are presented. The reduced temperatures studied were $T^* = T / T_c = 1.1$, in all cases, and *1.25* and *1.5* when available.

The AAD% of the total values are always very small (less than 5% in most of the cases), even close to the critical point. This is a direct consequence of the absolute value the ideal contribution has for these properties. On the contrary, the residual properties show greater AAD%. It should be kept in mind that these properties are obtained with the original equation using parameters from vapor-liquid equilibrium data. It is also important

to emphasize that these results for residual heat capacities are of the same order than those obtained from Laffite et al. (2006) with parameters fitted to vapor-liquid equilibria and the speed of sound simultaneously.
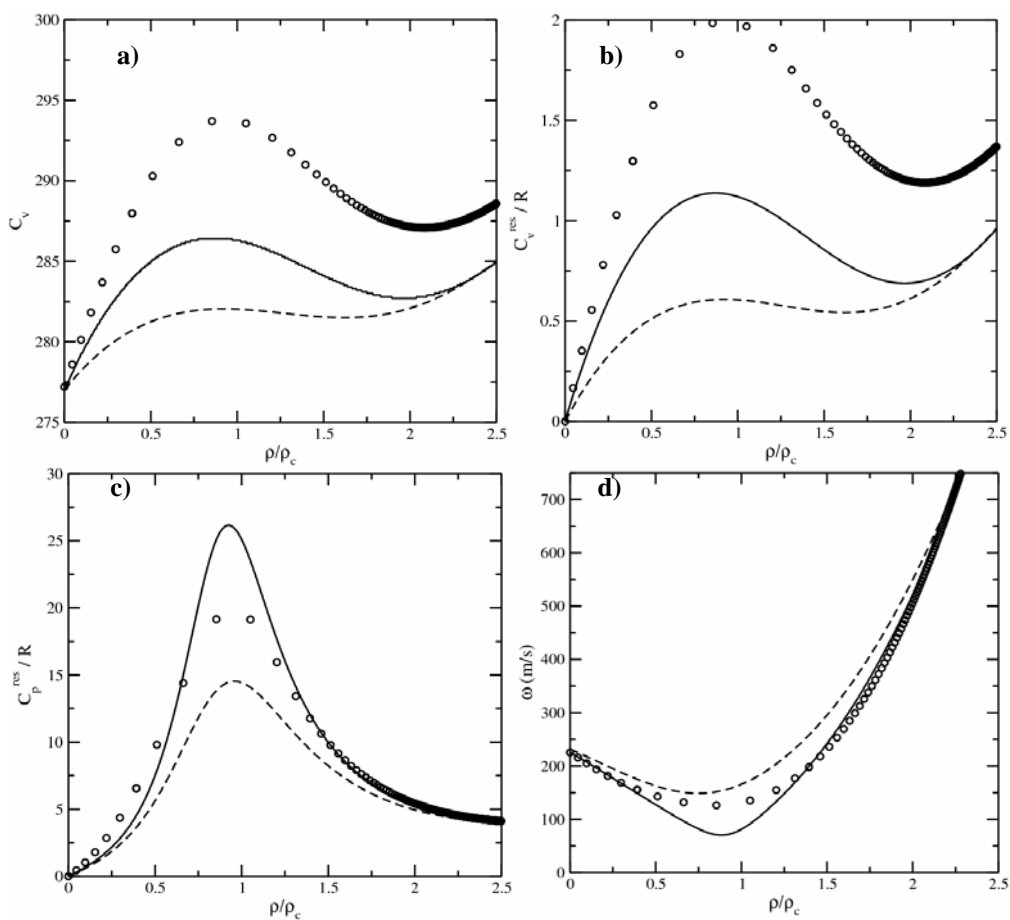
Figure 6.10: *The behavior of n-heptane. **a)** total isochoric heat capacity. **b)** residual isochoric heat capacity. **c)** residual isobaric heat capacity. **d)** speed of sound. Calculations are done at a reduced temperature of 1.1. Notation as in Figure 6.9.*

Table 6.5: *AAD% for residual and total isochoric and isobaric heat capacities, and speed of sound, for several n-alkanes at temperatures above the critical point, as obtained with the soft-SAFT equation.*

Compound	Property	T / T_c	AAD % Res Value	AAD % Total Value
methane	C_v	1.10	25.3	4.21
		1.25	19.8	2.49
		1.50	14.9	0.806
	C_p	1.10	9.72	5.48
		1.25	6.38	3.80
		1.50	3.19	1.46
	ω	1.10	---	3.11
		1.25	---	2.54
		1.50	---	1.82
n-propane	C_v	1.10	32.7	4.26
		1.25	27.9	1.07
		1.50	25.9	0.821
	C_p	1.10	13.6	4.61
		1.25	10.9	1.62
		1.50	9.20	1.17
	ω	1.10	---	5.91
		1.25	---	3.48
		1.50	---	2.88
		1.25	---	5.19
n-hexane	C_v	1.10	50.0	1.02
	C_p	1.10	27.7	4.87
	ω	1.10	---	20.2
n-heptane	C_v	1.10	55.9	1.46
	C_p	1.10	24.0	3.44
	ω	1.10	---	20.7

Regarding Table 6.5, it can be noticed that the greater deviations are obtained for the speed of sound of *n*-hexane and *n*-heptane, a direct consequence of the inaccuracy of the equation in providing the isochoric heat capacity of these compounds (see Figure 6.10a and Figure 6.10b).

Till now, the interest has been centered in the performance of the equation near the critical region. However, it is also interesting to see the behavior of the derivative properties far away of this region. As an example, Figure 6.11 shows speed of sound predictions for *n*-heptane at three different pressures, ranging from 0.1 MPa to 101.3 MPa. The AADs% for n-heptane range between 6.2% for 0.1MPa and 5.5% for 101.3MPa.

Although the equation is able to capture the correct trend, an underestimation of this property compared to the experimental data (Dzida and Ernst, 2003) is obtained in all cases. The deviations become more pronounced as the pressure increases. It can be established that as far as the *n*-alkanes series is concerned, the deviations obtained for the speed of sound with the soft-SAFT equation do not strongly depend on pressure, being always of the same order.
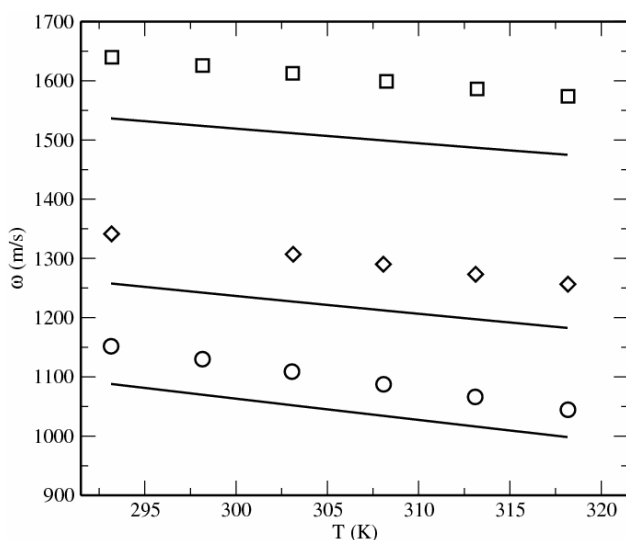
Figure 6.11: *Speed of sound-temperature diagram of heptane at 0.1 MPa, 30.4 MPa and 101.3 MPa. Symbols represent the experimental data taken from Dzida and Ernst (2003). Solid lines correspond to soft-SAFT predictions.*

A main advantage of having a molecular-based equation to perform the calculations is that the different microscopic contributions to the total derivative properties can be separated and quantified. Taking advantage of the way in which soft-SAFT is written, the reference term (segments forming the chain) and the chain term (way in which these different segments are jointed) into the derivative properties have been separated for analysis. This methodology helps to identify the leading contributions in each compound and acts in favor of a better understanding of the physics of the fluid. Moreover, the knowledge of the dominance of a particular term can be used for further modifications in the equation in order to improve the prediction of different thermodynamic properties.

Results for the residual isochoric heat capacity and the isothermal compressibility at a constant temperature of 1.1 times their critical value are shown as representative of an energetic and a volumetric property, respectively. They have been chosen because these two properties do not depend on the other derivative properties (see equations 5.25 and 5.26). Figures 6.12a-d depict results for ethane and *n*-heptane. All properties are calculated without the crossover term. Figures 6.12a and 6.12b represent the isochoric heat capacity as a function of the temperature for ethane and *n*-heptane respectively. The ideal term has been omitted for clarity (it is just a straight line at constant temperature). Results for the isothermal compressibility for the same two compounds are shown in Figures 6.12c and 6.12d.

The representation of the isochoric heat capacity looks quite similar because the increasing value of the chain length (reference term) in *n*-heptane is balanced by an increasing negative contribution of the chain term. It results in a similar soft-SAFT prediction for the isochoric heat capacity for both, a short and a longer alkane.

When analyzing the figures of the isothermal compressibility, it can be observed that, although both curves also present the same qualitative trend, the number of segments becomes the dominant term as the chain length increases. This is a result to be expected intuitively, since this property depends on the volume occupied by the molecules (see equatrion 5.26).
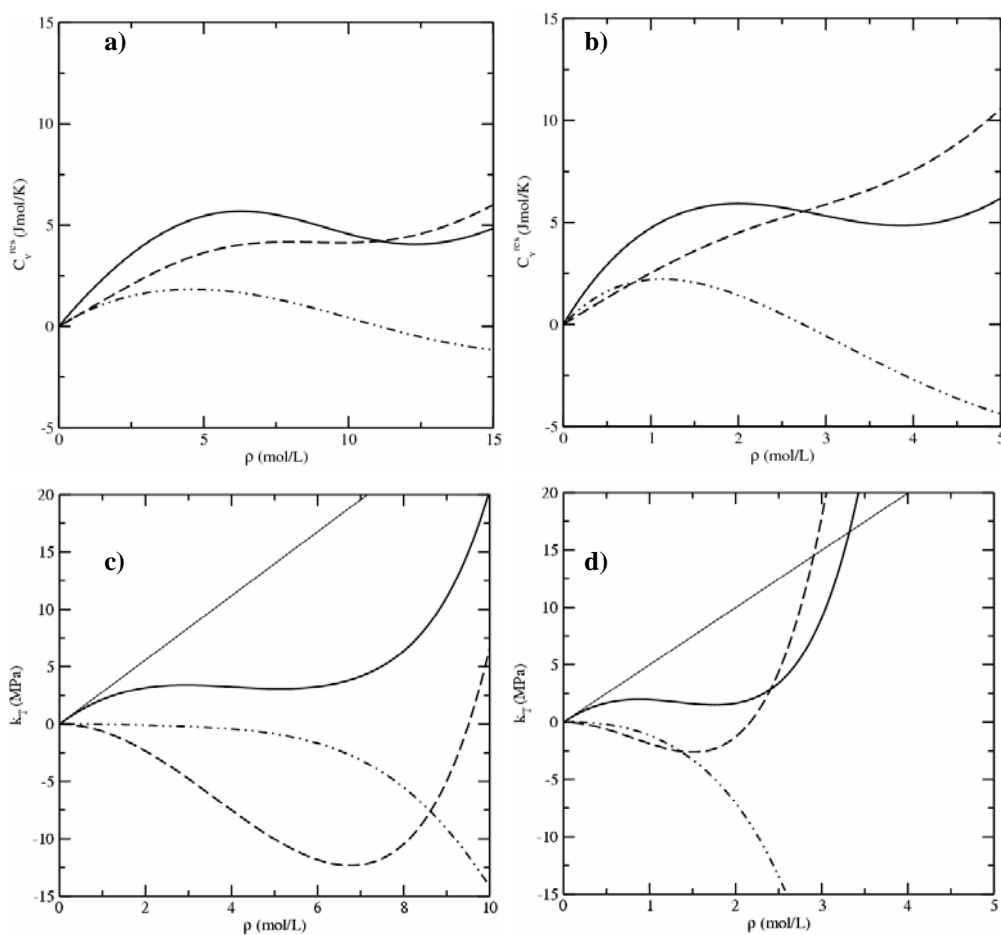
Figure 6.12: *Analysis of the different microscopic contributions to some derivative properties as obtained by the soft-SAFT equation. **a)** isochoric heat capacity of ethane. **b)** isochoric heat capacity of n-heptane. **c)** isothermal compressibility of ethane **d)** isothermal compressibility of n-heptane Solid line: total residual value; dashed line: segment term contribution; dashed-double dotted: chain term contribution.*

6.2.2. The 1-alkanols family[3]

The 1-alkanols family constitutes another hydrocarbon series of great interest from both the industry and the academic point of view. Alcohols are in wide use in industry and science as reagents, solvents, and fuels. Ethanol and methanol can burn more cleanly than gasoline or diesel. Because of its low toxicity and ability to dissolve non-polar substances, ethanol is often used as a solvent in medical drugs, perfumes, and vegetable essences such as vanilla. In organic synthesis, alcohols frequently serve as versatile intermediates. In the kitchen, alcoholic beverages are added to dishes not only for their inherent flavors, but also because the alcohol dissolves flavor compounds that water cannot.

From a theoretical point of view, they are strong associating molecules due to the presence of a hydroxyl group. For this reason, they tend to have higher boiling points than the corresponding *n*-alkanes. Moreover, the polarity due to the hydroxyl group makes the shortest member in the series (methanol, ethanol and 1-propanol) soluble in water.

Following the work done by Blas and Vega (1997) and Pàmies (2003), *1*-alkanols can be modeled as homonuclear chainlike molecules of equal diameter σ and the same dispersive energy ε. The hydroxil group in alkanols is mimicked by two square-well sites embedded off-centre in one of the LJ segments, with volume k_{HB} and association energy ε_{HB}. According to the model, these five molecular parameters (plus the crossover parameters ϕ and L), are enough to describe all thermodynamic properties. As it was done for the *n*-alkanes, all the parameters have been calculated fitting experimental saturated liquid densities and vapor pressures for each compound. Since the length of the chain should not affect the strength of the association bonds, except for very short molecules, the parameters of the association sites are set at constant values, except for methanol and ethanol.

The values of the fitted molecular parameters are presented in Table 6.6. All the parameters show physical trends (i.e. they increase as the molecular weight of the

---

[3] *The results of this section have been published in the J. Phys. Chem. B (Llovell and Vega, 2006a/b).*

compound increases, until they reach an asymptotic value for relatively long chains, as it should happens, since this is a united atom approach). The exception is methanol, which is already known for its anomalous behavior.

Table 6.6. *Molecular parameters for the 1-alkanols (C1-C8).*

	m	σ (Å)	ε/k (K)	ϕ	L/σ	ε^{HB}/k_B (K)	k^{HB} (Å^3)
methanol	1.481	3.390	227.4	7.70	1.390	3193	4907
ethanol	1.710	3.659	240.0	7.00	1.300	3470	2300
1-propanol	1.941	3.815	249.8	7.30	1.320	3600	2300
1-butanol	2.210	3.934	266.5	7.65	1.350	3600	2300
1-pentanol	2.470	4.020	279.5	7.83	1.370	3600	2300
1-hexanol	2.686	4.110	291.0	8.00	1.380	3600	2300
1-heptanol	2.920	4.170	299.5	8.10	1.390	3600	2300
1-octanol	3.148	4.212	306.0	8.25	1.395	3600	2300

As done in previous works with soft-SAFT (Blas and Vega, 1998; Pàmies and Vega, 2001; Llovell et al., 2004), a correlation from optimized parameters for the eight first members (excepting methanol) of the *1*-alkanols series is obtained:

$$m = 0.0173 M_w + 0.921 \tag{6.3a}$$

$$m\sigma^3 = 1.83 M_w - 0.725 \tag{6.3b}$$

$$m\varepsilon / k_B = 6.73 M_w + 93.1 \tag{6.3c}$$

$$m\phi = 0.168 M_w + 4.31 \tag{6.3d}$$

$$mL / \sigma = 0.0262 M_w + 1.03 \tag{6.3e}$$

Units of σ and ε/k_B are Å and K respectively. M_w is the *1*-alkanol molecular weight expressed in g/mol. The advantage of having a correlation is the ability to describe heavier

1-alkanols with the same degree of accuracy through the parameters extrapolation from these correlations. Moreover, this new set of parameters is able to describe equally well the vapor-liquid equilibria diagram and critical region of these fluids, in contrast to previous correlations, accurate for only one of the two regions.

As done before, the experimental critical temperature, pressure and density and those predicted from the original soft-SAFT and crossover soft-SAFT for the first eight members of the 1-alkanols series are presented in table 6.7 for comparison.

The values obtained show the same tendencies observed in the *n*-alkanes series. Good accuracy is obtained for the critical temperature and pressure values with the crossover treatment, while the critical density is overestimated. A correct evaluation of the density poses an interesting feature. The fact of correcting the long-range fluctuations of the critical region derives in a change of the shape of the curve, which is becoming almost planar in the critical point. It means that a extremely small change in temperature will modify the density in a significant way. This is the main reason for the inaccuracies observed in the critical density.

Table 6.7 *Critical constants for 1-alkanols (C_1-C_8).Experimental data from Smith and Srivastava (1986)*

	T_c (K)			P_c (MPa)		
1-alkanol	Exp.	Crossover soft-SAFT	soft-SAFT	Exp.	Crossover soft-SAFT	soft-SAFT
methanol	512.6	513.0	541.7	8.10	8.13	10.92
ethanol	513.9	514.6	540.5	6.15	6.30	8.47
1-propanol	536.8	537.4	561.0	5.17	5.24	7.06
1-butanol	563.1	563.5	588.1	4.42	4.69	5.96
1-pentanol	588.1	588.2	616.5	3.90	4.06	5.18
1-hexanol	611.4	611.9	642.3	3.51	3.65	4.53
1-heptanol	633.0	633.4	668.4	3.06	3.18	4.06
1-octanol	655.0	653.9	695.3	2.78	2.82	3.70

1-alkanol	Exp.	Crossover soft-SAFT	Soft-SAFT
		D_c (mol/L)	
methanol	8.48	7.61	7.96
ethanol	5.99	5.64	5.60
1-propanol	4.55	4.25	4.31
1-butanol	3.85	3.84	3.42
1-pentanol	3.06	3.14	2.81
1-hexanol	2.63	2.87	2.35
1-heptanol	2.30	2.50	2.02
1-octanol	2.01	2.19	1.76

Figure 6.13a shows the coexistence curve for the eight first members of the *n*-alkanols series. Circles are experimental data (Smith and Srivastava, 1986) while the solid line is from the crossover soft-SAFT equation. Agreement is excellent in all cases, correcting the behavior in the critical region due to the incorporation of density fluctuations into the equation. Figure 6.13b shows vapor pressures for the same members of the series. Again, excellent results are achieved.

Following the same procedure used for the *n*-alkanes, the evaluation of other properties outside the phase diagram remains an interesting test for the equation of state. Concerning the 1-alkanols derivative properties it is necessary to mention the work of Kiselev and coworkers (2000), who published the application of a crossover version of the original SAFT equation to obtain the thermodynamic properties of propan-1-ol. They calculated isochoric and isobaric specific heats, speed of sound, PVT, and VLE data far from and close to the critical region. They obtained excellent agreement with available experimental data. It seems to be the first published work on the application of a SAFT-type equation to the calculation of main derivative properties of a compound; unfortunately,

the extensive study was performed just for one compound and no systematic studies for other families of compounds was done.

The present work evaluates several compounds of the 1-alkanols family to give a general overview of the performance of the crossover equation for these properties. As it was done before, the optimized molecular parameters are used without any further adjustment to check the accuracy of the predictions.
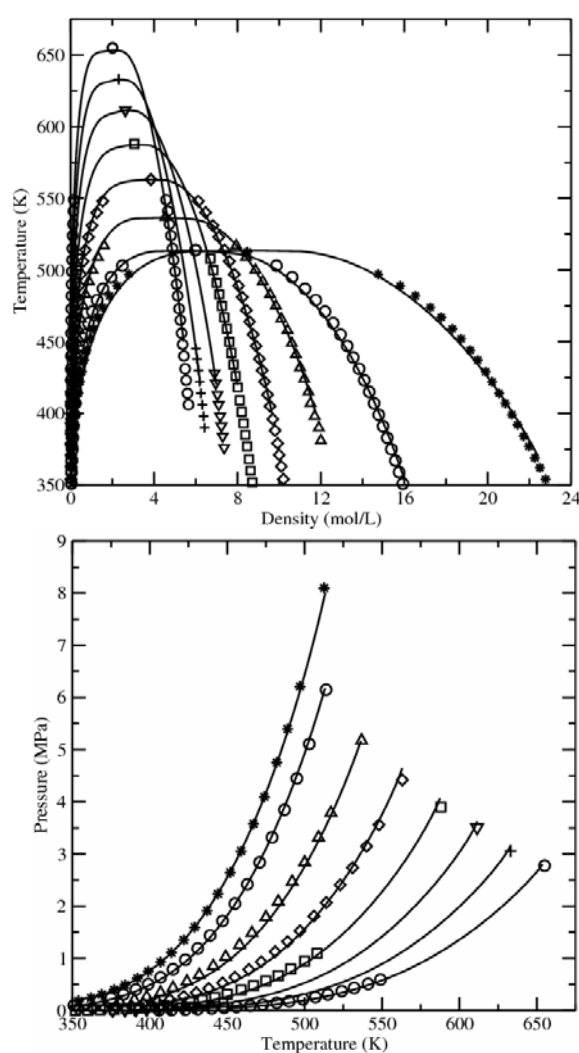
Figure 6.13 *Phase equilibrium diagram for the light members of the 1-alkanols series, from methanol to 1-octanol.*
a) *Temperature-density diagram*
b) *Pressure-density diagram.*
Symbols represent the experimental data taken from Smith and Srivastava (1986) and the critical points are from reference NIST Chemistry Webbook. Lines represent crossover soft-SAFT predictions.

Figure 6.14 shows some selected results for methanol. Figure 6.14a represents the phase equilibrium envelope for this compound while Figures 6.14b, 6.14c and 6.14d show the residual isochoric heat capacity, the residual isobaric heat capacity and the speed of sound, respectively, all of them at two reduced temperatures of *1.1* and *1.2*. As in the previous figures the soft-SAFT calculations with and without the crossover term are compared with correlated data taken from NIST Chemistry Webbook.
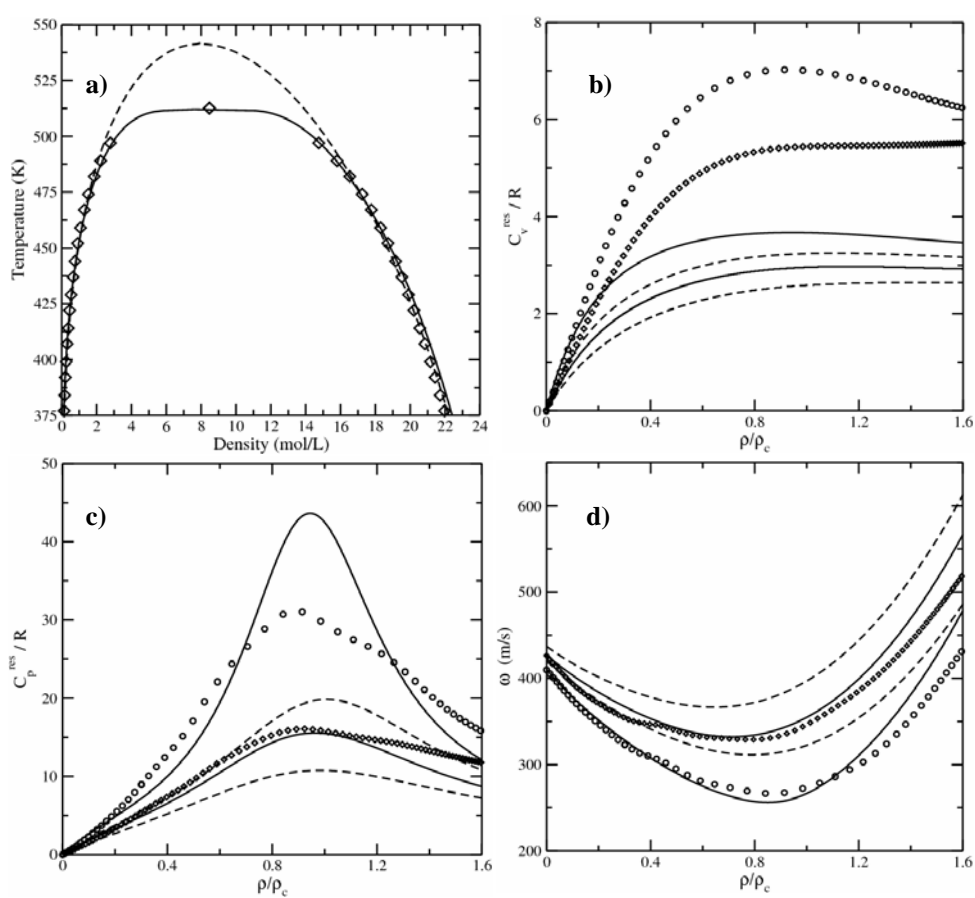
Figure 6.14: *The behavior of methanol. **a)** temperature-density diagram. **b)** residual isochoric heat capacity. **c)** residual isobaric heat capacity. **d)** speed of sound. Figures b), c) and d) were obtained at two reduced temperatures of 1.1 and 1.2. Notation as in 6.9.*

Figure 6.14a shows how accurate the optimized parameters are for the evaluation of the phase envelope. Looking at the heat capacities and the speed of sound, it is seen that, although the soft-SAFT equation is also able to capture the singular behavior of isothermal derivative properties of methanol versus density, important deviations with respect to the correlated experimental (NIST Chemistry Webbook) data are obtained, especially for the residual heat capacities.

Note that, as for the case of *n*-alkanes, the crossover term greatly improves the description of the isobaric heat capacity (see Table 6.8, where the absolute average deviation for C_v and C_p with and without crossover for methanol is provided at the two selected temperatures) and the speed of sound, except very close to the critical density and in the high density region. It has not been possible to find a clear explanation of the deviations obtained for the isochoric heat capacities and further research in this line should be performed. Probably, a global fitting including this property would improve their results.

Table 6.8: *Absolute average percentage deviation (AAD%) of isochoric and isobaric heat capacities for methanol. Results were obtained at two reduced temperatures above the critical point, using the original soft-SAFT and crossover soft-SAFT equations.*

Compound	Property	T / T_c	AAD % Res. Value soft-SAFT	AAD % Res Value crossover-soft-SAFT
methanol	C_v	1.10	50.3	40.1
		1.20	50.1	41.6
	C_p	1.10	34.4	18.4
		1.20	30.5	10.0

Although the description of the isobaric heat capacity versus density in the proximities of the critical point is not well reproduced, the soft-SAFT equation is able to capture the behavior of this property versus pressure in almost quantitative agreement with experimental data. Figure 6.15 depicts the total isobaric heat capacity of methanol as

obtained by the original soft-SAFT equation versus pressure as compared to experimental data (Vargaftik et al., 1996) at three temperatures: 533, 553 and 573K.
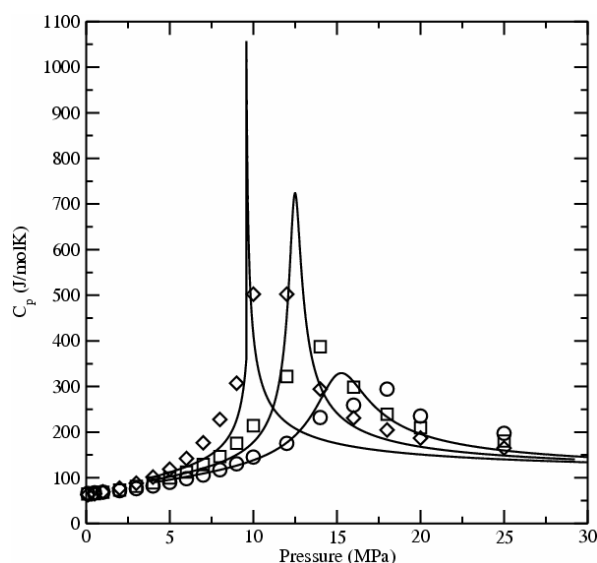
Figure 6.15: *Total isobaric heat capacity of methanol at three near critical isotherms, T= 533.15, 553.15 and 573.15 K. Symbols represent the experimental data obtained from Vargaftik et al. (1996) while the lines represent soft-SAFT calculations without a crossover term.*

Table 6.9 provides results obtained from the original soft-SAFT equation for other members of the 1-alkanol series. The obtained AAD% of the residual and total derivative properties versus available experimental data is presented. Results for methanol (Varkaftik et al., 1996) are given at constant temperature, while results for *1*-propanol (Peleteiro et al., 2001; Dzida and Ernst, 2003), *1*-hexanol (Fulem et al., 2002) and *1*-heptanol (Fulem et al., 2002) are specified at different pressure values, in accordance to the experimental data.

Again, soft-SAFT provides small AAD% for the total values, while the AAD% are greater for the residual values. It should be noted that, in fact, the greatest deviations are obtained for methanol; unfortunately, there is not available data to perform an exhaustive comparison of all properties at different conditions, as it happens for the *n*-alkanes series.

Table 6.9: *AAD% for residual and total isobaric heat capacities and speed of sound for some selected 1-alkanols at constant temperature or pressure.*

Compound	Property	T (K)	P (MPa)	AAD % Res Value	AAD % Total Value
methanol	C_p	533.15	---	30.0	18.1
		553.15	---	23.9	13.0
		573.15	---	19.6	8.34
1-propanol	C_p	---	0.1013	10.6	4.37
	ω	---	0.10	---	6.29
		---	15.2	---	4.11
		---	30.4	---	3.04
		---	60.8	---	1.48
		---	101.3	---	0.215
1-hexanol	C_p	---	10	15.6	4.68
		---	30	13.3	3.84
1-heptanol	C_p	---	10	13.9	6.20
		---	30	13.6	9.59

The effect of the temperature on some of these properties has also been investigated in subcritical conditions. Figures 6.16a and 6.16b show the evolution of the isobaric heat capacity and the speed of sound of ethanol at 1MPa as a function of temperature. Experimental results were taken from Dillon and Penoncello (2004). Soft-SAFT is able to capture the correct trend for the two properties considered, in both, the liquid and vapor phases. Very good predictions are obtained for the isobaric heat capacity (Figure 6.16a) in the liquid phase, while there is an overestimation of this property in the gas phase as it approaches the critical temperature. The speed of sound (see Figure 6.16b) is predicted in quantitative agreement in the vapor phase, while the liquid phase is slightly overestimated.
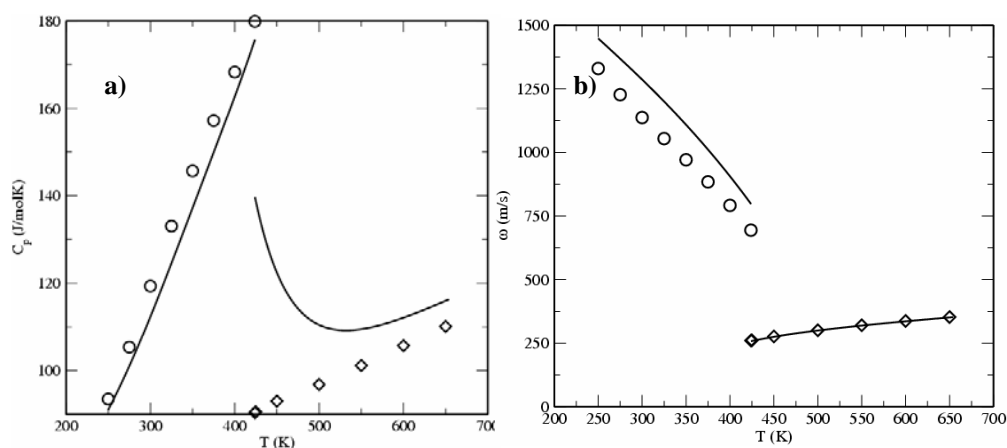
Figure 6.16: *Selected derivative properties of ethanol as a function of temperature, at 1MPa **a)** Isobaric heat capacity - temperature diagram. **b)** Speed of sound - temperature diagram of ethanol. Symbols are experimental data (Dillon and Penoncello, 2004) and solid lines the soft-SAFT predictions.*

The influence of the pressure in a selected property like the speed of sound has also been checked. Figure 6.17 depicts speed of sound predictions for *1*-propanol at five different pressures, in the range from 0.1MPa to 101.3 MPa. The AADs% remains in a range between 6.3% for 0.1MPa and 0.22% for 101.3MPa. Contrary to what happens to non-associating chains (*n*-alkanes), there is an overestimation of this property at low pressures that is corrected when the pressure increases. The overestimation may be due to the association contribution, which has a very strong effect in the calculations of the derivative properties. However, as the pressure increases, as already observed for *n*-alkanes, the underestimation of the other terms of the equation become more important and, as a result, there is a fortuitous error cancellation which provides quantitative predictions at high pressures.
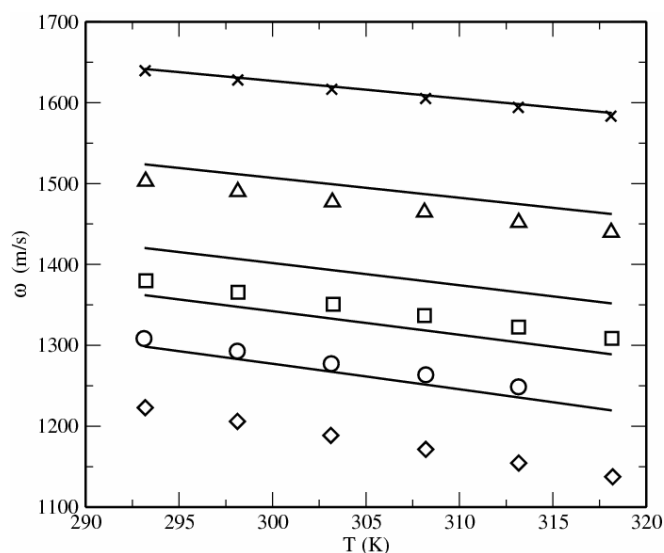
Figure 6.17: *Speed of sound-temperature diagram of 1-propanol at 0.1 MPa, 15.2 MPa, 30.4 MPa, 60.8 MPa and 101.3 MPa. Symbols represent the experimental data taken from Dzida and Ernst (2003). Solid lines correspond to soft-SAFT predictions.*

To complete the thermodynamic study of the *1*-alkanols family, the same contribution analysis made for the *n*-alkanes family has been performed for the *1*-alkanols. Again, the isochoric heat capacity and the isothermal compressibility are evaluated. The chosen compounds have been ethanol and *1*-heptanol, in order to establish a comparison with their two corresponding *n*-alkanes ethane and *n*-heptane, previously discussed. For a visual understanding, figure 6.12 (C_v and k_t contribution analysis for ethane and *n*-heptane) has been recovered and shown here with the corresponding diagrams of ethanol and *1*-heptanol.

Figures 6.18a-6.18d depict the different microscopic contributions to the second-order derivative properties as obtained from soft-SAFT for ethane, heptane, ethanol and heptanol at 1.1 times the critical temperature, respectively. The clear conclusion to be extracted from these figures is that the main contribution to the residual isochoric heat capacity comes from the association term (order of magnitude and shape of the curve). Note that the total residual isochoric heat capacity curves of ethanol and heptanol are similar, and very different from the ethane and heptane ones. In the case of ethanol, the association contribution accounts for almost the total residual value. In the case of heptanol, the shape

of the curve at high densities is a consequence of both, the chain length and the association contribution. These results show that for the case of energetic properties, such as heat capacities, the dominant role is played by the energetic intermolecular interactions.
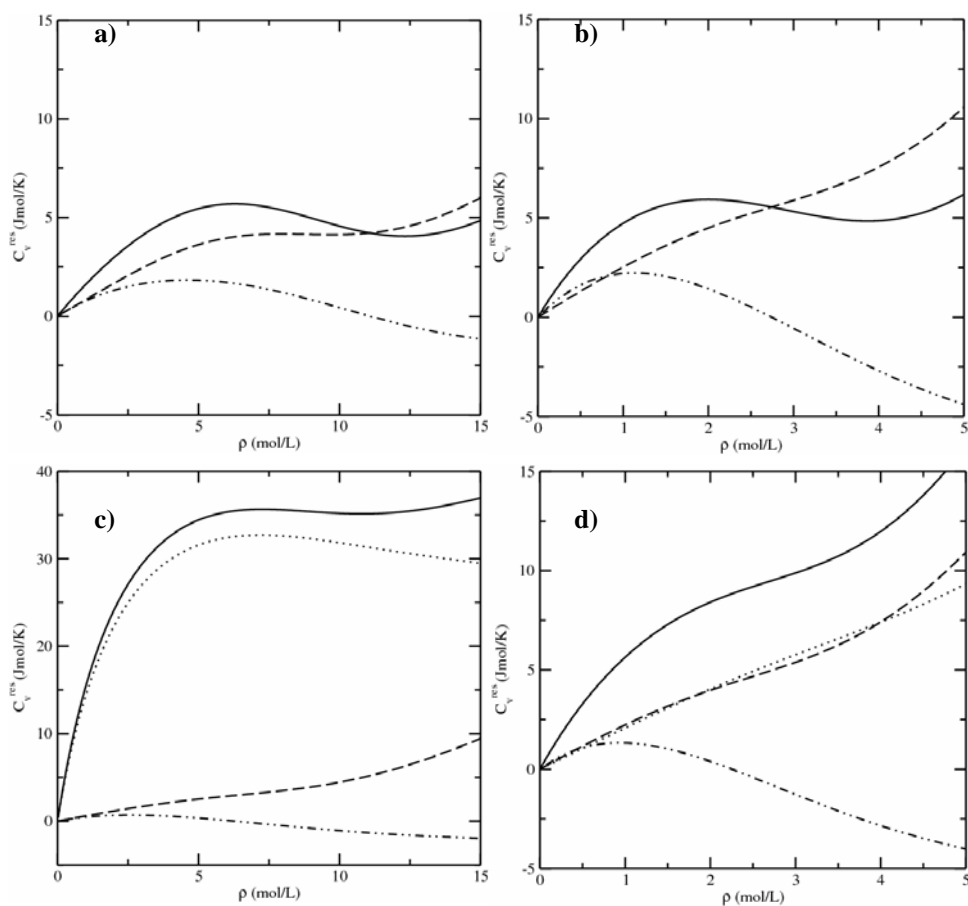
Figure 6.18: *Analysis of the different microscopic contributions to the residual isochoric heat capacity as obtained by the soft-SAFT equation.* ***a)*** *ethane.* ***b)*** *n-heptane.* ***c)*** *ethanol.* ***d)*** *1-heptanol. Solid line: total residual value; dashed line: segment term contribution; dotted line: association term contribution; dashed-double dotted: chain term contribution.*

Results for the isothermal compressibility for the same four compounds (ethane, heptane, ethanol and heptanol) are shown in Figures 6.19a-6.19d.
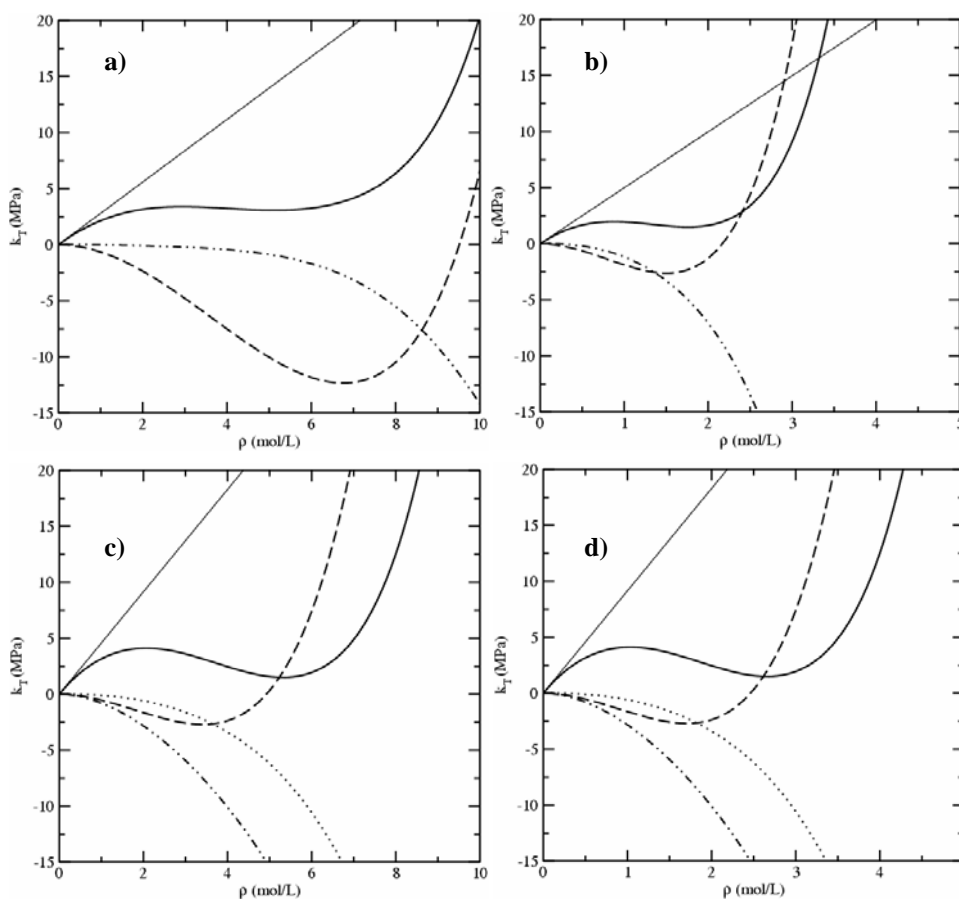
Figure 6.19: *Analysis of the different microscopic contributions to the isothermal compressibility as obtained by the soft-SAFT equation. **a)** ethane. **b)** n-heptane. **c)** ethanol. **d)** 1-heptanol. Thin solid line: ideal term contribution. Rest of notation as in Figure 6.18.*

In this case, all curves present the same qualitative trend, being the number of segments the dominant term as the chain length increases. The association does not play an important role since the isothermal compressibility is a volumetric property.

6.2.3. The perfluoroalkanes family

The perfluoroalkanes family constitutes another challenging series to evaluate. They are synthetic fluorinated hydrocarbons formulated by substituting the fluorine to replace hydrogen atoms on common organic compounds. These compounds are used in different fields like medicine, environment and industry and their number of applications increases every year. They can be used as substitutes for chlorinated solvents, as cosolovents in supercritical extraction, as medium in two-phase reaction mixture and as refrigerants, among other applications.

From a chemical point of view, fluorine's high ionization potential and relatively low polarizability lead to weak intermolecular forces (Fielding, 1979) which, together with the strong intermolecular forces give the perfluoroalkanes interesting properties, like the highest solubility known among organic liquids (Dias, 2006), an exceptional chemical and biological inertness, and excellent spreading characteristics.

From a molecular point of view, they can be modeled in the same way as the n-alkanes family: homonuclear chainlike molecules, modeled as m Lennard-Jones segments of equal diameter σ, and the same dispersive energy ε, bonded tangentially to form the chain, plus the crossover parameters L and ϕ to include the long-range fluctuations in the critical region. In order to minimize the number of adjusted calculations, and considering the analogy with the n-alkane series, the parameter L was fixed to the same value as the one previously adjusted for the respective n-alkane. The parameters are optimized, as done before, to the saturated liquid densities and vapor pressures for the eight first members of the series. The optimized parameters are presented in Table 6.10.

It can be noted that the parameters are quite similar to the ones for the n-alkanes family, excepting the value of the diameter σ, which is higher because of the presence of the fluorine atom instead of the smaller hydrogen.

Table 6.10. *Molecular parameters for the light members of the n-perfluoroalkanes family (C1-C8).*

	m	σ (Å)	ε/k (K)	ϕ	L/σ
perfluoromethane	1.025	4.152	182.0	5.00	1.04
perfluoroethane	1.392	4.335	203.8	5.50	1.10
perfluoropropane	1.750	4.400	216.0	6.12	1.16
perfluorobutane	2.134	4.430	222.5	6.63	1.22
perfluoropentane	2.471	4.460	229.0	7.10	1.27
perfluorohexane	2.752	4.475	234.0	7.45	1.33
perfluoroheptane	3.160	4.485	236.5	7.72	1.38
perfluorooctane	3.512	4.500	239.0	8.10	1.43

The correlations obtained from these parameters are shown below.

$$m = 0.0352CN + 0.689 \tag{6.4a}$$

$$m\sigma^3 = 34.65CN + 43.05 \tag{6.4b}$$

$$m\varepsilon/k_B = 92.55CN + 98.29 \tag{6.4c}$$

$$m\phi = 3.33CN + 1.08 \tag{6.4d}$$

$$mL/\sigma = 0.12CN + 0.11 \tag{6.4e}$$

In table 6.11, the values obtained for the critical constants for the light perfluroalkanes with the equation are compared with the experimental ones. While the critical temperature and pressure show good agreement with the experimental values, the critical density remains slightly overestimated, as stated in the previous cases.

Figure 6.20 shows the vapor-liquid equilibria for the first eight members of the *n*-perfluoroalkanes. The temperature-density and the pressure-temperature diagram are shown in 6.20a and 6.20b respectively.

Table 6.11 *Critical constants for n-perfluoroalkanes (C_1-C_8).Experimental data from various authors (see text for details).*

n-perfluoroalkane	T_c (K)			P_c (MPa)		
	Exp.	Crossover soft-SAFT	soft-SAFT	Exp.	Crossover soft-SAFT	soft-SAFT
perfluoromethane	227.6	226.6	249.6	3.74	3.70	4.55
perfluoroethane	293.0	292.9	314.0	3.04	3.01	5.70
perfluoropropane	345.1	345.2	370.1	2.67	2.60	5.14
perfluorobutane	386.5	386.4	417.5	2.31	2.21	4.70
perfluoropentane	421.4	422.0	460.7	2.04	1.96	4.29
perfluorohexane	450.6	448.8	498.4	1.88	1.81	3.88
perfluoroheptane	475.3	474.8	533.3	1.62	1.53	3.57
perfluorooctane	498.2	498.4	559.7	1.55	1.37	3.26

n-perfluoroalkane	D_c (mol/L)			Reference
	Exp.	Crossover soft-SAFT	Soft-SAFT	
perfluoromethane	7.17	8.76	6.86	Smith and Srivastava (1986)
perfluoroethane	4.49	5.61	4.44	Smith and Srivastava (1986)
perfluoropropane	3.34	3.68	3.18	Smith and Srivastava (1986)
perfluorobutane	2.65	2.86	2.46	Brown and Mears (1958)
perfluoropentane	2.16	2.50	1.99	Barber and Cady (1956) Burguer and Cady (1951)
perfluorohexane	1.84	2.20	1.65	Dias (2006); Dunlap et al. (1958); Crowder et al. (1967); Mousa (1978)
perfluoroheptane	1.60	1.88	1.40	Oliver et al. (1951); Steele et al. (1997); Oliver and Grisard (1951); Milton and Oliver (1952)
perfluorooctane	1.39	0.97	1.21	Dias (2006); Kreglewski (1962)
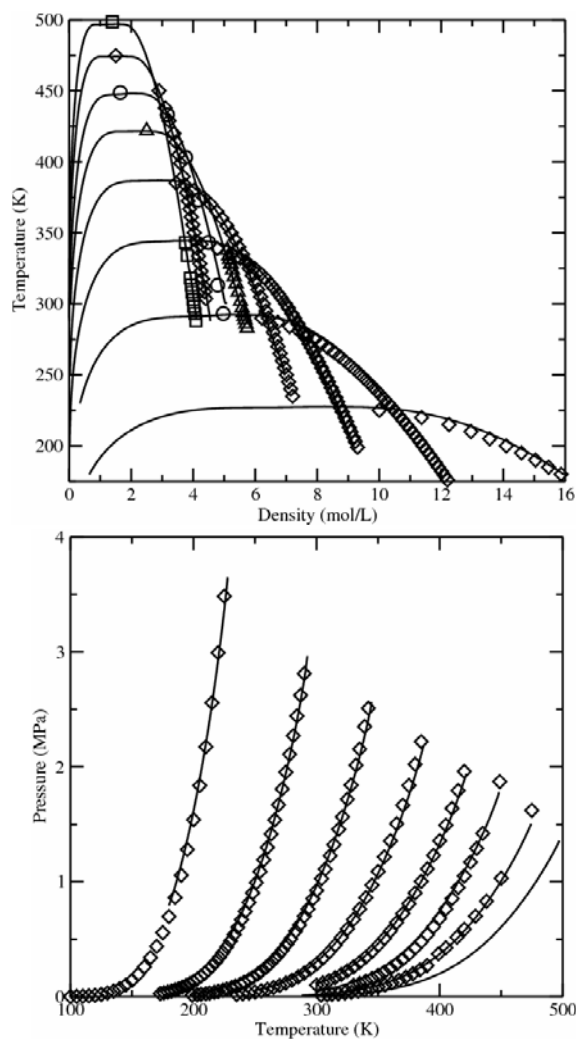
Figure 6.20 *Phase equilibrium diagram for the light members of the n-perfluoroalkanes series, from perfluoromethane to perfluorooctane.* ***a)*** *Temperature-density diagram* ***b)*** *Pressure-density. Symbols represent the experimental data taken from various authors (see table 6.11). Lines represent crossover soft-SAFT predictions.*

As in the other series, excellent agreement is obtained in all cases, although the multiple experimental sources employed does not help to obtain a clean fitting.

Following the same procedure done for the *n*-alkane and *1*-alkanol series, some of the most important derivative properties are calculated for a selected perfluoroalkane. The number of published works dealing with the evaluation of these properties in perfluoroalkanes is very scarce. In this sense, it is worthwhile mentioning the experimental evaluation of the isobaric heat capacity for the perfluoroalkanes family and the study of the transition of state for heavier perfluoroalkanes done by Jin et al. (1994). Perfluoropropane has been the chosen compound in order to establish a comparison with the results obtained for *n*-propane. Figure 6.21 shows the behavior of perfluoropropane for two isotherms close but above the critical point, at 1.1 and 1.25 times the critical temperature. Figure 6.21a represents the phase equilibrium diagram optimized and the following figures are predictions for the isochoric and isobaric heat capacity and the speed of sound respectively. Similar results are achieved compared to the n-propane study and the same conclusions can be extracted. The crossover treatment improves estimations for heat capacities and it also results in an improvement of the speed of sound prediction (see Table 6.12). However, there are still some significant deviations in the critical point, especially for the isochoric heat capacity, which is less accurate than in the case of *n*-propane. In spite of the important differences in the critical point, it is important to remark that the crossover treatment shows better qualitative agreement with the phenomena observed in the critical point.

Table 6.12: *AAD% for residual and total isochoric and isobaric heat capacities, and speed of sound, for perfluoropropane at temperatures above the critical point, as obtained with the soft-SAFT equation with and without crossover.*

Compound	Property	T / T_c	AAD % Without crossover	AAD % With crossover
Perfluoro-propane	C_v	1.10	63.2	52.5
		1.25	29.8	20.2
	C_p	1.10	24.0	15.6
		1.25	18.4	9.8
	ω	1.10	19.2	2.1
		1.25	16.8	4.9
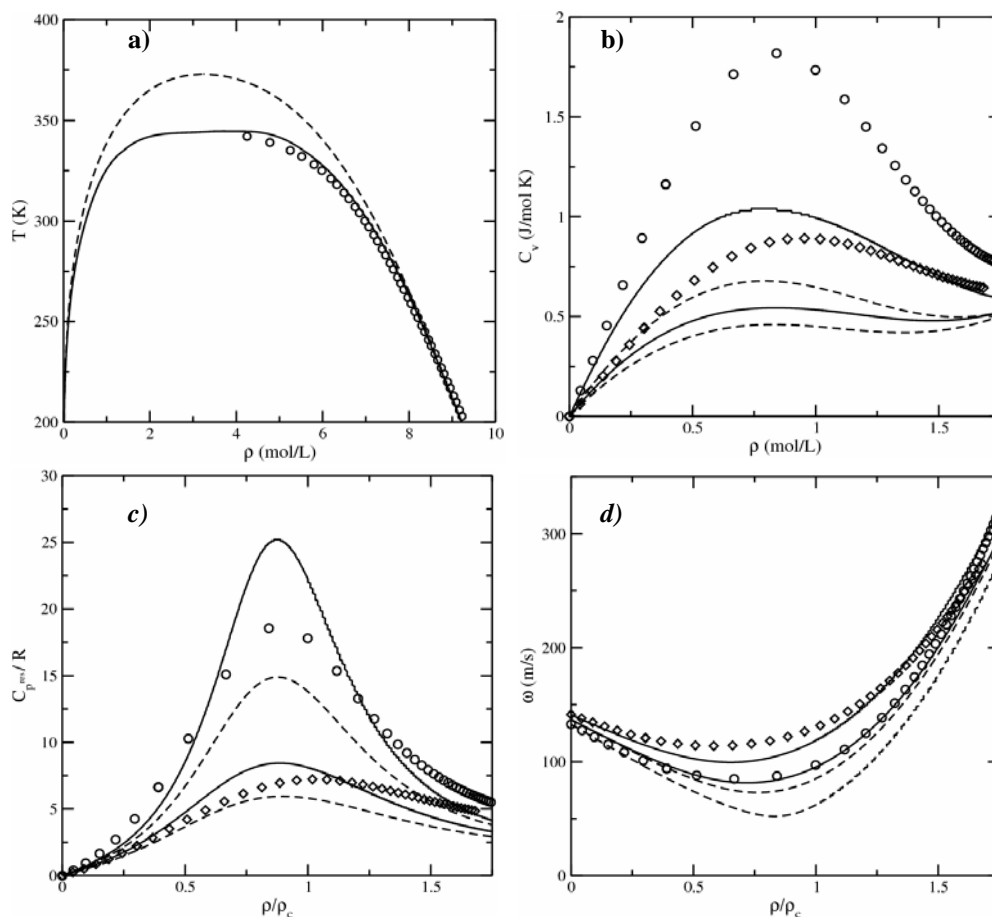
Figure 6.21*: The behavior of perfluoropropane. **a)** temperature-density diagram. **b)** residual isochoric heat capacity. **c)** residual isobaric heat capacity. **d)** speed of sound. Figures b), c) and d) were obtained at two reduced temperatures of 1.1 and 1.25. Notation as in Figure 6.9.*

Nevertheless, the predictions for derivative properties are comparable to the results obtained for the *n*-alkanes and *1*-alkanols family, in terms of qualitative agreement and percentage of deviation, and similar conclusions can be extracted.

6.2.4. Other selected compounds

As with any other EoS, there is a considerable amount of compounds whose parameters can be optimized using soft-SAFT. The purpose of this work is not to develop a library of parameters, but to show the capability of the crossover soft-SAFT equation of state to accurately predict an ensemble of properties using a unique set of parameters for some of them.

Several fluids have been studied because of its important industrial interest or its common use in binary and multicomponent mixtures. Their calculation always implies a previous study of the pure compound, in order to avoid unphysical values for the parameters. A realistic model of the molecular structure is the key for an accurate prediction of all properties. For example, it is possible to employ a high value of *m* for a small molecule, but it does not really represent the molecular structure and, probably, it will affect the calculation of mixtures. Moreover, the consideration about the quadrupolar moment or a possible association of the molecule is also crucial. In the following lines, some of these compounds are mentioned and its parameters summarized in Table 6.13.

Table 6.13 *Optimized molecular parameters for some selected compounds*

	m	σ (Å)	ε/k (K)	ϕ	L/σ	ε/k_B (K)	k (Å^3)
Acetic Acid	1.553	3.735	290.7	8.17	1.22	7701	95.0
CO_2*	1.606	3.158	159.9	5.79	1.18	---	---
Ethylenglycol	1.741	3.682	326.1	7.58	1.30	4484	4195
HCl	1.000	3.566	257.2	4.73	1.00	1321	1137
NO_2	1.300	3.200	249.8	7.70	1.39	6681	10.2
MTBE	2.725	3.837	251.0	8.70	1.32	---	---
SF_6	1.654	3.918	201.4	6.20	1.10	---	---

Quadrupole value: $4.4 \cdot 10^{-40}$ Cm^2

Among them, carbon dioxide and hydrogen chloride are described with more detail because they will be used in the performance of binary and ternary mixtures.

6.2.4.1. Carbon dioxide

Carbon dioxide is one of the most important compounds in the planet. It is present in the Earth's atmosphere at a low concentration and acts as a greenhouse gas. In its solid state, it is called dry ice. It is a major component of the carbon cycle.

Carbon dioxide is present in a huge amount of industrial processes. However, as stated in the second chapter of this work, the main interest remains in the fact that it is widely used as a near-critical solvent. Supercritical carbon dioxide is now well established as a solvent for use in extractions. It is used for the decaffeination of coffee and tea and the extraction of hops, natural products, high value pharmaceutical precursors, essential oils, and environmental pollutants. Other important commercial technologies are also emerging involving supercritical carbon dioxide, such as dry cleaning and paint spraying.

From the modeling point of view, the main feature of this simple molecule stays in the quadrupolar interactions present in CO_2. These interactions are taken into account by an additional term into the equation (Gubbins and Twu, 1978). This term involves a new molecular parameter Q that represents the quadrupolar moment of the molecule. For the case of carbon dioxide, the experimental value measured by Vrabec et al., (2001) is explicitly introduced in the equation, as well as the fraction of segments in the chain that contain the quadrupole (one third for carbon dioxide). As a result, Q is fixed and the other parameters $m, \sigma, \varepsilon, \phi$ and L are fitted to experimental vapor pressure and saturated liquid density.

Figure 6.22 shows the phase equilibrium diagram for carbon dioxide. 6.22a is the temperature-density diagram while 6.22b is the pressure-temperature diagram. The critical region is well reproduced due to crossover treatment.

The action of the quadrupole will improve the ability for mixtures prediction. In that sense, the molecular parameters obtained with the quadrupole contribution added are more realistic from a physical point of view. In the next chapter, the performance of the equation in mixtures involving CO_2 with alkanes and 1-alkanols will be described in detail.
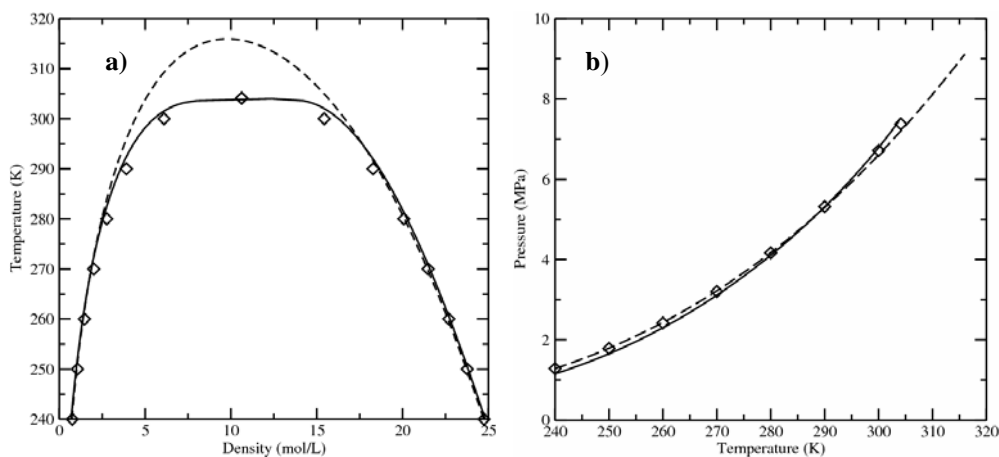
Figure 6.22. *Phase equilibria for carbon dioxide.* **a)** *Temperature-density diagram* **b)** *Pressure-temperature diagram. Circles are experimental data from NIST Chemistry Webbook, dashed lines are the original soft-SAFT and solid lines are the crossover soft-SAFT equation.*

6.2.4.2. Hydrogen chloride

Hydrogen chloride (HCl) is a very common compound used in several different industrial processes, like the regeneration of ion exchangers, the pH control, the pickling of steel and the production of organic and inorganic compounds. In many cases, it appears as one of the major constituents of a mixture and, for this reason, accurate basic thermodynamic data of the compound is needed. However, the corrosive nature of HCl makes it not easy to handle in experimental facilities and, as a result, thermodynamic information about hydrogen chloride is quite limited.

From a modeling point of view, HCl is considered as a single Lennard-Jones segment of diameter σ and dispersive energy ε with two square-well sites with volume k^{HB} and association energy ε^{HB}, representing its dipole moment. This approximation is done in a similar manner in a previous work of Galindo et al. (1999) using a different version of SAFT, SAFT-VR (Gil-Villegas et al., 1997). In that work, the authors modeled three

mixtures of hydrogen chloride with n-alkanes using two different approaches, a perturbed anisotropic chain theory (PACT) (Vimalchand and Donohue, 1985) and the already mentioned SAFT-VR. They obtained very good results using SAFT-VR although they had to rescale the parameters to the critical region due to the lack of a specific crossover treatment to take into account the fluctuations produced in that region.

Fig. 6.23 shows the vapor-liquid equilibrium for pure hydrogen chloride. Excellent agreement is obtained in the temperature-density and in the pressure-temperature diagrams between the experimental data and soft-SAFT.
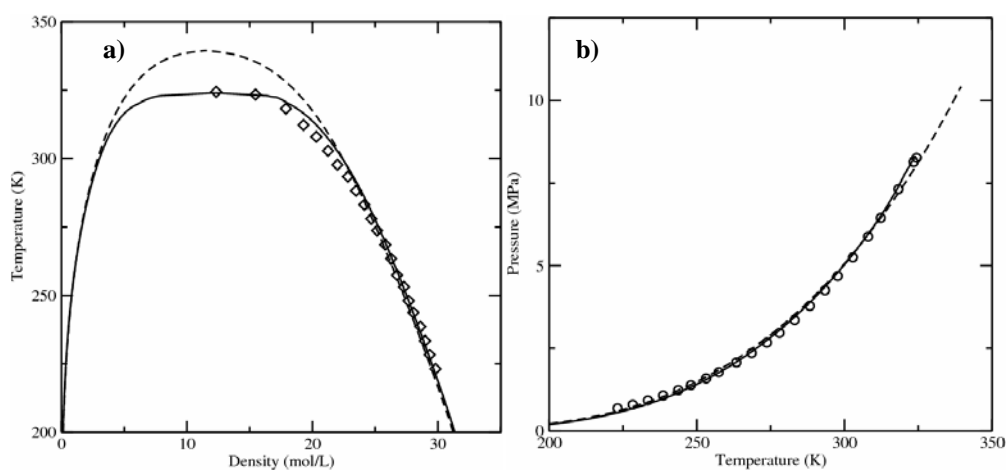
Figure 6.23 *Temperature-Density and Pressure-Temperature diagrams for hydrogen chloride. Symbols represent the experimental data (Galindo et al., 1999) and the solid line is the soft-SAFT calculation.*

The critical region is well described by the equation and the critical point is perfectly captured due to the crossover treatment included into the equation. The approximation made when modeling the dipole as an association contributions seems to be quite good, although it is necessary to test its influence when dealing with mixtures. This will be done in the study proposed in section 7.1.5 of this thesis work, where the performance of HCl with alkanes will be treated.

6.3. Comparison with a van der Waals type equation

As this PhD work is devoted to the improvement of a molecular-based equation for the description of the critical region, it has been considered and interesting test to study the performance of the selected crossover approach when it is implemented into a cubic equation of state. In fact, it is expected that the treatment has to be able to correct the behavior of the critical region in the same way as it was done for the soft-SAFT, although the capabilities of the original equation will affect the whole phase envelope calculations.

A refined van der Waals type equation has been selected for this purpose. The equation follows the general cubic form (Segura et al, 2006):

$$P = \frac{RT}{(V_m - b)} - \frac{a}{(V_m + c_1 b)(V_m + c_2 b)} \tag{6.5}$$

Parameters a, b, c_1 and c_2 are calculated for each compound using the experimental critical point data and a reference saturation point (usually the boiling point), following a mathematical procedure described in the work of Segura et al. (2006). The features of this parametrization approach are:

- The critical predicted compressibility is equivalent to the experimental one.

- The EoS describes almost exactly the reference boiling point.

- The EoS describes almost exactly the liquid volume at the reference boiling point.

- Only a reference experimental point, beside the critical temperature and pressure, is required for calculating the parameters. Possible reference saturation points could be the normal boiling point, the triple point or an arbitrary subatmospheric boiling point.

White's approach is implemented in the same way as it was done before with soft-SAFT. An additional term is added to the cubic Helmholtz energy obtained from equation 6.5. The equations are almost the same that those described in section 5.5 of this work with a slight simplification proposed by Cai and Prausnitz (2004) for their implementation in a cubic equation of state.

It has to be considered that the renormalization-group treatment is only applied to the attractive term of the equation. It means that the attractive part of the equation (initially evaluated as a mean-field theory) has to be sustracted and recalculated using the following numerical recursive procedure:

$$a = \lim_{n \to \infty} a_n - a_{vdW-type}\rho^2 \tag{6.6}$$

where the first iteration a_0 will correspond to the repulsive part of the equation of state before applying the renormalization group treatment.

$$a_n(\rho) = a_{n-1}(\rho) + da_n(\rho) \tag{6.7}$$

$$da_n(\rho) = -K_n \cdot \ln\frac{\Omega_n^s(\rho)}{\Omega_n^l(\rho)}, \tag{6.8}$$

$$K_n = \frac{k_B T}{2^{3n} \cdot L^3} \tag{6.9}$$

$$\Omega_n^\beta(\rho) = \int_0^{\min(\rho,\rho_{max}-\rho)} \exp\left(\frac{-G_n^\beta(\rho,x)}{K_n}\right) \cdot dx \tag{6.10}$$

$$G_n^\beta(\rho,x) = \frac{\bar{a}_n^\beta(\rho+x) + \bar{a}_n^\beta(\rho-x) - 2\bar{a}_n^\beta(\rho)}{2} \tag{6.11}$$

$$\overset{l}{\bar{a}}_{n}(\rho) = a_{n-1}(\rho) + \alpha \cdot \rho^{2} \tag{6.12}$$

$$\overset{s}{\bar{a}}_{n}(\rho) = a_{n-1}(\rho) + \frac{\alpha \cdot \rho^{2} \cdot \phi}{2^{2n+1}} \tag{6.13}$$

where Ω^{s} and Ω^{l} represent the density fluctuations for the short-range and the long-range attraction respectively. K_{n} is a coefficient that depends on the temperature T, the cutoff length L and the Boltzmann constant k_{B}. The superindex β refers to both long (l) and short (s) range attraction, respectively, and G^{β} is a function that depends on the evaluation of the function $\bar{a}$. The term $\alpha\rho^{2}$ corresponds to the theoretical mean-field attractive Helmholtz energy. The evaluation of this term depends on the intermolecular potential selected for each equation. Due to the fact that van der Waals type equations of state are mainly phenomenological, it would be too rough to assume that the attractive part of the equation is just the right term of equation 6.5 (the term where the attractive parameter is involved). As it is done in other published works (Cai and Prausnitz, 2004; Cai et al., 2006) renormalization group calculations are fitted to experimental data showing that the attractive part of the free energy is done by:

$$\alpha\rho^{2} \approx \frac{1}{2} a_{vdW-type}\rho^{2} \tag{6.14}$$

It is important to notice that equation 6.13 lacks of the term $(w/L)^{2}$ if it is compared to equation 5.13. In fact, ϕ is more or less a function of the initial shortest wavelength of density fluctuations but, for practical calculations the whole term $\phi\,(w/L)^{2}$ is considered an adjustable parameter with a constant value for a family of compounds. ρ_{max} is the maximum possible molecular density and it depends on the selected model. For a vdW-type equation, the maximum package density corresponds to the inverse of the covolume parameter b:

$$\rho_{max} = \frac{1}{b} \tag{6.15}$$

The integral in equation 6.10 is evaluated numerically, by the trapezoid rule. As done before, the density step is fixed to 500 and the number of iterations to 5.

The basis of the equation of state proposed includes the critical point properties as input information to calculate the different parameters of the equation. In some way, the EoS is forced to capture the critical point. However, due to the fact that the asymptotic behavior observed near the critical point is not achieved, the consequence is a remarkable deviation in the liquid density predictions. With the implementation of the crossover treatment, it is necessary to introduce "virtual" values for the critical properties that fit properly both phase densities far from the critical region. The renormalization group treatment will correct the critical point when approaching the critical region, obtaining a whole accurate description of the phase envelope. The critical pressure has been shown as the variable that most affect the calculations and has been used as an adjustable parameter, keeping the true critical temperature. As a result, the application of the renormalization group treatment introduces two new parameters into the equation, the cut-off length L and the virtual critical pressure $P_c^{'}$, while ϕ will be fixed to a constant value for a whole family of compounds.

Figure 6.24 represents the phase diagram for propane as a selected *n*-alkane. Temperature-density diagram is described and compared to experimental data from NIST Chemistry Webbook. Calculations have been done with the cubic equation of state (equation 6.5) with (solid line) and without (dotted line) the crossover treatment. Moreover, the propane calculation using crossover soft-SAFT has been added in order to establish a comparison of both equations.

It can be observed how the addition of a renormalization group term modifies the shape of the liquid phase curve giving very good agreement with experimental data. In this case, the critical region is not corrected because the original equation had included this correction in their implementation when optimizing the parameters. However, the price paid for that fitting (an inaccurate prediction of the liquid phase) can be improved with the crossover methodology. When compared to crossover soft-SAFT, this one captures better

the curve of the whole phase envelope, although there is not a remarkable difference between both performances.
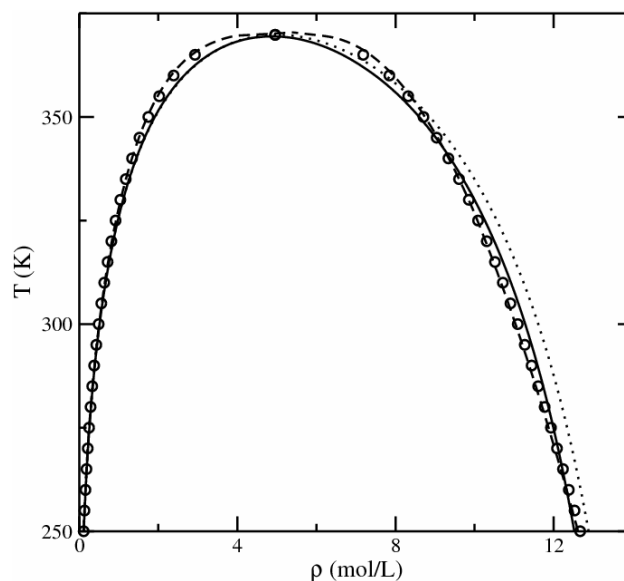
Figure 6.24 *Phase equilibrium diagram of n-propane. Temperature-density diagram. Circles are experimental data (NIST Chemistry Webbook). The solid and dotted lines are calculations done with and without crossover respectively, while the dashed line is the result obtained using crossover soft-SAFT..*

The crossover-vdW type equation has been applied to perform the *n*-alkane series in the same way as done by soft-SAFT in section 6.2.1. The original equation parameters have been previously parametrized following the procedure described in Segura et al. (2006). The new crossover parameters (the difference between the virtual critical pressure P_c' and the real critical pressure P_c and the cut off length parameter *L*) can be correlated with the molecular size into the same family of compounds. The correlation comes from optimized parameters for the seven first members of the alkanes series, obtained by fitting

experimental saturated liquid densities and vapor pressures. For all the compounds of this work, ϕ has been fixed to 1.40.

Figure 6.25 shows the vapor-liquid phase equilibrium diagram for the first seven members of the *n*-alkanes family. Figure 6.25a shows the temperature-density diagram while figure 6.25b is devoted to the pressure-temperature diagram. Symbols represent experimental data taken from the NIST Chemistry Webbook, while the full lines are calculations using the crossover-vdW-type equation. As it has been already said, the original vdW-type equation calculations use real critical point properties, which results in an accurate description of the critical point. However, due to the fact that the inherent density fluctuations are not taken into account, the asymptotic behavior when approaching the critical region is not reproduced. The consequence is an inaccurate calculation of the liquid volumes (see dashed line in Figure 6.24). When the renormalization group treatment is added, there is an automatic correction of the liquid volume because the shape of the curve changes to reproduce the asymptotic behavior.

In this case, the renormalization-group method is introducing two new parameters: a virtual critical pressure and a cut off length. Both, the cut-off length and the difference between the virtual critical pressure and the experimental critical pressure present a linear relationship respect to the molecular weight and can be directly correlated. However, in the case of the critical pressure, when a certain chain length is achieved, a constant difference between pressures is enough to obtain accurate results.

For the *n*-alkanes family, the following correlations for the crossover parameters are presented here:

$$\Delta P_c = -4.79 \times 10^{-2} M_w + 1.41 \qquad 1 \le CN \le 7$$
$$\Delta P_c = -0.93 \qquad\qquad\qquad\qquad CN \ge 7 \tag{6.15a}$$

$$L = 3.72 \times 10^{-12} M_w + 1.28 \times 10^{-9} \tag{6.15b}$$
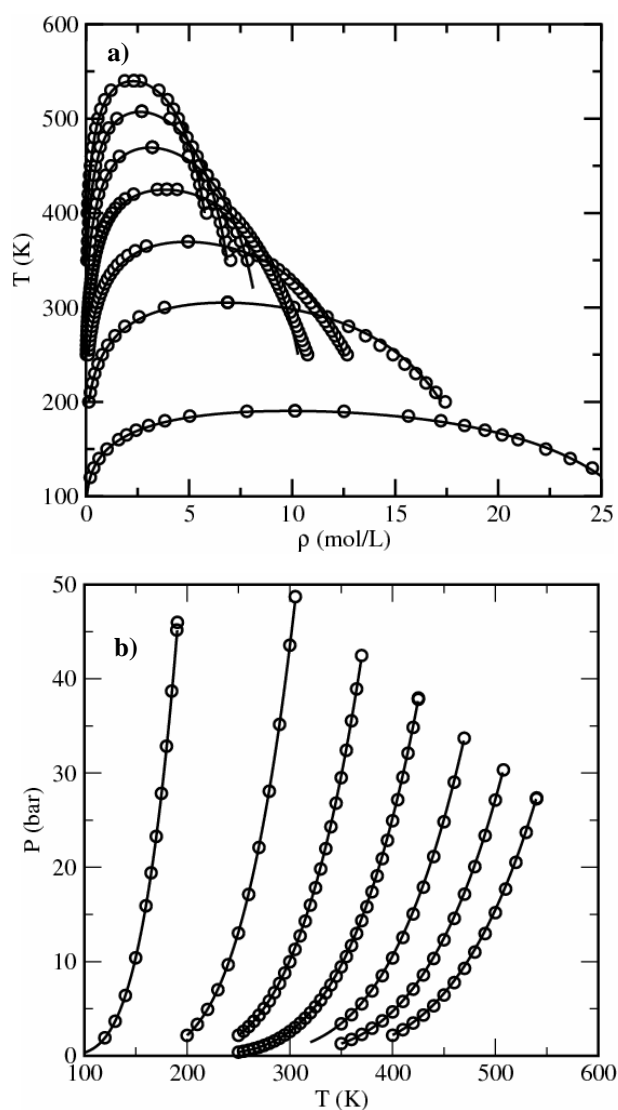
Figure 6.25 a*) Temperature-density diagram for the light members of the n-alkanes series, from methane to n-heptane.* ***b****) Pressure-density diagram for light members of the n-alkanes series, from methane to n-heptane. Symbols represent the experimental data taken from NIST Chemistry Webbook. Dashed lines correspond to vdW-type equation calculations, and the solid line to the crossover-vdW-type calculations.*

The advantage of a correlation is that the parameters can be extrapolated and heavier compounds can be predicted with accuracy. Figure 6.26 shows predictions for heavier alkanes like decane, dodecane, hexadecane and tetracosane.
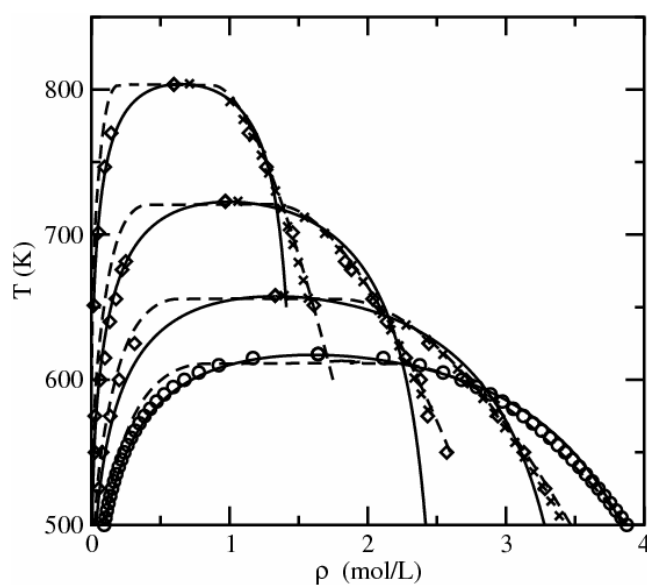
Figure 6.26*: Phase equilibria predictions for n-decane, n-dodecane, n-hexadecane and n-tetracosane. Circles for n-decane represent experimental correlated data from NIST Chemistry Webbook, while the rest of symbols are simulation data Nath et al. (1998). Simulation critical points are from Errington and Panagiotopoulos (1999). Solid Lines are crossover cubic equation predictions while dashed lines are crossover soft-SAFT predictions.*

The agreement between the experimental and simulation data and the crossover-vdW predictions is quite good, although some deviations are observed at low temperatures. These deviations increase with the chain length. The main reason for these deviations comes from the fact of having a set of vdW-type equation parameters calculated using the

experimental values for the critical pressure and now using a "virtual" critical pressure value different from the experimental one.

It is important to remark that this is not a problem of the crossover approach but the basis of the original equation. The crossover treatment takes into account the inherent fluctuations, correcting the calculation when the equation is able to give an approximate result but it will not modify completely the behavior observed without the treatment. The optimization procedure for parameters *a, b, c1* and *c2* gives a too steep decrease of the liquid density with the temperature which does not agree with the experimental and simulation data. Here, the goodness of a robust molecular-based equation of state like soft-SAFT is appreciated. In that sense, if predictions with crossover soft-SAFT (dashed lines) are compared to the results obtained with the cubic equation, it is easily observed how liquid density predictions are far better using the molecular equation.

The equation has also used to model the *1*-alkanols family. However, the same tendencies have been found: very good agreement for short *1*-alkanols and some deviations in the liquid volume predictions for the heavier compounds. Since results are very similar to the ones presented for *n*-alkanes and the conclusions are also very similar, they are omitted here for conciseness.

7

Mixtures

In this chapter, a compilation of results obtained for binary and ternary mixtures is presented. The chapter is split in several sections depending on the family of mixtures studied. First of all, mixtures between similar and dissimilar *n*-alkanes are treated. The critical transitions from Type I to type V are reproduced for the methane and ethane series. Secondly, some *n*-alkane/*1*-alkanol mixtures are tested, from vapor-liquid equilibria to derivative properties and critical behavior. The third and four sections study the transitions from Type II to Type III passing through Type IV for the CO_2/n-alkanes and CO_2/1-alkanols families, respectively. Section five presents several calculations for the not very well known HCl/n-alkanes family, giving some new information about the critical transitions. Finally, the last section presents some preliminary results for ternary mixtures of CO_2/*n*-alkane/*1*-alkanol mixtures.

7.1. Binary mixtures

The first part of this chapter is devoted to the study of several binary mixtures, paying special attention to the critical region. The mixtures are grouped by families and the goal is to test the ability of the crossover soft-SAFT equation of state for describing the different transitions observed when increasing the chain length of the second compound. Moreover, vapor-liquid, liquid-liquid and vapor-liquid-liquid equilibria for subcritical and supercritical states are evaluated, as well as the performance in the estimation of the heat capacities, compressibilities and the speed of sound.

7.1.1 n-Alkanes mixtures[1]

Mixtures among *n*-alkanes are commonly found in several industrial processes, including those of the petrochemical industry. Their study is also of interest from the fundamental point of view: when their chain length is similar, they exhibit an ideal behavior, showing a continuous critical line that joins both critical points (Type I, according to the classification of van Konynenburg and Scott [1980] for binary mixtures). However, although all the compounds are of the same nature, the dissimilarity between compounds as the chain of the second compound increases produces liquid-liquid and liquid-liquid-vapor equilibrium, leading to a transition from type I to type V in the critical behavior.

All the molecular parameters of the *n*-alkanes considered have been taken from the correlation proposed in section 6.2.1. When necessary, the binary parameters η and ξ are used take into account deviations between the size and energy of the segments forming the different compounds, allowing a quantitative description of the mixture. When needed, they have been obtained by fitting to one mixture at an intermediate temperature (pressure). Once this *Pxy* (*Txy*) diagram is optimized, the parameters are used to predict the phase

---

[1] *This work has been published in Llovell and Vega (2006a) and Llovell et al. (2006a) and Llovell and Vega (2006c).*

equilibria of the mixture at different temperatures as well as the critical lines in a purely predictive manner. Binary parameters for all the n-alkane mixtures studied here are presented in Table 7.1.

Table 7.1. *Binary parameters employed for different binary mixtures between n-alkanes (a value of 1.000 means predictions from pure compounds).*

Mixture	η	ξ
n-butane/*n*-pentane	1.000	1.000
n-butane/*n*-hexane	1.000	0.990
n-butane/*n*-heptane	1.010	0.980
n-butane/*n*-octane	1.030	0.960
methane/*n*-pentane	1.030	1.000
methane/*n*-hexane	1.030	1.000
ethane/*n*-decane	1.030	0.970
ethane/*n*-eicosane	1.030	0.970

The first four mixtures correspond to the *n*-butane series. As *n*-butane and *n*-pentane are very similar compounds no binary parameters are needed for this mixture. The binary parameters of the other *n*-butane mixtures are also very close to unity and they have been fitted just to obtain quantitative agreement with the experimental data, although a good description of the mixtures could be achieved when fixing them to unity. Some examples of the performance of the crossover soft-SAFT equation are shown in Figure 7.1a and 7.1b. They show *Txy* projections at two different pressures for the mixtures *n*-butane/*n*-hexane and *n*-butane/*n*-octane. Symbols represent experimental data extracted from the works of Kay et al. (1974, 1975), while the lines correspond to the crossover soft-SAFT predictions. Quantitative agreement is obtained in all cases. It is impossible to distinguish which one was the pressure used to fit the binary parameters and which one is the predicted one.
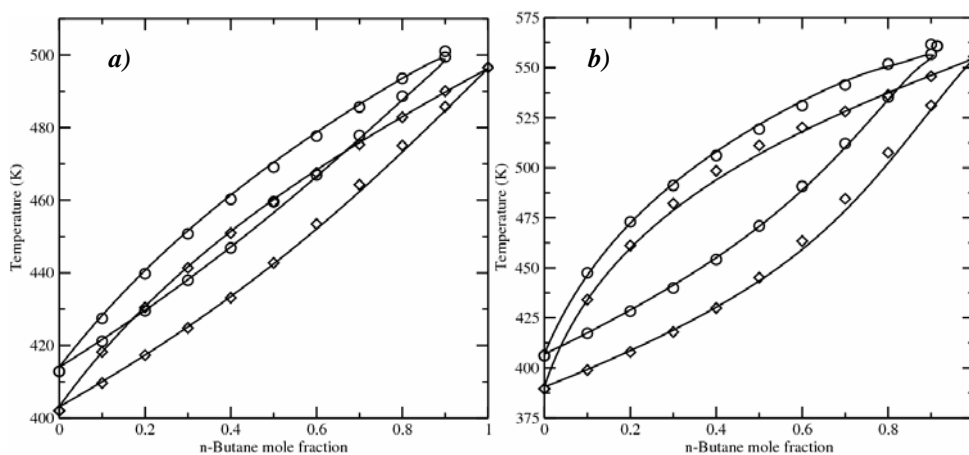
Figure 7.1*: Temperature-composition diagram of the binary mixtures a) n-butane/n-hexane at 2.58 and 3.10 MPa b) mixture n-butane/n-octane at 2.07 and 2.76 MPa. Symbols are experimental data from references Kay et al (1974, 1975). Solid lines are crossover soft-SAFT predictions.*

       Once the vapor-liquid equilibria was calculated, the same binary parameters were used to predict the critical lines of the mixtures. Figure 7.2 shows the *PT* projections of the *PTxy* surfaces for the *n*-butane series, with mixtures between *n*-butane and *n*-pentane, *n*-hexane, *n*-heptane and *n*-octane. As it was expected, crossover soft-SAFT predicts Type I critical behavior with quantitative agreement for all the mixtures.

       It is important to notice that if the parameters of the original soft-SAFT equation are rescaled to the critical point of the pure compounds, excellent predictions are also obtained (Blas and Vega, 1998). However, with the rescaling method, the behavior in the subcritical region is not accurately reproduced, and a different set of parameters is needed to predict the phase equilibria of the binary mixture far from the critical point. As a result, two sets of parameters are needed to describe the entire phase envelope of a fluid. The advantage of the crossover soft-SAFT equation is the ability to have a unique set of parameters for the whole range of a fluid.
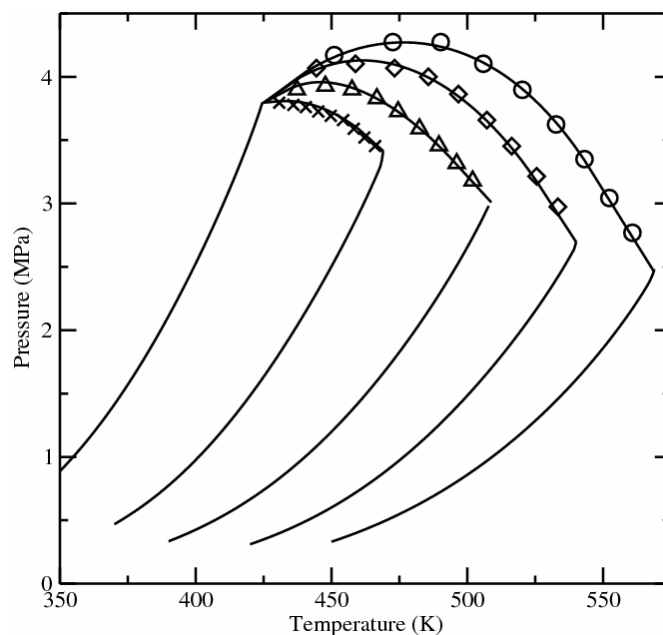
Figure 7.2: *PT projections of the binary mixtures of the n-butane series: n-butane/n-pentane, n-butane/n-hexane, n-butane/n-heptane and n-butane/n-octane. Symbols are experimental data from Kay et al. (1975). The solid lines are the predictions from the crossover soft-SAFT equation.*

The analysis of more dissimilar mixtures of *n*-alkanes has been performed in order to model the transition from one type of critical behavior to another one. This is the case for the last four mixtures presented next, corresponding to the methane and ethane series. Both series have been studied in the same manner and the binary parameters have been adjusted, in this case, to the critical line of one of these mixtures: the ethane-eicosane mixture, in order to assure Type V behavior.

It is well known that methane/*n*-pentane mixture exhibits type I behavior while the methane/*n*-hexane mixture shows a type V behavior, with a three phase region found near the critical point of methane. These two mixtures have been investigated with several

approaches. In particular, the critical behavior evolution was studied by Blas and Vega (1998) with the soft-SAFT equation. Since no crossover term was included in the version of the equation these authors used, they employed the rescaling alternative approach. Without any further adjustment, they were able to correctly predict the transitions from type I to type V in these mixtures. However, as it has been mentioned, this approach leads to two different sets of molecular parameters. The same rescaling approach was used by McCabe et al. (1998), focused on the particular system methane/n-hexane in order to describe the type V behavior with the SAFT-VR EoS. In 1999, Polishuk et al. studied the whole methane series up to n-octane using six different cubic equations of state. Their deep study showed that almost all the equations were predicting an incorrect liquid-liquid-vapor equilibrium in the methane/*n*-pentane mixture. Later on, the same authors (Polishuk et al., 2003) studied the series with three semipredictive approaches (Global Phase Diagram Semipredictive Approach GPDA, the predictive Soave-Redlich-Kwong PSRK and a linear combination of the Vidal and Michelsen mixing rules LCVM). The only one which was able to predict type I (i.e. no liquid-liquid phase) behavior was the GPDA, although it underestimated the dew point data at high temperatures and overestimated the buble point data at low temperatures. The present work is an improvement over these previous approaches, since the crossover term incorporated into the soft-SAFT equations allows the prediction of the subcritical and critical behavior with the same set of parameters in an accurate manner.

The phase behavior of the mixture methane/*n*-pentane is shown in Figure 7.3. Fig. 7.3a depicts the pressure-temperature projection of the phase diagram of this mixture predicted by both versions of the soft-SAFT equation, with and without the crossover term, as compared to available experimental data (Sage et al., 1942; Berry and Sage, 1970; Chen et al., 1974; Chu et al.; 1976).
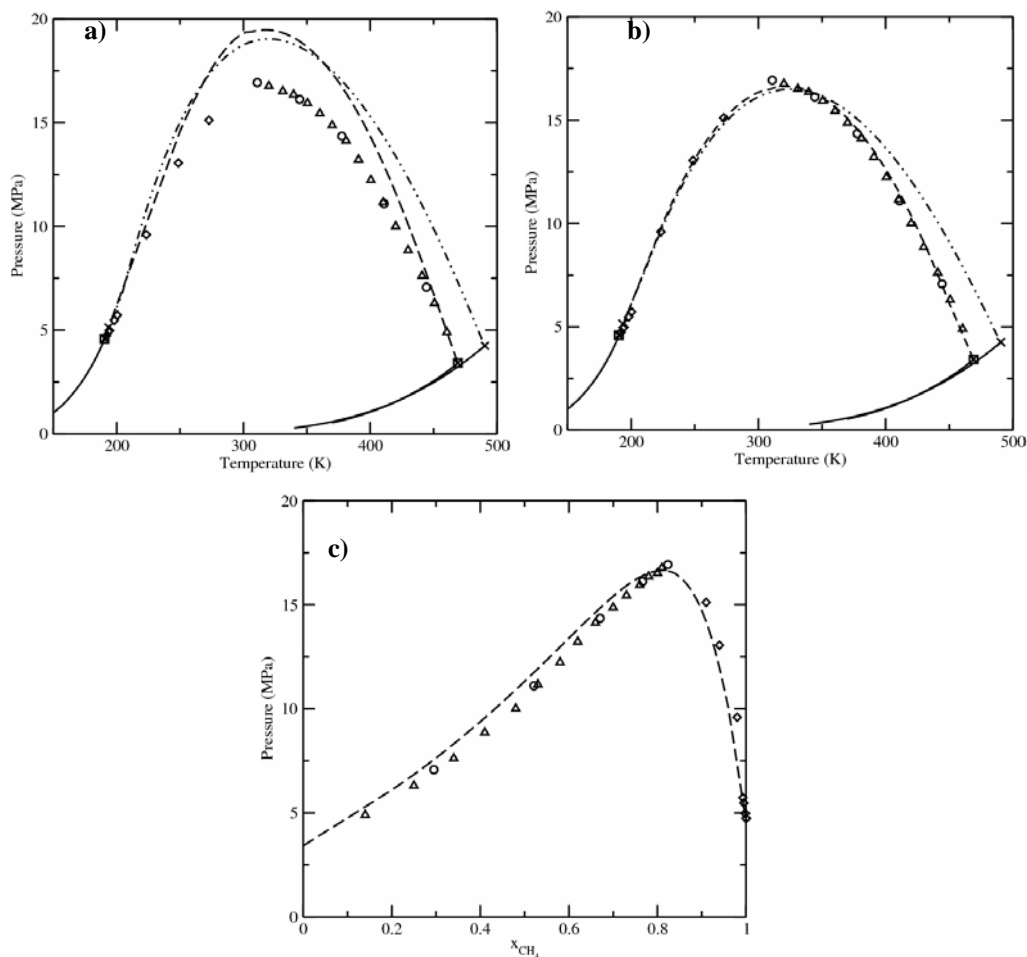
Figure 7.3: *Critical line of the methane/n-pentane mixture.* ***a)*** *PT diagram as predicted by the original soft-SAFT and crossover soft-SAFT using just pure component parameters (η=1.000).* ***b)*** *PT diagram of the original soft-SAFT and crossover soft-SAFT with η=1.030.* ***c)*** *Px critical diagram as described by the crossover soft-SAFT with η=1.030. Circles (Berry and Sage, 1970), triangles (Sage et al., 1942) and diamonds (Chen et al, 1974; Chu et al., 1976) represent experimental data; squares (experimental data) and crosses (equation calculations) are the critical points of the pure compounds. Solid lines stand for the pure compound vapor pressures; the dashed-double-dotted line represents predictions from original soft-SAFT while the dashed line stands from crossover soft-SAFT.*

As expected the equation predicts type I behavior for the methane/n-pentane mixture, with the critical line joining the critical points of both components in a continuous manner. However, as it can be observed in the figure, the classical version of the equation overestimates both, the critical points of the pure compounds and the critical points of the mixtures, over the whole range of compositions. The crossover soft-SAFT EoS is able to quantitatively predict the critical point of the pure compounds and the critical points of the mixture near the critical point of the pure compounds. Nevertheless, deviations are observed as the critical temperature and pressure of the mixture deviate from those of either pure compound. This behavior has been previously observed in mixtures where there is a dissymmetry in size/energy of the two compounds, as it happens for the methane/n-pentane case (see, for instance, Blas and Vega [1998] and McCabe et al. [1999], and references therein). The description of asymmetric mixtures is clearly improved when one or two binary parameters, independent of the thermodynamic conditions, are fitted to experimental data of the mixture at particular conditions and then used in a transferable manner for the rest of the mixtures. Fig. 7.3b shows the performance of the original and the crossover soft-SAFT equation when a binary parameter value η=1.030 is used in both cases, as compared to the same experimental data shown in Fig. 7.3a. The particular value of this parameter was chosen to assure the type V behavior of the ethane/eicosane mixture (i.e. it was not optimized for the methane/n-alkane mixtures). The agreement between crossover soft-SAFT EoS with this parameter and the experimental data is excellent for the whole range of compositions. The critical pressure-composition diagram of this mixture is depicted in Fig. 7.3c, using the same value of the binary parameter η=1.030. As it can be observed the predictions of the crossover equation are in excellent agreement with the experimental data.

The behavior of the methane/n-hexane binary mixture is shown in Fig. 7.4. Fig. 7.4a shows predictions with pure component parameters while Fig. 7.4b depicts calculations performed using the size binary parameter (η=1.030).
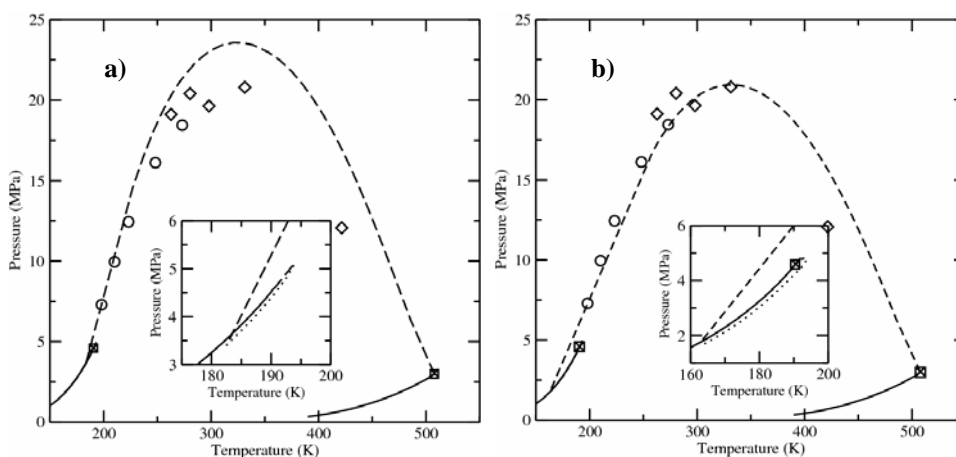
Figure 7.4: *PT diagram showing the critical line of the methane/n-hexane mixture. Diamonds are experimental data from Hicks and Young (1975), while circles correspond to data obtained from Lin et al. (1977). Crosses (experimental data) and squares (equation calculations) represent the critical points of the pure compounds. The insets show an enlargement of the region near the critical point of methane. The solid lines represent the vapor pressures of the pure compounds, the dashed lines stand for the critical line of the mixtures with crossover and the dotted lines represent the liquid-liquid-vapor equilibria. **a)** crossover soft-SAFT predictions from pure component parameters. **b)** crossover soft-SAFT with η=1.030. See text for details.*

As observed in Fig. 7.3, the binary parameter allows to better describe the critical region of the mixture far from the pure components critical points. A small three phase region in the vicinity of the more volatile compound (methane) is predicted with the two versions of the equation. An enlargement of this region (presented in the inset of the figures) shows the three-phase-line, a critical line arriving to a lower critical end point (LCEP) and another critical line going from pure methane till an upper critical end point (UCEP). It is important to remark how small this region is, making difficult accurate calculations with any EoS. A Pxy projection of the phase diagram at T=190K is shown in

Fig. 7.5, where the narrowness of the three phase region is clearly observed. A small three phase region in the vicinity of the pure methane compound is predicted in both cases.
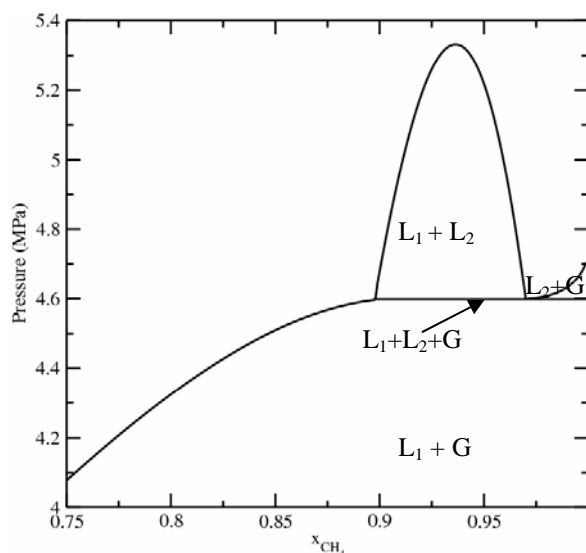
Figure 7.5: *Pxy projection of the phase diagram of the mixture methane/n-hexane at T=190K using the crossover soft-SAFT EoS.*

The values of the UCEP and LCEP calculated with the crossover soft-SAFT EoSs (with and without the binary parameter) are compared to the experimental values (Lin et al., 1977) in Table 7.2. Note that calculations performed with pure component parameters are in closer agreement with experimental data than those obtained with the binary parameter. In this later case the LCEP is clearly underestimated. It should be emphasized that the value of η was optimized for obtaining quantitative agreement in the liquid-vapor critical line, keeping the transition from Type I to Type V in the mixtures methane/n-pentane and methane/n-hexane. In any case, it is striking to see the predictive power of the crossover soft-SAFT equation with just pure component parameters, in excellent agreement with experimental data.

Table 7.2: *Critical end point (CEP) temperature and pressure for the methane/n-hexane mixture*

Mixture	Exp. Data	crossover soft-SAFT		Exp. Data	crossover soft-SAFT	
		η=1.00	η=1.03		η=1.00	η=1.03
methane/ n-hexane	T^{exp} (K)	T^{SAFT} (K)	T^{SAFT} (K)	P^{exp} (MPa)	P^{SAFT} (MPa)	P^{SAFT} (MPa)
UCEP	195.91	194.0	194.0	5.206	5.124	4.814
LCEP	182.46	182.50	164.0	3.415	3.399	1.697

The same procedure has been used to investigate the behavior of the ethane/n-alkane homologous series. The ethane/*n*-alkane homologous series is also of great interest. It seems that there is not a systematic study available of the application of SAFT-type equations to describe the critical behavior of this homologous series, although some other modeling approaches have been used. In particular, Polishuk et al. (2005) have used three semipredictive equations of state (the Global Phase Diagram Semipredictive Approach [GPDA], the predictive Soave-Redlich-Kwong [PSRK] and a linear combination of the Vidal and Michelsen mixing rules [LCVM]) to describe several mixtures of this family. They were able to reproduce with good accuracy several isotherms of the ethane/*n*-pentane, ethane/*n*-heptane, ethane/*n*-decane, ethane/*n*-hexadecane and ethane/*n*-tetracosane mixtures.

Results for the ethane/*n*-decane and ethane/*n*-eicosane mixtures are presented next. The ethane/decane system has been widely revised for his academic interest. Among several modeling approaches, two recent works have been implemented using a renormalization-group theory. Mi et al. (2005) performed several binary mixtures including ethane/decane. They used the original SAFT plus same White's crossover approach with two binary parameters to accurately describe vapor-liquid equilibria and the critical line of the mixture. Using the same crossover approach, Mi et al. (2006) obtained excellent predictions for this mixture with the use of the first-order mean spherical approximation (Tang and Lue, 1993, 1995) applied to the SAFT equation. Unfortunately, these two excellent works did not perform other ethane/alkane mixtures to complete the information

about this family. The ethane/eicosane mixture has not been yet studied using a crossover technique, although there are some previous works, like the one from Voutsas et al. (2004), who used different classical and molecular equations of state to describe vapor-liquid equilibria of ethane/decane and ethane/eicosane mixtures. It is also necessary to mention the molecular simulations made by Errington and Panagiotopoulos (1999) and Nath et al. (1998b) for both systems, achieving very good agreement respect to the available experimental information.

Ethane/decane and ethane/eicosane are very asymmetric mixtures since the chain length of the second compound is much greater than that of the first compound. In order to accurately describe the behavior of the mixtures two binary parameters, independent of the thermodynamic conditions, are needed. They correct the difference in size and energy of interaction between the segments belonging to the two compounds. The size binary parameter value previously used for the methane/n-alkane mixtures (η=1.030) is also used now, while a value of ξ=0.970 is used for the energy binary parameter. This second parameter is fitted to the subcritical data of the mixture ethane/decane at T=410.9K, and used in a transferable manner for the rest of the ethane/decane and ethane/eicosane mixtures investigated here. Although values are very close to unity (the ideal value), there is a significant difference in the phase diagrams obtained with these two parameters and the one obtained with no binary parameters.

The performance of the crossover soft-SAFT EoS for the ethane/decane mixtures is shown in Fig. 7.6. Fig. 7.6a depicts the *Pxy* projections of the phase diagram at the subcritical temperatures T = 310.9, 344.3, 377.6 and 410.9 K. Note that the second binary parameter was fitted to the highest temperature, the rest of the isotherms are pure predictions. The agreement with available experimental data from Bufkin et al. (2006) is excellent in all cases. Mixtures with asymmetric compounds are also characterized for having curved critical lines. Using the same set of parameters, some calculations at constant high pressure have also been performed to complete vapor-liquid equilibria calculations.
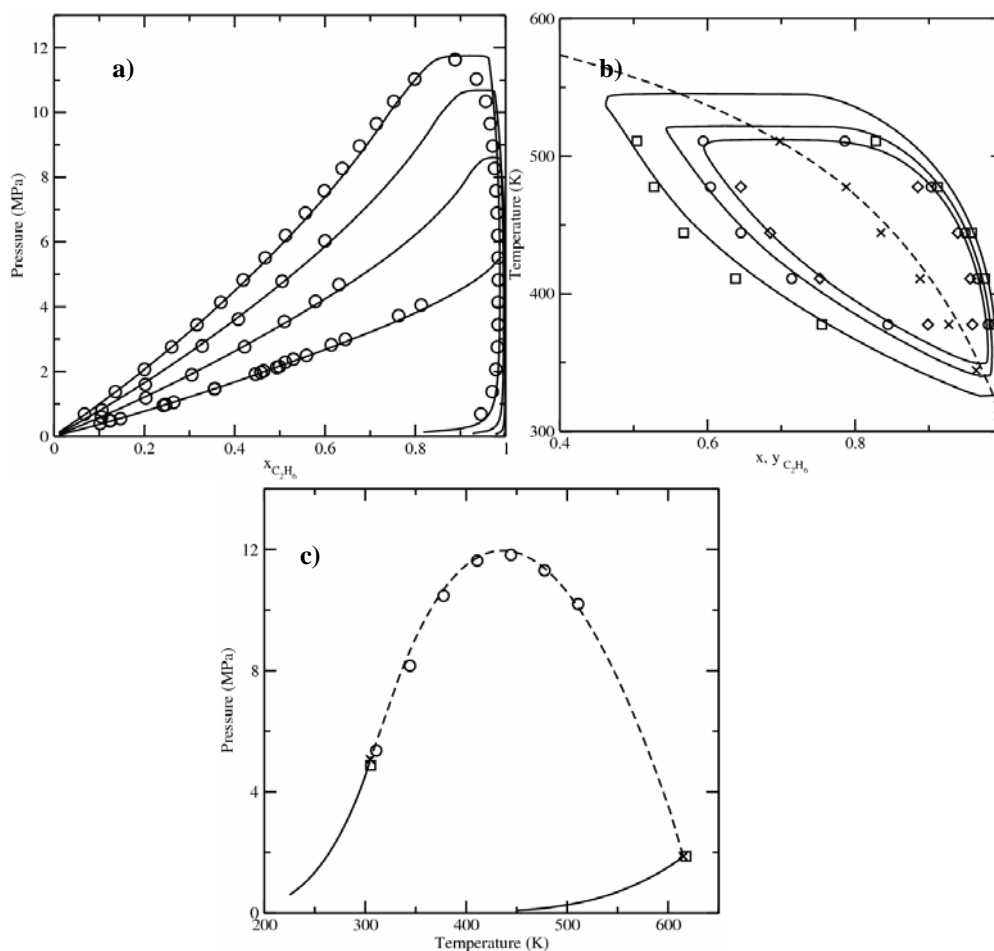
Figure 7.6: *The ethane/n-decane binary mixture. Lines represent the crossover soft-SAFT calculations. **a)** Pxy diagram of the mixture ethane/n-decane at several temperatures, from bottom to top: T = 310.9, 344.3, 377.6 and 410.9 K. Symbols represent experimental data from Bufkin et al. (1986) **b)** Txy diagram of the same mixture from outside to inside at P = 8.27 (squares); 9.65 (circles) and 10.34 (diamonds) MPa; crosses indicate the critical line experimental data; all symbols are from Reamer and Sage (1962). The dashed line is the critical line of the mixture **c)** PT diagram showing the critical line of the mixture. Symbols represent the experimental data from Reamer and sage (1962), while squares*

(experimental) and crosses (calculations) represent the critical point of the pure compounds.

Fig. 7.6b shows a *Txy* diagram of the ethane/decane mixture at three different constant pressures of 8.27, 9.65 and 10.34MPa. The overall agreement between predictions from the equation and experimental data is very good, including the critical points. However, some inaccuracies are observed in the ethane rich phase at high temperatures; the upper part of the phase behavior predicted by the crossover soft-SAFT equation is too flat, as compared to the experimental data (Reamer and Sage, 1962). A similar behavior of the equation has been observed when studying the phase diagram of pure systems, as the chain length increases (see figure 6.2.3), and it may be due to the some approximations made when developing the crossover term. Nevertheless, the equation is able to provide the two critical points, one at a high temperature and a second one at a lower temperature (see the dashed line in the figure), as it happens experimentally.

Finally, Fig. 7.6c shows the PT diagram of the mixture, with the calculated critical line in excellent agreement with available experimental data (Reamer and Sage, 1962). As expected, a classical type I behavior is obtained.

As it was done with the methane/*n*-pentane mixture, the interest remains in obtaining the transition of the mixture from type I to type V, as the length of the second compound increases, with the same set of parameters. Contrary to what happens with the methane/n-alkane homologous series, there are some discrepancies concerning where this transition takes place for the ethane/n-alkane homologous series. Gregorowicz (2003) stated that it appears in the ethane/octadecane mixture, while Rowlinson and Swinton (1982) declared that it occurs in the ethane/nonodecane mixture. In any case, it is absolutely sure that ethane/eicosane mixture exhibits type V behavior, with a very narrow range of temperature and pressure in which the liquid-liquid-vapor equilibrium region exists. The subcritical phase diagrams and critical line of this mixture have been obtained using the same binary parameters employed to describe the ethane/decane mixture; moreover, two

Pxy and one *Txy* equilibrium diagrams are shown to ensure a global accurate description of the fluid. All these results are presented in 7.7.

Figure 7.7a shows a *Pxy* diagram at two constant temperatures of 340 and 450K, while figure 7.7b presents the *Txy* diagram at a constant pressure of 9.65MPa. In both cases, the same set of binary parameters employed in the ethane/decane mixture is able to correctly describe the thermodynamic behavior at these conditions. Figure 7.7c depicts the critical line of the mixture. The inset shows an enlargement of the region near the critical point of ethane, where a type V behavior is clearly observed.
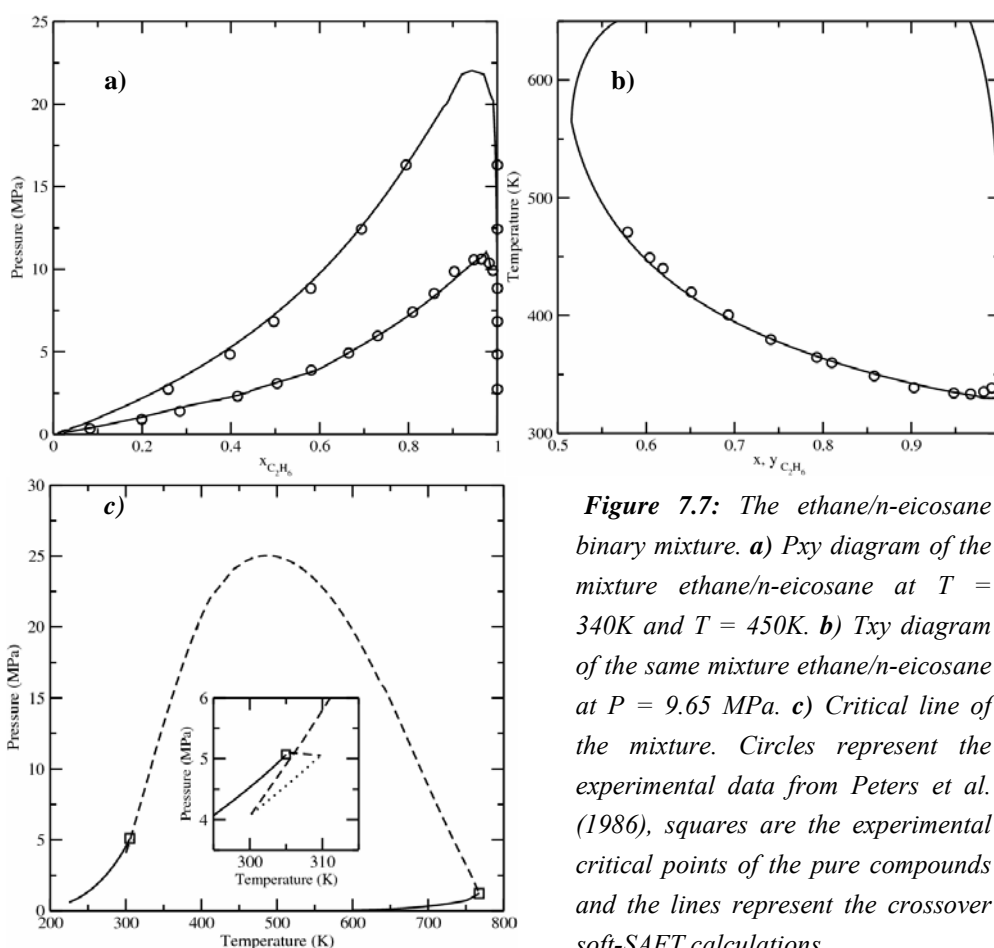
Figure 7.7: *The ethane/n-eicosane binary mixture. a) Pxy diagram of the mixture ethane/n-eicosane at T = 340K and T = 450K. b) Txy diagram of the same mixture ethane/n-eicosane at P = 9.65 MPa. c) Critical line of the mixture. Circles represent the experimental data from Peters et al. (1986), squares are the experimental critical points of the pure compounds and the lines represent the crossover soft-SAFT calculations.*

The predicted values for the UCEP and LCEP are compared with the experimental data (Specovius, 1981) in Table 7.3. As it happens for the methane/*n*-hexane mixture the LCEP is underestimated, while there is an excellent agreement between the predicted and the experimental UCEP.

Table 7.3*: Critical end point (CEP) temperature and pressure for the ethane/eicosane mixture*

Mixture	Exp.Data	Crossover soft-SAFT	Exp. Data	Crossover soft-SAFT
ethane/eicosane	T(K)	η=1.03	P(MPa)	η=1.03
UCEP	309.62	309.80	5.260	5.056
LCEP	307.69	300.20	4.927	4.089

Next step concerns the application of the soft-SAFT equation to the calculation of second order thermodynamic derivative properties of some *n*-alkane mixtures. The mixtures are selected and the tests are performed according to the available experimental information. Firstly, a mixture between propane and isobutene is selected. Propane has been deeply treated before as a pure fluid in section 6.2.1. The molecular parameters of isobutane (m=1.942, σ=4.032Å, ε/k_B=240.3K, ϕ=6.95, L/σ=1.20) are obtained by fitting vapor-liquid equilibrium data (NIST Chemistry Webbook). Once both pure fluids are well described, the performance to calculate derivative properties of a mixture is shown. Figure 7.8 is split in two graphics. Figure 7.8a depicts several *P-xy* diagrams of the mixture propane/isobutane at different temperatures ranging from 260 to 320K. Circles represent the experimental data extracted from Kayukawa et al. (2005). The agreement between calculated results and experimental data is excellent, as expected, given the ideal behavior of the mixture. Figure 7.8b shows the isochoric heat capacity as a function of temperature at two different isopleths, at a propane composition equal to 0.7006 (diamonds) and 0.2979 (circles).

Again, the soft-SAFT calculations (full lines) are in good agreement with the experimental data from Duarte-Garza and Magee (1999), with an absolute average deviation (AAD%) of 3% in both cases.
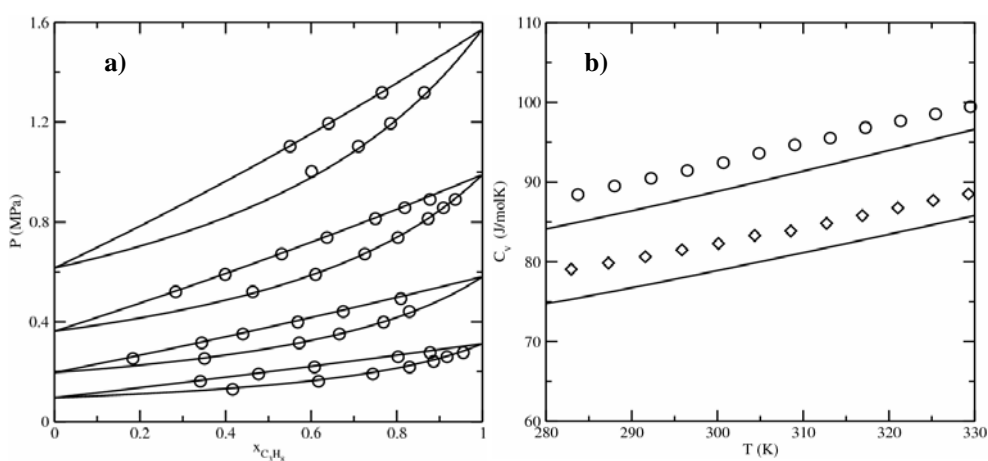
Figure 7.8: *The propane / isobutane mixture.* ***a)*** *Vapor-liquid equilibrium at T=260K, T=280K, T=300K and T=320K* ***b)*** *Isochoric heat capacity-temperature diagram of a mixture propane (1) / isobutane (2) at two constant compositions of x_1=0.7006 (Diamonds) and x_1=0.2979 (Circles). Symbols represent experimental data from Kayukawa et al. (2005) and Duarte-Garza and Magee (1999) and the solid lines are the soft-SAFT predictions.*

Finally, one of the most sensitive derivative properties has also been evaluated. Fig. 7.9 depicts the speed of sound of the mixture methane/*n*-butane as a function of the pressure, at the critical temperature (311K) and at a methane composition of 0.894, as compared to available experimental data (Plantier et al., 2005). The line represents the crossover soft-SAFT calculations with molecular parameters of the pure compounds taken from table 6.1, and the same value of the size binary parameter used in the rest of the calculations for the methane series. Note that the speed of sound is a challenging property to be accurately described with any EoS, especially close to the critical point. The crossover

soft-SAFT equation is able to quantitatively reproduce the experimental behavior, including the minimum observed near the critical pressure.
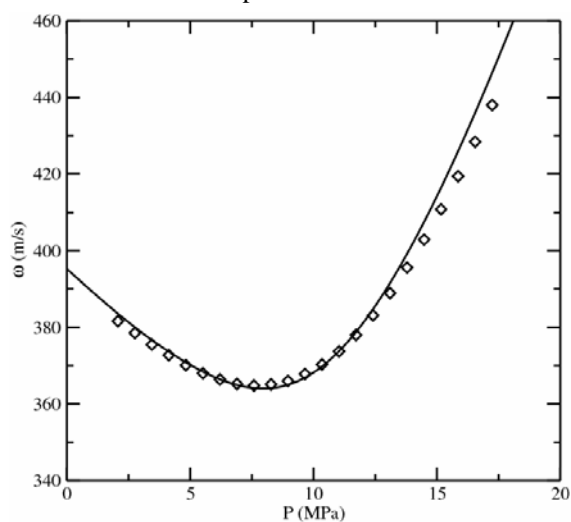
Figure 7.9: *Speed of sound versus pressure of the methane/n-butane binary mixture, at 311K and a methane composition of 0.894. Symbols represent the experimental data taken from Plantier et al. (2005) while the solid lines represent crossover soft-SAFT predictions.*

7.1.2. Mixtures of n-alkanes / 1-alkanols[2]

The behavior of *n*-alkane/1-alkanol mixtures is also of interest due to the non-ideal behavior found in these mixtures, because of the presence of the hydroxyl group in the *1-*alkanol molecules. The performance of the crossover soft-SAFT EoS to predict the critical and subcritical behavior of the n-alkane/1-alkanol mixture is checked with two model mixtures, the *1*-propanol/*n*-hexane and ethanol/n-butane mixtures. They have been chosen for two reasons, because there is experimental data available for comparison and also for the particular phase behavior they show, with an azeotropic line. These two mixtures are dissimilar regarding not only the hydrogen bonding interactions (which are accounted for in

---

[2] *This work has been published in the Journal of Supercritical Fluids (Llovell and Vega, 2006c)*

the two molecular parameters of the alkanols) but also because one of the compounds is slightly larger than the other one. This dissymmetry has been taken into account by the use of one size binary parameter, the same one used for the n-alkane asymmetric mixtures, in a transferable manner (η=1.030).

The mixture 1-propanol/*n*-hexane shows an interesting type I behavior, in which the critical line presents a minimum in temperature at an intermediate composition. This is a challenging behavior to be predicted with any EoS. Fig. 7.10a, shows the Pxy diagram of this mixture at different temperatures: 483.15, 493.15, 503.15 and 513.15 K; this figure also includes the critical line of the mixture (dashed line). Fig. 7.10b shows the critical line of the mixture 1-propanol/*n*-hexane in a pressure-temperature diagram. The calculated diagrams are compared with experimental data taken from Oh et al. (2004).
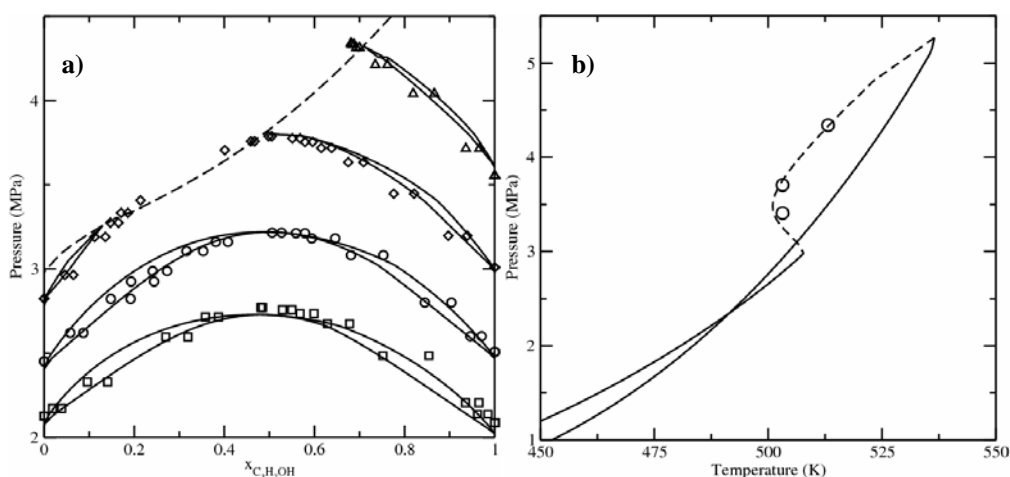
Figure 7.10*: The 1-propanol/n-hexane binary mixture. a) Pxy diagram of the mixture at 483.15, 493.15, 503.15 and 513.15K. Solid lines, phase equilibria crossover soft-SAFT predictions; dashed line, crossover soft-SAFT prediction of the critical line; symbols, experimental data from Oh et al. (2004). b) PT diagram showing the critical line of the mixture. Symbols represent the experimental data from Oh et a. (2004). Solid lines stand for the pure compounds vapor pressures; the dashed line represents the critical line of the mixture and the dotted line the predicted liquid-liquid-vapor equilibrium.*

It is striking to see the excellent agreement found between soft-SAFT predictions and experimental data in all cases. Soft-SAFT is able to capture both the subcritical and critical behavior in excellent agreement with experimental data in the whole composition range. Note that these are pure predictions since the parameters used were obtained from pure component parameters and one binary parameter from the n-alkanes mixtures.

Results for the ethanol/n-butane mixture are shown in Fig. 7.11. The lines correspond to soft-SAFT predictions with pure component parameters and the same value of the size binary parameter as in the previous cases. Again, no experimental data about the mixture was used in the equation calculations. Fig. 7.11a shows Pxy diagram at three different subcritical temperatures, far from the critical point: 273.15, 293.15 and 313.15 K. The behavior of the mixture, also at subcritical conditions, but close to the critical region is shown in Fig. 7.11b, in which different isotherms at T= 423.25, 443.25 and 463.25K are presented; in this case the critical line of the mixture is also shown. The study is completed with the prediction of the pressure-temperature critical line of the mixture, shown in Fig. 7.11c. In all graphics, symbols represent experimental data from the works of Goral et al. (2002) and Deak et al. (1995).

Again, crossover soft-SAFT is able to quantitatively predict the behavior of the mixture at subcritical and critical conditions, in excellent agreement with experimental data. This acts in favor of the transferability of the parameters used in the equation to describe the different binary mixtures.
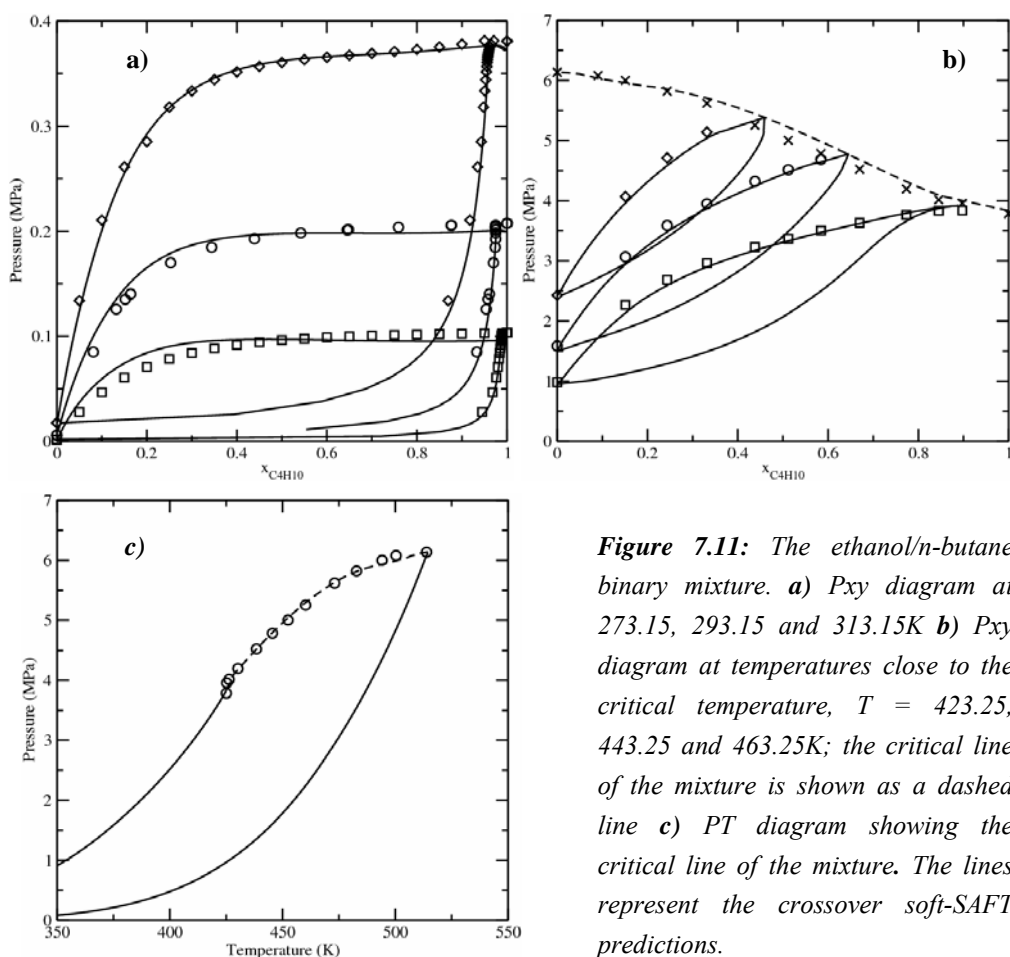
Figure 7.11: *The ethanol/n-butane binary mixture.* ***a****) Pxy diagram at 273.15, 293.15 and 313.15K* ***b****) Pxy diagram at temperatures close to the critical temperature, T = 423.25, 443.25 and 463.25K; the critical line of the mixture is shown as a dashed line* ***c****) PT diagram showing the critical line of the mixture. The lines represent the crossover soft-SAFT predictions.*

The performance of the equation for capturing the behavior of derivative properties in this kind of mixtures between associating and non-asocciating compounds is also checked. Two mixtures between *1*-propanol and *n*-alkanes have been selected for this purpose. Figure 7.12 shows the isobaric heat capacity – composition diagram of two mixtures between *1*-propanol/*n*-decane and *1*-propanol/*n*-tridecane at two given temperatures (280K and 318K). Circles (280K) and diamonds (318K) represent

experimental data obtained from Peleteiro et al. (2001, 2002) while the lines are the soft-SAFT predictions at 280K (solid line) and 318K (dashed line). These calculations were performed with the same binary parameter (η=1.030) used for vapor-liquid equilibria of *1*-propanol + *n*-hexane, in a transferable manner.
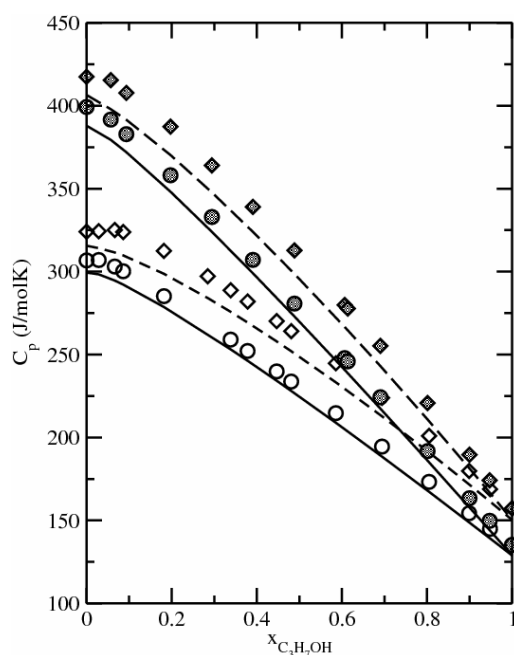
Figure 7.12: Isobaric heat capacity-composition diagram of two binary mixtures of 1-propanol with n-decane (non-filled symbols) and n-tridecane (filled symbols) at 280 K (circles) and 318K (diamonds). Open and filled symbols stand for experimental data from Peleteiro et al. (2001, 2002), while the solid lines correspond to the soft-SAFT prediction.

Excellent agreement between the experimental and the predicted values are observed in all cases, with 3% of AAD% at 280K and 5% at 318K for both mixtures.. The shape of the curve is perfectly reproduced. In the case of *1*-propanol/decane mixture, the maximum of the C_p value is reached at the same composition as the experimental value, while the maximum disappears for the *1*-propanol/tridecane, as it happens experimentally. It is also noticeable that the agreement slightly deteriorates as the temperature increases.

The same approach has been used to calculate other second order derivative properties, and, unfortunately, not all of them show the same accuracy as the previous results. In fact, it is known that the derivatives performed to calculate the isothermal and

isentropic compressibility are more sensitive to deviations, since a small error in the density is multiplied in the prediction of these properties due to their formulation (see equation 5.26 and C.21 in appendix). The accuracy of the calculation in these properties for the same mixture *1*-propanol/*n*-decane has been checked. Predictions of the isentropic compressibility for this mixture at 280K and 318K are depicted in Figure 7.13.
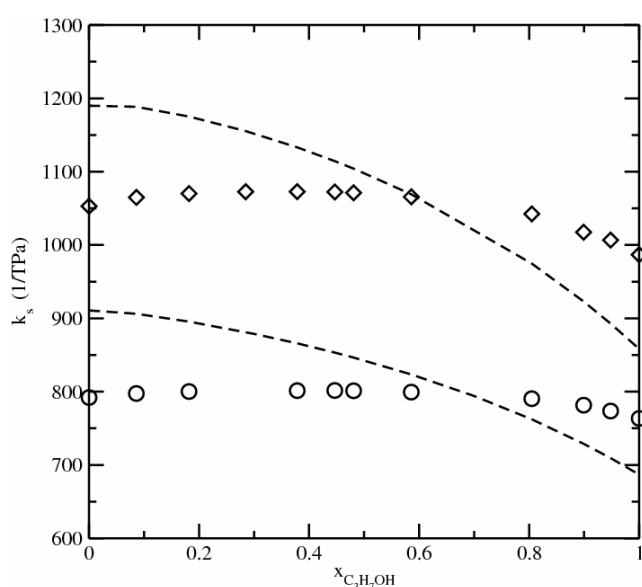
Figure 7.13: Isentropic compressibility-composition diagram of a mixture 1-propanol n-decane at 280 K (circles) and 318K (diamonds). Experimental source from Peleteiro et al.(2002). Dashed lines are the soft-SAFT predictions.

It is observed that the value of k_s was underestimated from soft-SAFT for the associating fluid (*1*-propanol) while this property was overestimated for the non-associating fluid (*n*-decane) with respect to the experimental data. The combination of these inaccuracies in the pure compounds is shown in the estimation of the mixture behavior.

A further way to check if the deviations come from inaccuracies in the pure components description and/or from the non-ideal behavior of the mixtures is to evaluate the excess properties. The excess properties reflect the deviations from ideality due to several factors: the self-association of 1-alkanols in solution which produces a strong departure from random mixing, the change in the non-specific interactions during mixing, the packing effects, etc. In fact, a good prediction of the excess properties reflects the

accuracy of the method in capturing the non-ideality of the mixing (dos Ramos and Blas, 2005). Hence, it is decided to calculate some excess properties of the non-ideal mixtures under investigation. Figure 7.14a shows the excess C_p for the mixture *1*-propanol / *n*-decane at 280 and 318K (the same temperatures provided in Figures 7.12 and 7.13). Quantitative agreement with experimental data at 280K is predicted with the soft-SAFT equation, while the agreement deteriorates at 318 K. Figure 7.14b shows the excess k_s for the same mixture at the same fixed temperatures 280K and 318K. The trend of the calculated points is exactly the same in the experimental data and the soft-SAFT predictions. Although there is not quantitative agreement at the intermediate compositions, the behavior of the mixture (self-association, non specific interaction, etc.) is well captured by the theory. In that way, it can be assumed that if one is able to better estimate the pure fluid property, the mixture will be automatically corrected.
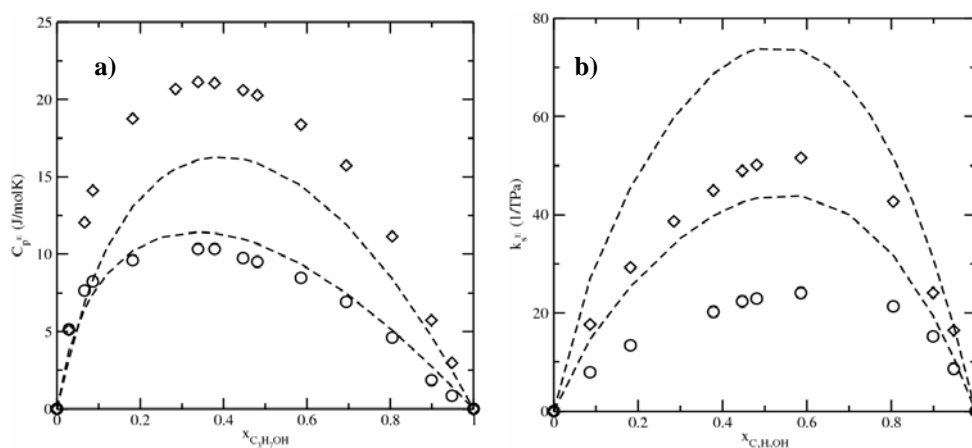
Figure 7.14: *Some excess properties of the mixture 1-propanol/n-decane at 280K (circles) and 318K (diamonds). **a**) Excess isobaric heat capacity. **b**) Excess isentropic compressibility. Legend as in Figure 7.13.*

Finally, some estimations of the speed of sound for the mixture *1*-propanol / *n*-heptane are presented. The modeling is compared with experimental data from Dzida and Ernst (2003).

The speed of sound is, in fact, a stringent test to any EoS since it involves the combination of several second-order derivative properties, in which the inaccuracies can be magnified. In the section devoted to pure fluids, some inaccuracies for estimating the speed of sound of alkanes and *1*-alkanols had been observed. Soft-SAFT underestimated the speed of sound of *n*-heptane, while it overestimated the speed of sound of pure 1-propanol at low pressures. As a result, the prediction of the mixture is affected by these discrepancies, as it is observed in Figure 7.15.
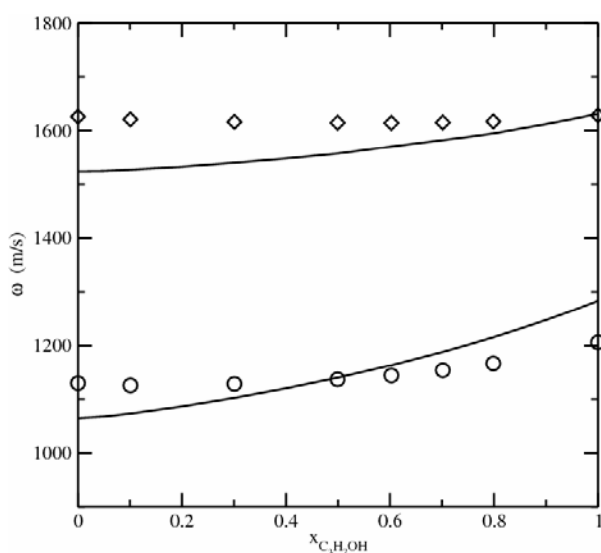
Figure 7.15: *Speed of sound – density diagram at 0.1 (circles) and 101.3 MPa (diamonds) for the 1-propanol / n-heptane mixture. Symbols represent experimental data from Dzida and Ernst (2003) and the lines stand for the soft-SAFT predictions.*

However, it should be emphasized that the AADs% obtained for the mixture is only 3.5% and 3.3% for 0.1MPa and 101.3 MPa, respectively, which can be considered as a good approximation for a pure prediction.

7.1.3. The CO$_2$ / n-alkanes mixtures[3]

The next step in the applicability of the crossover soft-SAFT is to test the accuracy of the equation when dealing with mixtures that involve a compound of different nature mixed with a hydrocarbon. Among many possibilities, CO$_2$ remains like one of the most used compounds in the industry, especially as a supercritical fluid. Moreover, as it has been described in Chapter 2, CO$_2$ is the best constituent for supercritical applications. As a consequence, a good modeling for CO$_2$ mixtures is crucial and necessary for engineering applications.

The CO$_2$/*n*-alkanes series has been selected to check the capabilities of the equation. It is especially interesting to revise if the equation is able to reproduce the continuous change of behavior observed in these mixtures when the chain length of the second compound is increased. For this purpose, four different systems have been selected with increasing chain length: CO$_2$/ethane, to see the effect of carbon dioxide in a short alkane, and then the three mixtures CO$_2$/*n*-decane, CO$_2$/tridecane and CO$_2$/hexadecane, as representative of the three different types of behavior experimentally observed in these mixtures. It has been shown that the CO$_2$/decane mixture shows type II behavior. When the chain length of the second compound increases and evolves till tridecane, the type IV behavior appears and the critical line is splitted in two parts, with a liquid-liquid-vapor region joining both. Finally, the CO$_2$/hexadecane mixture has already evolved to type III, with a continuous critical line ending at infinite pressures.

Figure 7.16a shows the vapor-liquid equilibria of the mixture CO$_2$/ethane at different temperatures. Symbols represent experimental data (Fredenslund and Mollerup, 1974) and solid lines are the equation predictions. Although pure predictions without binary parameters were in good agreement with experimental data, the energy binary parameter ξ has been slightly adjusted to experimental data to an intermediate subcritical temperature of

---

[3] *This work has been published in J. Phys. Chem. B (Llovell and Vega, 2006a)*

283K (ξ=0.990). Very good agreement is observed between the modeling and the experimental values at all temperatures. The azeotropes are predicted at the correct pressure and mole fraction. Figure 7.16b depicts the predicted critical line of this mixture.
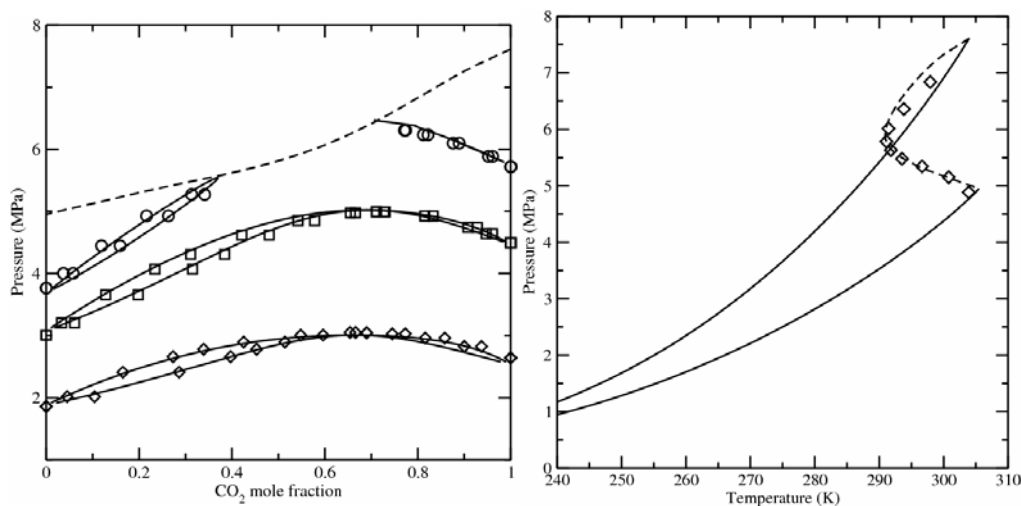
Figure 7.16 a) *Pxy projections of the CO$_2$/ethane mixtures at 263.15, 283.15 and 293.15 K.* ***b)*** *PT projection of the PTxy surface for the CO$_2$/ethane mixtures. Symbols represent experimental data (Fredenslund and Mollerup, 1974) and solid lines are the soft-SAFT predictions. The dashed line corresponds to the critical line of the mixture.*

The trend of the curve is perfectly captured by the equation, providing an excellent description of the behavior of this mixture, including the azeotropic line. It is important to notice that, although this mixture correspond to the type I behavior, the shape of the critical line, with a temperature minima between the two compounds, is not straightforward to obtain with an EoS. It is assumed that the particular behavior of this mixture is due to the quadrupolar interactions of the CO$_2$ molecule as well as the short length of the *n*-alkane. For instance, in some other works (Galindo and Blas, 2002) it was necessary to use some binary parameters far away from unity, since quadrupolar interactions were not explicitly considered in that case. In our case, just one binary parameter, very close to unity, is enough to obtain an excellent representation of this mixture.

Figures 7.17a, 7.17b and 7.17c show the *PT* projections for the mixtures CO$_2$/decane, CO$_2$/tridecane and CO$_2$/hexadecane as obtained from the crossover soft-SAFT equation. As it has been said, the goal is to study the evolution of the critical behavior. In this case, and due to the lack of experimental vapor-liquid equilibria data, the parameters η= 1.025 and ξ=0.950 have been fitted to the critical points data of the CO$_2$/tridecane mixture and used to predict the behavior of the homologous series. In general, very good agreement is achieved in all cases. CO$_2$/decane shows type II behavior, with the critical line joining the critical point of both pure compounds. CO$_2$/tridecane, belonging to type IV behavior, becomes the most difficult mixture to predict because it is in the intermediate changing behavior with a very narrow range before the series evolves to type III as the chain length of the second compound increases. However, crossover soft-SAFT is able to reproduce this shape, with the appropriate binary parameters. The three-phase-line is found and the UCEP and the LCEP are compared to experimental values in Table 7.4.

Table 7.4: *Critical end point (CEP) temperature and pressure for the type IV binary mixture CO$_2$/n-tridecane. Experimental data obtained from Ziegler and Chester (1995).*

CO$_2$/tridecane mixture	T^{exp}	T^{SAFT}	P^{exp}	P^{SAFT}
UCEP	279.0	289.0	3.933	4.408
LCEP	310.8	305.6	8.114	5.751
UCEP	314.0	315.2	8.716	7.625

Finally, CO$_2$/hexadecane exhibits a clear type III behavior. The critical line goes to infinite pressures and very good agreement is obtained with experimental data, although the border between the gas-liquid and the liquid-liquid could be better predicted. Note that this could be achieved if binary parameters were optimized for this particular mixture, but in this case the binary parameters were taken from the CO$_2$/tridecane mixture. The purpose of this study is to use the same binary parameters to predict the evolution in the CO$_2$/*n*-alkanes homologous series; the results indicate this achievement, and the capability of the crossover

soft-SAFT equation to predict critical behavior of this type of mixtures in excellent agreement with experimental data.
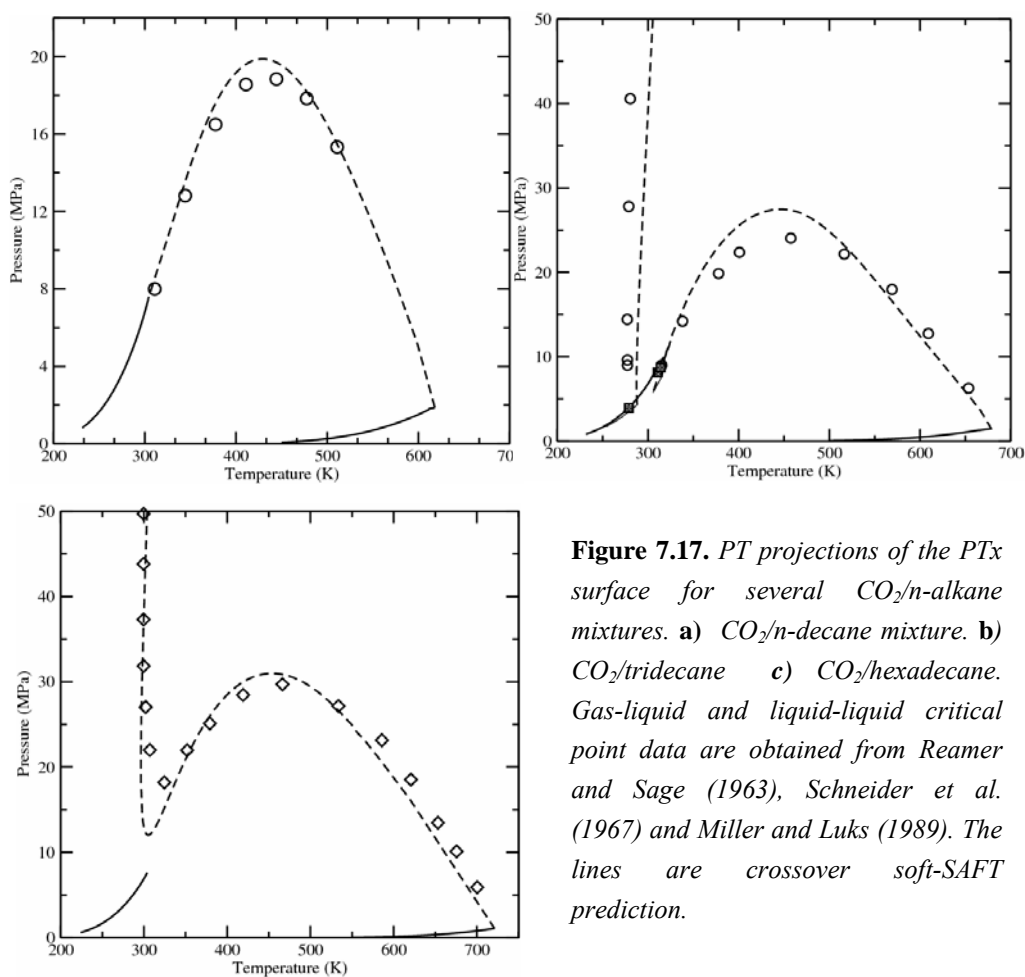
Figure 7.17. *PT projections of the PTx surface for several CO$_2$/n-alkane mixtures.* **a)** *CO$_2$/n-decane mixture.* **b)** *CO$_2$/tridecane* **c)** *CO$_2$/hexadecane. Gas-liquid and liquid-liquid critical point data are obtained from Reamer and Sage (1963), Schneider et al. (1967) and Miller and Luks (1989). The lines are crossover soft-SAFT prediction.*

7.1.4. Mixtures of CO$_2$ / 1- alkanols[4]

In a similar manner as done in the last section, mixtures of CO$_2$ with *1*-alkanols are studied because of both, its industrial and academic interest. In order to check the continuous change of behavior in this homologous series the mixtures from *1*-propanol till *1*-hexanol have been selected to examine the critical region. According to the literature (Raeissi et al., 1998; Polishuk et al., 2001), CO$_2$/alkanol mixtures evolve from type II to type III behavior. CO$_2$/*1*-propanol and CO$_2$/*1*-butanol have been confirmed to show type II behavior, while the mixture with *1*-hexanol is already a type III. Some discussion has been reported about CO$_2$/1-pentanol binary mixture: Raeissi et al. (1998) have identified it as a type IV, finding that this particular mixture exhibits a very narrow part of the limited liquid-liquid inmiscibility, which has been missed by other authors (Lan et al., 1990.; Gurdial et al., 1993). Due to the narrow range in which this behavior appears this is a very challenging mixture for any theoretical approach. The performance of the crossover soft-SAFT equation is investigated with these mixtures, trying to find a global modeling for the homologous series, as it was done for the CO$_2$/*n*-alkanes homologous series.

Figure 7.18 show the critical lines for the CO$_2$/*1*-propanol, CO$_2$/*1*-butanol, CO$_2$/*1*-pentanol and CO$_2$/*1*-hexanol binary mixtures. Symbols represent the experimental data taken from Sang-Do et al. (2000), Ziegler and Chester (1995) and Scheidgen (1997). As previously done for the *n*-alkane binary mixtures, binary parameters could be fitted to experimental data from a single subcritical isotherm for each mixture and used to predict the behavior of the same mixture at other thermodynamic conditions, including the critical lines. Alternatively, as it was done with the CO$_2$/n-alkanes mixtures with heavy compounds, binary parameters can also be fitted to one selected mixture and used to predict the evolution of the critical line of the homologous series and the subcritical behavior of these mixtures. As the interest mainly remains in describing the critical line evolution in the

---

[4] *This work has been published in the J. Phys. Chem. B (Llovell and Vega, 2006a)*

homologous series as the length of the second compound increases, this second approach is followed in order to check the capability of the equation to predict this behavior with a unique set of binary parameters for the whole series (although in some cases, this may not be the best fit to the available data). Using a value of η= 0.970 and ξ = 1.010 an accurate description of the overall critical behavior is achieved.
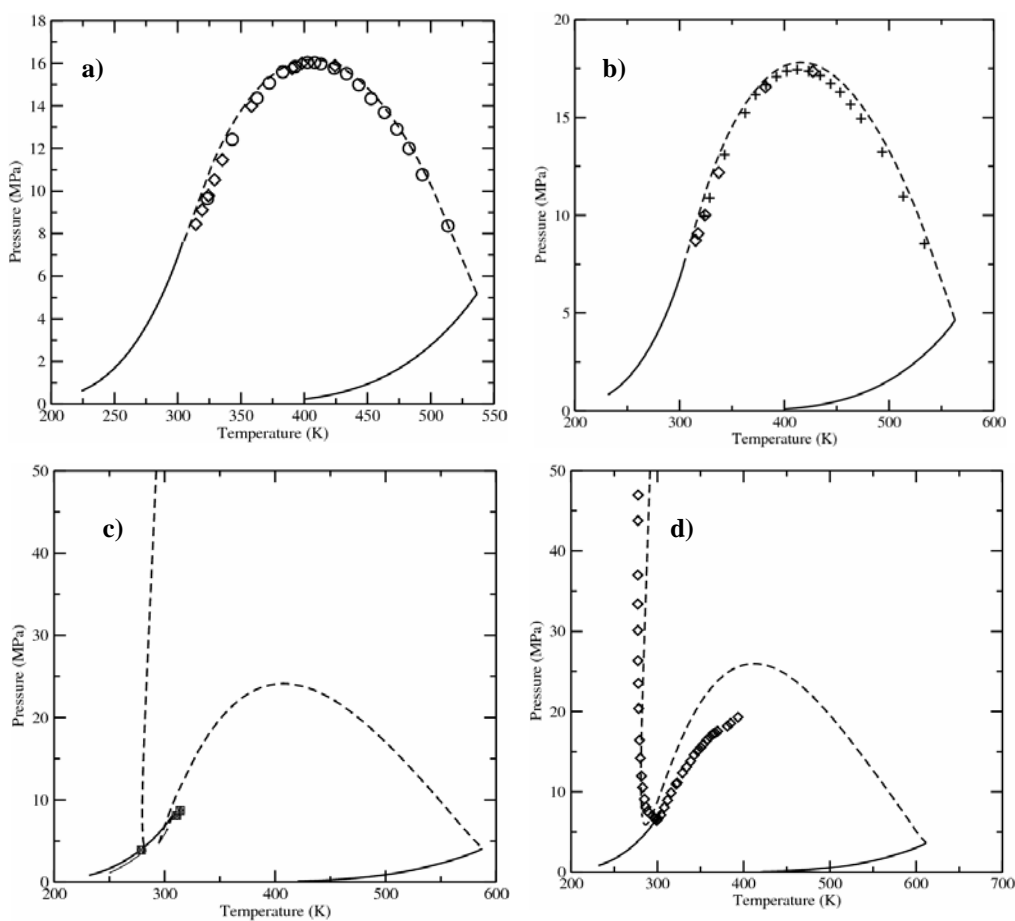
Figure 7.18*: PT projection of the PTx surface for some CO$_2$/1-alkanol binary mixtures. **a)** CO$_2$/1-propanol **b)** CO$_2$/1-butanol **c)** CO$_2$/1-pentanol **d)** CO$_2$/1-hexanol. Symbols represent experimental data (Sang-Do et al., 2000) and solid lines are the crossover soft-SAFT predictions.*

CO$_2$/1-propanol and CO$_2$/1-butanol show type II behavior, with the critical line of the mixture ending at the critical point of the pure compounds. Excellent agreement between the soft-SAFT description and the experimental data is achieved for the two mixtures. The CO$_2$/1-pentanol mixture falls into type IV behavior, as experimentally measured by Raeissi et al. (1998), and theoretically obtained by Polishuk et al. (2001). A short three phase line is found and an UCEP and a LCEP could be determined with the equation. However, it is important to remark that a slight variation of the binary parameters makes this region to disappear, becoming a type II or type III mixture. A comparison between the calculated critical end points and the experimental values is presented in Table 7.5.

Table 7.5: *Critical end point (CEP) temperature and pressure for type IV binary mixture CO$_2$/1-pentanol. Experimental data obtained from Ziegler and Chester (1995).*

CO$_2$/1-pentanol mixture	T^{exp}	T^{SAFT}	P^{exp}	P^{SAFT}
UCEP	273.5	283.4	3.413	3.981
LCEP	317.0	294.7	8.752	4.689
UCEP	317.0	301.8	8.950	7.325

As expected, this mixture is particularly difficult to model, being extremely sensitive to the selected parameters. Finally, the CO$_2$/1-hexanol mixture shows type III behavior. Note that, although the binary parameters chosen for the whole homologous series are not the best to quantitatively describe this last data, they are still good enough to capture the overall behavior of the mixture. In particular, the gas-liquid critical line of the CO$_2$/1-hexanol mixture is overpredicted, as compared to experimental data (Scheidgen, 1997).

Moreover, the capability of the two selected binary parameters ($\eta = 0.970$ and $\xi = 1.010$), fitted to describe the critical behavior of the mixtures, has to be checked predicting the subcritical behavior of them. The four mixtures of this homologous series studied above, representing type II, type III and type IV behavior, are also investigated here. *Pxy*

projections of the CO$_2$/*1*-propanol, CO$_2$/*1*-butanol, CO$_2$/*1*-pentanol and CO$_2$/*1*-hexanol mixtures as obtained by crossover soft-SAFT are compared to available experimental data in figure 7.19.
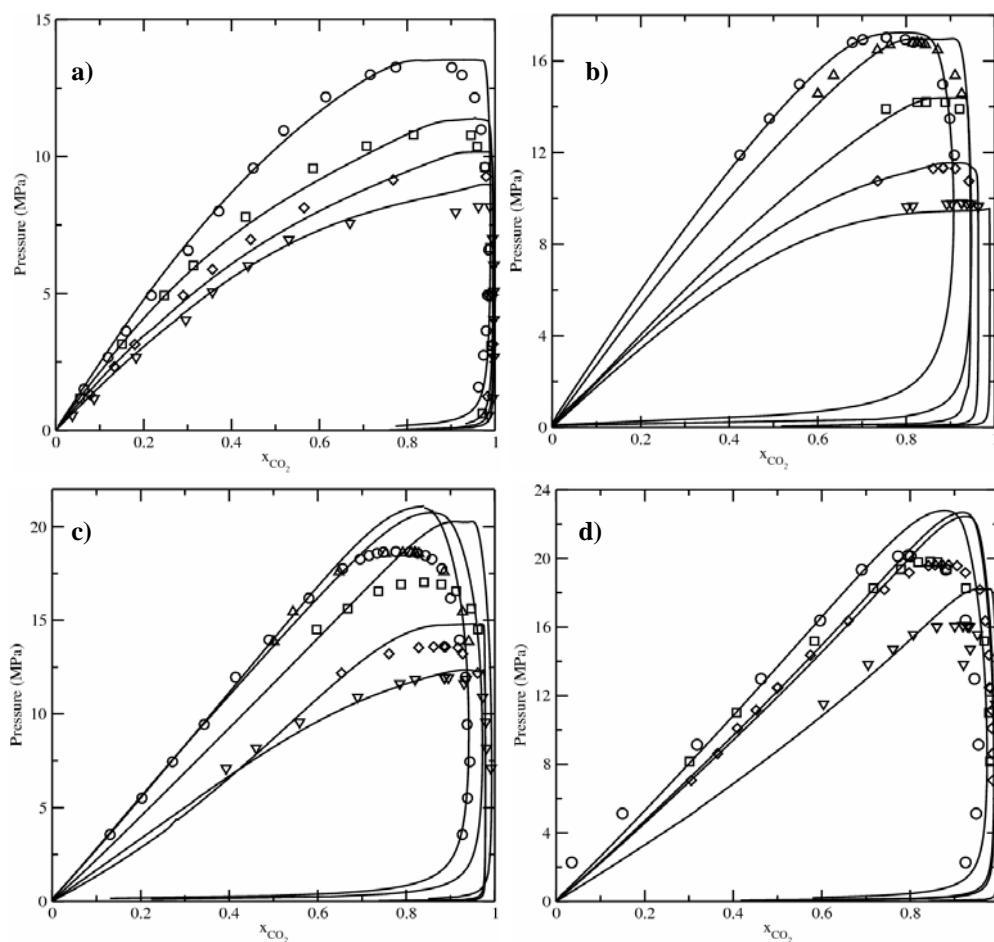
Figure 7.19: *Pxy projections of the **a)** CO$_2$/1-propanol mixtures at four different temperatures: 313.4 ($\triangledown$), 322.36 ($\diamond$), 333.4 ($\square$) and 352.83 K ($\bigcirc$). Symbols are experimental data: T = 322 and 352K taken from Mendoza de la Cruz and Galicia-Luna (1999), while data for T = 313 and 333K was taken from Suzuki and Sue (1990). **b)** CO$_2$/1-butanol mixtures at five different temperatures 324.16 ($\triangledown$), 333.58 ($\diamond$), 355.38 ($\square$), 392.72 ($\triangle$) and 427.95K ($\bigcirc$). Symbols are experimental data from Silva-Oliver and Galicia-Luna*

(2001). ***c)*** *CO$_2$/1-pentanol mixtures at five different temperatures 333.08 ($\triangledown$), 343.69 ($\lozenge$), 374.93 ($\square$), 414.23 ($\triangle$) and 427.86K ($\bigcirc$). Symbols are experimental data from Silva-Oliver et al. (2002).* ***d)*** *CO$_2$/1-hexanol mixtures at four different temperatures 353.93 ($\triangledown$), 397.78 ($\lozenge$), 403.39 ($\square$) and 432.45K ($\bigcirc$). Symbols are experimental data from Elizalde-Solis et al. (2003). In all cases, solid lines represent soft-SAFT predictions.*

It is remarkable to see the excellent agreement obtained for the CO$_2$/*1*-propanol and CO$_2$/*1*-butanol mixtures, in quantitative agreement with experimental data. The agreement is also very good for the CO$_2$/*1*-pentanol and CO$_2$/*1*-hexanol mixtures far from the critical point, although, as expected from the Px projections (figures 7.19a and 7.19b), it deteriorates as the mixtures approach their critical point, overestimating them. It should be emphasized that a better description of each mixture could be achieved if the parameters were fitted to their particular data. However, it has been decided to use a unique set of parameters to describe the behavior of the homologous series, in a transferable manner.

A final remark should be made regarding the quadrupolar interactions found in the two homologous series: since in the case of CO$_2$/*1*-alkanol there are strong associating forces, this effect screens the quadrupolar interactions, which are more relevant in the CO$_2$/*n*-alkane mixtures where no association is present.

7.1.5. Mixtures of HCl / n-alkanes[5]

Mixtures of HCl / *n*-alkanes can be found in several industrial processes. The most important application is the production of organic compounds, although they are also found in the industry of leather processing, household cleaning, and building construction. Their accurate modeling poses a solution to avoid the difficult experimental measurements due to the corrosive nature of the hydrogen chloride. From an academic point of view, these mixtures remain quite unexplored and their critical behavior has not been studied yet.

The modeling of hydrogen chloride has been already treated in section 6.2.4. Once the pure fluids have been studied, next step concerns the modeling of the binary mixtures between hydrogen chloride/*n*-alkanes. The only available experimental data has been found for the mixtures with ethane, *n*-propane and *n*-dodecane (Galindo et al. 1999). Hence, the efforts have been devoted to the modeling of vapor-liquid equilibria of two of these three mixtures: hydrogen chloride/n-propane and hydrogen chloride/*n*-dodecane.

Pure component parameters were obtained by fitting to vapor-liquid equilibrium data. The mixtures have been calculated using the parameters for the pure fluids. However, it has been observed that the energy parameter ξ was needed to be adjusted in mixtures to obtain quantitative agreement in the modeling. The procedure was done adjusting the energy parameter to one single *Pxy* diagram to experimental data just at an intermediate temperature. Once the adjusted value for ξ is obtained, it is used to calculate all the other equilibriums and the critical line. Moreover, due to the transferability power of the equation, it is expected that the same binary parameter will be good enough to model any other mixture of HCl / *n*-alkanes. The diagram selected was for the mixture HCl / n-propane at a constant temperature of 313K, and a value of ξ=0.920 was obtained.

---

[5] *The experimental data was measured at Delft University of Technology by L.J. Florusse. The new experimental data and the modeling work have been submitted to J. Phys. Chem. B. (2006).*

Fig. 7.20a shows some Pxy diagrams at constant temperatures in the range from 273 to 353K. Circles, squares, diamonds, triangles and crosses represent experimental data of this work at 273, 293, 313, 333 and 353K, and the solid lines are the results from soft-SAFT. As it is observed, quantitative agreement is obtained for all the temperatures using the same binary parameter ξ in all cases. The vapor-liquid critical line is also shown in this graphic and the agreement between the theory and the experimental measurements is very good. In Fig. 7.20b, a pressure-temperature projection of the mixture is presented. Symbols are experimental data measured in Delft (Llovell et al, 2006b), while the dashed line is the soft-SAFT prediction.
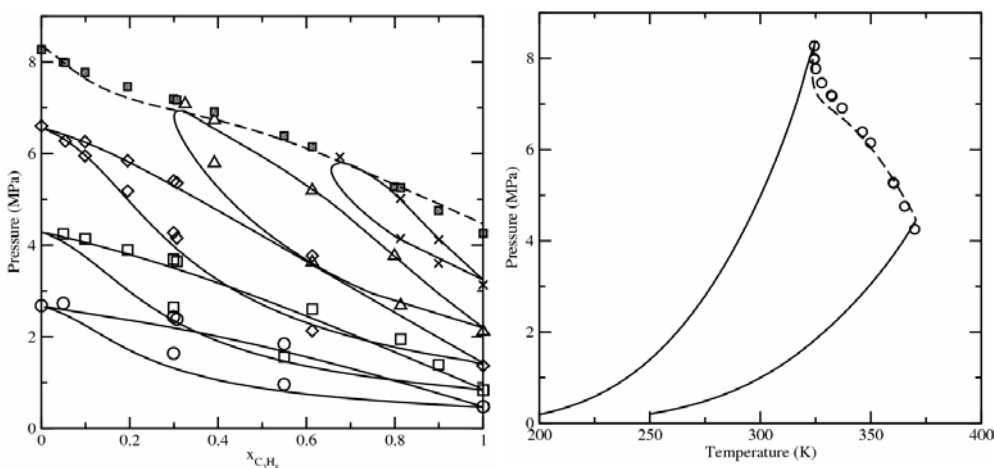
Figure 7.20 a*) Pxy projections of the hydrogen chloride(1) / n-propane(2) mixture at five different temperatures of 273 (○), 293 (□), 313 (◇), 333 (△) and 353K (✕) plus critical line. Symbols are the experimental data, the filled squares represent the critical line points, the solid lines are the soft-SAFT predictions for each isotherm and the dashed line is the equation prediction for the critical line.* ***b****) Pressure-Temperature diagram of the same mixture showing the critical line. Symbols represent the experimental data from Llovell et al. (2006), solid lines are the pure fluid soft-SAFT calculations while the dashed line is the critical line predicted by the equation.*

Soft-SAFT is able to reproduce the nature of the critical line showing quantitative agreement for the whole critical composition, with slight deviations close to the critical point of hydrogen chloride. The theory has confirmed that HCl / *n*-propane exhibits a Type I behavior, with a continuous vapor-liquid critical line connecting both critical points.

Following the same procedure, HCl / *n*-dodecane mixture has been studied. In Fig. 7.21a, several *Px* diagrams are depicted in a range from 283 to 363K. Circles, squares, diamonds, triangles and crosses are experimental data at 283, 303, 323, 343 and 363K respectively. The solid lines correspond to soft-SAFT predictions. As it has already been stated, the same value for the binary energy parameter ξ is used here. Quantitative agreement is obtained at higher concentrations of hydrogen chloride while some deviations are shown when increasing the mole fraction of *n*-dodecane. The global agreement is very good at all temperatures. Although the results could be still improved changing the value of the binary parameter, it would result in a loss of predictive power from the soft-SAFT equation. As the actual prediction seems accurate enough, it is preferable remaining with the same value and to use it to study other mixtures of chlorhydric acid and *n*-alkanes. Fig. 7.21b shows a pressure-temperature projection with the calculation of the critical line for this mixture. As far as we know, no experimental data is available to compare with the soft-SAFT prediction. A type II critical behavior has been found. The effect of the presence of a longer *n*-alkane has produced the creation of a second critical line that shows that there is a liquid-liquid equilibrium at low temperatures.
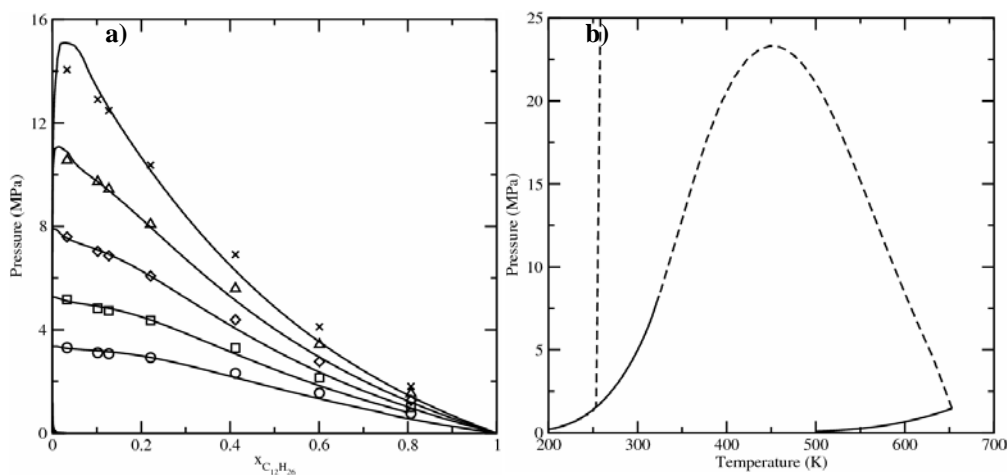
Figure 7.21 a) *Pxy projections of the hydrogen chloride(1) / n-dodecane(2) mixture at five different temperatures of 283 (○), 303 (□), 323 (◊), 343 (△) and 363K (✕).* ***b)*** *Pressure-Temperature diagram of the mixture showing the critical line. Symbols and lines as in Figure 7.20.*

A further step in this research is to investigate the behavior of the mixture as the chain length of the *n*-alkane is increased. This is the first time that this transition is studied. It is expected that both, the gas-liquid and the liquid-liquid critical line, will be joined forming a Type III behavior, but it is difficult to precisely define where this transition will take place. Moreover, the formation of a Type IV (a transition between Type II and III) could also be achieved in a particular *n*-alkane length. Using the same binary parameter ξ, it has been determined that the transition to Type III is clear for the *n*-heneicosane. Fig. 7.22 shows a PT projection where the critical line of the mixture hydrogen chloride / n-heneicosane ($C_{21}H_{44}$) exhibits a Type III behavior. The influence of the binary parameter selected is very strong and a small modification of this value can produce the formation of this critical behavior at lower or higher chain lengths. It is not clear at this point if the mixture between hydrogen chloride and *n*-eicosane exhibits Type II, IV or III behavior. Some experimental work would be really useful in order to check this transition.
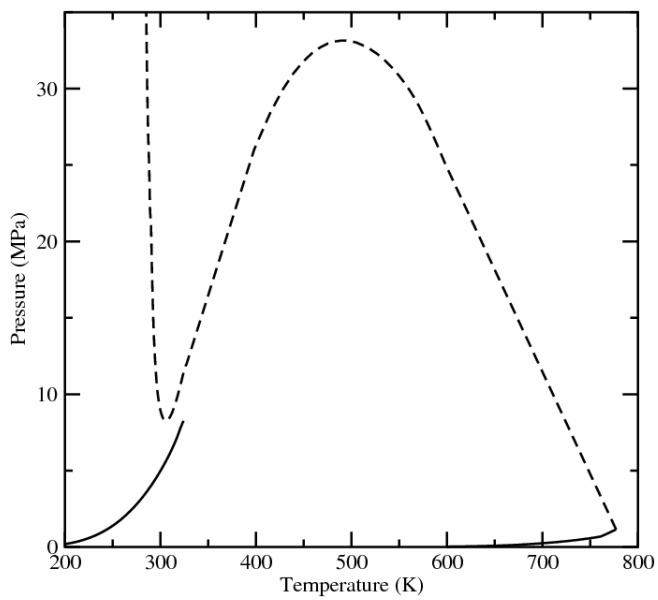
Figure 7.22 Pressure-Temperature diagram of a mixture hydrogen chloride / n-heneicosane. Lines as in Figure 7.20b.

7.2. Ternary mixtures

Ternary mixtures can be used as model systems for some important applications in supercritical and near-critical fluid technology. However, when working at supercritical conditions, complex multiphase equilibria can occur in these mixtures, especially close to the critical point of the solvent. For small changes in temperature, pressure or composition, a variety of unexpected phenomena can be encountered and not directly be anticipated regarding only the binary subsystems. This makes clear that a need for systematic research on the fluid phase behavior of multicomponent mixtures is in order, especially since experimental information in literature on systems with three or more components is very limited.

The last part of the results of this work concerns the study of some ternary mixtures of particular interest. Based on the discovery of Patton et al. (1993), founding two-phase holes enclosed in three-phase surfaces liquid-liquid-vapor (LLV) for some mixtures of CO$_2$/alkane/1-alkanol, some preliminary results for modeling this particular thermodynamic behavior in ternary systems containing near-critical CO$_2$ and two heavier solutes is carried out.

7.2.1. Closed miscibility loops

In 1993, Patton et al. conducted phase equilibrium experiments in ternary mixtures of carbon dioxide / *n*-tetradecane / *1*-decanol. Much attention was given to determine critical endpoints of the three phase equilibrium liquid-liquid-vapor in mixtures with about 95 mol% of carbon dioxide and various ratios of both solutes with total concentration of the two solutes of about 5 mol%. Their measurements showed an unexpected two-phase hole liquid-vapor (associated to Type IV critical behavior) in the three phase surface LLV for a

certain mole fraction of tetradecane. In fact, this result could not be predicted from the binary mixtures CO$_2$ / tetradecane and CO$_2$ / *1*-decanol , which exhibit Type III behavior.

Patton et al. (1993) explained the occurrence of a two-phase hole in the three-phase surface by assuming the formation of aggregates of decanol molecules due to hydrogen bonding. Starting from a binary mixture between CO$_2$ and tetradecane, a continuous replacing of tetradecane by decanol in the mixture would result in a decrease of the average carbon number of the solute mixture tetradecane/decanol. In a certain moment, the mixture would tend to change its fluid phase behavior into that exhibited by a mixture CO$_2$ / tridecane (type IV). However, if the amount of decanol continues increasing, the aggregation of the decanol molecules due to its increasing concentration would play a significant role. The consequence would be an increasing of the average carbon number due to this aggregation phenomena, changing the phase behavior again into Type III. Some spectroscopic studies of Fulton et al. (1993) confirmed that at the study conditions alkanols aggregates of four molecules are formed, giving to the theory a higher credibility.

Later on, Scheidgen (1997) argued that this behavior was a consequence of a cosolvency effect. Cosolvency is defined as the effect whereby a mixture of two solutes A and B is better solvable in a solvent than any of the solutes A and B individually. In this case, the cosolvency effect would decrease the value of the pressure minimum of the liquid-liquid critical locus. Once that minimum crosses the liquid-liquid-vapor surface, Type IV behavior would appear. At a certain decanol concentration, the solubility of the mixture would begin to decrease returning to the original Type III behavior.

Both concepts seem quite reasonable for explaining these phenomena. It is clear that these "physical" effects will only be modeled with accuracy using a tool that takes into account the physics of each compound involved.

7.2.2. Mathematical approaches to modeling miscibility loops

There are only few published papers in the literature devoted to the modeling of these ternary mixtures. Gauter and Peters (1999) modeled several mixtures of CO$_2$ / tetradecane / *1*-alkanols using the Soave-Redlich-Kwong equation of state.

Two different approaches can be used for modeling closed miscibility loops of ternary mixtures: a quasi-binary mixture approach and a strict calculation of the critical endpoints for ternary mixtures.

The quasi-binary approach is a methodology based on the principle of congruence. This principle was firstly described by Brønsted and Koefoed (1946) and proposed that for a mixture of components belonging to a homologous series, an index ν can be found characterizing the mixture. Other mixtures, having the same ν are supposed to have the same values for some of their thermodynamic properties. These mixtures are called congruent to each other. For this particular case, there would be an index ν supposing that the average chain length is equal to the carbon number of the alkane belonging to the corresponding mixture of the homologous series CO$_2$ / *n*-alkanes.

The average solute chain length (CL^{av}) for a ternary CO$_2$ / *1*-alkanol / *n*-alkane system can be obtained as (Brønsted and Koefoed, 1946; Smits et al., 1998):

$$CL^{av} = zCL^{CH(1)} + (1-z)CL^{COH(av)} \tag{7.1}$$

where z is the mole fraction of the alkane in the mixture, $CL^{CH(l)}$ represents the chain length of a single alkane molecule (equal to the carbon number) and $CL^{COH(av)}$ is the average chain length of the alkanol aggregates. This value is calculated assuming a monodisperse aggregate distribution of aggregate sizes. It means that the average size of the aggregates is a constant value independent of the total alkanol mole fraction for a given temperature. With this assumption, the value of $CL^{COH(av)}$ can be obtained from:

$$CL^{COH(av)} = yCL^{COH(1)} + (1-y)CL^{COH(agg)} = yCL^{COH(1)} + (1-y)\beta CL^{COH(1)} \quad (7.2)$$

being y the fraction of alkanol molecules present as single molecules, $CL^{COH(l)}$ the chain length of a single alkanol molecule and β the aggregation number.

The formation of mono-disperse aggregates is given by the equation:

$$\beta C_N H_{2N+1} OH \leftrightarrow (C_N H_{2N+1} OH)_\beta \quad (7.3)$$

The method assumes that the equilibrium constant K of this reaction can be calculated considering a first order approximation of an ideal solution.

$$K = \frac{(C_N H_{2N+1} OH)_\beta}{(C_N H_{2N+1} OH)^\beta} = \frac{x_\beta}{x_{mono}^{\ \beta}} \quad (7.4)$$

Using the approximation:

$$x_{total} = x_{mono} + \beta x_\beta \quad (7.5)$$

$$\ln(x_{total} - x_{mono}) = \beta \ln(x_{mono}) + \ln(\beta K) \quad (7.6)$$

An expression for the fraction of alkanol molecules present as single molecules y can be found as a function of the average aggregation number β.

$$y = \frac{x_{mono}}{x_{mono}(1 - 1/\beta) + x_{total}/\beta} \quad (7.7)$$

In the same manner, an expression for the mole fraction of the alkane in the mixture z is developed.

$$z = \frac{x_{CH}}{x_{CH} + x_{mono}(1 - 1/\beta) + x_{total}/\beta} \qquad (7.8)$$

Combining equations 7.1, 7.2, 7.7 and 7.8, there is a system of equations that is solved for a given composition of tetradecane over a constant mole free basis of CO$_2$, having three degrees of freedom: the chain length of the alkanol molecules present as single molecules $CL^{OH(l)}$, the equilibrium constant K and the aggregation number β.

The value of $CL^{OH(l)}$ depends on the consideration of the hydroxyl group. Some works consider that the effect of the group can be neglected (Vimalchand et al., 1988; Peters, 1994). Other authors consider that the hydroxyl group can be assimilated to a full carbon group (Stamoulis, 1994). Gauter (1999) had considered an intermediate solution, adding 0.5 to the number of carbons of the alkanol molecule. As a first approach, this work has followed Gauter's idea.

The values of K and β can be determined in a certain range from measuring the monomer concentration of a mixture by infrared (IR) spectroscopy. Fulton et al. (1993) reported aggregation numbers for several alkanols in supercritical CO$_2$ at 313K and 20 MPa (from 4.3 ± 1 for dodecanol to 4.9 ± 1 for butanol). Aveyard et al. (1973) showed a value of 4 for dodecanol in liquid octane at 303.15K and Pacynko et al. (1989) found an aggregation value of 5 ± 1 for dodecanol in liquid heptane at 303.15K. The introduction of CO$_2$ in the system should not modify strongly these values, because aggregates of about the same size are formed in CO$_2$ and in alkanes in a similar manner (Gauter, 1999). Although this value is taken in an effective way, the decision has been based in the comparison of the m value between methane and methanol, where the difference in the chain length parameter m approaches 0.5. In any case, as the difference changes when the chain length increases, this assumption must be taken with care. It is crucial to remark that this is done as a first approximation to see the performance of the crossover soft-SAFT equation in the same conditions as other equations of state. In fact, crossover soft-SAFT can directly calculate the fraction of aggregates in a mixture (Blas and Vega, 2000; Herdes et al. 2004), which

would save an adjustable parameter like β. At present, a comparison between the adjusted value (by fitting procedure) and the calculated value of β is being done, although the results were not at time to be included in the present work.

Concerning the equilibrium constant K, Fulton et al. (1993) also reported values for the systems CO$_2$/1-dodecanol and CO$_2$/1-butanol at 313.15K and 20MPa. He estimated a value of 37000 and 15000 respectively. These values can be taken as a range for their optimization, because the temperature at which they were measured is close to the used in this work. Moreover, although the pressure value is higher than the values obtained in this study, it is assumed that the aggregates are mostly present in the liquid phase, where the pressure influence can be neglected.

With this approach, ternary interactions among the molecules are neglected. Moreover, the interactions alkane/alkane, CO$_2$/alkane, CO$_2$/CO$_2$ and alkane/alkanol are not taken into account in the calculation of the average chain length because they are considered to be weaker compared to those of alkanol/alkanol and alkanol/CO$_2$ molecules.

As it has been mentioned, it is also possible to strictly calculate the critical end points where the three compounds are considered independently. For that purpose, the general calculation method for the evaluation of critical points proposed by Heidemann and Khalil (1980) is followed. However, it is necessary an extra condition to find a CEP, which is related to the occurrence of an additional phase in equilibrium with the critical point. Following the work of Gauter (1999) the Gibbs tangent plane criterion in the formulation of Michelsen (1982) is added to find this extra phase.

The mathematical model proposes the resolution of the critical conditions for a mixture (Heidemann and Khalil, 1980), that have to satisfy:

$$Q = Det\left|q_{ij}\right| \quad where \quad q_{ij} = \left(\frac{\partial^2 A}{\partial n_j \partial n_i}\right) \tag{7.9}$$

$$\sum_i \sum_j \sum_k \left(\frac{\partial^3 A}{\partial n_k \partial n_j \partial n_i}\right) = 0 \tag{7.10}$$

Then, once a critical point is obtained, the Gibbs tangent criterion plane is applied, looking for the minimum tangent plane distance *D*:

$$D = \ln(f_i) - \ln(f_i^{crit}) \qquad\qquad (7.11)$$

When the value of *D* is zero, it means that an additional phase in equilibrium with the critical phase has been found.

Gauter (1999) applied this methodology to the Peng-Robinson equation of state and reproduced several miscibility loops of CO$_2$ / tetradecane / 1-alkanols with qualitative agreement with experimental data in most of the cases.

This second approach is more realistic than the quasibinary approach, although it requires more computational time and a careful evaluation of the derivatives.

The purpose of this work is to check the capabilities of the crossover soft-SAFT equation for modeling these miscibility loops. The quasibinary approach has been chosen for a first modeling approximation. In a second step, the rigorous calculation of the critical points will be done and the results will be compared with the first approach. Preliminary results for the quasibinary approach are presented here, while the rigorous treatment is a matter of future work.

7.2.3. Preliminary results for CO$_2$ / tetradecane / 1-alkanols

The quasi-binary approach was used for calculating the miscibility loop in the CO$_2$ / *n*-tetradecane / *1*-decanol mixture. The molecular parameters transferability capacity of the crossover soft-SAFT equation was used to define the ternary mixture.

The molecular parameters for CO$_2$ were taken from table 6.13. Tetradecane and decanol parameters are calculated from correlations 6.1 and 6.3 respectively. Binary parameters between CO$_2$ and tetradecane were the same that the used for CO$_2$/*n*-tridecane. Binary parameters between CO$_2$ and *1*-decanol were the same used for studying the critical transitions in the CO$_2$/*1*-alkanols family. Finally, only one binary parameter was employed

for the interaction tetradecane/1-decanol, the same one employed for the alkane/alkanol mixtures evaluated in section 7.1.2.

The parameters β and K were optimized looking for the best agreement with the experimental data to reproduce the closed miscibility loop. The range for the aggregation number β was taken between 3 and 6, while K has been optimized in a range from 10000 to 50000. Figure 7.23 shows the modeling of a closed miscibility loop of the mixture. Figure 7.23a represents a temperature-composition diagram while figure 7.23b shows the pressure-composition diagram. The *n*-tetradecane composition is calculated respect to the solute mole fraction (alkane + alkanol), without considering the CO$_2$ (which is 95% of the total mole fraction). A composition of zero means that there is only a CO$_2$/1-alkanol mixture while a composition of one means that there is a CO$_2$/alkane mixture. Symbols represent experimental data (Gauter, 1999) while the solid line correspond to the crossover soft-SAFT calculations.
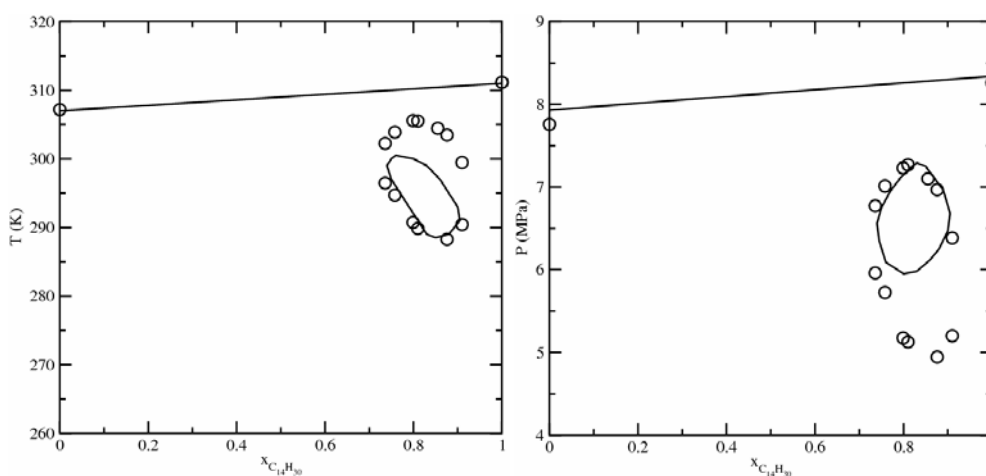
Figure 7.23. *Closed solubility loop for the mixture CO$_2$ / n-tetradecane / 1-decanol. Circles are experimental data (Gauter, 1999) and the solid line represents crossover soft-SAFT calculations. Aggregation number β = 3.94; Equilibrium constant K= 39500.*

Qualitative agreement has been found using the equilibrium constant value of *K=39500* and an aggregation number β = 3.94. Both values are inside the range where

experimental measurements for similar systems were performed. The closed miscibility loop is reproduced although it is smaller than it should be. In some way, the equation is considering that either the tetradecane or the 1-decanol molecules are longer than they are and they for a miscibility gap in a smaller region of the phase space. Nevertheless, the prediction of the lower critical end points (LCEP) is accurate in temperature, while the upper critical end points (UCEP) have better pressure predictions. In any case, several options should be studied, like the possibility of not considering the hydroxyl group as 0.5 carbon numbers.

It is interesting to check the performance of the methodology when the chain length of the alkanol decreases. Experimental measurements show that *1*-hexanol seems to be the last alkanol which exhibits a miscibility loop. This loop is open and connected to the two-phase critical line. Its modeling is also very challenging because we are in the limit of appearance of this phenomena.

The calculations were done using the same binary parameters than before. Unfortunately, no miscibility loops were predicted for the selected ranges of β and K. As it happened in Gauter's work (1999), the only way to achieve qualitative agreement is for extremely high values of K (more than 10^6). Figure 7.24, shows the best calculation obtained. The model would be acceptable (with quantitative agreement at low compositions of alkane) for a reasonable value of *K*. However, the value of this parameter was increased to 3.000.000 to observe this behavior. The value of β remains in the reasonable range *(β=5.57)*. It seems clear that for a better representation the model has to be improved.
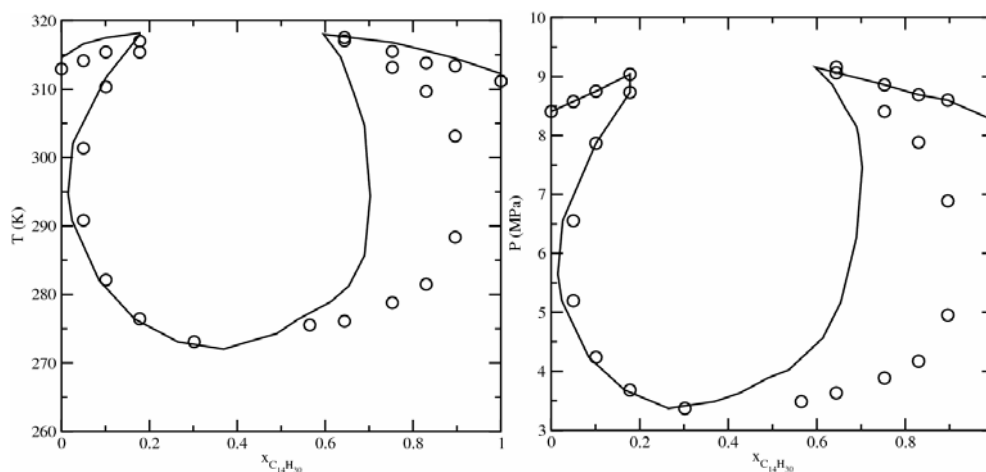
Figure 7.24*. Critical end point modeling for the mixture CO$_2$/n-tetradecane/1-hexanol. Circles are experimental data (Gauter, 1999) and the solid line represents crossover soft-SAFT calculations. Aggregation number β = 5.57; Equilibrium constant K= 3000000.*

As it has been said there are several crude assumptions that could be improved: the monodispersity of the alkanol aggregates, the linear shape of the alkanol agglomerates, the ideality of the solution and the size of the oxygen atom of 0.5 carbon atom.

In any case, the results obtained are preliminary and further research has to be done in this field, but the simplicity of the method offers several options to improve the results.

D. Conclusions

I think and think for months and years. Ninety-nine times, the conclusion is false. The hundredth time I am right.

(Albert Einsten) (1879-1955)
German-Swiss-U.S. scientist

8

Conclusions

This thesis work has been devoted to the improvement of a versatile molecular equation of state, in order to develop a powerful tool applicable under several conditions for thermodynamic calculations. The robust Statistical Associating Fluid Theory has been coupled with a renormalization group theory that account for the contributions of long-wavelength fluctuations. The new equation has been tested against molecular simulations and has been used to evaluate several compounds and their mixtures, in a systematic manner.

First of all, the equation was evaluated for several phase envelopes of Lennard-Jones chains of different chain lengths from $m=1$ till $m=16$. In all cases, very good agreement was obtained respect to the molecular simulations with the same underlying model. A good representation of the critical region was found without a prejudice far away from this region. In these calculations, the only adjustable parameters were the crossover parameters L and ϕ.

Crossover soft-SAFT was then used to obtain optimized molecular parameters for the first eight members of the *n*-alkanes, *1*-alkanols and *n*-perfluoroalkanes families. All molecular parameters followed physical trends and were linearly correlated respect to their molecular weight. Predictions of heavier compounds for the *n*-alkanes family demonstrated the parameters transferability. In all cases, a single set of parameters accurately describes the whole phase envelope, close to and far from the critical region. The evaluation of the universal critical exponents was calculated to show that the correct asymptotic approach to the critical point was reproduced with the equation.

The same crossover approach was also implemented into a vdW type equation of state to check its validity in a different equation of state. Good results were achieved for the *n*-alkanes and *1*-alkanols, although soft-SAFT performed better far from the critical region. This is not a limitation of the crossover treatment, but the basis of the equation of state.

Different families of binary mixtures were treated with crossover soft-SAFT, paying special attention to the transitions from one type of critical behavior to another one:

- Dissimilar mixtures of *n*-alkanes were described using the same binary parameters. The transitions from Type I to type V in the methane and ethane series were reproduced with accuracy.

- Mixtures among *n*-alkanes and *1*-alkanols were also treated. Vapor-liquid equilbria and the critical line showed the same degree of accuracy.

- The transition from Type II to Type III passing through Type IV behavior was performed for the CO_2/alkanes family. Using the same binary parameters adjusted to the CO_2/tridecane mixture, several phase diagrams and critical lines were reproduced with qualitative and quantitative agreement with experimental data.

- The same transition (Type II – IV – III) was studied for the CO_2/*1*-alkanols. Phase equilibrium diagrams and critical lines reproduced mixtures of CO_2/*1*-propanol, CO_2/*1*-butanol, CO_2/*1*-pentanol and CO_2/*1*-hexanol. Type IV was found for the CO_2/*1*-pentanol mixture.

- The unknown critical behavior series of the HCl/*n*-alkanes was also evaluated. It was the first time that the critical behavior of these mixtures was described for alkanes higher than *n*-dodecane. The equation predicted an expected Type III behavior for the mixture HCl/*n*-heneicosane, although some experimental measurements would be necessary to evaluate this prediction

A preliminary work for multicomponent mixtures was started in this thesis work. The study of the thermodynamic behavior of near critical CO_2/*n*-alkanes/*1*-alkanol mixtures was performed with a preliminary study of the mixture CO_2/tetradecane/*1*-decanol and CO_2/tetradecane/*1*-hexanol. Two-phase holes of these mixtures were calculated with the equation, obtaining qualitative agreement with experimental data.

Finally, a complete evaluation of several derivative properties, like heat capacities, compressibilities and the speed of sound, was performed for pure fluids and binary mixtures. They were calculated using the same parameters optimized for phase equilibria properties. Good agreement was found for most of the properties, reproducing some extrema observed in the vicinity of the critical point. Excess properties were also evaluated in mixtures to study the inaccuracies observed in some predictions. Derivative properties have constituted a powerful test to demonstrate that the underlying model behind crossover soft-SAFT is able to capture the physics of the behavior shown by these compounds.

Of course, this is not the end in the searching for a general equation of state. Although the examples shown in this thesis work indicate that crossover soft-SAFT is a strong tool for thermodynamic calculations, there is still room for some improvements to be made in order to increase its capabilities.

- A specific modification in the crossover theory has to be made for liquid-liquid calculations. In vapor-liquid equilibria, the order parameter selected to take into account the fluctuations is the density. However, in a liquid-liquid equilibria, the mole fraction is a better choice, because it is

the property that suffers the stronger fluctuations in the vicinity of the critical point.

- Dipole and other multipolar expansion terms should be implemented into the code to model the effects of electrostatic interactions among molecules.

- An appropriate term should be introduced for solid-liquid equilibria. This field remains quite unexplored for almost all equations of state.

- A deeper work in multicomponent mixtures has to be performed. The intrinsic behavior of some ternary mixtures should be studied.

- The study of interfacial properties in the critical region is another important test to do. The coupling of the density gradient theory and the crossover theory in the soft-SAFT equation has to be used to study surface tensions and density profile in the near critical region.

- New ways of fitting the molecular parameters should be studied. The fact that derivative properties are more sensitive to errors than first order-thermodynamic properties opens the possibility of using them to get the molecular parameters of the equation, in order to check their performance for phase equilibria calculations (as a complementary approach to the one usually done with soft-SAFT).

BIBLIOGRAPHY

Abrams, D.S.; Prausnitz, J.M. Statistical thermodynamics of liquid mixtures-New expression for excess Gibbs energy of partly or completely miscible systems. *AIChE J.* **21**, 16 (1975).

Adidharma, H.; Radosz, M. Prototype of an Engineering Equation of State for Heterosegmented Polymers. *Ind. Eng. Chem. Res*. **37**, 4453 (1998).

Alder, B.J.; Young, D.A.; Mark. M.A. Studies in Molecular Dynamics. X. Corrections to the Augmented van der Waals Theory for the Square Well Fluid. *J. Chem. Phys.* **56**, 3013 (1972).

Al-Matar, A.K.; Rockstraw, D.A.; A Generating Equation for Mixing Rules and Two New Mixing Rules for Interatomic Potential Energy Parameters, *J. Comp. Chem*. **25**, 660 (2004).

Andersen, H.C. Clusters expansions for hydrogen bonding fluids. 1. Molecular association in dilute gases. *J. Chem. Phys*. **59**, 4714 (1973).

Andersen, H.C. Clusters expansions for hydrogen bonding fluids. 2. Dense liquids. *J. Chem. Phys*. **61**, 4985 (1974).

Anisimov, M.A.; Senger, J.V. *Equations of State for Fluids and Fluid Mixtures, Critical, Chapter 11 Critical Region*, Editors J.V. Senger, R.F. Kayser, C.J. Peters, H.J. White Jr., Elsevier, Amsterdam (2000).

Arce, P.F.; Mattedi, S.; Aznar, M. Vapor-liquid equilibrium of copolymer plus solvent mixtures: Thermodynamic modeling by two theoretical equations of state. *Fluid Phase Equilib*. **246**, 52 (2006).

Aveyard, R.; Briscoe, B.J.; Chapman, J. Activity coefficients and association of n-alkanols in n-octane. J. Chem. Soc. Faraday Trans. I **69**, 1772 (1973).

Banaszak, M.; Chiew, Y.C.; Radosz, M. Thermodynamic perturbation theory. Sticky chains and square-well chains. *Phys. Rev. E*, **48**, 3760 (1993).

Banaszak, M.; Chen, C.K.; Radosz, M. Copolymer SAFTEquation of State. Thermodynamic Perturbation Theory Extended to Heterobonded Chains. Macromolecules. **29**, 6481(1996).

Barber, E.J.; Cady, G.H. Vapor pressures of Perfluoropentanes. *J. Phys. Chem*. **60**, 504 (1956).

Barker, J.A.; Henderson, D. Perturbation theory and equation of state for fluids: I. The square-well potential. *J. Chem. Phys*., **47**, 2856 (1967).

Barker, J.A.; Henderson, D. Perturbation theory and equation of state for fluids: I. A succesful theory of liquids. *J. Chem. Phys*., **47**, 4714 (1967).

Bearman, R.J.; Freasier, B.C.; Smith D.K. Heat-capacity extrema - Monte-Carlo simulations for the truncated Lennard-Jones fluid. *J. Phys. Chem*., **96**, 4093 (1992).

Behzadi, B.; Patel, B.H.; Galindo, A.; Ghotbi, C. Modeling electrolyte solutions with the SAFT-VR equation using Yukawa potentials and the mean-spherical approximation. *Fluid Phase Equilib*. **236**, 241 (2005).

Benedict, M.; Webb, G.B.; Rubin, L.C., An Empirical Equation for Thermodynamic Properties of Light Hydrocarbons and Their Mixtures: I. Methane, Ethane, Propane, and n-Butane, *J. Chem. Phys*., **8**, 334 (1940).

Berry, V.M.; Sage, B.H. *NSRDS-NBS* **32** (1970).

Beret, S.; Prausnitz, J.M., Perturbed Hard-Chain Theory – Equation of State for Fluids Containing Small or Large Molecules. *AIChE J*., **18**, 1123 (1975).

Beysens, D. *A world without gravity: Critical Point Phenomena*. B. Fitton and B. Battrick (Eds). European Space Agency, 2001.

Blas, F.J.; Vega, L.F. Thermodynamic behaviour of homonuclear and heteronuclear Lennard-Jones chains with association sites from simulation and theory, *Mol. Phys*., **92**, 135 (1997).

Blas, F.J.; Vega, L.F. Prediction of Binary and Ternary Diagrams Using the Statistical Associating Fluid Theory (SAFT) Equation of State. *Ind. Eng. Chem. Res*. **37**, 673 (1998).

Blas, F.J.; Vega, L.F.; Critical behavior and partial miscibility phenomena in binary mixtures of hydrocarbons by the statistical associating fluid theory. *J. Chem. Phys.*, **109**, 7405 (1998).

Blas, F.J.; Excess thermodynamic properties of chainlike mixtures. 1. Predictions from the Soft-SAFT equation of state and molecular simulation, *J. Phys*. *Chem. B* **104**, 9239 (2000).

Blas, F.J.; Vega, L.F. Improved vapor-liquid equilibria predictions for Lennard-Jones chains from the statistical associating fluid dimer theory: Comparison with Monte Carlo simulations. *J. Chem. Phys*. **115**, 4355 (2001).

Blas, F.J.; Vega, L.F. Thermodynamic properties and phase equilibria of branched chain fluids using first- and second-order Wertheim's thermodynamic perturbation theory. *J. Chem. Phys*. **115**, 3906 (2001).

Blas, F.J.; Excess thermodynamic properties of chainlike mixtures. II. Self-associating systems: predictions from soft-SAFT and molecular simulation, *Mol. Phys*. **100**, 2221 (2002).

Boublik, T. Hard sphere equation of state. *J. Chem. Phys*., **53**, 471 (1970).

Brønstead, J.N.; Koefoed, J., *The thermodynamic properties of paraffin mixtures*, Kgl. Danske Videnkabernes Selskab, Matematish-Fysische Meddelelser. **22**, 1 (1946).

Brown, J.A.; Mears, W.H. Physical Properties of n-Perfluorobutane. *J. Phys. Chem.* **62**, 960 (1958).

Bufkin, B.A.; Robinson Jr., R.L.; Estrera, S.S.; Luks, D.K. Solubility of ethane in n-decane at pressures to 8.2 MPa and temperatures from 278K to 411K, *J. Chem. Eng. Data* **31**, 421 (1986).

Burguer, L.L.; Cady, C.H. Physical Properties of Perfluoropentanes. J. Am. Chem. Soc. **73**, 4243 (1951).

Cahn, J.W.; Hilliard, J.E. Free energy of a nonuniform system. I. Interfacial free energy. *J. Chem. Phys*. **28**, 258 (1958).

Cai, J.; Prausnitz, J.M. Thermodynamics for fluid mixtures near to and far from the vapor–liquid critical point, *Fluid Phase Equilib*., **219**, 205 (2004).

Cai, J.; Qiu, D.; Zhang, L; Hu, Y. Vapor-liquid critical properties of multi-component fluid mixture, *Fluid Phase Equilib*., **241**, 229 (2006).

Carnahan, N.F.; Starling, K.E., Equation of State of non-attracting rigid spheres. *J. Chem. Phys.*, **51**, 635 (1969).

Carnahan, N.F.; Starling, K.E., Thermodynamic properties of a rigid-sphere fluid. *J. Chem. Phys.*, **53**, 600 (1970).

Cerdeiriña, C.A.; Gonzalez-Salgado, D.; Romani, L.; Delgado, M.C.; Torres, L. A.; Costas, M.; Towards an understanding of the heat capacity of liquids. A simple two-state model for molecular association. *J. Chem. Phys*., **120**, 6648 (2004).

Chandler, D.; Pratt L., Statistical mechanics of chemical equilibria and intramolecular structures of nonrigid molecules in condensed phases. *J. Chem. Phys*. **65**, 2925 (1976).

Chang, J.; Sandler, S.I. An equation of state for the hard-sphere chain fluid: theory and Montecarlo simulation. *Chem. Eng. Sci*., **49**, 2777 (1994).

Chapman, W.G.; Gubbins, K.E.; Joslin, C.G.; Gray, C.G. Theory and simulation of associated liquid mixtures. *Fluid Phase Equilib*. **29**, 337 (1986).

Chapman, W.G.; Jackson, G.; Gubbins, K.E. Phase equilibria of associating fluids. Chain molecules with multiple bonding sites. *Mol. Phys*., **65**, 1057 (1988).

Chapman, W.G. *Theory and simulation of associating liquid mixtures*. Ph. D. thesis, Cornell Univerity, Ithaca, NY, 1988.

Chapman, W.G.; Gubbins, K.E.; Jackson, G.; Radosz, M. SAFT-equation-of-state solution model for associating fluids. *Fluid Phase Equilib*. **52**, 31 (1989).

Chapman, W.G.; Gubbins, K.E.; Jackson, G.; Radosz, M. New reference equation of state for associating liquids, *Ind. Eng. Chem. Res.*, **29**,1709 (1990).

Chen, R.J.J.; Chappelear, P.S.; Kobayashi, R. Dew-point loci for methane-n-pentane binary system*, J. Chem. Eng. Data*, **19**, 58 (1974).

Chen, Z.Y.; Albright, P.C.; Senger, J.V. Crossover from singular critical to regular classical thermodynamic behavior of fluids, *Phys. Rev. A*, **41**, 3161 (1990).

Chen, Z.Y.; Abbaci, A.; Tang, S.; Senger, J.V. Global Thermodynamic behavior of fluids in the critical region. *Phys. Rev. A*, **42**, 3370 (1990).

Chien C.H., Greenkorn, R.A.; Chao, K.C., Chain-of-Rotators Equation of State, *AIChE J.*, **29**, 560 (1983).

Chu, T.C.; Chen, R.J.J.; Chappelear, P.S.; Kobayashi, R. Vapor-liquid-equilibrium of methane-normal-pentane system at low-temperatures and high-pressures, *J. Chem. Eng. Data,* **21,** 41 (1976).

Colina, C.M.; Turrens, L.F.; Olivera-Fuentes, C.; Gubbins, K.E.; Vega, L.F. Predictions of the Joule-Thomson Inversion Curve for the n-Alkane Series and Carbon Dioxide from the Soft-SAFT Equation of State. *Ind. Eng. Chem. Res*. **41**, 1069 (2002).

Colina, C.M.; Galindo A.; Blas, F.J.; Gubbins, K.E. Phase behavior of carbon dioxide mixtures with n-alkanes and n-perfluoroalkanes. Fluid Phase Equilib. **222**, 77 (2004).

Cooper, A.; Materials HIPE - creating nanostructures using SCFs. Materials World. 10, 24 (2002).

Cotterman, R.L.; Schwarz B.J.; Prausnitz J.M. Molecular Thermodynamics for Fluids at Low and High Densities. Part I: Pure Fluids Containing Small or Large Molecules. *AIChE J*. **32**, 1787 (1986).

Crowder, G.A.; Taylor, Z.L.; Reed, T.M. Young, J.A. Vapor Pressures and Triple Point Temperatures for Severals Pure Fluorocarbons, *J. Chem. Eng. Data* **12**, 481 (1967).

Davies, L.A.; Gil-Villegas, A.; Jackson, G. Describing the properties of chains of segments interacting via soft-core potentials of variable range with the SAFT-VR approach. *Int. J. Thermophys*. **19**, 675 (1998).

Davies, L.A.; Gil-Villegas, A.; Jackson, G. An analytical equation of state for chain molecules formed from Yukawa segments. *J. Chem. Phys*. **111**, 8659 (1999).

Deák, A.; Victorov, A.I.; de Loos, Th. W. High pressure VLE in alkanol + alkane mixtures. Experimental results for n-butane + ethanol, + 1-propanol, + 1-butanol systems and calculations with three EOS methods, *Fluid Phase Equilib*. **107**, 277 (1995).

Deiters, U.K. A new semi-empirical equation of state for fluids – I. Derivation. *Chem. Eng. Sci*. **36**, 1139 (1981).

de Melo, M.J.P.; Dias, A.M.A.; Blesic, M.; Rebelo, L.P.N.; Vega, L.F.; Coutinho, J.A.P., Marrucho, I.M. Liquid–liquid equilibrium of (perfluoroalkane + alkane) binary mixtures. *Fluid Phase Equilib*. **242**, 210 (2006).

Dias, A.M.A.; Pàmies, J.C.; Coutinho, J.A.P., Marrucho, I.M.; Vega, L.F., SAFT modeling of the solubility of gases in perfluoroalkanes. *J. Phys. Chem. B* **108**, 1450 (2004).

Dias, A.M.A.; Gonçalves, C.M.B.; Caço, A.I.; Santos L.M.N.B.F; Pineiro M.M.; Vega L.F.; Coutinho, J.A.P.; Marrucho, I.M. Densities and vapor pressures of highly fluorinated compounds. *J. Chem. Eng. Data* **50**, 1328 (2005).

Dias, A.M.A.; Carrier, H.; Daridon, J.L.; Pàmies, J.C.; Vega, L.F.; Coutinho, J.A.P., Marrucho, I.M. Vapor-liquid equilibrium of carbon dioxide-perfluoroalkane mixtures: Experimental data and SAFT modeling. *Ind. Eng. Chem. Res*. **45**, 2341 (2006).

Diaz Peña M.; Pando, C.; Renuncio J.A.R. Combination rules for intermolecular potential parameters. I. Rules based on approximations for the long-range dispersion energy. *J. Chem. Phys*. **76**, 325 (1982).

Dillon, H.E.; Penoncello, S.G. A fundamental equation for calculation of the thermodynamic properties of ethanol. *Int. J. Thermophys.* **25**, 321 (2004).

Dolezalek, F. Zur Theorie der binären Gemische und konzentrierten Lösungen. *Z. Phys. Chem.* **64**, 727 (1908).

dos Ramos, M.C.; Blas, F.J.; Examination of the excess thermodynamic properties of n-alkane binary mixtures: A molecular approach. *J. Phys. Chem. B* **109**, 12145 (2005).

Duarte-Garza, H.A.; Magee, J.W.; Isochoric p-rho-T and heat capacity C-v measurements on {xC(3)H(8)+(1-x)i-C4H10, x approximate to 0.7, 0.3} from 200 to 400 K at pressures to 35 MPa. *J. Chem. Eng. Data* **44**, 1048 (1999).

Dunlap, R.D.; Murphy, C.J.; Bedford, R.G. Some Physical Properties of Perfluoro-n-hexane. *J. Am. Chem. Soc*. **80**, 83 (1958).

Duque D., Pamies J.C., Vega L.F. Interfacial properties of Lennard-Jones chains by direct simulation and density gradient theory. *J. Chem. Phys*. **121**, 11395 (2004)

Dzida, M.; Ernst, S. Speed of sound in propan-1-ol plus heptane mixtures under elevated pressures. *J. Chem. Eng. Data* **48**, 1453 (2003).

Economou, I.G.; Tsonopoulos, C. Associating models and mixing rules in equations of state for water/hydrocarbons mixtures. *Chem. Eng. Sci.* **52**, 511 (1997).

Economou, I.G.; Statistical Associating Fluid Theory: a successful model for the calculation of thermodynamic and phase equilibrium properties of complex fluid mixtures, *Ind. Eng. Chem. Res*. **41**, 953 (2002).

Elizalde-Solis, O.; Galicia-Luna, L.A.; Sandler, S.I.; Sampayo-Hernández, J.G. Vapor-liquid equilibria and critical points of the CO2+1-hexanol and CO2+1-heptanol systems. *Fluid Phase Equilib.* **210,** 215 (2003).

Errington, J.R.; Panagiotopoulos, A.Z. A new intermolecular potential model for the n-alkane homologous series. *J. Phys. Chem. B*, **103**, 6314 (1999).

Escobedo, F.A.; de Pablo, J.J. Simulation and prediction of vapour-liquid equilibria for chain molecules. *Molec. Phys.*, **87**, 347 (1996).

Fisher, M. Renormalization of critical exponents by hidden variables, *Phys. Rev.*, **176**, 257 (1968).

Florusse, L.J.; Pàmies, J.C.; Vega, L.F.; Peters C.J.; Meijer, H. Solubility of hydrogen in heavy n-alkanes: experiments and SAFT modeling. *AIChE J.* **49**, 3260 (2003).

Flory, P.J. *Principles of polymer chemistry.* Cornell University Press, Ithaca, NY, 1953.

Fotouh, K; Shukla, K. A comparative study of numerical methods for calculating phase equilibria in fluid mixtures from an equation of state. *Chem. Eng. Sci.* **51**, 3763 (1996).

Freasier, B.C.; Woodward, C.E.; Bearman, R.J. Heat capacity extrema on isotherms in one-dimension: Two particles interacting with the truncated Lennard-Jones potential in the canonical ensemble. *J. Chem. Phys.*, **105**, 3686 (1996).

Freasier, B.C.; Woodward, C.E.; Bearman, R.J. C-v extrema on isotherms for simple fluids and why they exist. *J. Chem. Phys.*, **106**, 10318 (1997).

Fredenslund, A.; Mollerup, J. Measurement and prediction of equilibrium ratios for C2H6+CO2 system *J. Chem. Society-Faraday Transactions I*, **70**, 1653 (1974).

Fredenslund, Aa.; Gmehling, J. Rasmussen, P. *Vapor-Liquid Equilibria using UNIFAC*; Elsevier, Amsterdam, 1977.

Fulem, M.; Ruzicka, K.; Ruzicka, V. Heat capacities of alkanols Part I. Selected 1-alkanols C-2 to C-10 at elevated temperatures and pressures. *Termochimica Acta*, **382**, 119 (2002).

Fulton, J.L.; Yee, G.G.; Smith, R.D., Hydrogen bonding in simple alcohols on supercritical fluids; an FTIR study. *Supercritical Fluid Engineering Science, Fundamentals and Applications*, E. Kiran and J.F. Brennecke (Eds.), ACS Symposium Series Nº 514, 175 (1993).

Furman, D.; Dattagupta, S.; Griffiths, R.B. Global phase diagram for a three-component model. *Phys. Rev. B* **15**, 441 (1977).

Galindo, A.; Davies, L.A.; Gil-Villegas, A.; Jackson, G. The thermodynamics of mixtures and the corresponding mixing rules in the SAFT-VR approach for potentials of variable range, *Mol. Phys*. **93**, 241 (1998).

Galindo, A; Florusse, L.J.; Peters, C.J. Prediction of phase equilibria for binary systems of hydrogen chloride with ethane, propane and n-dodecane. *Fluid Phase Equlib*. **158-160**, 123 (1999).

Galindo, A.; Gil-Villegas, A.; Jackson, G.; Burgess, A. N. SAFT-VRE: Phase Behavior of Electrolyte Solutions with the Statistical Associating Fluid Theory for Potentials of Variable Range. *J. Phys. Chem. B* **103**, 10272 (1999).

Galindo A.; Blas, F. J. Theoretical examination of the global fluid phase behavior and critical phenomena in carbon dioxide plus n-alkane binary mixtures. *J. Phys. Chem. B*, **106**, 4503 (2002).

Gauter, K.; *Fluid Multiphase Behavior in Ternary Systems of Near-Critical CO$_2$, Ph Dissertation*, Delft University of Technology, The Netherlands, 1999.

Gauter, K.; Heidemann R.A.; Peters, C.J. Modeling of fluid multiphase equilibria in ternary systems of carbon dioxide as the near-critical solvent and two low-volatile solutes. *Fluid Phase Equilib*. **158**, 133 (1998).

Ghonasgi, D.; Chapman, W.G. A new equation of state for hard chain molecules. *J. Chem. Phys.*, **100**, 6633 (1994).

Gibbons, R.M.; Scaled particle theory for particles of arbitrary shape. *Mol. Phys.*, **17**, 81 (1969).

Gil-Villegas, A.; Galindo, A; Whitehead, P.J.; Mills, S.J.; Jackson, G.; Burgess, A.N. Statistical Associating Fluid Theory for chain molecules with attractive potentials of variable range, *J. Chem. Phys.*, **106**, 4168 (1997).

Gmehling J.; Liu, D.D.; Prausnitz, J.M., High pressure vapor-liquid equilibria for mixtures containing one or more polar components. Application of an equation of state which includes dimerization equilibria. *Chem. Eng. Sci.*, **34**, 951 (1979).

Goral, M.; Oracz, P.; Skrzecz, A.; Bok, A.; Maczynski, A. Recommended Vapor-Liquid Equilibrium Data. Part 1: Binary n-Alkanol + n-Alkane Systems, *J. Phys. Chem. Ref. Data*, **31**, 701 (2002).

Gregorowicz, J.; O'Connell, J.P.; Peters, C.J. Some characteristics of pure fluid properties that challenge equation-of-state models. Fluid Phase Equilib., **116**, 94 (1996).

Gregorowicz, J. Solubility of eicosane in supercritical ethane and ethylene, *J. Supercrit. Fluids* 26, 95 (2003).

Gross, J.; Sadowski, G.; Perturbed-chain SAFT: an equation of state based on a perturbation theory for chain molecules, *Ind. Eng. Chem. Res*. **40**, 1244 (2001).

Gross, J.; Sadowski, G.; Application of the perturbed-chain SAFT equation of state to associating systems, *Ind. Eng. Chem. Res*. **41**, 5510 (2002).

Gubbins, K.E.; Twu, C.H. Thermodynamics of polyatomic fluid mixtures- I Theory. *Chem. Eng. Sci*. **33**, 863 (1978).

Guggenheim, E.A. Statistical thermodynamics of mixtures with zero energies of mixing. *Proc. R. Soc. London A*, **183**, 213 (1944).

Guggenheim, E.A. Statistical thermodynamics of cooperative systems (a generalization of the quasi-chemical method). *Trans. Faraday Soc.*, **44**, 1007 (1944).

Gurdial, G.S.; Foster, N.R.; Yun, S.L. J.; Tilly, K.D. *Supercritical fluid engineering science, fundamentals and applications*. Washington: American Chemical Society. Eds. E. Kiran and J.F. Brennecke, 1993; p. 34.

Halgren, T.A.; Representation Of Vanderwaals (Vdw) Interactions in Molecular Mechanics Force-Fields - Potential Form, Combination Rules, and vdW Parameters. J. Am. Chem. Soc., **114**, 7827 (1992).

Heidemann, R.A.; Prausnitz, J.M. A van der Waals type equation of state for fluids of associating molecules. *Proc. Natl. Acad. Sci. USA*, **73**, 1773 (1976).

Heidemann, R.A.; Khlail, A. M. The calculation of critical points. *AiChE Journal*. **26**, 769 (1980) *Proc. Natl. Acad. Sci. USA*, **73**, 1773 (1976).

Herdes, C.; Pàmies, J.C.; Marcos, R.M.; Vega, L.F. Thermodynamic properties and aggregate formation of surfactant-like molecules from theory and simulation. *J. Chem. Phys*. **120**, 9822 (2004).

Hicks, C.P.; Young, C.L. The Gas-Liquid critical properties of binary mixtures, *Chemical Reviews,* **75**, 119 (1975).

Hoye, J.S.; Olaussen, K. Statistical mechanical model with chemical reaction. *Physica A*, **104**, 435 (1980).

Hu, Y.; Liu, HL; Prausnitz, J.M. Equation of state for fluids containing chainlike molecules, *J. Chem. Phys*., **104**, 396 (1996).

Hu, Z-Q; Yang, J-C; Li, Y-G; Crossover SAFT equation of state for pure supercritical fluids, *Fluid Phase Equilibria,* **205**, 1 (2003).

Huang, S.H.; Radosz, M. Equation of state for small, large, polydisperse and associating molecules, *Ind. Eng. Chem. Res*., **29**, 2284 (1990).

Huang, S.H.; Radosz, M. Equation of state for small, large, polydisperse and associating molecules – Extension to fluid mixtures. *Ind. Eng. Chem. Res*., **30**, 1994 (1991).

Ikonomou, G.D.; Donohue, M.D. Thermodynamics of hydrogen-bonded molecules: The associated perturbed anisotropic hard chain theory. *AIChE J.* **32**, 1716 (1986).

Ikonomou, G.D.; Donohue, M.D. COMPACT. A simple equation of state for asscoiated molecules. *Fluid Phase Equilib.* **33**, 61 (1987).

Jackson, G.; Chapman, W.G.; Gubbins, K.E. Phase equilibria of associating fluids. Spherical molecules with multiple bonding sites. *Molec. Phys.* **65**, 1 (1988).

Jackson, G. Theory of closed-loop liquid-liquid immiscibility in mixtures of molecules with directional attractive forces. *Mol. Phys.* **72**, 1365 (1991).

Jiang, J.; Prausnitz, J.M., Equation of state for thermodynamic properties of chain fluids near-to and far-from the vapor–liquid critical region, *J. Chem. Phys.* **111**, 5964 (1999).

Jiang, J.; Prausnitz, J.M., Phase equilibria for chain-fluid mixtures near to and far from the critical region, *AIChE J.* **46**, 2525 (2000).

Jin, Y.; Boller, A.; Bunderlich, B.; Lebedev B.V. Heat-Capacities and Transitions in N-Perfluoroalkanes and Poly(Tetrafluoroethylene), *Termochimica Acta* **234**, 103 (1994).

Johnson, J.K.; Gubbins, K.E. Phase equilibria for associating Lennard-Jones fluids from theory and simulation. *Molec. Phys.* **77**, 1033 (1992).

Johnson, J.K.; Zollweg, J.A.; Gubbins, K.E. The Lennard-Jones equation of state revisited, *Mol. Phys.* **78**, 591 (1993).

Johnson, J.K.; Müller, E.A.; Gubbins, K.E. Equation of state for Lennard-Jones chains. *J. Phys. Chem.* **98**, 6413 (1994).

Joslin, C.G.; Gray, C.G.; Chapman, W.G.; Gubbins, K. E. Theory and simulation of associating liquid mixtures. II. *Molec. Phys.* **62**, 843 (1987).

Karakatsani, E.K.; Spyriouni, T.; Economou, I.G. Extended statistical associating fluid theory (SAFT) equations of state for dipolar fluids. *AIChE J.* **51**, 2328 (2005).

Karakatsani, E.K.; Economou, I.G. Perturbed chain-statistical associating fluid theory extended to dipolar and quadrupolar molecular fluids. *J. Phys. Chem. B.* **110**, 9252 (2006).

Kay, W.B.; Genco, J.; Fichtner, D.A. Vapor-liquid-equilibrium relationships of binary-systems propane octane an butane octane, *Journal of Chem. Eng. Data* **19**, 275 (1974).

Kay, W.B.; Hoffman, R.L.; Davies, O. Vapor-liquid-equilibrium relationships of binary-systems normal-butane normal-pentane and normal-butane normal-hexane. *Journal of Chem. Eng. Data* **20**, 333 (1975).

Kayukawa, Y.; Fujii, K.; Higashi, Y. Vapor-liquid equilibrium (VLE) properties for the binary systems propane (1) plus n-butane (2) and propane (1) plus isobutane (3). *J. Chem. Eng. Data* **50**, 579 (2005).

Kim, C.H.; Vimalchand, P.; Donohue, M.D.; Sandler, S.I., Local composition model for chainlike molecules: a new simplified version of the perturbed hard chain theory. *AIChE J*. **32**, 1726 (1986).

Kiselev, S.B.; Kostyukova, I.G.; Povodyrev, A.A.; Universal crossover-behavior of fluids and fluid mixtures in the critical region, *Int. J. Thermophys*. **12**, 877 (1991).

Kiselev, S.B., Cubic crossover equation of state, *Fluid Phase Equilibria*, **147**, 7 (1998).

Kiselev, S.B.; Ely, J.F. Crossover SAFT equation of state: application for normal alkanes. *Ind. Eng. Chem. Res*. **38**, 4993 (1999).

Kiselev, S.B.; Friend, D. Cubic crossover equation of state for mixtures, *Fluid Phase Equilib*. **162**, 51 (1999).

Kiselev, S.B.; Ely, J.F.; Abdulagatov, I.M.; Magee, J.W. Crossover SAFT equation of state and thermodynamic properties of propan-1-ol. *Int. J. Thermophys*. **21**, 1373 (2000).

Kiselev, S.B.; Ely, J.F.; Adidharma, H; Radosz, M. A crossover equation of state for associating fluids. *Fluid Phase Equilib*. **53**, 183 (2001).

Kiselev, S.B.; Ely, J.F.; Tan, S.P.; Adidharma, H; Radosz, M. HRX-SAFT Equation of State for Fluid Mixtures: Application to Binary Mixtures of Carbon Dioxide, Water, and Methanol. *Ind. Eng. Chem. Res*. **45**, 3981 (2006).

Kojima, K.; Tochigi, K. *Prediction of Vapor-Liquid Equilibria y the ASOG Method*, Elsevier, Amsterdam, 1979.

Kolafa, J.; Nezbeda, I. The Lennard-Jones fluid - an accurate analytic andtheoretically-based equation of state. *Fluid Phase Equilib*. **100**, 1 (1994).

Kortekaas, W.G.; Peters, C.J. ; de Swaan Arons, J. Joule-Thomson expansion of high-pressure-high-temperature gas condensates. *Fluid Phase Equilib*. **139**, 205 (1997).

Kraska, T.; Gubbins, K.E. Phase equilibria calculations with a modified SAFT equation of state. 1. Pure alkanes, alkanols, and water. *Ind. Eng. Chem. Res*. **35**, 4727 (1996).

Kreglewski, A. Vapour Pressure and Molar Volumes of Liquid Perfluoro-n-Octane, Trifluoroacetic Acid and its Anhydride, Bulletin de L'Academie Polonaise des Sciences, **vol. X,** 629 (1962).

Lagache, M.H.; Ungerer, Ph.; Boutin, A. Prediction of thermodynamic derivative properties of natural condensate gases at high pressure by Monte Carlo simulation *Fluid Phase Equilib*. **220**, 211 (2004).

Lagache, M.; Ungerer, Ph.; Boutin, A.; Fusch, A.H.; Prediction of thermodynamic derivative properties of fluids by Monte Carlo simulation. *Phys. Chem. Chem. Phys.* **3**, 4333 (2001).

Laffite, T.; Bessieres, D.; Piñeiro, M.M.; Daridon, J.L. Simultaneous estimation of phase behavior and second-derivative properties using the statistical associating fluid theory with variable range approach. *J. Chem. Phys.* **124**, 024509 (2006).

Lam, D. H.; Jangkamolkulchai, A.; Luks, K. D. Liquid liquid vapor-phase equilibrium behavior of certain binary carbon dioxide + n-alkanol mixtures. *Fluid Phase Equilib.* **60**, 131 (1990).

Lee B.I.; Kesler M.G. A generalized thermodynamic correlation based on three-parameters corresponding states. *AIChE J*. **21**, 510 (1975).

Lee K.H.; Lombardo, M.; Sandler, S.I., The generalized Van der Waals partition function. II: Application to the square-well fluid. *Fluid Phase Equilib*. **21**, 177 (1985).

Lin, Y.N.; Chen, R.; Chappelear, P.; Kobayashi, R. Vapor-Liquid Equilibrium of the methane + n-hexane system at low temperature, *J. Chem. Eng. Data* **22**, 402 (1977).

Lofti, A.; Vrabec, J.; Fischer, J. Vapor-liquid-equilibria of the Lennard-Jones fluid from the NPT plus test particle method. *Molec. Phys.* **76**, 1319 (1992)

Lue, L.; Prausnitz, J.M. Renormalization-group corrections to an approximate free-energy model for simple fluids near to and far from the critical region*, J. Chem. Phys.* **108**, 5529 (1998).

Lue, L; Prausnitz, J.M. Thermodynamics of fluid mixtures near to and far from the critical region, *AIChE J*. **44**, 1455 (1998).

McCabe, C.; Gil-Villegas, A.; Jackson, G. Predicting the High-Pressure Phase Equilibria of Methane + n-Hexane Using the SAFT-VR Approach, *J. Phys. Chem. B* **102**, 4183 (1998).

McCabe, C.; Galindo, A; Gil-Villegas, A; Jackson, G. Predicting the high-pressure phase equilibria of binary mixtures of perfluoro-n-alkanes plus n-alkanes using the SAFT-VR approach. *J. Phys. Chem. B* **102**, 8060 (1998).

McCabe, C.; Jackson, G. SAFT-VR modelling of the phase equilibrium of long-chain n-alkanes. *Phys. Chem. Chem. Phys*. **1**, 2057 (1999).

McCabe, C.; Kiselev, S.B, A crossover SAFT-VR equation of state for pure fluids: preliminary results for light hydrocarbons, *Fluid Phase Equilib*. **219**, 3 (2004).

McCabe, C.; Kiselev, S.B, Application of crossover theory to the SAFT-VR equation of state: SAFT-VRX for pure fluids, *Ind. Eng. Chem. Res*. **43**, 2839 (2004).

Medeiros, M. Monte Carlo study of the temperature dependence of the residual heat capacity of pure fluids. The case of compressed supercritical methanol, *J. Phys. Chem. B*, **108**, 2676 (2004).

Mejía A.; Pàmies J.C.; Duque D.; Segura H.; Vega L.F. Phase and interface behaviors in type-I and type-V Lennard-Jones mixtures: Theory and simulations. *J. Chem. Phys*. **123**, 034505 (2005).

Mejía, A.; Vega, L.F. Perfect wetting along a three-phase line: Theory and molecular dynamics simulations. *J. Chem. Phys*. **124**, 244505 (2006).

Mendoza de la Cruz, J.L.; Galicia-Luna, L.A. *The International Electronic Journal of Physico Chemical Data* **5**, 157 (1999).

Meroni, A.; Parola, A.; Reatto, L.; Differential approach to the theory of fluids. *Phys. Rev. A* **42**, 6104 (1990).

Mi, J.; Zhong, C; Li, Y-G.; Tang, Y.P. An improved renormalization group theory for real fluids. *J. Chem. Phys*. **121**, 5372 (2004).

Mi, J.; Zhong, C; Li, Y-G. Renormalization group theory for fluids including critical region. II. Binary mixtures. *Chem. Phys*. **312**, 31 (2005).

Mi, J.; Zhong, C; Li, Y-G.; Tang, Y. Prediction of Global VLE for Mixtures with Improved Renormalization Group Theory. *AIChE. J*. **52**, 342 (2006).

Michelsen, M.L. The isothermal flash problem. Part I: Stability, *Fluid Phase Equilib*. **9**, 1 (1982).

Miller, M.M.; Luks, K.D. Observations on the multiphase equilibria behavior of co-2-rich and ethane-rich mixtures. *Fluid Phase Equilib*. **44**, 295 (1989).

Milton, H.T.; Oliver, G.D. High Vapor Pressure of n-Hexadecafluoroheptane. *J. Am. Chem. Soc*. **72**, 3951 (1952).

Morris, W.O.; Vimalchand, P.; Donohue, M.D. The Perturbed-Soft-Chain Theory - An Equation Of State Based On The Lennard-Jones Potential. *Fluid Phase Equilib*. **32**, 103 (1987).

Mousa, A.E.H.N. Study of Vapor Pressure and Critical Properties of Perfluoro-n-hexane, *J. Chem. Eng. Data* **23**, 133 (1978).

Müller, E.A.; Vega, L.F.; Gubbins, K.E. Theory and simulation of associating fluids: Lennard-Jones chains with association sites, *Molec. Phys*. **83**, 1209 (1994).

Müller, E.A.; Gubbins, K.E. An equation of state for water from a simplified intermolecular potential. *Ind. Eng. Chem. Res*. **34**, 3662 (1995).

Müller, E.; Gubbins, K.E. Molecular-based equations of state for associating fluids: a review of SAFT and related approaches, *Ind. Eng. Chem. Res*. **40**, 2193 (2001).

Nath, S.K.; Escobedo, F.A.; de Pablo, J.J. On the simulation of vapor-liquid equilibria for alkanes. *J. Chem. Phys*. **108**, 9905 (1998).

Nath, S.K.; Escobedo, F.A.; de Pablo, J.J.; Patramai, I. Simulation of Vapor-Liquid Equilibria for Alkane Mixtures. *Ind. Eng. Chem. Res*. **37**, 3195 (1998).

Negele, J.W.; Orland, H. *Quantum Many-Particle Systems*, Addison-Wesley, Redwood City, CA (1988) p.204

Nezbeda, I.; Leland, T.W. Conformal theory of hard non-spherical molecule fluids. *J. Chem. Soc. Faraday Trans. II*, **75**, 193 (1979).

NIST Chemistry Webbook, *http://webbook.nist.gov/chemistry*.

Oh, B.C.; Kim, Y.; Shin, H.Y.; Kim, H. Vapor-liquid equilibria for the system 1-propanol + *n*-hexane near the critical region, *Fluid Phase Equilib*. **220**, 41 (2004).

Oishi, T.; Prausnitz, J.M. Estimation of Solvent Activities in Polymer-Solutions Using a Group-Contribution Method, *IEC Proc. Des. Dev*. **17**, 333 (1978).

Oliver, G.; Blumkin, S.; Cunningham, Some Physical Properties of Hexadecafluoroheptane, *J. Am. Chem. Soc*. **73**, 5722 (1951).

Oliver, G.; Grisard, J.; Some Thermodynamic P Properties of Hexadecafluoroheptane, *J. Am. Chem. Soc*. **73**, 1688 (1951).

Pacynko, W.F.; Yarwood, J.; Tiddy, G.J.T., Infrared spectroscopic studies on the aggregation of polyoxyethylene surfactants in hydrocarbon solvents. J. Chem. Soc. Faraday Trans. I **86**, 1397 (1989).

Pàmies, J.C.; Vega, L.F. Vapor-liquid equilibria and critical behavior of heavy n-alkanes using transferable parameters from the soft-SAFT equation of state. *Ind. Eng. Chem. Res.* **40**, 2532 (2001).

Pàmies, J.C.; Vega, L.F. Critical properties of homopolymer fluids studied by a Lennard-Jones statistical associating fluid theory. *Molec. Phys.* **100**, 2519 (2002).

Pàmies, J.C. *Bulk and interfacial properties of chain fluids: a molecular modelling approach.* PhD. Dissertation, Universitat Rovira i Virgili, Tarragona, Spain, 2003.

Panayiotou, C.G.; Sanchez, I.C. Hydrogen bonding in fluids: Equation of state approach. *J. Phys. Chem.* **95**, 10090 (1991).

Parola, A.; Meroni, A.; Reatto, L. Comprehensive theory of simple fluids, critical-point included, *Phys. Rev. Lett.* **62**, 2981 (1989).

Parola, A.; Meroni, A.; Reatto, L. Theory of the universal and non-universal quantities of fluids at the critical-point, *Int. J. Thermophys.* **10**, 345 (1989)

Patel, N.C.; Teja A.S. New Cubic Equation of State for Fluids and Fluid Mixtures. *Chem. Eng. Sci.* **37**, 463 (1982).

Patel, B.H.; Paricaud, P.; Galindo, A.; Maitland, G.C. Prediction of the salting-out effect of strong electrolytes on water plus alkane solutions. Ind. Eng. Chem. Res. 42, 3809 (2003).

Patel B.H.; Docherty, H.; Varga, S.; Galindo, A.; Maitland, G.C.; Generalized equation of state for square-well potentials of variable range. *Mol. Phys.* **103**, 129 (2005).

Patton, C.L.; Kisler, S.H.; Luks, K.D., Multiphase equilibrium behavior of a mixture of carbon dioxide, *1*-decanol and n-tetradecane. *Supercritical Fluid Eng. Sci. Fundamentals and Applications*, ACS Symposium Series Nº**514**, 55 (1993).

Pedrosa, N.; Pàmies, J.C.; Coutinho, J.A.P.; Marrucho, I.M.; Vega, L.F. Phase equilibria of ethylene glycol oligomers and their mixtures, *Ind. Eng. Chem. Res*. **44**, 7027 (2005).

Pedrosa, N.; Vega, L.F., Coutinho, J.A.P.; Marrucho, I.M. Phase equilibria calculations of polyethylene solutions from SAFT-type equations of state. *Macromolecules*. **39**, 4240 (2006).

Pedrosa, N.; Vega, L.F., Coutinho, J.A.P.; Marrucho, I.M. The phase behavior of polystyrene systems as described by molecular-based equations of state. *submitted* (2006).

Peleteiro, J.; Gonzalez-Salgado, D.; Cerdeiriña, C.A.; Valencia, J.L.; Romani, L. Thermodynamics of 1-alkanol plus n-alkane mixtures: new data and predictions from the NTGC model. *Fluid Phase Equilib*. **191**, 83 (2001).

Peleteiro, J.; González-Salgado, D.; Cerdeiriña, C.A.; Romaní, L. Isobaric heat capacities, densities, isentropic compressibilities and second-order excess derivatives for (1-propanol plus n-decane). *J. Chem. Thermodynamics* **34**, 485 (2002).

Peleteiro, J.; González-Salgado, D.; Cerdeiriña, C.A.; Valencia, J.L.; Romaní, L. Thermodynamics of 1-alkanol plus n-alkane mixtures: new data and predictions from the NTGC model. *Fluid Phase Equilib*. **191**, 83 (2001).

Peng, D.Y.; Robinson, D.B. New Two-Constant Equation of State. *Ind. Eng. Chem. Fundam.* **15**, 59 (1976).

Perry, R.H.; Green, D. W. *Perry's Chemical Engineers' Handbook*; Ed.McGraw-Hill, pp. 2-170, 1999.

Perrut, M. Supercritical Fluid Applications: Industrial Developments and Economic Issues. *Ind. Eng. Chem. Res*. **39**, 4531 (2000).

Peters, C.J.; de Roo, J.L.; Lichtenthaler, R.N. Measurements and calculations of phase-equilibria of binary mixtures of ethane + eicosane. 1. Vapor-liquid equilibria, *Fluid Phase Equilib*. **34**, 287 (1987).

Peters, C.J.; Multiphase equilibria in near-critical solvents, in *Supercritical Fluids*. E. Kiran and J.M.H. Levelt Sengers (Eds.). Kluwer Academic Publishers, 117, 1994.

Pfohl, O.; Brunner, G; 2. Use of BACK to Modify SAFT in Order to Enable Density and Phase Equilibrium Calculations Connected to Gas-Extraction Processes. *Ind. Eng. Chem. Res*. **37**, 2966 (1998).

Plantier, F.; Danesh, A.; Sohrabi, M.; Daridon, J.L.; Gozalpour, F.; Todd, A.C. Measurements of the Speed of Sound for Mixtures Methane + Butane with a Particular Focus on the Critical State, *J. Chem. Eng. Data* **50**, 673 (2005).

Polishuk, I.; Wisniak, J.; Segura, H. Prediction of the critical locus in binary mixtures using equation of state I. Cubic equations of state, classical mixing rules, mixtures of methane-alkanes, *Fluid Phase Equilib*. **164**, 13 (1998).

Polishuk, I; Wisniak, J.; Segura, H. Simultaneous prediction of the critical and sub-critical phase behavior in mixtures using equation of state I. Carbon dioxide-alkanols, *Chem. Eng. Sci.* **56**, 6485 (2001).

Polishuk, I.; Wisniak, J.; Segura, H. Simultaneous prediction of the critical and sub-critical phase behavior in mixtures using equations of state III. Methane-n-alkanes, *Chem. Eng. Sci..* **58**, 4363 (2003).

Polishuk, I.; Wisniak, J.; Segura, H. Simultaneous Prediction of the Critical and Subcritical Phase Behavior in Mixtures of Ethane-n-Alkanes, *Ind. Eng. Chem. Res.* **44**, 2292 (2005).

Prausnitz, J.M.; Tavares, F.W. Theromdynamics of Fluid-Phase Equilibria for Standard Chemical Engineering Operations, AIChE J. **50**, 739 (2004).

Prigogine, I., *The Molecular Theory of Solutions*, North-Holland, Amsterdam (1957).

Raeissi, S; Gauter, K.; Peters, C. J., Fluid multiphase behavior in quasi-binary mixtures of carbon dioxide and certain 1-alkanols, *Fluid Phase Equilib.*, **147**, 239 (1998).

Reamer, H.H.; Sage, B.H. Phase Equilibria in Hydrocarbons Systems: Volumetric and Phase Behavior of the Ethane-n-Decane System, *J. Chem. Eng. Data* **7**, 161 (1962).

Reamer, H.H.; Sage, B.H. Phase Equilibria in Hydrocarbon Systems. Volumetric and Phase Behavior of the n-Decane-CO2 System. *J. Chem. Eng. Data* **8**, 508 (1963).

Reid, R.C.; Prausnitz, J.M.; Poling, B.E.; The properties of gases and liquids, 4th ed., McGraw-Hill, New York, 1987.

Renon, H.; Prausnitz, J.M. Local compositions in thermodynamic excess functions for liquid mixtures. *AIChE J.* **14**, 135 (1968).

Rowlinson, J.S.; Swinton, F.L. *Liquid and Liquid Mixtures*. Butterworth Scientific, London, 1982.

Sadowski, G. A square-well based equation of state taking into account the connectivity in chain molecules. *Fluid Phase Equilib.* **149**, 75 (1998).

Sadus, R. J. *High-pressure phase behaviour of multicomponent fluid mixtures*. Elsevier: Amsterdam, The Netherlands, 1992.

Sage, B.H.; Reamer, H.H.; Olds, R.H.; Lacey, W.N. *Ind. Eng. Chem.* **34**, 1108 (1942).

Sala, S. Desenvolupament del nou mètode DELOS® de cristal•lització amb fluids comprimits. Estudi a nivell molecular dels seus fonaments, *PhD. Dissertation*, Universitat Autònoma de Barcelona, Bellaterra, 2005.

Salvino, L.W.; White, J.A. Calculation of density fluctuation contributions to thermodynamic properties of simple fluids. *J. Chem. Phys.* **96**, 4559 (1992).

Sanchez, I. C., and R. H. Lacombe, Elementary Molecular Theory of Classical Fluids - Pure Fluids, *J. Phy. Chem.* **80**, 2352 (1976).

Sanchez, I. C., and R. H. Lacombe, Statistical Thermodynamics of Polymer-Solutions, *Macromolecules* **11**, 1145 (1978).

Sang-Do, Y.; Su-Jin, P.; Jin-Woo, K.; Jae-Chang, K. Critical Properties of Carbon Dioxide + Methanol, + Ethanol, + 1-Propanol, and + 1-Butanol. *J. Chem. Eng. Data* **45**, 932 (2000).

Scheidgen, A. Fluidphasengleichgewichte binärer und ternärer Kohlendioxidmischungen mit schwerflüchtigen organischen Substanzen bis 100 MPa – Cosolvency effect, Miscibility windows und Löcher in der krtischen Fläche, *Ph. D. dissertation*, Ruhr-University at Bochum, Germany, 1997.

Schneider, G.M.; Alwani, Z.; Heim, W.; Horvath, E., Franck, E.U. Phase equilibria and critical phenomena in binary mixtures (CO2 with n-octane n-undecane n-tridecane and n-hexadecane up to 1500 bar). *Chem. Eng. Technol.* **39**, 649 (1967).

Scott, R.L.; van Konynenburg, P.H. Van der Waals and related models for hydrocarbon mixtures, *Discuss. Faraday Soc.* **49**, 87 (1970).

Segura, H.; Kraska, T.; Mejía, A.; Wisniak, J.; Polishuk, I. Unnoticed pitfalls of soave-type alpha functions in cubic equations of state. *Ind. Eng. Chem. Res.* **42**, 5662 (2003).

Segura, H.; Mejía, A. A generalized vdW-type equation of state. In preparation (2006).

Silva-Oliver, G.; Galicia-Luna, L.A. Vapor-liquid equilibria near critical point and critical points for the CO2+1-butanol and CO2+2-butanol systems at temperatures from 324 to 432 K. *Fluid Phase Equilib.* **182**, 145 (2001).

Silva-Oliver, G.; Galicia-Luna, L.A.; Sandler, S.I. Vapor-liquid equilibria and critical points for the carbon dioxide + 1-pentanol and carbon dioxide + 2-pentanol systems at temperatures from 332 to 432 K *Fluid Phase Equilib.* **200**, 161 (2002).

Smith, D.; Srivastava, R. *Thermodynamic data for pure compounds: part A hydrocarbons and ketones*. Elsevier: Amsterdam, The Netherlands, 1986.

Smits, J.C.; Gauter, K.; Peters, C.J.; de Swaan Arons, J. A novel approach to the modelling of the fluid multiphase behaviour of ternary mixtures of carbon dioxide + n-alkane + 1-alkanol. *Fluid Phase Equilib.* **145**, 239 (1998).

Soave, G. Equilibrium Constants from a Modified Redlich-Kwong Equation of State. *Chem. Eng. Sci.* **27**, 1197 (1972).

Specovius, J.; Leiv, M.A.; Scott, R.L.; Knobler, C.M. Tricritical phenomena in quasi binary mixtures of hydrocarbons 2. Binary ethane mixtures, *J. Phys. Chem.* **85**, 2313 (1981).

Stamoulis, D. *Patterns of fluid phase behavior in ninary and quasi-binary mixtures*. PhD Dissertation. Delft University of Technology. The Netherlands, 1994.

Starling, K.E. *Fluid Properties for Light Petroleum Systems*. Gulf Publishing Company, 1973.

Steele, W.V.; Chirico, R.D.; Knipmeyer, S.E.; Nguyen, A., Vapor Pressure, Heat Capacity and Density along the Saturation Line, Measurements for Cyclohexanol, 2-Cyclohen-1-one, 1,2-Dichloropropane, 1,4-Di-tert-butylbenzene, 2-Ethylhexanoic Acid, 2-(Methylamino)ethanol, Perfluoro-n-heptane, and Sulfolane, *J. Chem. Eng. Data*. **42**, 1021 (1997).

Stryjek, R.; Vera, J.H. PRSV: An Improved Peng-Robinson Equation of State for Pure Compounds and Mixtures, *Can. J. Chem. Eng*. **64**, 323 (1986).

Sun, L.; Zhao, H.; Kiselev, S. B.; McCabe, C. *Fluid Phase Equilib*. **275**, 228 (2005).

Suzuki, K.; Sue, H. Isothermal vapor-liquid-equilibrium data for binary-systems at high-pressures - carbon-dioxide methanol, carbon-dioxide ethanol, carbon dioxide-1-propanol, methane ethanol, methane-1-propanol, ethane ethanol, and ethane-1-propanol systems. *J. Chem. Eng. Data* **35**, 63 (1990).

Tang Y.P., Lu BCY. A New solution of the Ornstein–Zernike equationfrom the perturbation theory. *J Chem Phys*. **99**, 9828 (1993).

Tang Y.P., Lu BCY. Analytical solution of the Ornstein–Zernike equation for mixtures. *Mol Phys*. **84**, 89 (1995).

Tang, Y. Outside and inside the critical region of the Lennard-Jones fluid, *J. Chem. Phys*. **109**, 5935 (1998).

Tavares, F.W.; Chang, J.; Sandler, S.I. A completely analytic equation of state for the square-well chain fluid of variable well width. *Fluid Phase Equilib*. **140**, 129 (1997).

Thiele, E. Equation of state for hard spheres. *J. Chem. Phys*. **39**, 474 (1963).

Tumakaka, F.; Gross, J.; Sadowski, G.; Thermodynamic modeling of complex systems using PC-SAFT. Fluid Phase Equilib. 228, 89 (2005).

Valderrama, J.O. The State of the Cubic Equations of State, *Ind. Eng. Chem. Res*. **42**, 1603 (2003).

Vandana, V.; Rosenthal, D.J.; Teja, A.S. The Critical properties of Perfluoron-alkanes. *Fluid Phase Equilib*. **99**, 209 (1994).

van der Waals, J.D. *On the continuity of the Gaseous and Liquid States*, Dissertation Universiteit Leiden., 1873 (in Dutch).

van der Waals, J.D. Thermodynamische theorie der kapillarität unter voraussetzung stetoger dichteänderung. *Z. Phys. Chem*. **13**, 657 (1894).

van Konynenburg, P.H.; Scott, R.L. Critical lines and phase-equilibria in binary van der Waals mixtures, *Philos. Trans. R. Soc. London A* **298**, 495 (1980).

Vargaftik, N.B.; Vinogradov, Y.K.; Yargin, V.S. *Handbook of Physical Properties of Fluids and Gases: Pure Substances and Mixtures*; Begell House Publishers, p. 714 (1996).

Vega, C.; Mc Bride, C.; de Miguel, E.; Blas, F.J.; Galindo, A. The phase diagram of the two center Lennard-Jones model as obtained from computer simulation and Wertheim's thermodynamic perturbation theory. *J. Chem. Phys*. **118**, 10696 (2003).

Vega, L.F.; Blas, F.J. Tricritical phenomena in chain-like mixtures from a molecular-based equation of state. *Fluid Phase Equilib*. **171**, 91 (2000).

Ventosa, N.; Sala, S.; Veciana, J.; Torres, J.; Llibre, J. Depressurization of an expanded liquid organic solution (DELOS): A new procedure for obtaining submicron- or micron-sized crystalline particles. *Cristal Growth and Design*. **1**, 299 (2001).

Vimalchand, P.; Donohue, M.D.; Thermodynamics of quadrupolar molecules - the Perturbed-Anisotropic-Chain Theory. *Ind. Eng. Chem. Fund*. **24**, 246 (1985).

Vimalchand, P.; Ikonomou, G.D.; Donohue, M.D. Correlation of equation of state parameters for the Associated Perturbed Anisotropic Chain Theory. *Fluid Phase Equilib*. **43**, 121 (1988).

Vimalchand, P.; Thomas, A.; Economou, I.G.; Donohue, M.D. Effect of hard-sphere structure on pure-component equation of state calculations. *Fluid Phase Equilib*. **73**, 39 (1992).

von Solms, N.; Michelsen, M.L.; Kontogeorgis, G.M. Prediction and correlation of high-pressure gas solubility in polymers with simplified PC-SAFT. Ind. Eng. Chem. Res. 44, 3330 (2005).

Voutsas, E.C.; Pappa, G.D.; Magoulas, K.; Tassios, D.P. Vapor liquid equilibrium modeling of alkane systems with Equations of State: "Simplicity versus complexity", *Fluid Phase Equilib*. 240, 127 (2006).

Vukalovich, M.P.; Novikov, I.I. *Equation of State of Real Gases*, State Energy Publishers Moscow (USSR), 1948 (in Russian).

Walsh, J.M.; Gubbins, K.E. The liquid structure and thermodynamic properties of Lennard-Jones spheres with association sites, *Molec. Phys*. **80**, 65 (1993).

Wertheim, M.S. Exact solution of the Percus-Yevick integral equation for hard spheres, *Phys. Rev. Lett*. **10**, 321 (1963).

Wertheim, M.S. Fluids with highly directional attractive forces. 1. Statistical Thermodynamics, *J. Stat. Phys*. **35**, 19 (1984).

Wertheim, M.S. Fluids with highly directional attractive forces. 2. Thermodynamic-perturbation theory and integral-equations, *J. Stat. Phys*. **35**, 35 (1984).

Wertheim, M.S. Fluids with highly directional attractive forces. 3. Multiple attraction sites, *J. Stat. Phys*. **42**, 459 (1986).

Wertheim, M.S. Fluids with highly directional attractive forces. 4. Equilibrium polymerization, *J. Stat. Phys*. **42**, 477 (1986).

Wertheim, M.S. Thermodynamic perturbation theory of polymerization. *J. Chem. Phys*. **87**, 7323 (1987).

White, J.A. Contribution of fluctuation to thermal properties of fluids with attractive potential force of limited range: Theory compared with pρT and CV data for argon, *Fluid Phase Equilib*. **75**, 53 (1992).

White, J.A.; Zhang, S.; Renormalization group theory for fluids, *J. Chem. Phys*. **99**, 2012 (1993).

White, J.A.; Zhang, S. Renormalization theory of nonuniversal thermal properties of fluids. *J. Chem. Phys*. **103**, 1922 (1995).

Wilson, G.M. Vapor-liquid equilibrium. XI: A new expression for the excess free energy of mixing. *J. Am. Chem. Soc.* **86**, 127 (1964).

Wilson, K.G. Renormalization group and critical phenomena, 2. Phase space cell analysis of critical behavior, *Phy. Rev. B* **4**, 3174 (1971).

Wilson , K.G.; Fischer, M.E.; Critical exponents in 3.99 dimensions, *Phys. Rev. Lett*,. **28**, 240 (1972).

Wyczalkowska, A.K.; Sengers, J.V.; Anisimov, M.A. Critical fluctuations and the equation of state of Van der Waals. *Physica A* **334**, 482 (2004).

Ziegler J.W.; Chester, T.L. *Innovations in Supercritical Fluids. Science and Technology*; ACS Symposium series, 1995.

Appendix

A. Dimensionless variables

Although the user can choose if they want to work with or without units in the interface, the mathematical code is all written in a dimensionless form. A reference component is needed. In multicomponent systems, each component has its own σ_i parameter, and σ corresponds to the "averaged" value computed from mixing and combination rules.

Dimensionless parameters:

$$\sigma' = \frac{\sigma}{\sigma_R} \quad (A.1) \qquad\qquad \sigma'_{i,i\neq i_R} = \frac{\sigma_i}{\sigma_R} \quad (A.5)$$

$$\varepsilon' = \frac{\varepsilon}{\varepsilon_R} \quad (A.2) \qquad\qquad \varepsilon'_{i,i\neq i_R} = \frac{\varepsilon_i}{\varepsilon_R} \quad (A.6)$$

$$k^{\alpha_i\beta_j}{}' = \frac{k^{\alpha_i\beta_j}}{\sigma_R^3} \quad (A.3) \qquad\qquad \varepsilon^{\alpha_i\beta_j}{}' = \frac{\varepsilon^{\alpha_i\beta_j}}{\varepsilon_R^3} \quad (A.7)$$

$$L' = \frac{L}{\sigma_R} \quad (A.4)$$

Dimensionless variables

$$T' = \frac{Tk_B}{\varepsilon_R} \qquad \text{(A.8)}$$

$$H' = \frac{H}{N_A \varepsilon_R} \qquad \text{(A.14)}$$

$$\rho' = \rho N_A \sigma_R^3 \qquad \text{(A.9)}$$

$$G' = \frac{G}{N_A \varepsilon_R} \qquad \text{(A.15)}$$

$$A' = \frac{A}{N_A \varepsilon_R} \qquad \text{(A.10)}$$

$$S' = \frac{S}{\varepsilon_R} \qquad \text{(A.16)}$$

$$P' = \frac{P\sigma_R^3}{\varepsilon_R} \qquad \text{(A.11)}$$

$$C_v' = \frac{C_v}{N_A k_B} \qquad \text{(A.17)}$$

$$\mu' = \frac{\mu}{N_A \varepsilon_R} \qquad \text{(A.12)}$$

$$C_p' = \frac{C_p}{N_A k_B} \qquad \text{(A.18)}$$

$$U' = \frac{U}{N_A \varepsilon_R} \qquad \text{(A.13)}$$

$$\kappa_T' = \frac{\kappa_T \varepsilon_R k_B}{\sigma_R^3} \qquad \text{(A.19)}$$

B. Crossover terms for phase equilibria properties

The following mathematical relationships constitute de expressions for the calculation of the crossover contribution of the three thermodynamic variables needed to evaluate phase equilibrium.

$$A^{cross} = A^{soft-SAFT} + \sum_{i=1}^{5} \frac{f^{cross}}{\rho} \qquad \text{(B.1)}$$

$$P^{cross} = P^{soft-SAFT} + \sum_{i=1}^{5} \rho_c^{rf} \left(\frac{df^{cross}}{d\rho} \right) - f^{cross} \qquad \text{(B.2)}$$

$$\mu^{cross} = \mu^{soft-SAFT} + \sum_{i=1}^{5} \frac{1}{\rho}\left(\frac{df^{cross}}{dx_i}\right) \tag{B.3}$$

$$f^{cross} = -K_n \ln\left(\frac{\Omega_n^s}{\Omega_n^l}\right) \tag{B.4}$$

$$K_n = \frac{T^{rf}}{\left(2^n L\right)^3} \tag{B.5}$$

$$\Omega_n^\alpha(\rho) = \int_0^{\min(\rho,\rho_{max}-\rho)} \exp\left(\frac{-G_n^\alpha(\rho,x)}{K_n}\right) dx \tag{B.6}$$

$$G_n^\beta(\rho,x) = \frac{\overline{f}_n^\beta(\rho+x) + \overline{f}_n^\beta(\rho+x) - 2\overline{f}_n^\beta(\rho)}{2} \tag{B.7}$$

$$\overline{f}_n^l(\rho) = f_{n-1}(\rho) + \alpha \cdot \rho_c^{rf\,2} \tag{B.8}$$

$$\overline{f}_n^s(\rho) = f_{n-1}(\rho) + \frac{\alpha \cdot \rho_c^{rf\,2} \cdot \phi}{2^{2n+1} L^2} \tag{B.9}$$

Combining equations A.4-A.9 a general expression for the Helmholtz free energy density is obtained.

$$f^{cross} = -K_n \ln\left| \frac{\int_0^{\min(\rho,\rho_{max}-\rho)} \exp\left(\left(\frac{-1}{2}\right)\left(\frac{f_{n-1}(\rho+x)+f_{n-1}(\rho-x)-2f_{n-1}(\rho)+2ax^2}{K_n}\right)\right) dx}{\int_0^{\min(\rho,\rho_{max}-\rho)} \exp\left(\left(\frac{-1}{2}\right)\left(\frac{f_{n-1}(\rho+x)+f_{n-1}(\rho-x)-2f_{n-1}(\rho)+\frac{ax\varphi^2}{\left(2^n L\right)^2}}{K_n}\right)\right) dx} \right| \tag{B.10}$$

The fully developed expression would be:

$$A^{cross} = -\frac{T^{rf}}{\rho\left(2^n L\right)^3}$$

$$\ln\left(\frac{\int_0^{\min(\rho,\rho_{max}-\rho)} \exp\left(\left(\frac{-2^{3n-1}L^3}{T^{rf}}\right)\left(f_{n-1}(\rho+x) + f_{n-1}(\rho-x) - 2f_{n-1}(\rho) + 2ax^2\right)\right)dx}{\int_0^{\min(\rho,\rho_{max}-\rho)} \exp\left(\left(\frac{-2^{3n-1}L^3}{T^{rf}}\right)\left(f_{n-1}(\rho+x) + f_{n-1}(\rho-x) - 2f_{n-1}(\rho) + \frac{ax\varphi^2}{\left(2^n L\right)^2}\right)\right)dx}\right)$$

(B.11)

The calculation of the crossover term for the pressure requires the evaluation of $\dfrac{df}{d\rho}^{cross}$

$$\frac{df}{d\rho}^{cross} = -K_n\left(\frac{\left(\frac{\partial \Omega^s}{\partial \rho}\right)}{\Omega^s} - \frac{\left(\frac{\partial \Omega^l}{\partial \rho}\right)}{\Omega^l}\right)$$

(B.12)

$$\frac{\partial \Omega^\alpha}{\partial \rho} = \int_0^\rho\left[\exp\left(\frac{-G^\alpha(\rho,x)}{K_n}\right)\left(\frac{-1}{K_n}\right)\left(\frac{\partial G(\rho,x)}{\partial \rho}\right)\right] + \exp\frac{\left(G^\alpha(\rho,\rho)\right)}{K_n}$$

(B.13)

$$\frac{\partial G(\rho,x)}{\partial \rho} = \frac{1}{2}\left(\left(\frac{df}{d\rho}(p+x)\right)_{n-1} + \left(\frac{df}{d\rho}(p-x)\right)_{n-1} - 2\left(\frac{df}{d\rho}(p)\right)_{n-1}\right)$$

(B.14)

$$\left(\frac{df}{d\rho}\right)_{n-1} = \frac{P_{n-1}}{\rho} + A_{n-1}$$

(B.15)

The combination of equations B12-B15 gives a global expression for P^{cross}

Finally, the chemical potential requires de evaluation of $\left(\dfrac{df}{dx_i}^{cross}\right)$

$$\mu^{cross} = \left(\frac{\partial A^{cross}}{\partial x_i}\right) = \frac{1}{\rho}\left(\frac{\partial f^{cross}}{\partial x_i}\right) \tag{B.16}$$

$$\frac{df}{dx_i}^{cross} = -\left(\frac{dK_n}{dx_i}\right)\cdot\ln\frac{\Omega^s}{\Omega^l} - K_n\left(\frac{\left(\frac{\partial\Omega^s}{\partial x_i}\right)}{\Omega^s} - \frac{\left(\frac{\partial\Omega^l}{\partial x_i}\right)}{\Omega^l}\right) \tag{B.17}$$

$$\frac{\partial\Omega^\alpha}{\partial x_i} = \int_0^\rho\left[\exp\left(\frac{-G^\alpha(\rho,x)}{K_n}\right)\left[\frac{\left(\frac{\partial G(\rho,x)}{\partial x_i}\right)}{K_n} + \frac{\left(\frac{\partial K_n}{\partial x_i}\cdot G^\alpha(\rho,x)\right)}{K_n^2}\right]\right]dx \tag{B.18}$$

$$\frac{\partial G(\rho,x)}{\partial\rho} = \frac{1}{2}\left(\left(\frac{d\overline{f}}{dx_i}(p+x)\right)_{n-1} + \left(\frac{d\overline{f}}{dx_i}(p-x)\right)_{n-1} - 2\left(\frac{d\overline{f}}{d\rho}(p)\right)_{n-1}\right) \tag{B.19}$$

$$\frac{\partial\overline{f}^l_n}{\partial x_i} = \frac{\partial\overline{f}^l_{n-1}}{\partial x_i} + \frac{\partial(a\rho^{rf})}{\partial x_i} \tag{B.20}$$

$$\frac{\partial\overline{f}^s_n}{\partial x_i} = \frac{\partial\overline{f}^s_{n-1}}{\partial x_i} + \frac{\partial\left(a\rho^{rf}\phi w^2 \middle/ 2^{2n+1}L^2\right)}{\partial x_i} \tag{B.21}$$

$$\frac{\partial K_n}{\partial x_i} = K_n\left(\frac{\frac{\partial\sigma^3}{\partial x_i}}{\sigma^3} - \frac{L_i^3}{L_m^3} - \frac{\frac{\partial\varepsilon^3}{\partial x_i}}{\varepsilon^3}\right) \tag{B.22}$$

$$\frac{da}{dx_i} = \frac{16}{9}\pi\left(\frac{d\sigma^3\varepsilon}{dx_i}\right) \tag{B.23}$$

$$\frac{dw^2}{dx_i} = \frac{6}{(7\sigma)} \left(\frac{d\sigma^3}{dx_i} \right)$$ (B.24)

The combination of equations B16-B24 gives the total contribution of μ^{cross}

C. Crossover terms for derivative properties

In this part of the appendix, the details for the derivation of the crossover terms for the main derivative properties are shown. Derivative properties are second-order derivatives from a primary thermodynamic function (the Helmholtz energy in this case). It means that they will be obtained derivating the free energy respect to temperature and density twice.

The first derivative from the Helmholtz energy permits to calculate de internal energy of the system. As it will be necessary for the calculation of the heat capacity, we also show the crossover term for its calculation.

The internal energy U of a system has the following expression:

$$U = -T^2 \left(\frac{\partial A/T}{\partial T} \right) = A - T \frac{\partial A}{\partial T} = A - \frac{T_{ref}}{\rho_{ref}} \left(\frac{\partial f}{\partial T} \right)$$ (C.1)

The crossover contribution for $\left(\frac{\partial f}{\partial T} \right)^{crossover}$ is expressed in the following equations:

$$\left(\frac{\partial f}{\partial T} \right)^{cross} = \frac{-K_n}{T} \log\left(\frac{\Omega^l}{\Omega^s} \right) - K_n \left[\frac{\left(\frac{\partial \Omega^s}{\partial T} \right)}{\Omega^s} - \frac{\left(\frac{\partial \Omega^l}{\partial T} \right)}{\Omega^l} \right]$$ (C.2)

$$\frac{\partial \Omega^\alpha}{\partial T} = \int_0^\rho \left[\exp\left(\frac{-G^\alpha(\rho,x)}{K_n} \right) \left(\frac{\frac{G(\rho,x)}{T} - \frac{\partial G(\rho,x)}{\partial T}}{K_n} \right) \right] dx \qquad (C.3)$$

$$\frac{\partial G(\rho,x)}{\partial T} = \frac{\frac{\partial f}{\partial T}(\rho+x) + \frac{\partial f}{\partial T}(\rho-x) - 2\frac{\partial f}{\partial T}(\rho)}{2} \qquad (C.4)$$

Combination of equation C1-C4 gives an expression for the internal energy crossover contribution.

The second derivative of the Helmholtz energy respect to the temperature is needed to obtain the isochoric heat capacity C_v.

$$C_v = -T\left(\frac{\partial^2 A}{\partial T^2} \right) = \frac{-T}{\rho_{ref}}\left(\frac{\partial^2 f}{\partial T^2} \right) \qquad (C.5)$$

The following expressions show the evaluation of the second derivative of the free Helmholtz energy density for the crossover term $\left(\frac{\partial^2 f}{\partial T^2} \right)^{crossover}$

$$\left(\frac{\partial^2 f}{\partial T^2} \right)^{cross} = \frac{-2K_n}{T}\left[\frac{\left(\frac{\partial\Omega^s}{\partial T}\right)}{\Omega^s} - \frac{\left(\frac{\partial\Omega^l}{\partial T}\right)}{\Omega^l} \right] + K_n\left[\frac{\left(\frac{\partial^2\Omega^s}{\partial T^2}\right)}{\Omega^s} - \left(\frac{\left(\frac{\partial\Omega^s}{\partial T}\right)}{\Omega^s}\right)^2 - \frac{\left(\frac{\partial^2\Omega^l}{\partial T^2}\right)}{\Omega^l} + \left(\frac{\left(\frac{\partial\Omega^l}{\partial T}\right)}{\Omega^l}\right)^2 \right] \qquad (C.6)$$

$$\frac{\partial^2\Omega^\alpha}{\partial T^2} = \int_0^\rho \left[\frac{\partial\Omega^\alpha}{\partial T}\left(\frac{\frac{G(\rho,x)}{T} - \frac{\partial G(\rho,x)}{\partial T}}{K_n} \right) + \exp\left(\frac{-G^\alpha(\rho,x)}{K_n} \right)\left(\frac{2T\frac{\partial G(\rho,x)}{\partial T} - 2G(\rho,x) - T^2\frac{\partial^2 G(\rho,x)}{\partial T^2}}{K_n T^2} \right) \right] dx \qquad (C.7)$$

$$\frac{\partial^2 G(\rho, x)}{\partial T^2} = \frac{\dfrac{\partial^2 f}{\partial T^2}(\rho + x) + \dfrac{\partial^2 f}{\partial T^2}(\rho - x) - 2\dfrac{\partial^2 f}{\partial T^2}(\rho)}{2} \tag{C.8}$$

The combination of equations C3-C8 gives a global expression for the evaluation of the crossover contribution to the isochoric heat capacity.

Next property is the isothermal compressibility. The general form has been given in equation 5.26:

$$\frac{1}{k_t} = \rho \left(\frac{\partial P}{\partial \rho} \right)_T \tag{C.9}$$

The pressure is obtained deriving the Helmholtz energy respect to the density. In fact, as all derivative properties, we have to perform a derivative of second order. In this case, both are respect to the density. If equations B.12 and B.15 are combined and introduced into equation C.9, the following expression is obtained:

$$\frac{1}{k_t} = \rho \left(\frac{\partial \left(\rho \dfrac{\partial f}{\partial \rho} - f \right)}{\partial \rho} \right) = \rho^2 \frac{\partial^2 f}{\partial \rho^2} \tag{C.10}$$

Next equations show the expressions to solve $\left(\dfrac{\partial^2 f}{\partial \rho^2} \right)^{cross}$

$$\left(\frac{\partial^2 f}{\partial \rho^2} \right)^{cross} = -K_n \left[\frac{\left(\dfrac{\partial^2 \Omega^s}{\partial \rho^2} \right)}{\Omega^s} - \left(\frac{\left(\dfrac{\partial \Omega^s}{\partial \rho} \right)}{\Omega^s} \right)^2 - \frac{\left(\dfrac{\partial^2 \Omega^l}{\partial \rho^2} \right)}{\Omega^l} + \left(\frac{\left(\dfrac{\partial \Omega^l}{\partial \rho} \right)}{\Omega^l} \right)^2 \right] \tag{C.11}$$

$$\frac{\partial^2 \Omega^\alpha}{\partial \rho^2} = \int_0^\rho \exp\left(\frac{-G^\alpha(\rho,x)}{K_n}\right)\left(\frac{\partial^2 G^\alpha(\rho,x)}{K_n}\right)\left(\frac{1}{K_n^2} - \frac{1}{K_n}\right)dx - \frac{2}{K_n}\left(\frac{\partial G^\alpha(\rho,\rho)}{\partial \rho}\right)\exp\left(\frac{-G^\alpha(\rho,\rho)}{K_n}\right) \quad \text{(C.12)}$$

$$\frac{\partial^2 G(\rho,x)}{\partial \rho^2} = \frac{\dfrac{\partial^2 f}{\partial \rho^2}(\rho+x) + \dfrac{\partial^2 f}{\partial \rho^2}(\rho-x) - 2\dfrac{\partial^2 f}{\partial \rho^2}(\rho)}{2} \quad \text{(C.13)}$$

Again, the combination of equations C.10-C.15, joined with those for the pressure contribution (B.12-B-15), give a global expression for the isothermal compressibility.

Another relevant property is the thermal expansion coefficient which is expressed in equation 5.28, and needed for the calculation of C_p.

$$\alpha = k_T \left(\frac{\partial P}{\partial T}\right)_\rho \quad \text{(C.14)}$$

The evaluation of the thermal expansion coefficient requires the previous calculation of k_T. As it was already done, the efforts are concentrated in the evaluation of $\left(\frac{\partial P}{\partial T}\right)_\rho^{cross}$. Again, combining eq. C.14 with expressions B.12 and B-15, we obtain:

$$\alpha = k_T\left(\rho\left(\frac{\partial^2 f}{\partial \rho \partial T}\right) - \frac{\partial f}{\partial T}\right) \quad \text{(C.15)}$$

The evaluation of $\left(\frac{\partial f}{\partial T}\right)^{cross}$ has been already done (see eq. C.2). The evaluation of the derivative $\left(\frac{\partial^2 f}{\partial \rho \partial T}\right)^{cross}$ is shown in the following equations.

$$\left(\frac{\partial^2 f}{\partial \rho \partial T}\right)^{cross} = \frac{-K_n}{T}\left[\frac{\left(\frac{\partial \Omega^s}{\partial \rho}\right)}{\Omega^s} - \frac{\left(\frac{\partial \Omega^l}{\partial \rho}\right)}{\Omega^l}\right] - K_n\left[\frac{\left(\frac{\partial^2 \Omega^s}{\partial \rho \partial T}\right)\left(\Omega^s - 1\right)}{\left(\Omega^s\right)^2} - \frac{\left(\frac{\partial^2 \Omega^l}{\partial \rho \partial T}\right)\left(\Omega^{ls} - 1\right)}{\left(\Omega^l\right)^2}\right] \quad (C.16)$$

$$\frac{\partial^2 \Omega^\alpha}{\partial \rho T^2} = \int_0^\rho\left[\frac{1}{K_n}\exp\left(\frac{-G^\alpha(\rho,x)}{K_n}\right)\left(\frac{\partial G(\rho,x)}{\partial \rho}\left(\frac{-G(\rho,x)}{K_n T} + \frac{1}{T}\right) + \frac{\partial^2 G(\rho,x)}{\partial \rho \partial T}\left(\frac{1}{K_n} - 1\right)\right)\right]dx$$

$$+ \frac{1}{K_n}\exp\left(\frac{-G(\rho,\rho)}{K_n}\right)\left(\frac{1}{T}G(\rho,\rho) - \frac{\partial G(\rho,\rho)}{\partial T}\right)$$

$$(C.17)$$

$$\frac{\partial^2 G(\rho,x)}{\partial \rho \partial T} = \frac{\frac{\partial^2 f}{\partial \rho \partial T}(\rho + x) + \frac{\partial^2 f}{\partial \rho \partial T}(\rho - x) - 2\frac{\partial^2 f}{\partial \rho \partial T}(\rho)}{2} \quad (C.18)$$

Combination of equations C.15-C.18 gives a global expression for the thermal expansion coefficient. The rest of derivative properties can be obtained from the three described:

$$\mu = T\left(\frac{\partial P}{\partial T}\right)_\rho - \rho\left(\frac{\partial P}{\partial \rho}\right)_T = \frac{\alpha T - 1}{k_T} \quad (C.19)$$

$$C_p = C_v + \frac{T\alpha^2}{k_T \rho} \quad (C.20)$$

$$k_S = k_T \frac{C_v}{C_p} \quad (C.21)$$

$$\omega = \sqrt{\frac{C_p}{C_v}\left(\frac{\partial P}{\partial \rho}\right)_T} = \sqrt{\frac{C_p}{C_v k_T \rho}} \quad (C.22)$$

The Joule-Thomson coefficient, the isobaric heat capacity, the isentropic compressibility and the speed of sound are calculated using equations C.19-C.22 respectively. The values inside the equation include already the crossover contribution.

Resum

El progrés i les millores assolides en el camp industrial han empès els investigadors a buscar eines més refinades per tal de modelar aquests processos amb un major grau de precisió. Les propietats termofísiques són necessàries i el seu coneixement ha de ser molt precís, ja que una predicció poc acurada pot afectar el disseny d'una operació unitària, amb una conseqüent pèrdua de rendiment i diners.

El treball experimental ha constituït sempre el pilar per disposar d'una base de dades de fluids purs i mescles. Tanmateix, actualment els models teòrics han progressat com a eines modernes que poden proveir a l'usuari d'una quantitat ingent d'informació sobre un fluid de manera ràpida, neta i barata. En qualsevol cas, manca encara un llarg camí per trobar una eina poderosa capaç de calcular el comportament termodinàmic de qualsevol compost en qualsevol condició.

Aquest treball utilitza una robusta equació d'estat anomenada soft-SAFT. El nom original prové de la Teoria Estadística de Fluids Associants (SAFT), que és una equació basada en principis de mecànica estadística. Posseeix una molt forta base molecular,

proposant un model "físic" per a descriure el compost. Soft-SAFT és una variant de la SAFT original que utilitza un terme de referència basat en una interacció de tipus Lennard-Jones entre les molècules.

Malgrat que l'equació prèvia ja havia estat provada de manera exitosa en un conjunt molt variat de treballs, encara fallava en una regió molt important del diagrama de fases: la regió crítica. En aquesta regió, les propietats sofreixen fortes fluctuacions i canvien dràsticament degut a les llargues correlacions que es produeixen entre les molècules. La versió original de la soft-SAFT no pot tenir en compte aquestes fluctuacions de llarg abast perquè està basada en una teoria de camp mig. Tanmateix, aquesta fallida de la teoria ha estat superada introduint un tractament específic de "crossover", que considera les fluctuacions inherents. El procediment està basat en la teoria del grup de renormalització de Wilson (1971) i va ser desenvolupada per White (1992). S'escriu com un joc de relacions recursives on les correlacions entre les molècules són considerades al llarg de vàries iteracions.

L'objectiu d'aquest treball de tesi s'ha dedicat a la millora d'una equació d'estat amb base molecular anomenada soft-SAFT afegint el tractament específic de "crossover" mencionat abans. La meta general implica el desenvolupament d'una poderosa eina predictiva aplicable a tot tipus de condicions per càlculs termodinàmics. Un tractament específic per calcular les fluctuacions inherents presents a la regió crítica s'ha implementat dins de la equació. Un cop l'equació fou millorada, la seva aplicació a sistemes experimentals ha cobert un ampli rang de famílies de compostos com els *n*-alcans, *1*-alcanols i *n*-perfluoroalcans, així com mescles entre ells i amb diòxid de carboni i àcid clorhídric. Diferents propietats incloent l'equilibri líquid-vapor, les línies crítiques i les propietats derivades de segon ordre han estat calculades amb aquesta eina, provant la seva validesa en la majoria de casos.

La nova equació, anomenada "crossover soft-SAFT" és en primer lloc comparada amb simulacions moleculars d'equilibris líquid-vapor de cadenes de Lennard-Jones. Per totes les diferents longituds de cadena, s'obté un acord excel·lent. A continuació, l'equació s'utilitza per estudiar tres famílies diferents d'hidrocarburs: els alcans, els alcanols i els

perfluoroalcans. Els paràmetres moleculars s'optimitzen emprant dades de densitat de líquid i pressió de vapor experimental pels primers vuit member de cada família. Es proposa una correlació per a cada paràmetre respecte el pes molecular, i els paràmetres s'extrapolen per predir el comportament termodinàmic d'altres membres més pesats de la mateixa família, amb un grau de precisió similar a l'obtingut pels membres més lleugers.

Un altre important test per l'equació ampliada dut a terme en aquesta tesi doctoral ha estat l'avaluació de propietats termodinàmiques derivades de segon ordre. Les capacitats calorífiques, la compressibilitat isotèrmica o isentròpica i la velocitat del so han estat calculats per totes aquestes famílies de compostos, obtenint novament un molt bon acord amb les dades experimentals en la majoria de casos. Els resultats obtinguts per a aquestes propietats resulta molt esperançador degut al fet que aquests càlculs s'han realitzat d'una manera purament predictiva, usant paràmetres moleculars obtinguts per ajust de dades a l'equilibri líquid-vapor. S'han pogut reproduir les diferents singularitats observades experimentalment en la regió veïna al punt crític, mentre que el càlcul dels exponents crítics universals també ha revelat un acord amb les mesures experimentals.

Finalment, també es presenta l'extensió dels càlculs a la regió crítica de mescles binàries i ternàries. S'han estudiat diferents grups de mescles entre alcans, alcà/alcanol, CO_2/alcà, CO_2/alcanol i HCl/alcà, posant un èmfasi especial en l'estudi de les diferents transicions crítiques observades al augmentar la longitud de la cadena de l'hidrocarbur. L'equació crossover soft-SAFT es capaç de descriure totes aquestes transicions a partir del paràmetres ajustats pels compostos purs, tot i que l'ajust de paràmetres binaris és necessari en alguns casos. Finalment, també es presenten alguns resultats preliminars de prediccions de bosses de miscibilitat observades en mescles ternàries amb CO_2 supercrític / alcà / alcanol, com una darrera mostra de la força predictiva d'aquesta eina.

Aquest treball pretén ser un pas endavant en la millora de les eines de modelat molecular per aplicacions enginyerils. Malgrat que la natura sigui sempre sorprenent i difícil de reproduir, l'esforç dedicat a aquesta tasca és prou encoratjador per continuar buscant noves fórmules que ens donin la possibilitat d'acostar-nos una mica més al món real.

Resumen

El progreso y las mejoras conseguidas en el campo industrial han impulsado a los investigadores a buscar herramientas más refinadas a fin de modelar estos procesos con un mayor grado de precisión. Las propiedades termofísicas son necesarias y su conocimiento debe ser muy preciso, ya que una predicción inexacta puede afectar al diseño de una operación unitaria, con una consiguiente pérdida de rendimiento y dinero.

El trabajo experimental ha constituido siempre la base para disponer de una base de datos de fluidos puros y mezclas. Sin embargo, actualmente los modelos teóricos han progresado como herramientas modernas que pueden proveer al usuario de una cantidad ingente de información sobre un fluido de manera rápida, limpia y barata. En cualquier caso, falta aún un largo camino para encontrar una herramienta poderosa capaz de calcular el comportamiento termodinámico de cualquier compuesto bajo cualquier condición.

Este trabajo utiliza una robusta ecuación de estado llamada soft-SAFT. El nombre original proviene de la Teoría Estadística de Fluidos Asociantes (SAFT), que es una ecuación basada en principios de mecánica estadística. Posee una base molecular muy fuerte, proponiendo un modelo "físico" para describir el compuesto. Soft-SAFT es una variante de la SAFT original que utiliza un término de referencia basado en una interacción de tipo Lennard-Jones entre las moléculas.

Pese a que la ecuación previa ya había sido probada de forma exitosa en un conjunto muy variado de trabajos, aún fallaba en una región muy importante del diagrama de fases: la región crítica. En esta región, las propiedades del compuesto sufren fuertes fluctuaciones y cambian drásticamente debido a las largas correlaciones que se producen entre las moléculas. La versión original de la soft-SAFT no puede tener en cuenta estas fluctuaciones de largo alcance porque está basada en una teoría de campo medio. Sin embargo, esta limitación de la teoría ha sido superada introduciendo un tratamiento específico llamado de *crossover*, que considera las fluctuaciones inherentes. El procedimiento está basado en la teoría del grupo de renormalización de Wilson (1971) y fue desarrollada por White (1992). Se escribe como un conjunto de relaciones recursivas donde las correlaciones entre las moléculas son consideradas a lo largo de varias iteraciones.

El objetivo de este trabajo de tesis ha sido dedicado a la mejora de una ecuación de estado con base molecular llamada soft-SAFT mediante la implementación del tratamiento específico de *crossover* anteriormente mencionado. El propósito global ha sido el de desarrollar una poderosa herramienta predictiva aplicable a todo tipo de condiciones para cálculos termodinámicos. Una vez la ecuación fue mejorada, su aplicación a sistemas experimentales ha cubierto un amplio rango de familias de compuestos, como los *n*-alcanos, *1*-alcanoles y *n*-perfluoroalcanos, así como mezclas entre ellos y con dióxido de carbono y ácido clorhídrico. Diferentes propiedades incluyendo el equilibrio líquido-vapor, las líneas críticas y las propiedades derivadas de segundo orden han sido calculadas con esta herramienta, constatando su validez en la mayoría de casos.

La nueva ecuación, llamada "crossover soft-SAFT" es, en primer lugar, comparada con simulaciones moleculares de equilibrios líquido-vapor de cadenas de Lennard-Jones. Para todas las diferentes longitudes de cadena, se obtiene un acuerdo excelente. A continuación, la ecuación se utiliza para estudiar tres familias diferentes de hidrocarburos: los alcanos, los alcanoles y los perfluoroalcanos. Los parámetros moleculares se optimizan usando datos de densidad de líquido y presión de vapor experimental para los primeros ocho miembros de cada familia. Se propone una correlación

para cada parámetro respecto al peso molecular, y los parámetros se extrapolan para predecir el comportamiento termodinámico de otros miembros más pesados de la misma familia, con un grado de precisión similar al obtenido para los miembros más ligeros.

Otro test importante para la ecuación extendida llevado a cabo en esta tesis doctoral ha sido la evaluación de propiedades termodinámicas derivadas de segundo orden. Las capacidades caloríficas, la compresibilidad isotérmica o isentrópica y la velocidad del sonido han sido calculadas para todas estas familias de compuestos, obteniendo nuevamente un muy buen acuerdo con los datos experimentales en la mayoría de casos. Los resultados obtenidos para estas propiedades resultan muy esperanzadores debido al hecho que estos cálculos se han realizado de un modo puramente predictivo, usando parámetros moleculares obtenidos por ajuste de datos al equilibrio líquido-vapor. Se han podido reproducir las diferentes singularidades observadas experimentalmente en la vecindad del punto crítico, mientras que el cálculo de los exponentes críticos universales también ha revelado un acuerdo con las medidas experimentales.

Finalmente, también se presenta la extensión de los cálculos a la región crítica de mezclas binarias y ternarias. Se han estudiado diferentes grupos de mezclas entre alcanos, alcano/alcanol, CO_2/alcano, CO_2/alcanol y HCl/alcano, poniendo un énfasis especial en el estudio de las diferentes transiciones críticas observadas al aumentar la longitud de la cadena del hidrocarburo. La ecuación crossover soft-SAFT es capaz de describir todas estas transiciones a partir de los parámetros ajustados para los compuestos puros, aunque el ajuste de parámetros binarios es necesario en algunos casos. Finalmente, también se presentan algunos resultados preliminares de predicciones de "bolsas" de miscibilidad observadas en mezcles ternarias de CO_2 supercrítico / alcano / alcanol, como una última muestra de la fuerza predictiva de esta herramienta.

Este trabajo pretende ser un paso adelante en la mejora de las herramientas de modelado molecular para aplicaciones ingenieriles. Pese a que la naturaleza sea siempre sorprendente y difícil de reproducir, el esfuerzo dedicado a esta tarea es lo suficiente estimulador para continuar buscando nuevas fórmulas que nos den la posibilidad de acercarnos un poco más al mundo real.

Curriculum Vitae

Felix Llovell was born in Tarragona, Spain, on the 21st of September in 1979. He started his studies in chemical engineering in 1997 at the *Universitat Rovira i Virgili*. In summer 2001, he did a three-month stay in the industry, working in the quality control laboratory of Basell Polyolefins in Tarragona. Later on, that year, he spent the first semester of his last year in Toulouse (France). He worked in the research group of "Functional Process Analysis", working on the modeling of liquid-liquid-vapor equilibria following an optimization procedure called "the method τ".

After graduating in 2002, he returned eight months to Toulouse to continue working in the same research project, collaborating with the simulator enterprise ProSim.

He then decided to join the Molecular Simulation Group to begin a PhD under the supervision of Prof. Lourdes F. Vega. He planned to work in the improvements of the molecular soft-SAFT equation of state, introducing a specific treatment for calculating the fluctuations produced in the critical region. He enrolled in the graduate studies in Chemical

and Process Engineering at the *Universitat Rovira I Virgili*, holding a FPU grant from the Spanish Government. A few months later, Prof. Vega got a senior researcher position in the *Institut de Ciència de Materials de Barcelona*, and the whole group moved there. Felix worked three years and a half in the Molecular Simulation Group in this Institute, doing two short stays abroad during this period.

He obtained the *Diploma d'Estudis Avançats* (Diploma of Advanced Studies) in September 2004, which stated that he was suitable to do research. In October 2004, he moved to Delft (Holland) during three months into the Laboratory of Applied Sciences under the supervision of Prof. Cor J. Peters. He modeled the vapor-liquid equilibrium of several mixtures of hydrogen chloride with n-alkanes, studying the critical transition when increasing the chain length of the hydrocarbon. He also applied the code for the calculation of derivative properties of binary mixtures, including heat capacities, isothermal compressibilities and the speed of sound.

In October 2005, he moved to Concepción (Chile) during two months into the Department of Chemical Engineering to work with Prof. Hugo Segura. He applied the crossover treatment to a cubic equation of state and studied the performance of the new equation compared to the soft-SAFT equation of state. He also studied some singularities observed in the vicinity of the critical point when calculating derivative properties.

Felix Llovell has published six research articles in international journals and he is actually preparing some more. He has more than ten publications in international conference proceedings, and has contributed by means of oral or poster presentations to more than 15 conferences. He has been a member of the organizing committee of one international symposium based on the lights of the present study. On 18th December 2006, the evaluation committee, formed by several experts in the field, will decide if he deserves the doctor's degree.

LIST OF PUBLICATIONS

1. Llovell, F.; Pàmies, J.C.; Vega, L.F. Thermodynamic properties of Lennard-Jones chain molecules: Renormalization-group corrections to a modified statistical associating fluid theory, *J. Chem. Phys*. **121**, 10715 (2004).

2. Llovell, F.; Vega, L.F. Global Fluid Phase Equilibria and Critical Phenomena of Selected Mixtures using the crossover soft-SAFT Equation, *J. Phys. Chem. B* **110**, 1350 (2006a).

3. Llovell, F.; Vega, L.F. Prediction of thermodynamic derivative properties of pure fluids through the soft-SAFT equation of state, *J. Phys. Chem. B* **110**, 11427 (2006b).

4. Llovell, F.; Peters, C.J.; Vega, L.F. Second-order thermodynamic derivative properties of selected mixtures by the soft-SAFT equation of state, *Fluid Phase Equilib.* **248**, 115 (2006).

5. Llovell, F.; Vega, L.F.; Phase equilibria, critical behavior and derivative properties of selected n-alkane/n-alkane and n-alkane/1-alkanol mixtures by the crossover soft-SAFT equation of state, *J. Supercritical Fluids*, doi:10.1016/j.supflu.2006.10.001 (2006c).

6. Llovell, F.; Florusse, L.J., Peters, C.J.; Vega, L.F. Vapor–liquid and critical behavior of binary systems of hydrogen chloride and certain n-alkanes: experimental data and soft-SAFT modeling, *J. Phys. Chem. B.*, submitted (2006).

7. Llovell, F.; Vega, L.F.;. Mejía, A.; Segura, H. Phase Equilibrium Near to and Far from the Critical Region for Different Families of Compounds Applying a Crossover Treatment to a vdW - Type Equation of State. In preparation.

8. Llovell, F.; Dias, A.; Marrucho, I.M.; Coutinho, J.A.P., Vega, L.F. Study of the critical behavior of CO_2 + n-perfluoroalkanes mixtures using crossover soft-SAFT. In preparation.